UNIVERSITY OF SOUTHAMPTON

FACULTY OF ENVIRONMENTAL AND LIFE SCIENCES

BIOLOGICAL SCIENCES

Volume 1 of 1

Phenotypic and Genotypic Characterisation of Single and Dual Species Biofilms of *Pseudomonas aeruginosa* and *Staphylococcus aureus* Treated With A Novel Antimicrobial Compound

by

Connor James Frapwell

Thesis for the degree of Doctor of Philosophy

August 2018

UNIVERSITY OF SOUTHAMPTON

ABSTRACT

FACULTY OF ENVIRONMENTAL AND LIFE SCIENCES
Biological Sciences

Thesis for the degree of Doctor of Philosophy

Phenotypic and Genotypic Characterisation of Single and Dual Species Biofilms of *Pseudomonas aeruginosa* and *Staphylococcus aureus* Treated With A Novel Antimicrobial Compound

Connor James Frapwell

Bacterial infections are becoming increasingly difficult to treat due to the emergence of antimicrobial resistance, (AMR), which renders current antimicrobial therapies ineffective. Further complicating matters is the ability of bacteria to form communities called biofilms, which are infamous for their tolerance to antimicrobial therapy. Biofilm mediated tolerance and AMR contribute to disease chronicity. Consequently, there is a need for novel antimicrobial interventions. The aim of this thesis was to characterise a novel antimicrobial, HT61, against biofilms of clinically relevant bacterial pathogens, particularly *Pseudomonas aeruginosa* and *Staphylococcus aureus.*

Phenotypic studies showed that HT61 was effective against biofilms formed by Gram-positive species with limited efficacy towards biofilms of Gram-negative species. Scanning electron microscopy of HT61 treated biofilms of *S. aureus* and *P. aeruginosa* suggested a mechanism of action targeting the cell envelope. Quantitative proteomic analysis of HT61 treated *S. aureus* cultures supported this, identifying upregulation of proteins associated with the cell wall stress stimulon and division cell wall cluster.

To investigate the effect of interspecies interactions on bacterial adaptation to HT61, a dual species biofilm model of *P. aeruginosa* and *S. aureus* was developed and characterised. Fluctuation analysis suggested that biofilm co-culture increased the mutation rate of *S. aureus* over 500-fold compared to planktonic culture and almost 100-fold compared to culture as a single species biofilm.

Whole genome sequencing of single and dual species biofilm derived *P. aeruginosa* and *S. aureus* isolates revealed significant genomic variation in both coding and intergenic sequences, but no change in evolutionary trajectory between isolates derived from mono- or co-culture biofilms. Following HT61 treatment, mutations in *S. aureus* were identified in *graS* and *fmtC*, which encode products that modulate the cell envelope and may suggest routes to HT61 adaptation.

In summary, the data presented in this thesis suggests potential mechanisms of action and adaptation to HT61, which could inform future antimicrobial development. This thesis also reinforces the need to understand the impact of interspecies interactions on bacterial evolution and shows that biofilms are important hubs of genomic diversity, which could have dangerous implications for the emergence of AMR.

Table of Contents

Table of Tables

Table of Figures

Academic Thesis: Declaration Of Authorship

I, Connor James Frapwell, declare that this thesis and the work presented in it are my own and has been generated by me as the result of my own original research.

Phenotypic and Genotypic Characterisation of Single and Dual Species Biofilms of *Pseudomonas aeruginosa* and *Staphylococcus aureus* Treated With A Novel Antimicrobial Compound

I confirm that:

1. This work was done wholly or mainly while in candidature for a research degree at this University;
2. Where any part of this thesis has previously been submitted for a degree or any other qualification at this University or any other institution, this has been clearly stated;
3. Where I have consulted the published work of others, this is always clearly attributed;
4. Where I have quoted from the work of others, the source is always given. With the exception of such quotations, this thesis is entirely my own work;
5. I have acknowledged all main sources of help;
6. Where the thesis is based on work done by myself jointly with others, I have made clear exactly what was done by others and what I have contributed myself;
7. Parts of this work have been published as:

Manuscripts

Frapwell C.J *et al*. Increased rates of genomic mutation in a biofilm co-culture model of *P. aeruginosa* and *S. aureus*. **Preprint available on bioRxiv.org, https://doi.org/10.1101/387233**

Conference Proceedings

Frapwell C.J. *et al*. Increased Rate of Evolution of Antimicrobial Resistance in Polymicrobial Biofilm Communities. **Eurobiofilms 2017, Amsterdam, The Netherlands**

Frapwell C.J. *et al*. A Novel Quinoline Derivative That Targets Non-Dividing Bacterial Cells Is Effective Against Biofilms of *S. aureus*, *S. epidermidis* and *P. aeruginosa, in vitro*. **Biofilms7, Porto, Portugal**

Frapwell C.J. *et al* Antibiofilm Efficacy of Antibiotic-Loaded Synthetic Calcium Sulfate Beads in a *P. aeruginosa*/*S. aureus* co-culture model for prosthetic infections. **Milano Biofilm Meeting 2017, Milan, Italy**

Signed: .....

Date: .....

Acknowledgements

I would like to thank Professor Jeremy Webb, Dr Yanmin Hu and Professor Anthony Coates of Helperby Therapeutics, for providing me with the opportunity to undertake this project. Furthermore, I would like to thank everyone at Helperby Therapeutics and St George's University of London for making me feel welcome during my placement. Thanks are also extended to Dr David Johnston and Dr Elizabeth Angus of the Southampton Biomedical Imaging Unit and Dr Mark Willett of the Imaging and Microscopy Centre for their assistance and expertise using the confocal laser scanning microscope and scanning electron microscope. In addition, I thank Dr Paul Skipp for his assistance in planning my proteomic investigations and for performing the mass spectrometry. I would also like to acknowledge the contributions of Benjamin McDonagh and Odel Soren for providing whole genome sequence data for *P. aeruginosa* PAO1 and crystal violet data for *P. aeruginosa* PA21, respectively. Portions of these datasets are presented in Chapter 4.

This PhD project would not have been possible without my excellent support network of friends and family, of which I have been lucky to have. Dr Rob Howlin, your guidance over the duration of my PhD has been invaluable; there isn't enough terrible, overpriced, hazelnut flavoured coffee in the world to repay you! Gratitude must also be paid to Dr Ray Allan who bravely demonstrated that one man can eat a frankly terrifying amount of sushi. As the "Connor F Support Network" the two of you have allowed me to somewhat retain my sanity, especially over my final year; for that, I am incredibly grateful.

To my labmates, in particular Dr Callum Highmore, Robert Hull, Odel Soren, Benjamin McDonagh, Dr Yuming Cai, Priscila Vitola, Chris Winnard and Dr Euan Scott; thank you for sharing in the laughs, late nights, the misery, the pain, the frustration and the odd speckle of optimism. Somehow, we all seem to have fumbled our way through this!

Thomas Bailey, thank you for almost 5 years of procrastination and takeaway pizza; I don't think we can put off going into the real world any longer! Ollie White and Oliver Cheshire, you helped me develop something resembling a work-life balance. It wasn't perfect, but neither are the two of you; perhaps you should both listen to me more? Further thanks must go to Emma Joslin, Chloe Rose, Dr Ben Yarnall and Dr Emily Farthing, all of whom have managed to make my life just that little brighter during my time in Southampton.

To my friends from home and otherwise; Aimæ Wood, Jemma Stewart, Dickon Moore, Madeleine Kelly, Naomi Parnell, Daniel Collis, Neo Phoenix and Laura Millard. Each and every one of you has supported me in some form over the past 4 years. This thesis is as much yours as it is mine, although, for obvious reasons, I will be the only one who can actually understand it.

Also, thank you to those who I have forgotten to name: please do not take it personally; I am tired and this thesis is already far too long.

Rosie Brigham; thank you for putting up with me, dealing with my tantrums, my PhD based sulks and everything in between. Most importantly, thank you for believing in me and everything that I was doing, even when I had given up. Now, let us step into the night and pursue that flighty temptress, adventure!

Finally, I would like to thank my family; Gina, Steve, Emily and Bridie Fry and Neilus and Janet O'Connor (Nanjan) for their unending support. And of course, thanks must be given to Smudge the cat, who motivated me to actually finish my writing. Last but not least, I must thank my parents, Lorraine Frapwell and Colin Frapwell. The two of you have been there every step of the way and without your relentless love and support, none of this would have been possible.

This thesis is dedicated to the memories of two people that I miss dearly.
Callum Wooldridge, may you never be broken again.
Helen Frapwell, I wish you were here to see this finished, but I know that you would be proud.

Definitions and Abbreviations

Full Term	Abbreviation
Antimicrobial Resistance	AMR
Autoinducers	AIs
Baird-Parker Agar	BPA
Bis-(3'-5')-cyclic dimeric guanosine monophosphate	c-di-GMP
Bovine Serum Albumen	BSA
Brain Heart Infusion	BHI
Carbapenem Resistant *Enterobacteriaceae*	CRE
Coding Sequences	CDS
Colony Forming Units	CFUs
Community Associated MRSA	CA-MRSA
Confocal Laser Scanning Microscopy	CLSM
Crystal Violet	CV
Cyclic-di(3'-5')-adenylic acid	c-di-AMP
Cystic Fibrosis	CF
Derjaguin-Landau-Verwey-Overbeek	DLVO
Dithiothreitol	DTT
Extended Spectrum β-lactamases	ESBLs
Extra Polymeric Substances	EPS
Extracellular DNA	eDNA
False Discovery Rate	FDR
Fractional Biofilm-Cidal Concentration	FBCI
Fractional Inhibitory Concentration Index	FICI
Guanidine Hydrochloride	G-HCl
Hanks Balanced Salt Solution	HBSS
Homoserine Lactone	HSL
Horizontal Gene Transfer	HGT
Hospital Associated MRSA	HA-MRSA
Insertions and Deletions	INDELS
Lipopolysaccharide	LPS
Liverpool Epidemic Strain	LES
Luria-Bertani	LB
Methicillin Resistant *Staphylococcus aureus*	MRSA
Methicillin Sensitive *Staphylococcus aureus*	MSSA
Microbial Evolution and Growth Arena	MEGA
Minimum Bactericidal Concentration	MBC
Minimum Biofilm Eradication Concentration	MBEC
Minimum Duration of Killing	MDK
Minimum Inhibitory Concentration	MIC
Minimum Stationary Phase Cidal Concentration	MSC
Multi-drug Resistant	MDR
New Delhi Metalloprotease 1	NDM-1
Next Generation Sequencing	NGS

Nitric Oxide	NO
Optical Density at X nm	OD_X
P. aeruginosa Variants	PAV
Penicillin Binding Protein	PBP
Primary Ciliary Dyskinesia	PCD
Pseudomonas Quinolone Signal	PQS
Quorum Sensing	QS
S. aureus Variants	SAV
Scanning Electron Microscopy	SEM
Single Nucleotide Polymorphism	SNP
Small Colony Variants	SCV
Solid Phase Extraction	SPE
Toxin-Antitoxin	TA
Tricarboxylic Acid	TCA
Triethylammonium Bicarbonate	TEAB
Tryptic Soy Agar	TSA
Tryptic Soy Broth	TSB
Ultra-Performance Liquid Chromatography-Mass Spectrometry$^{\text{Elevated Energy}}$	$UPLC/MS_E$
Vancomycin Insensitive/Intermediate *Staphylococcus aureus*	VISA
Vancomycin Resistant Enterococcus	VRE
Vancomycin Resistant *Staphylococcus aureus*	VRSA
World Health Organisation	WHO

Chapter 1

Introduction and Literature Review

1 Introduction

1.1 Historical Context of Antimicrobials and Bacterial Resistance

Prior to the 20th century, bacterial infections were a major global cause of morbidity and mortality. In 1910, Paul Ehrlich and Sahachiro Hata pioneered targeted microbial therapies with the development of Salvarsan 606; the first ever chemical therapeutic that specifically targeted a microbial organism, (in this case, *Treponema pallidum*). This finding showed that it was possible to identify compounds to target disease causing microbes, which could potentially eradicate infections[1]. The next major breakthrough would not come until the summer of 1928, with Alexander Fleming's discovery of penicillin, produced by the mould, *Penicillium rubens*[2]. Fleming found that penicillin was able to inhibit the growth of *Staphylococci* and further work by Howard Florey and Ernst Chain would result in the mass production of the compound for clinical use in a multitude of bacterial infections, 12 years later[3].

The period of time following, (1945-1960), has been colloquially described as the golden era of antimicrobial discovery due the discovery of many novel antimicrobial classes, of which, the majority are still in use today[4]. However, post-1960, pharmaceutical research deviated from the discovery of novel compounds and instead focused on the chemical modification and synthesis of analogues of already existing antimicrobial classes. Hence, the rate of antimicrobial discovery slowed significantly[4,5].

The lack of novel antimicrobial development is a major problem because antimicrobial resistance, (AMR), has been associated with every antimicrobial class currently in clinical use. Complicating matters further is the fact that bacteria typically exist as surface attached, multicellular communities, called biofilms[6]. Biofilms are phenotypically tolerant to external stress, (including antimicrobial treatment), which facilitates bacterial survival and contributes to the chronic nature of certain diseases[6,7]. Biofilms have also been described as hubs of genetic diversity and as such, could act as reservoirs of novel AMR mechanisms[8,9].

1.2 Research Justification

Consequently, novel antimicrobial compounds are of great interest, especially if they are efficacious against biofilms[10]. HT61 is a novel antimicrobial compound that is highly effective against non-dividing cultures of *Staphylococcus aureus and Staphylococcus epidermidis*[11–13]. Non-dividing bacterial cells are typically far less susceptible to the majority of antimicrobial therapies[11] and it is thought that a portion of biofilm tolerance can be attributed to the presence of non-dividing cellular sub-populations[7].

This thesis describes research investigating the cellular responses of planktonic and biofilm cultures of clinically relevant bacterial pathogens to HT61, with a particular focus on *Pseudomonas aeruginosa* and *Staphylococcus aureus*. With HT61 as a unifying component, there were two broad objectives.

The first was to characterise HT61 against biofilms in order to understand the phenotypic bacterial response and shed light on the mechanism of action of HT61. As biofilms can harbour non-dividing sub-populations, it was predicted that HT61 would be effective at treating bacterial biofilms. If so, this could ultimately inform the development of future antimicrobials.

The second objective was to explore how biofilm growth affected bacterial evolvability and whether HT61 treatment was associated with the selection of resistant or adapted phenotypes. By studying the emergence of AMR mechanisms during biofilm growth, the results could provide insight into potential adaptive mechanisms to HT61 as well as the role of the biofilm lifestyle during bacterial evolution.

In Chapter 2, standard antimicrobial susceptibility testing was performed alongside high-resolution microscopy to characterise the efficacy of HT61 against planktonic and biofilm cultures of multiple bacterial species. Upon confirming the efficacy of HT61 towards cultures of *S. aureus*, the results of a quantitative proteomic analysis investigating the cellular response to treatment are described in Chapter 3. To investigate adaptation to HT61 as well as determine its effectiveness against a more clinically relevant model, a dual species model of *P. aeruginosa* and *S. aureus* was created and is described in Chapter 4. This chapter also describes findings that suggest bacteria in biofilms exhibit increased rates of mutation, particularly during co-culture, which may have important implications for the emergence of AMR. Finally, in Chapter 5, whole genome sequencing was utilised to

characterise isolates derived from biofilms of *P. aeruginosa* and *S. aureus* in order to explore bacterial adaptation to HT61 and evaluate how interspecies interactions affected bacterial evolvability.

The remainder of this chapter reviews the available literature and details the physiology of biofilms, the impact and evolution of AMR and potential links between the two phenomena, which demonstrates why novel therapeutic strategies are necessary.

1.3 Overview of the ESKAPE Pathogens

The majority of resistant, nosocomial infections are caused by a small cohort of bacterial species known as the ESKAPE pathogens, encompassing ***E****nterococcus faecium,* ***S****taphylococcus aureus,* ***K****lebsiella pneumoniae,* ***A****cinetobacter baumannii,* ***P****seudomonas aeruginosa* and ***E****nterobacter* species, respectively[14]. Additionally, as detailed by the World Health Organisation's, (WHO), priority list on antimicrobial resistant bacteria (published in 2017), a number of other bacterial species are becoming significantly resistant to current antimicrobial therapies including *Escherichia coli*, *Helicobacter pylori*, Nontyphoidal *Salmonella*, *Campylobacter spp.* and *Neisseria gonorrhoea*[15]. While the ESKAPE pathogens are the current archetypal species linked to AMR, where relevant, other organisms will also be discussed in this review.

An in-depth review of the bacterial physiology of each of these species is beyond the scope of this thesis. However, to supply context, the following sections briefly summarise the characteristics of the ESKAPE pathogens and bacterial physiology that are relevant to infection and AMR.

1.3.1 The Gram Classification System

Prior to discussing the numerous bacterial species associated with AMR and the associated mechanisms, it is necessary to briefly discuss the most common form of bacterial classification: the Gram classification. It is necessary to understand the physiology underlying this definition as it is a recurring theme in both this thesis and the field of AMR and bacterial pathogenesis.

Probably the most utilised descriptor in microbiology is whether a bacterial species is Gram-positive or Gram-negative. The Gram categorisation method was devised by Carl Friedlander and Christian Gram in the late 1800's whereby the two scientists found that bacteria could be classified depending on whether they retained a crystal violet stain. If the stain was retained, the bacteria were classed as Gram-positive and if the stain was lost, the bacteria were classified as Gram-negative[16]. Crystal violet stains bacterial peptidoglycan and differentiates bacteria based on the composition of their cell envelope. In short, Gram-negative species are constrained by the cell membrane, followed by a thin (a few nm) layer of peptidoglycan and finally an additional outer membrane. On the other hand, Gram-positive bacteria are surrounded by the cell membrane and a comparatively thicker (30-100

nm thick) peptidoglycan wall, only[17]. There are also differences in the actual cell wall composition between classes. Specifically, the cell wall of Gram-positive species will contain components such as wall teichoic acids that are linked to the cell wall and lipoteichoic acids, which are linked to the cell membrane[17,18]. These differences are illustrated in Figure 1. The exception to this classification system are the *Mycobacterium spp.* which due to a differing cell envelope composition are neither Gram-positive or Gram-negative[18]. However, an examination of this genus would be out of scope with the rest of the thesis.

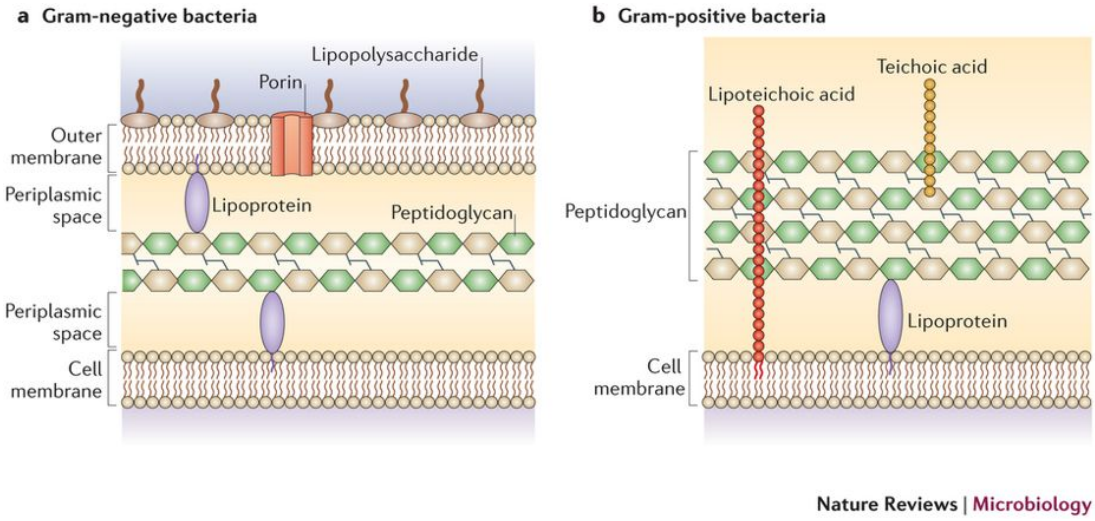

Figure 1: Cell envelope structure of Gram-negative and Gram-positive bacterial species

A) The Gram-negative cell is protected by a double membrane that sandwiches a thin layer of peptidoglycan. Proteins can be integral to both membranes and can often include specific outer membrane porins, important for influx/efflux and bacterial attachment. B) Gram-positive cells possess a simpler cell envelope, consisting only of the cell membrane and a thick peptidoglycan layer incorporating wall teichoic and lipoteichoic acids. Reprinted and adapted with permission from Springer Nature: Nature Reviews Microbiology. Through the wall: extracellular vesicles in Gram-positive bacteria, mycobacteria and fungi. Brown L., Wolf JM., Prados-Rosales R., Casadevall A. Copyright 2015.

1.3.2 Enterococcus faecium

E. faecium is a Gram-positive facultative anaerobe, comprising a portion of the commensal gut flora. As such, colonisation by *E. faecium* is usually asymptomatic. However, if an individual is immunocompromised, it can be implicated in a number of ailments including urinary tract infections, wound infections, bacteraemia and endocarditis[19]. Treatment of these conditions has been made more difficult due to the emergence of resistance mechanisms towards a broad selection of compounds including β-lactam antimicrobials, such as ampicillin, as well as other antimicrobial classes including aminoglycosides,

macrolides, fluoroquinolones and vancomycin, with the latter designated as Vancomycin Resistant Enterococcus, (VRE)[14,20].

1.3.3 Staphylococcus aureus

Alongside *E. faecium*, *S. aureus* is the only other Gram-positive ESKAPE pathogen. It is often a commensal of the human nares and while generally asymptomatic, carriage is considered a significant risk factor for infection, especially in individuals following surgery or other invasive procedures such as catheterisation, or are otherwise immunocompromised[21,22]. Penicillin resistance was first documented in 1942 and resistance can now be identified in approximately 80% of all *S. aureus* strains[22]. Methicillin resistant *S. aureus*, (MRSA, also resistant to all currently used β-lactam antimicrobials), was first identified in 1961 and can be divided into two genotypically distinct clonal subtypes: hospital associated MRSA (HA-MRSA) and community associated MRSA (CA-MRSA)[22,23]. In the US, the prevalence of MRSA is such that more people die as a result of MRSA infections than the combined total of deaths resulting from HIV/AIDS and tuberculosis[14]. Furthermore, vancomycin resistant strains have emerged in the form of Vancomycin Insensitive *S. aureus,* (VISA, which was first identified in Japan in the mid 1990s)[20], and Vancomycin Resistant *S. aureus,* (VRSA), which was first identified in the US in 2002) and evolved via interspecies interactions and genetic transfer with VRE[20,24].

1.3.4 Klebsiella pneumoniae

K. pneumoniae is a commensal, Gram-negative bacterium that is a common asymptomatic coloniser of the nasopharynx and intestines. Similar to *Streptococcus pneumoniae*, it is surrounded by a polysaccharide capsule that acts as protection from immune cell phagocytosis as well as an important virulence factor[25]. It is a common cause of a number of medical conditions including pneumonia, urinary tract infections, bacteraemia and a distinct class of pyogenic liver abscesses.[27,28] Resistant *K. pneumoniae* are often associated with a group of bacteria known as the carbapenem resistant *Enterobacteriaceae,* CRE, which are highly resistant to β-lactam antimicrobials including the "last resort" carbapenems[26]. This is typically due to the expression of plasmid encoded extended spectrum β-lactamases, (ESBLs), which hydrolyse β-lactam antimicrobials. An example ESBL is the infamous New Delhi Metalloprotease 1 (NDM-1)[26,27].

1.3.5 Acinetobacter baumannii

The Gram-negative bacterium, *A. baumannii,* has only become clinically relevant in the past 20 years, coinciding with the finding that it could readily become highly multi-drug resistant, (MDR)[28]. This concern was not unfounded; 70% of *A. baumannii* isolates from Latin America and the Middle East were found to be MDR, which is considerably higher than other Gram-negative species[29]. *A. baumannii* is more likely to infect immunocompromised individuals meaning that the incidence of nosocomial infection is high, encompassing ventilator associated pneumonia and septicaemia[28,30]. A particularly infamous outbreak occurred between 2002 and 2004 in members of the US military following operations in Iraq, where individuals suffered from *A. baumannii* associated wound and bone infections[31].

1.3.6 Pseudomonas aeruginosa

P. aeruginosa is an opportunistic, Gram-negative bacterium that is implicated in an array of nosocomial infections including soft tissue infections, urinary tract infections, bacteraemia, otitis media folliculitis as well as both acute and chronic lung infections[32,33]. It is associated with increased morbidity and mortality during chronic infections of the cystic fibrosis, (CF), lung and is difficult to treat due to an array of intrinsic AMR mechanisms[32,33]. *P. aeruginosa* is the archetypal biofilm forming pathogen, exhibiting increased tolerance and survival towards antibacterial slights, including both antimicrobial compounds and attack by the immune system[33]. While the majority of bacteria can employ this lifestyle, *P. aeruginosa* is considered to be the model biofilm organism and the majority of biofilm research has focused on this pathogen.

1.3.7 Enterobacter spp.

The *Enterobacter* genus encompasses a number of Gram-negative species that are increasingly emerging as common nosocomial pathogens. They are often associated with conditions such as septicaemia, endocarditis, skin and soft tissue infections, lower respiratory tract infections, intra-abdominal infections, ophthalmic infections, urinary tract infections and infections of the central nervous system, although, like all opportunistic pathogens, rarely cause disease in those who are immunocompetent[34]. The two most commonly isolated species are *Enterobacter cloacae* and *Enterobacter aerogenes* and resistance against β-lactam antimicrobials via expression of ESBLs makes treatment difficult[35,36].

1.4 Biofilms

1.4.1 Definition

The majority of bacteria possess the ability to form communities of cells, otherwise known as biofilms. Biofilms are tolerant to antimicrobial treatment as well as other harsh environments such as extreme temperatures, pH, the immune system, biocides and dessication[6]. There is no exact definition of a biofilm but they are most commonly thought of as sessile aggregates of cells that have attached to a surface[10]. However, in certain instances, cells can form aggregates called flocs, which do not attach to a surface and are inherently mobile[6,37]. Once aggregated, cells typically begin to surround themselves in a self-produced hydrogel matrix, (extracellular polymeric substances, EPS), which can contain a number of components including, but not limited to proteins, polysaccharides, extracellular DNA (eDNA), enzymes and metal ions. The EPS provides protection, structural stability, increased adhesive capability as well as the majority of the overall biofilm biomass[6,38]. Biofilms are highly heterogenous and usually harbour numerous species and/or phyla alongside gradients of nutrients and metabolic activity, as well as altered gene expression compared to free floating planktonic cultures[6,7,10].

These aforementioned features mean that biofilms are of great concern within healthcare environments and have been predicted to account for up to 80% (NIH Public Announcements PA-03-047)[39], of all nosocomial infections. Due to their antimicrobial tolerance, biofilms are typically implicated in long-term chronic infections[6,7,10]. When biofilms are formed by genotypically resistant pathogens, for example MRSA and β-lactam resistant *P. aeruginosa* in cystic fibrosis sputum samples[40], the issue of biofilm tolerance is further exacerbated. Aside from healthcare, biofilms are also a problem in industry. For example, in the shipping industry biofilms can attach to the hulls of shipping vessels, increasing drag and operating costs. Biofilms can also form within pipes causing microbially induced corrosion, and also pose problems across the food processing industry[41,42].

1.4.2 Biofilm Development

While many bacteria will form biofilms readily, there is evidence suggesting that biofilm formation is a type of bacterial stress response that is implemented to prolong their survival. The effectiveness of this sessile lifestyle is undisputed but worryingly, a number of studies have shown that the stress levied by antimicrobial treatments can also be sufficient at promoting biofilm development. For example, the use of thiopeptide antimicrobials (which are naturally produced metabolites of *Bacillus cereus*), have been shown to stimulate formation of *Bacillus subtilis* biofilms[43], while sub-inhibitory concentrations of aminoglycosides, (including tobramycin, amikacin, streptomycin and gentamicin) has been shown to increase biofilm formation of *P. aeruginosa*[44]. This link is concerning; as biofilms survive antimicrobial treatment, ineffective use of antimicrobials to treat them may promote further biofilm formation, which would make future treatments even less likely to succeed.

P. aeruginosa is often utilised as the model biofilm forming organism and proteomic studies have identified four stages of biofilm development that can be broadly applied to all biofilm forming organisms. These stages, (depicted in Figure 2), are adhesion, (which includes reversible and irreversible elements), early development, microcolony maturation and dispersal[10].

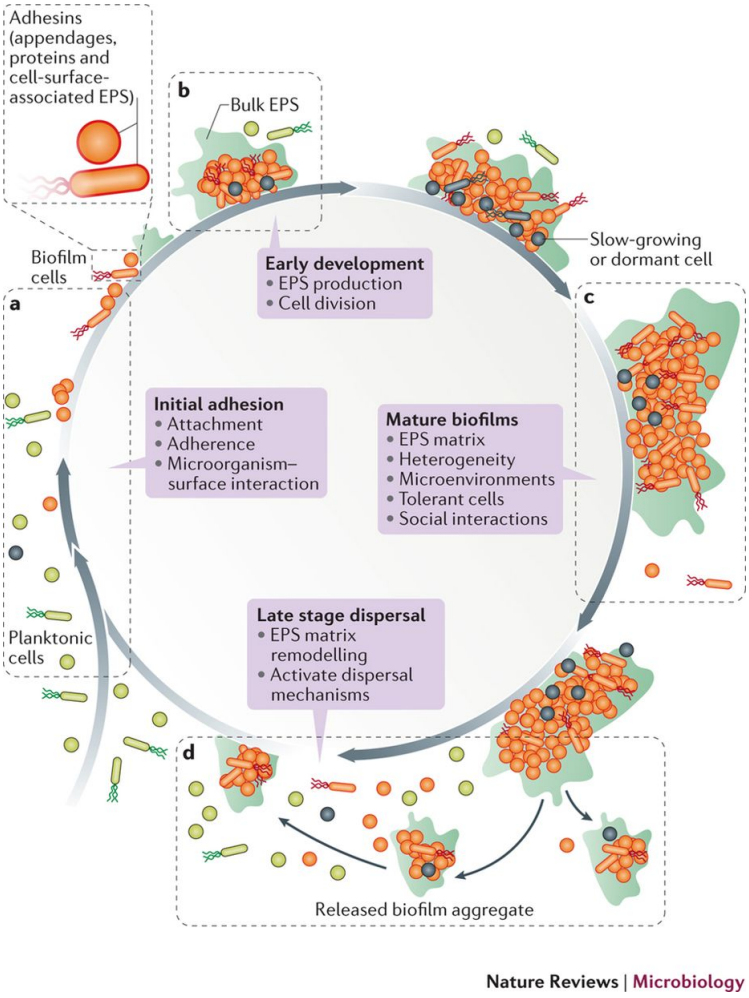

Figure 2: The lifecycle of a biofilm

During biofilm formation, bacteria follow a distinct developmental process, which includes several stages. A) During attachment, planktonic cells contact the surface using a combination of non-specific (e.g. electrostatic), and specific (e.g. receptor mediated) interactions. B) Once a critical cell number is reached, bacterial communication via the production and recognition of quorum sensing molecules causes the bacterial cells to start producing “biofilm factors” such as further attachment proteins and EPS components. C) As the biofilm matures, quorum sensing molecules, as well as environmental signals, continue to influence development. This can lead to the development of distinct microcolonies and the establishment of microenvironments and gradients across the biofilm. Bacterial cells exhibit a division of labour, with certain cells designated to certain functions, such as EPS production. Furthermore, as public goods begin to arise (such as certain metabolites), social interactions begin to occur, including a rise in both co-operators and cheaters. D) Dispersal of the biofilm can occur actively, as a result of signal molecules, which can be produced by the bacteria, or therapeutically administered (e.g. nitric oxide). Alternatively, dispersal can be passive and caused by shear forces. Reprinted with permission from Springer Nature: Nature Reviews Microbiology. Targeting microbial biofilms: current and prospective therapeutic strategies. Koo H., Allan R., Howlin R., Stoodley P., Hall-Stoodley L. Copyright 2017.

1.4.2.1 Role of Bacterial Communication During Biofilm Formation

Bacterial communication is of critical importance for coordinating biofilm development[45]. One branch of communication is quorum sensing, QS, which is a cell density dependent form of communication. QS can occur in both sessile and planktonic populations but is more widespread in biofilms because they are, by definition, cell dense. A typical quorum sensing signalling cascade begins with the release of extracellular signalling molecules called autoinducers, (AIs). These initiate a positive feedback loop whereby their detection elicits further AI production; as the cell density increases, so does the production of AIs. Once the local concentration of AIs reaches a threshold level (which is intrinsically linked to cell density), they can be detected and bound by specific bacterial cell receptors, ultimately leading to changes in gene expression[45]. While QS systems are widespread throughout the bacterial kingdom, they are distinct between Gram-positive and Gram-negative species. Gram-negative species predominantly utilise *N*-acyl homoserine lactones (AHLs, also called autoinducer-1, AI-1 molecules), while Gram-positive species predominantly utilise modified oligopeptides (autoinducer-peptides, AIPs)[46]. Both Gram-negative and Gram-positive species can utilise boron-furan type signals, such as autoinducer-2 (AI-2), produced by the conserved enzyme LuxS, thereby facilitating interspecies communication[46,47].

Differences in QS system complexity can be observed by comparing the systems of *P. aeruginosa* and *S. aureus*. *P. aeruginosa* utilises 4 main quorum sensing systems in a hierarchical network. The homoserine lactone (HSL) based *las* and *rhl* systems revolve around the production and binding of the respective cognate signal molecules, modulating gene expression in a concentration dependent (which is itself mediated by cell density) manner[48,49]. The third system is the *Pseudomonas* quinolone signal (PQS) system which utilises the 2-heptyl-3-hydroxy-4(1H)-quinolone (PQS) and 2-heyptyl-4-hydroxyquinoline (HHQ) alongside the cognate PqsR transcriptional regulator/receptor[48,49]. During growth in nutrient rich environments, the *las* system coordinates the activity of both *rhl* and *pqs* systems[48,49]. However, during stressful conditions, the *las* system can be superseded by the fourth signalling system, the IQS system, which is modulated by stressful environmental cues[48,49]. Conversely, in *S. aureus* (also numerous other *Staphylococcal spp.*), the most important and well-studied QS system is the Agr system which functions alongside the *luxS* mediated AI-2 system[50]. In both species, the related systems are important for the regulation of genes associated with stress, virulence and biofilm formation.

Despite their ubiquity across bacterial species, the production of quorum sensing molecules can be an exploitable, metabolic burden. A study by Mund *et al* (2017) demonstrated that in an environment where quorum sensing was necessary for survival, *lasI* mutants of *P. aeruginosa* (which could not produce the *las* autoinducer), were able to scavenge the quorum sensing molecules produced by the wild type cells and subsequently outcompete them, thereby acting as metabolic cheats[51]. However, the authors also showed that limiting the diffusion of quorum sensing molecules via supplementation of increasing concentration of agar, limited cheater exploitation[51]. It is possible that the biofilm structure, particularly EPS composition, can act in a similar manner to protect "public good producers" from exploitative cheaters.

Second messenger systems are also important for biofilm development. Of particular interest is the second messenger bis-(3'-5')-cyclic dimeric guanosine monophosphate, (c-di-GMP), which has been shown to be critical in biofilm formation and controlling other associated factors regarding properties such as adhesion and motility[52]. The intracellular concentration of c-di-GMP is maintained by two opposing classes of enzymes: the diguanylate cyclases and the phosphodiesterases. The former contain a highly conserved GGDEF domain and create c-di-GMP from two molecules of GTP, whereas the latter utilise either an EAL or HD-GYP domain to degrade c-di-GMP into either a linear 5'-phosphoguanylyl-(3'-5')-guanosine, (pGpG) dinucleotide or two GMP molecules, respectively[52,53]. The activity of the catalytic domains is typically coordinated by additional sensor domains; for example, the protein motility regulator A, (MorA), found in *P. aeruginosa* contains both GGDEF and EAL domains alongside four PAS sensor domains, which respond to nitric oxide, (NO), oxygen and carbon monoxide. In this example, binding of NO to the PAS domain upregulates the EAL activity resulting in a decrease in c-di-GMP, stimulating *P. aeruginosa* biofilm dispersal[54].

The second messenger cyclic di-(3'-5')-adenylic acid, (c-di-AMP) has also been discovered as an important signal molecule in a number of bacterial species including *S. aureus*[55], *B. subtilis*[56], *L. monocytogenes*[57], among others, where it has been implicated in cell wall regulation, sporulation, and DNA damage stress responses[58].

Where relevant to biofilm development, the role of specific bacterial communication pathways will be discussed as appropriate, in the following sections.

1.4.2.2 Biofilm Attachment

Initial biofilm development is largely driven serendipitously, relying on bacterial cells suspended in liquid to periodically interact with a surface. The process of non-specific cell attachment can be characterised with the Derjaguin-Landau-Verwey-Overbeek (DLVO) theory. In classical terms, this theory can be used to describe the interactions between flat surfaces and colloidal objects (i.e. cells), relying on the balance of typically attractive van der Waals interactions and the repulsive forces formed between the electric double layers, (two layers of charge surrounding an object) of the cell and the attachment surface[59]. The DLVO theory has been extended (xDLVO theory) to incorporate polar interactions between both bacterial cells and substrata[60]. However, neither theory consider the role of specific attachment factors, such as cell surface receptors that can interact directly with surface ligands, which are vital factors in bacterial attachment. A study by Ramsey and Whiteley (2004), demonstrated the importance of cell surface proteins in terms of bacterial attachment by creating a series of transposon mutants of *P. aeruginosa* PA14, (referred to as the dynamic attachment deficient (dad) mutants)[61]. The constructed strains of *P. aeruginosa* contained mutations in genes encoding both motility (such as *flhF* and *pilA*, coding for flagellar and type IV pilin subunits respectively), and non-motility proteins, (such as *phoQ*, a Mg^{2+} sensor kinase and *ginK*, a PII-type nitrogen regulatory protein). In all cases, the mutants exhibited impaired attachment during the initial stages of biofilm formation[61]. Another study by Secor *et al* (2015) showed that negatively charged filamentous prophages could improve adhesion of *P. aeruginosa* by interacting with positively charged polymers[62].

Reversible adhesion can then progress into irreversible adhesion, which utilises covalent interactions rather than electrostatic interactions. This process has been likened to that of a lock and key mechanism whereby bacterial surface adhesins selectively bind with structures located on the attachment surface. At this stage, a subpopulation of the bacterial cells will begin to produce EPS to aid in attachment and aggregation of the bacterial cells[10]. QS is important for initial biofilm formation, although different species have different QS requirements. For example, in *S. aureus*, decreased expression of the *agr* system is linked to increased biofilm formation[63]. while the opposite is true for *P. aeruginosa*, whereby expression of the *las* system promotes initial biofilm formation and is important for instigating acute infections[64].

1.4.2.3 Biofilm Maturation and Development

As the attached cells continue to divide and multiply, they can form distinct microcolony structures. The morphology of these structures varies depending on the bacterial species as well as environmental cues including, but not limited to, the nutrient availability, levels of shear stress placed on the biofilm, genetic profiles of the cells within a biofilm, and the precise constituents of the bacterially produced EPS. For example, *P. aeruginosa* grown under flow can form biofilms with distinct mushroom shaped microcolonies[65], whereas biofilms of *S. pneumoniae* can form honeycomb-like structures[66]. Microcolony maturation is not a gene-independent process (it does not occur automatically, without regulation). The *dad*

P. aeruginosa PA14 mutants (described previously) also presented with altered microcolony formation. For example, when the *phoQ* mutant, dad5, was cultured within a flow cell, it formed a biofilm lacking large cell aggregates/microcolonies, unlike the wild type *P. aeruginosa* PA14[61].

1.4.2.4 Biofilm Dispersal

The final stage of biofilm development is dispersal, characterised by a breakdown of the biofilm and a reversion of the cells to a planktonic phenotype. Typically this is associated with downregulation of biofilm associated genes and upregulation of genes associated with a planktonic lifestyle such as those associated with increased motility[54]. There are two classes of dispersal: active, which is initiated by the bacteria and passive, which occurs as a result of external factors such as increased shear forces[54]. Across these classes, there are three types of dispersal mechanism: erosion, where small clusters of cells are released continuously over the course of biofilm formation; sloughing, where large clumps of the biofilm are detached periodically and seeding, which is preceded by cell death of particular subpopulations within the micro colony structures and the escape of cells from within. Erosion and sloughing can be both active and passive mechanisms but seeding is exclusively an active mechanism[67].

Much like the preceding stages of the biofilm lifecycle, dispersal (specifically, active dispersal), is a highly coordinated process, relying on QS systems, second messengers and other factors. For example, QS is vital for the seeding dispersal of *P. aeruginosa* as the microcolonies of QS mutants (lacking the *lasI* and *rhlI* genes), do not hollow out and disperse, compared to the wild type strains[68]. In *S. aureus,* dispersal is mediated by increased expression of the *agr* system[63]. As discussed previously, the breakdown of c-di-

GMP is often associated with biofilm dispersal and low levels of NO have been shown to induce dispersal by upregulating phosphodiesterase activity in a number of bacterial species[54]. *P. aeruginosa* has even been shown to produce low levels of endogenous NO to induce its own dispersal[69].

A variety of other factors have also been implicated in biofilm dispersal. In biofilms of *P. aeruginosa* PAO1, the presence of a filamentous prophage, Pf4, has been linked to cell death mediated dispersal[70] and D-amino acids have been linked to biofilm dispersal in *B. subtilis* (as well as reduced biofilm formation for *P. aeruginosa* and *S. aureus*)[71].

1.4.3 Physiological and Chemical Heterogeneity

A key characteristic of biofilms is their marked chemical, physiological and genetic heterogeneity[6,72,73]. Oxygen gradients are particularly common, with areas of high oxygen concentration at the apical surface of a biofilm and anaerobic, or even completely anoxic environments occurring at the basal side of the biofilm[72]. Oxygen gradients generally do not arise as a result of limited oxygen penetration; instead the concentrations will vary due to the metabolic demands of the bacteria within the biofilm. For example, bacteria in the upper layers utilise the oxygen before it can diffuse throughout the entire structure. Ultimately, the final concentration of a solvent within a biofilm is a product of its rate of diffusion and its rate of metabolism by nearby bacteria. Other gradients can also occur including but not limited to microscale pH gradients[74], QS molecules and gradients of sulphate metabolic products[75].

Naturally, variations in the biofilm microenvironment can promote physiological adaptation by the surrounding cells and stratification of different sub-populations. For example, cells deplete of oxygen at the base of a 350 μM *P. aeruginosa* biofilm contained high numbers of mRNA transcripts for Ribosomal hibernation proteins, indicating a hypoxia mediated reduction in metabolic activity[76]. In a more complex multispecies environment, specific bacteria could be spatially separated to take advantage of certain niches e.g. aerobic bacteria would be nearer the apical surface to take advantage of higher oxygen concentrations. Both of these concepts are illustrated in Figure 3. It should not be surprising that physiological adaptation is typically facilitated by changes in gene expression[6,72].

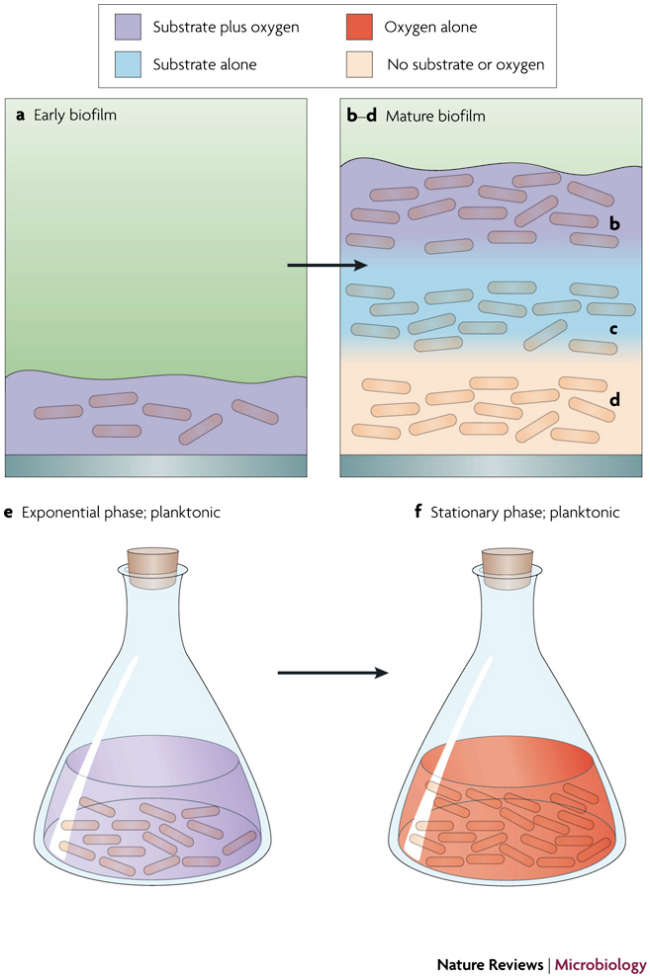

Figure 3: The effect of chemical gradients on the physiological heterogeneity of a biofilm

a) A naïve biofilm is usually thin, with a low cell density, ensuring that there is suitable amounts of metabolic substrates and oxygen, facilitating cell division. b-d) As the biofilm grows, at least three general chemical microenvironments can be established. b) The cells are located at the apical surface and have ready access to both oxygen and metabolic substrates. If appropriate, aerobic species will likely associate within this region of the biofilm. c) The cells at an intermediate depth within a biofilm may no longer be able to access oxygen as it is being utilised by the cells in the apical layer. However, there is sufficient quantities of metabolic substrate available that they can continue to divide via fermentation. d) However, at the bottom of the biofilm, both oxygen and metabolic substrates are depleted, forcing the cells to enter a dormant, metabolically inactive state (unless they are adapted to anaerobic/anoxic environments). e and f) The concept of metabolic substrate depletion within the depths of a biofilm is analogous to growth of bacteria within liquid culture. Initially, when there is a suitable quantity of substrate available, bacteria will readily enter the exponential growth phase. However, once the substrate is depleted, the culture will enter stationary phase; a balance of dividing and non-dividing cells. Figure from Stewart & Franklin (2008).

1.4.4 Genetic Heterogeneity and the Emergence of Novel Genotypes

1.4.4.1 Biofilm Derived Variants

Genetic heterogeneity is an important characteristic of biofilms and can be linked to the emergence of novel bacterial lineages[8,9]. The diversity that is generated within biofilm populations can lead to the emergence of variants with markedly altered phenotypic profiles compared to their respective wild type. Typically, biofilm derived genomic variants are described in terms of their colony morphology, the most well-known being the small colony variants, (SCVs)[77]. SCVs are usually characterised by their slow growth and, as their name implies, small colony diameter. However, they can also possess different traits including altered ability to form biofilms and altered antimicrobial susceptibility. Colony variants have been identified for numerous bacterial species including *P. aeruginosa*[78,79], *S. aureus*[80,81], *Burkholderia cenocepacia*[82], *E. coli*[83] and *S. pneumoniae*[84–86]. Specific genomic changes have often been linked to the observed phenotype but these mechanisms can be incredibly diverse. For example, small rugose colony variants of *P. aeruginosa* are the result of increased c-di-GMP production and can be induced by mutations in *wspF*[78], while SCVs of *S. pneumoniae* have been linked to mutations in *rpoE*[84] and certain *E. coli* variants have been shown to form via the insertion of a Tn1000 transposon element into *hemB*[83]. Similar mutations in *hemB* have also been linked to *S. aureus* SCV formation during biofilm co-culture with *P. aeruginosa*[87].

Parallel evolutionary dynamics have also been identified in biofilm populations. Parallel evolution refers to a mutation that occurs at an identical gene, or nucleotide, in evolutionary independent populations. For example, long term analysis of cystic fibrosis clinical isolates of *P. aeruginosa* biofilms revealed 24 genes that were consistently altered between different isolates over 8 years/39, 000 generations[88]. Parallel evolution over a short time period has also been recorded. Parallel mutations in *wspA* were identified in biofilm derived variants of *B. cenocepacia* after 4 days[82], while a separate experiment investigating *P. aeruginosa* 18A, a cystic fibrosis clinical isolate, identified parallel evolution of nonsynonymous mutations in genes responsible for alginate production and biofilm attachment after only 4 days of biofilm growth[89].

The appearance of similar colony phenotypes across numerous bacterial species and growth conditions is technically an example of convergent evolution, whereby similar ecosystem pressures facilitate the emergence of similar genotypes/phenotypes across independent populations. An elegant example of this was demonstrated by Sommer *et al*

(2016). In this study, the authors compared the evolutionary trajectories of *P. aeruginosa* isolates taken from both CF and primary ciliary dyskinesia (PCD) patients and found six genes (alginate associated: *mucA, algU*; quorum sensing: *lasR*; efflux pumps: *mexZ, mexS, mexA)* that were commonly mutated across isolates from both conditions, suggesting that they were important for pathogen adaptation to the lung environment[90].

1.4.4.2 Mechanisms for Genomic Change

The acquisition of novel genetic traits typically occurs using one of two mechanisms: chromosomal mutations or acquisition and integration of external elements such as plasmids and transposons. It is critical to note that these mechanisms are applicable to all bacteria, regardless of whether they are part of a biofilm community. However, there are certain characteristics of biofilm growth that can influence these mechanisms and may explain why biofilms appear to be hubs for diversification[8,9].

Numerous studies have linked biofilm growth to increased mutation frequency (fraction of mutants within a population), usually utilising resistance to rifampicin or ciprofloxacin as a proxy for mutation. These antimicrobials are chosen because single point mutations can be sufficient to confer resistance. The frequency of *P. aeruginosa* spontaneous resistance to rifampicin and ciprofloxacin increased 15 and 105 fold, respectively following biofilm culture, compared to planktonic growth[91]. In *S. aureus* and *S. epidermidis,* biofilm culture was linked to a 60 and 4 fold increase in the occurrence of spontaneous rifampicin resistance[92]. A 55-fold increase in the frequency of rifampicin resistance was also observed in biofilms of *S. pneumoniae*[86]. The three aforementioned studies all link the increased frequency of mutation seen in biofilms to environmental stressors, namely increased oxidative stress/a reduction in oxidative stress protection and DNA repair mechanisms. While the conclusions appear to be sound, it is worth noting that for the experiments looking at *P. aeruginosa*, *S. aureus* and *S. epidermidis*, biofilms were grown for longer time frames than the comparative planktonic cultures. This limitation was acknowledged in the *Staphylococcal spp.* study, and while the authors say that no difference was observed in planktonic cultures, the data was not shown[92]. Increased mutation frequency has also been associated with an increase in microcolony structures within biofilms of *P. aeruginosa*, which may act as important foci for diversification[93].

As for the acquisition of novel genetic elements, (encompassing both conjugation and transformation mechanisms), horizontal gene transfer, (HGT), is predicted to be increased

in biofilms[6]. For example, plasmids harbouring genes for AMR were incorporated into *S. aureus* 16, 000 fold more efficiently during biofilm growth[94]. *Streptococcus mutans* was found to be 10 to 600 fold more effective at incorporating chromosomal DNA sequences and plasmid-borne elements if cultured as a biofilm, rather than planktonic culture[95].

At first glance, it would seem axiomatic for biofilms to greatly increase rates of HGT between bacteria as the cells are spatially locked in place. However, the reality is more nuanced[96]. Transmission of plasmid-borne GFP was found to only occur during the first 20 hours of growth in biofilms of *Pseudomonas putida*[97]. Factors limiting HGT have been associated with reduced penetration of the exogenous DNA as well as physiological heterogeneity of bacteria within a biofilm. The incorporation of exogenous DNA elements is usually metabolically costly[98]. As certain biofilm sub-populations can be deprived of nutrients (such as those situated away from the apical surface-air interface), in certain cases the penetration of elements such as plasmids can actually be reduced in these areas[96,99]. Furthermore, the presence of sub-populations can limit plasmid transmission as these populations are by definition, separated from the other. Disturbing this structure (i.e. thoroughly mixing a population) has been linked to increased levels of plasmid penetration[99].

1.4.5 Natural Selection and Evolutionary Dynamics in Biofilm Populations

While the previous examples demonstrate cases where biofilm growth increases the levels of genomic diversity, (such as a stress mediated increase in mutation frequency), this is not an example of adaptive mutation *per se*. Natural selection (the fixation of genotypes that result in greater fitness phenotypes within a population) is still a fundamental driver of variation within biofilms[100]. Even though the frequencies of mutation or HGT can be increased, the associated genomic changes that occur may only be relevant to a population if the resulting phenotype is under positive selection i.e. the fitness cost is less than that of a wild type genotype[101]. An example of natural selection within a biofilm was observed with biofilms of the acid producing bacterium, *S. mutans.* Following colonisation of rats, a series of *gtfBC* deletion mutants were isolated at a frequency of 22%, from populations lacking the *gbpA* gene. The *gbpA* mutants formed biofilms which were smaller and, (due to less nutrient restriction), more metabolically active, with a corresponding increase in acid load on the bacteria. This increased acid stress selected for genotypes harbouring *gtfBC*

deletions which could produce thicker biofilms, mitigate the loss of *gbpA* and reduce the acid burden on the bacteria[100].

Due to the spatial and physiological heterogeneity of cells within a biofilm, numerous genetic and phenotypic lineages exist in concert as distinct sub-populations. In evolutionary terms this is known as population fragmentation[102]. Because populations are physically separated and not homogenously mixed, (until a dispersal event, which can result in the biofilm reforming in novel arrangements), there is less access to rare, low cost, high benefit mutations. This means that within biofilm populations, the beneficial mutations that do fix will typically be of smaller (i.e. lower risk) effect. The subpopulations may ultimately reach the same genotypic outcome as that of cells acquiring a single rare, low cost, high benefit mutation however in order to this, more diverse adaptive routes may have been taken[102]. The fixation of smaller mutations can actually slow down the rate of bacterial adaptation[102]. However, if biofilms possess higher mutation rates, it may be possible for the cells to navigate these longer routes of adaptation in a shorter evolutionary time frame.

The number of diversifying lineages within a biofilm at any one time means that competition is inevitable. A common observation is that the strongest competition occurs at the growing edge of the biofilm where nutrients are rich and growth is promoted. Consequently, natural selection for phenotypes that enable bacteria to reach the edge is often high. This specific point may explain the observed division of labour during the construction of microcolonies in biofilms of *P. aeruginosa* cultured in a flow cell. In this example, two distinct populations have been identified: a non-motile population that forms the stalks of the microcolonies and a motile population which can form the mushroom shaped cap[103].

However, if two identical beneficial phenotypes arise, (e.g. improved capacity for biofilm formation), the lineages will compete. One of these lineages will eventually be eradicated from the population. However, due to the competition, fixation of the most beneficial mutation will be delayed, in a process known as clonal interference[101,104]. Delayed fixation due to clonal interference, combined with population fragmentation will mean that when taken as a whole population, diversity will be higher in a spatially structured population, opposed to a planktonic culture.

While the previous examples of evolutionary dynamics have been largely competitive in nature, the dynamics can also be co-operative although these appear to be rarer. A documented example of evolved co-operation can be seen with members of the gut microbiome. In this instance, *Bacteroides ovatus* digests numerous polysaccharides extracellularly which benefits *Bacteroides vulgans,* albeit at a cost to itself[105].

1.4.6 Bacterial Survival During Biofilm Growth

1.4.6.1 Resistance vs Tolerance vs Persistence

Biofilms are tolerant to antimicrobial treatment. Tolerance is distinct from resistance however the two terms are often used interchangeably. The concept of bacterial persistence, a third form of bacterial survival, complicates definitions further[10,106]. However, all can be defined in terms of the bacterial response to an antimicrobial and are summarised in Figure 4. Resistance is typically a heritable genetic trait that renders an antimicrobial ineffective by increasing its minimum inhibitory concentration (MIC, the concentration required to inhibit growth)[106]. In the context of biofilms, tolerance is a typically transient phenotype, which is lost following biofilm dispersal[107]. The MIC of an antimicrobial is not altered against tolerant cells; instead tolerance is linked to an increase in the minimum bactericidal concentration (MBC, the concentration required to kill 99.9% of a bacterial population) as well as increase in the time required to kill the bacterial population. Persistence refers to a phenotypic sub-population of cells that can survive an antimicrobial therapy. This results in bi-phasic killing kinetics where the susceptible population is first killed and the persistent population is killed at a slower rate. Persistence can be split into two types: time dependent and dose dependent persisters. Time dependent persisters present with an extended lag phase or a slower growth rate, ultimately limiting antimicrobial effectiveness, requiring longer treatment times and higher concentrations. On the other hand, dose-dependent persisters transiently alter factors that affect antimicrobial susceptibility; for example, a transient overexpression of efflux pumps[106].

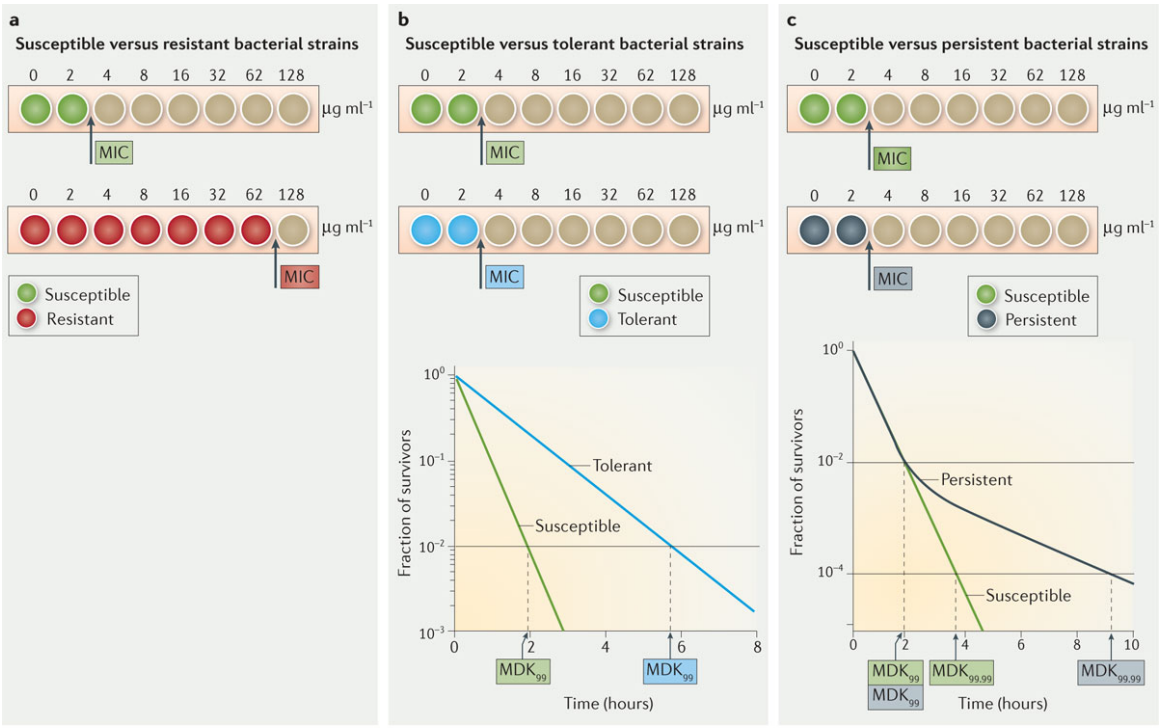

Figure 4: Comparison of resistance, tolerance and persistence

A) Resistance is defined by an increase in the minimum inhibitory concentration, MIC of an antimicrobial. B) Tolerance does not alter the MIC of an antimicrobial; instead the time required (minimum duration of killing, MDK) to elicit the same killing effect as sensitive cells is increased. This can also be linked to an increase in the minimum bactericidal concentration, MBC. C) Persistence is similar to tolerance, but is a phenotype displayed by a much smaller sub-population. For the persisters subpopulation, the MDK will be even higher than that of sensitive or tolerant populations. Reprinted and with permission from Springer Nature: Nature Reviews Microbiology. Distinguishing between resistance, tolerance and persistence to antibiotic treatment. Brauner A., Fridman O., Gefen O., Balaban N. Copyright 2016.

1.4.6.2 Biofilm Tolerance Mechanisms

Biofilm tolerance mechanisms are varied and extensive and have been discussed thoroughly in several excellent review articles[7,108,109]. This section aims to briefly summarise the main biofilm associated tolerance mechanisms.

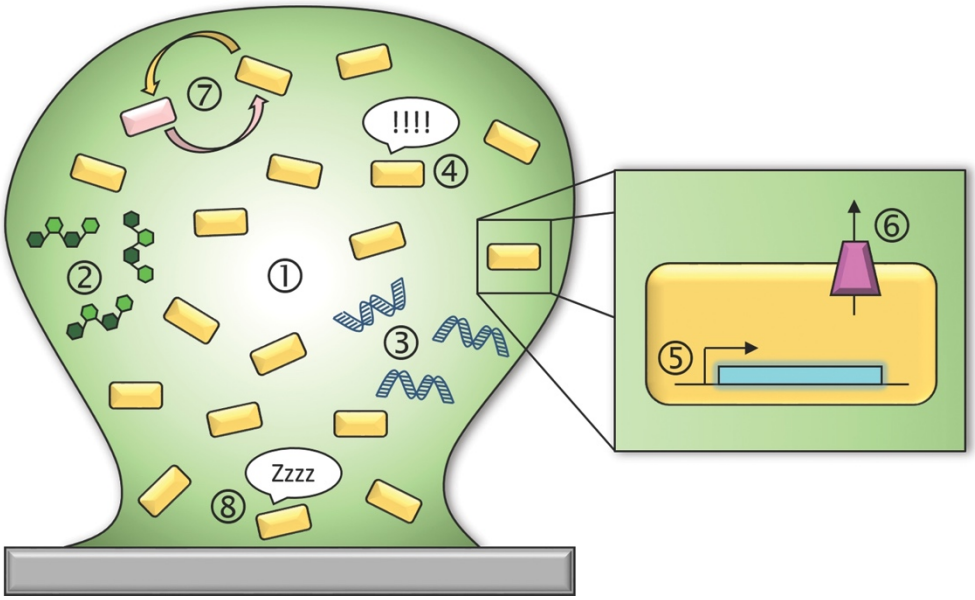

Figure 5: Mechanisms of biofilm tolerance

Biofilms contain numerous characteristics and mechanisms that facilitate tolerance to antimicrobials. 1) Nutrient gradients, (depicted with colour gradient), facilitate the emergence of micro-environments, contributing to physiological heterogeneity. Factors such as matrix polysaccharides (2), eDNA (3), increased stress responses (4) and expression of biofilm specific genes (5) such as efflux pumps (6) act in concert to reduce susceptibility of bacteria to antimicrobials. Due to high cell densities, there is increased levels of cellular communication and potential for the horizontal gene transfer (7). Reprinted with permission from Oxford University Press: FEMS Microbiology Reviews. Molecular mechanisms of biofilm-based antibiotic resistance and tolerance in pathogenic bacteria. Hall C., Mah T. Copyright 2017.

The biofilm EPS is the first line of defence to bacteria during antimicrobial treatment. However, for the majority of antimicrobials, the mere presence of a barrier is not enough to impede diffusion[110,111]. Yet the EPS can contain additional components that do retard antimicrobial penetration. For example, in biofilms of *K. pneumoniae*, matrix bound β-lactamases impede ampicillin diffusion, whereas ciprofloxacin can diffuse freely[112]. In *P. aeruginosa,* tobramycin diffusion can be limited by the presence of a negatively charged filamentous prophage[62], alginate[113], and polysaccharide components such as Psl[114]. A study of *S. epidermidis* biofilms revealed that sub-optimal vancomycin treatment led to an increase in eDNA within the EPS, (likely as a result of increased cell autolysis), which directly impeded further vancomycin transport through the biofilm[115].

The physiological heterogeneity of biofilms can also influence antimicrobial susceptibility. Variations in chemistry have been shown to directly affect the efficacy of certain antimicrobial compounds. The presence of oxygen gradients throughout biofilms of *P. aeruginosa* results in the occurrence of slowly dividing, "stationary-phase" like sub-populations that are less susceptible to numerous antimicrobials[116]. This poses a problem as the majority of antimicrobials in use today are more active against dividing cells[117]. This principle was demonstrated in a paper by Pamp *et al* (2008) where the authors were able to selectively target both metabolically active and metabolically inactive subpopulations using ciprofloxacin and colistin, respectively[118]. This study lends credence to the idea that targeting physiologically separate sub-populations could be a viable strategy for the development of novel antimicrobials that are effective against biofilm populations.

Low pH environments have been shown to reduce the effectiveness of levofloxacin against *A. baumannii, E. coli, Klebsiella spp.* and *Enterobacter spp.*, although effectiveness was increased against chronic isolates of *P. aeruginosa*[119]. While this study was not performed in biofilms, the fact that pH gradients are known to occur in biofilms, suggests that understanding the interactions between pH and antimicrobial efficacy is important. A study by Wilton *et al* (2016) investigated how biofilm acidification affected aminoglycoside tolerance of *P. aeruginosa*[120]. The authors found that eDNA production acidified spatial microdomains throughout the biofilm. This led to the activation of the PhoPQ and PmrAB systems and activation of genes to incorporate spermidine into the outer membrane. The end result was that eDNA mediated acidification of *P. aeruginosa* biofilms resulted in membrane modifications, reducing susceptibility to aminoglycosides[120].

Contributing to biofilm heterogeneity are antimicrobial tolerant, persister cell sub-populations[121]. Persisters have been identified in a number of species including but not limited to, *E. coli*, *P. aeruginosa*, *A. baumannii and S. aureus* and often occur thanks to a transient, stochastic genetic switch[121–123]. Activation of the persistent phenotype has been associated with the expression of toxin-antitoxin related genes, such as *hipA*, *RelE* and *MazF*, which leads to cellular dormancy and multidrug tolerance in *E. coli*[121,124]. Other mechanisms have also been identified; activation of the stringent response due to nutrient starvation is linked to *P. aeruginosa* persister formation[125], while ATP depletion is associated with the formation of persisters by *S. aureus*[126].

Altered gene expression and the activation of particular stress responses has also been linked to biofilm tolerance. Activation of the stringent response appears to be important for *P. aeruginosa* tolerance to fluoroquinolone antimicrobials as associated double knock out mutants (*ΔrelA ΔspoT*) were more susceptible to antimicrobial treatment than wild type biofilms[125]. A study by Stewart *et al* (2015) provided further evidence for this by demonstrating that transcripts for numerous stress responses were enriched in biofilm cultures of *P. aeruginosa*[127]. Furthermore, the authors found that *P. aeruginosa* strains defective in *rpoS*, *relA* and *spoT* formed biofilms that were more susceptible to ciprofloxacin treatment than the respective wild type[127].

Altered expression profiles of biofilms is also linked to specific biofilm-associated genes. For example, the periplasmic glucan, ndvB, was upregulated 20-fold in biofilms of *P. aeruginosa* compared to planktonic cultures. Knockout of this gene was subsequently linked to increased susceptibility to tobramycin[128]. Efflux pumps are also often upregulated during biofilm formation which can lead to reduced antimicrobial susceptibility[129].

QS systems can also confer biofilm tolerance. Biofilms of *P. aeruginosa* QS mutants, (Δ*rhlI* and Δ*lasI*), exhibit reduced tolerance to tobramycin, hydrogen peroxide and the oxidative burst and phagocytosis of polymorphonuclear leukocytes[130]. Another study of *P. aeruginosa* has shown that the QS signal, HQNQ, can induce cell autolysis and expulsion of DNA into the surrounding EPS, which as discussed earlier, can facilitate antimicrobial tolerance. This was subsequently confirmed by the authors who found that meropenem tolerance was increased in HQNQ-deficient (*ΔpqsA*) mutants[131].

Ultimately, biofilm tolerance is not conferred by one specific mechanism and it is instead the product of numerous factors.

1.4.7 Biofilms as Complex Communities

The majority of biofilm studies focus on single species communities. However, *in vivo*, biofilms can incorporate numerous species and phyla. Oral biofilms are notorious for harbouring sometimes hundreds of different bacterial and fungal species[132]. CF lung infections typically include *P. aeruginosa,* alongside numerous other pathogens including *B. cenocepacia, S. aureus*, *Haemophilus influenzae* and *Stenotrophomonas maltophila*[133] and nasopharyngeal swabs can be associated with colonisation by *S. pneumoniae*, *H. influenzae* and *M. catarrhalis*[134]. Consequently, it is now accepted that understanding these

interspecies interactions is necessary in order to tackle chronic infections[135]. To highlight how these interspecies interactions can alter bacterial phenotypes, examples of *in vitro* research of *P. aeruginosa* and *S. aureus* will be discussed to emphasises the importance of these interactions within biofilm communities. While certain interactions will be unique to these bacterial species, the general themes surrounding them will be applicable to all multispecies communities.

P. aeruginosa and *S. aureus* are most frequently investigated in the context of the CF lung and chronic wounds[136]. In the CF lung, *S. aureus* will dominate early infection before *P. aeruginosa* increases in abundance during late stage infection[137]. For wound infections, the bacteria appear to be spatially separated, with *S. aureus* at the surface, and *P. aeruginosa* deep within the wound[138]. However, in both cases, co-isolation of these species is associated with increased disease severity and reduced recovery suggesting that *in vivo* bacterial interactions increase virulence to the host[139–144]. For example, Seth *et al* (2012) demonstrated that co-infection of a rabbit ear wound model using the two bacterial species was linked to increased expression of host pro-inflammatory cytokines[140,142].

Co-culture of *P. aeruginosa* and *S. aureus* has also been associated with altered antimicrobial susceptibility compared to single species biofilm culture, which has important implications for the treatment of chronic infections. For example, *S. aureus* becomes less susceptible to numerous antimicrobials including vancomycin, tobramycin, and penicillin during co-culture with *P. aeruginosa*[145]. This increase in tolerance was linked to *P. aeruginosa* production of PQS (the QS signal) and numerous siderophore (iron scavenging) molecules[145]. The authors predicted, based on their previous research, that the improved tolerance was associated with a decrease in *S. aureus* growth, linked to a change to fermentative metabolism[146]. Conversely, a study by Radlinski *et al* (2017) suggested that co-culture of certain strains of *S. aureus* with *P. aeruginosa* increased *S. aureus* susceptibility to vancomycin and tobramycin by promoting cell lysis with the LasA endopeptidase and increasing *Staphylococcal* tobramycin uptake via the production of extracellular rhamnolipids[147]. A similar study showed that *P. aeruginosa* became more tolerant to tobramycin treatment when co-cultured with *S. aureus*[148]. This was due to interactions between *P. aeruginosa* produced Psl and *S. aureus* produced staphylococcal protein A, resulting in *P. aeruginosa* aggregation and increased tobramycin tolerance[148].

Aside from changes in antimicrobial susceptibility, interspecies interactions can alter the metabolic properties of the bacterial species, in both beneficial and detrimental ways, depending on the species[135]. Despite their co-isolation from infection sites, numerous *in vitro* studies have shown antagonism between *P. aeruginosa* and *S. aureus*, usually with the latter being outcompeted[149–151]. This has been linked to the production of anti-staphylococcal compounds by *P. aeruginosa,* such as HQNQ, which is regulated by the PQS QS system, pyocyanin and the aforementioned LasA endopeptidase[136].

Iron is known to be an extremely important factor for biofilm growth, particularly within the CF lung[152,153]. *P. aeruginosa* harbours numerous mechanisms for iron acquisition, such as the production of siderophores pyoverdine and pyochelin, *pvdS* and *pchD.* During co-culture, *P. aeruginosa* has been shown to lyse *S. aureus* as a mechanism for iron acquisition. Mashburn *et al* (2005) found that the transcriptional profiles of iron inducible genes in *P. aeruginosa* were the same, whether the bacteria was part of an *in vivo* infection with *S. aureus* or whether it was cultured alone in an iron-rich medium *in vitro*[149]. They showed that a mutant deficient in PQS signalling (*P. aeruginosa* PA14-LM1, harbouring a Tn5 insertion in *pqsA)* was unable to lyse *S. aureus* on an agar plate and by measuring the transcript levels of *pvdS* (induced under perceived low-iron conditions) in both WT PA14 and PA14-LM1 during *in vivo* co-culture with *S. aureus*, found that the *pvdS* transcript was low in the WT and high in the mutant. This implied that as the mutant was not lysing *S. aureus*, environmental iron remained low, leading to increased expression of *pvdS.* The conclusion of the paper was that *P. aeruginosa* could lyse *S. aureus* as a source of exogenous iron[149]. In order to counteract the typically stressful environments, *S. aureus* can switch to fermentative metabolism and form a SCV with a slower rate of growth than wild type colonies[87,136,146]. In these cases, SCV generation is associated with upregulation of the alternative sigma B transcription factor, which is important for promoting the stress response in Gram-positive bacteria[136].

Recent planktonic co-culture experiments have suggested that evolutionary trajectories are also affected by interspecies interactions. Following co-culture with *S. aureus,* numerous populations of *P. aeruginosa* were shown to have acquired mutations (leading to inactivation/reduced function) in lipopolysaccharide biosynthesis genes, specifically *wbpL*[154]. *wbpL* encodes a glycosyltransferase involved in the synthesis of O-specific antigens contained in the outer membrane. Importantly, these mutations were only identified in *P. aeruginosa* populations that were co-evolved with *S. aureus*. Further

investigation revealed that these mutations increased *P. aeruginosa* resistance to β-lactam antimicrobials and also conferred a fitness benefit to *P. aeruginosa* during co-culture with *S. aureus*[154]. This finding, paired with the high level of parallelism suggests strong selection when in the presence of *S. aureus*. While this study was performed for planktonic cultures, there is no reason why the findings (namely the concepts of altered evolutionary trajectories during co-culture), would not be applicable to more complicated, multi-species biofilm communities.

1.5 Antimicrobial Resistance

1.5.1 Human Factors Contributing to the Emergence of Antimicrobial Resistance

Antimicrobial resistance genes have been identified in bacterial populations pre-dating antimicrobial use in a healthcare or industrial environment by many thousands of years[155,156] Antimicrobials are typically produced by bacterial species in order to gain a competitive advantage; as such, AMR mechanisms evolved both to prevent auto-toxicity and to compete with antagonistic microscopic neighbours[155]. However, since the discovery of penicillin, antimicrobial use and the incidence of antimicrobial resistance has risen steadily. This is the result of increased selective pressure on antimicrobial resistant phenotypes. While antimicrobial use is not intrinsically an issue, the catastrophic increase in resistance has arisen due to misuse and overuse of antimicrobials, including over prescription, poor patient compliance and excessive use in both clinical and industrial environments.

A study of prescription practices in the United States revealed that 44% of patients diagnosed with the common cold, (caused by a viral infection), were prescribed antimicrobials, resulting in excessive selective pressure for resistance mechanisms on the bacterial population[157]. A related issue is of patients not following the correct prescription regimen; if a patient does not complete a treatment course, bacteria may survive, develop resistance and cause an infection to reoccur that is even more dificult to treat. Conversely, if a patient continues treatment for longer than necessary, they could be contributing to the development of resistance by increasing the selective pressure on the bacterial population. A randomised clinical trial studying the effect of antimicrobial therapy length for patients suffering with ventilator associated pneumonia showed that upon infection recurrence, resistant bacteria were identified less frequently in the cohort treated for a shorter period of time (8 days opposed to 15 days)[158].

Antimicrobials are also used in agriculture and aquaculture as pest control agents, biocides in cleaning products and for various purposes within research and industry[155]. The interplay between these industries and the routes of AMR dissemination are displayed in Figure 6.

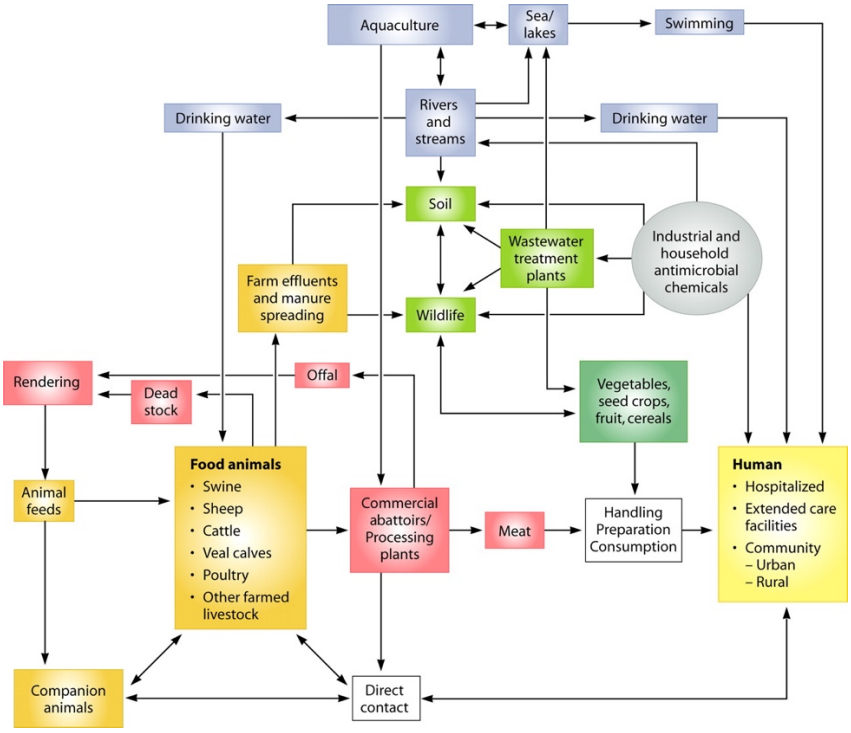

Figure 6: Routes of antimicrobial and antimicrobial resistance dissemination between healthcare, agriculture, aquaculture and industry

Hospitals and other healthcare facilities are not the only environment where bacteria are placed under evolutionary pressure to develop antimicrobial resistance. Factors from agriculture, aquaculture and industry all contribute and the interconnectedness of each environment readily enables the dissemination of genes throughout different bacterial populations. Reprinted with permission from The American Society for Microbiology: Microbiology and Molecular Biology Reviews. Origins and Evolution of Antibiotic Resistance. Davies J., Davies D., Copyright 2010

Perhaps the most infamous example of agricultural misuse is that of avoparcin. Avoparcin was primarily used in Europe for its growth promoting side effects. This led to the inadvertent colonisation of livestock and the surrounding land with vancomycin resistant bacterial species, such as VRE. Colonisation of livestock enables resistant bacterial species to enter the food chain and readily spread throughout both human and other animal populations, which naturally has health risks[159]. In the US, avoparcin was never used as a growth promoter and as such VRE is rarely, if ever, found in livestock[160]. By the late 1990s, an EU wide ban of avoparcin was enforced and additional studies performed after this time have shown that the decrease in antimicrobial use is correlated to a decrease in levels of VRE within livestock[161].

The MCR-1 plasmid which harbours a polymyxin resistance gene was originally isolated from a strain of *E. coli* from a Chinese pig. It is currently believed that MCR-1 evolved due to China's overuse of colistin within the agriculture, aquaculture and veterinary industries[162].

Finally, large scale releases of antimicrobials into the environment are not unheard of. For example, the daily processed sludge disposed of by a sewage treatment plant in Sweden was shown to contain a total of 8 g and 20 g of norfloxacin and ciprofloxacin, respectively[163], and a study of the Almendares River in Cuba, (infamous for its high level of industrial pollution), revealed the presence of 13 different antimicrobial resistance genes (encompassing various classes of tetracycline, erythromycin and β-lactamase genes), in the water[164]. While these studies do not conclusively link the rise of antimicrobial resistance to specific industrial pollution, they do suggest a link between pollution and promotion of AMR evolution.

1.5.2 Mechanisms of Resistance

The increased emergence of AMR further complicates treatment strategies, particularly when considered alongside biofilm tolerance. Heritable resistance has been observed against all current antimicrobial classes in clinical use. While the number of antimicrobials, and the number of antimicrobial classes available is reasonably large, their mechanisms of action are relatively narrow. The majority of currently used antimicrobials inhibit protein synthesis by either binding to the ribosome directly or inhibiting the transcription of mRNA, (such as the aminoglycoside antimicrobials). Other cellular processes that can be targeted include cell wall synthesis, DNA gyrase activity and folic acid synthesis. An in-depth review of each antimicrobial class is out of scope for this thesis. However, for reference, the most common antimicrobial classes are listed in Table 1, alongside example compounds and a brief overview of their mechanisms of action.

Regardless of the mechanism of action of an antimicrobial, mechanisms of resistance can be broadly split into one of three categories: efflux pumps, inactivating enzymes and target alteration mechanisms.

Antimicrobial Class		Examples	Mechanism of Action
Aminoglycosides		Gentamicin, Streptomycin, Tobramycin	Inhibits protein synthesis by binding to the 30S subunit of the ribosome.
Ansamycins		Rifampicin, Rifabutin	Reduces protein synthesis by inhibiting RNA polymerase and preventing transcription of mRNA.
β-lactamase Inhibitors		Clavulanate, Sulbactam	Prevents the action of β-lactamase enzymes which would degrade β-lactam antimicrobials, thereby increasing their efficacy.
β-lactams	***Subclass***		Suicide substrates for a number of penicillin binding proteins, (PBPs), and inhibit cell wall synthesis, resulting in cell lysis.
	Penicillins	Penicillin G, Methicillin, Ampicillin, Amoxicillin	
	Carbapenem	Imipenem, Meropenem, Doripenem	
	Cephalosporin	1st gen: Cephalothin, Cephradrine 2nd gen: Cefamandole, Cefprozil 3rd gen: Cefotaxime, Cefdinir 4th gen: Cefpirome, Cefepime 5th gen: Ceftaroline, Ceftobipirole, Ceftolozane	
Amphenicols		Chloramphenicol	Inhibits protein synthesis by blocking the protein exit channel located on the 50S subunit of ribosome.
Diarylquinolines		Bedaquiline	Inhibits the proton pump of ATP synthase. Specific to *Mycobacterium tuberculosis.*
Dihydrofolate Reductase Inhibitors		Trimethoprim and derivatives	Inhibits folic acid synthesis
Macrolactones		Fidaxomicin	Inhibits RNA polymerase, preventing the formation of mRNA. Selective for *Clostridium difficile.*
Glycopeptides		Vancomycin, Teicoplanin	Inhibits cell wall synthesis by preventing cross linking reactions.
Lincosamides		Lincomycin, Clindamycin	Inhibits peptidyl transferase activity by binding to the 50S ribosomal subunit.
Lipid Binding		Teixobactin	Binds to lipid II and III components, precursors of peptidoglycan and wall teichoic acids, inhibiting cell wall synthesis.
Lipopeptides		Daptomycin	Inserts into the bacterial membrane in a calcium dependent manner, depolarising the bacterial cell.
Macrolides		Erythromycin, Azithromicin. Also includes the ketolide ,Telithromycin.	Inhibits protein synthesis by blocking the protein exit channel located on the 50S subunit of ribosome.
Nitroimidazoles		Metronidazole	Disrupts and damages the bacterial DNA.
Oxazolidinones		Linezolid	Inhibits protein synthesis by blocking the formation of ribosomal initiation complexes.
Phosphonics		Fosfomycin, Fosmidomycin, Alafosfalin	Inhibits synthesis of phospoenolpyruvate, required for peptidoglycan and cell wall synthesis.
Pleuromutilins		Retapamulin	Inhibits protein synthesis by binding to the 50S ribosomal subunit.
Polymyxins		Colistin, Polymyxin B	Disrupts membranes of bacterial membrane by binding to lipopolysaccharide, (LPS)
Quinolones		Ciprofloxacin, Nalidixic Acid	Inhibits action of topoisomerase enzymes such as DNA gyrase.
Streptogramins		Quinupristin, Dalfopristin, Pristinamycin	Inhibits protein synthesis by blocking binding to the ribosome at overlapping regions of the peptidyl site.
Sulphadrugs		Sulphamethoxazole, Sulphanilamide	Inhibits folic acid synthesis
Tetracyclines		Tetracycline, doxycycline, Minocycline	Inhibits protein synthesis by preventing initial binding of tRNA to the ribosome.[100]

Table 1: An overview of current antimicrobial classes

1.5.2.1 Efflux Pumps

Efflux pumps are membrane proteins that actively export foreign compounds from the cell utilising either an ion gradient or the energy produced from the hydrolysis of ATP[165,166]. Compared to other mechanisms of resistance, such as inactivating enzymes or target altering mechanisms, efflux pumps do not tend to confer high level resistance in isolation. By lowering the intracellular antimicrobial concentration, other antimicrobial mechanisms can function in concert[166].

Efflux pumps can be divided into one of five categories based on their constituent components. The five classes are the major facilitator, (MFS), superfamily, the resistance-nodulation-cell division (RND, exclusive to Gram-negative bacteria due to membrane spanning regions), family, the small multidrug resistance, (SMR), family, the ATP binding cassette, (ABC), superfamily and finally the multidrug and toxic compound extrusion, (MATE), family. Of these classes the MFS and ABC family are the most widely represented[165,166]. Example pump systems include NorA pump (MFS class), expressed in *S. aureus*[167], the MexAB-OprM system of *P. aeruginosa*[168], and the AcrAB-TolC system of *Salmonella enterica* serotype Typhimurium[129] (both RND class).

1.5.2.2 Inactivating Enzymes

Inactivating enzymes directly modify an antimicrobial to reduce its activity. Thousands of examples have been identified but they can be divided into two subclasses: enzymes that that are hydrolytically active and cleave structural bonds that are vital for an antimicrobial to function, and those enzymes that transfer chemical groups to an antimicrobial, preventing it from interacting with its target. Examples of the former include β-lactamases, macrolide esterases, (which cleave and inactivate macrolide antimicrobials) and epoxidases, (which cleave and inactivate fosfomycin), while examples of the latter include acyl- and phosphotransferases[169].

The most prevalent hydrolytic enzymes are the β-lactamases, which break down β-lactam antimicrobials, (penicillins, cephalosporins, monobactams and carbapenems), via cleavage of a vital covalent bond found within a 4 membered lactam ring. This ring mimics a D-alanyl-D-alanine motif, which is the substrate of bacterial Penicillin Binding Proteins, (PBPs), (see Figure 7). By binding to PBPs, cell wall synthesis is ultimately interrupted[170,171]. β-lactamases are categorised as either serine or metallo-β-lactamases,

(MβL) based on whether their active site contains a serine or a bivalent metal ion (usually Zn^{2+})[171].

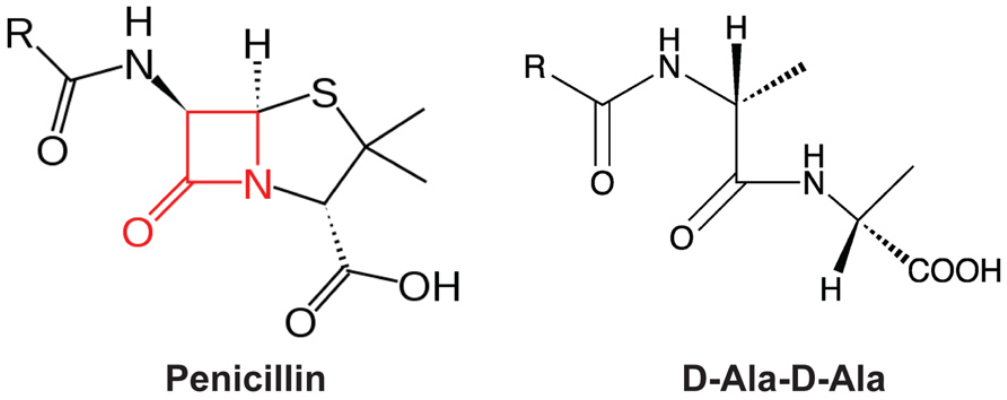

Figure 7: Structural comparison of penicillin and D-alanyl-D-alanine

The 4-member lactam ring, highlighted in red, along with the general structure of the penicillin molecule, shows marked mimicry to the PBP substrate, D-ala-D-ala. This enables the molecule to antagonise the action of PBPs and inhibit cell wall synthesis. Figure taken from Zeng and Lin (2013).

An alternative method of enzymatic mediated resistance is that of chemical group transfer. Here, specific transferase enzymes attach different biochemical groupings to the antimicrobial compound leading to its inactivation. These transferase enzymes comprise the largest and most diverse subset of enzyme controlled resistance and utilise strategies such as acylation, phosphorylation, thiol transfer, nucleotidylation, (transfer of nucleotide monophosphates), ribosylation (transfer of an ADP-ribose moiety) and glycosylation[169]. Examples include the specific acyltransferases *aacA29a* and *aacA29b*, isolated from MDR isolates of *P. aeruginosa,* (conferring aminoglycoside resistance)[172]; aminoglycoside and macrolide phosphotransferases, identified in *E. coli*, *S. aureus, S. epidermidis, K. pneumoniae* and *P. aeruginosa*[173–175]; and the specific thioltransferases enzyme FosB associated with fosfomycin resistance in *B. subtilis*[176].

1.5.2.3 Target Alteration

The final mechanism of antimicrobial resistance involves alterations to an antimicrobial's target, reducing its binding affinity. This culminates in reduced antimicrobial efficacy. Alterations associated with antimicrobial resistance have been observed in a large number of antimicrobial targets including, but not restricted to, PBPs, cell wall peptidoglycans, the ribosome, elongation factors and topoisomerases, to name a small selection[177]. Probably

the two best understood instances of resistance as a result of target alteration are those for β-lactams and the glycopeptide antimicrobial, vancomycin.

β-lactam resistance has been linked to alterations in the PBPs of many bacteria including *S. pneumoniae, S. aureus (*MRSA*), N. gonorrhoeae, A. baumannii, P. aeruginosa,* and *E. faecium*[178–183]. MRSA is without doubt, the most infamous example. MRSA expresses an altered, acylated PBP, (PBP2a), encoded by the *mecA* gene. This modification means that PBP2a binds to β-lactam compounds at a rate that is 3-4 fold lower than the wild type. PBP2a also has a higher dissociation constant regarding β-lactam antimicrobials. Together, these factors reduce the greatly increase the resistance of *S. aureus* to β-lactam therapies[184].

Vancomycin resistance can occur via modification of peptidoglycan structure. In VRSA, resistance can occur due to "affinity trapping". Here, synthesis of N-acetylglucosamine is increased, which increases cell wall thickness. This prevents vancomycin binding to the D-ala-D-ala motif, necessary for its crosslinking mechanism of action[185]. In VRE, different peptidoglycan biosynthesis enzymes are expressed, leading to reduced vancomycin binding. For example, expression of the VanA gene cluster results in peptidoglycan containing a D-ala-D-lac motif instead of the D-ala-D-ala motif[24]. This mechanism can also occur in VRSA.

1.6 Evolution and Acquisition of Antimicrobial Resistance

1.6.1 Sources of Antimicrobial Resistance

Antimicrobial resistance can be intrinsic, acquired or adaptive[186]. Intrinsic resistance relates to those mechanisms that are fundamental to the physiology of the organism. In general, Gram-negative species are more resistant than Gram-positive species due to the presence of an additional outer membrane, which impedes antimicrobial entry into the cell. Additionally, some species such as *A. baumannii* and *P. aeruginosa,* supplement their intrinsic Gram-negative defences with more specific mechanisms such as the constitutive expression of β-lactamases such as AmpC, TEM, SHV and VIM, aminoglycoside modifying enzymes and efflux pumps[187].

Acquired resistance refers to traits acquired when bacteria that are susceptible to antimicrobial treatment, acquire and accumulate novel resistance via a genetically mediated mechanism e.g. genetic recombination utilising plasmids, transposons, integrons or raw DNA, or simply thanks to the product of cumulative mutations. Finally, adaptive resistance refers to mechanisms that are enhanced or activated by altering gene expression in response to environmental fluctuations, (usually environmental stresses, such as the presence of sub-inhibitory concentrations of antimicrobials).

1.6.2 Mechanisms of Resistance Acquisition

AMR mechanisms can be acquired via genetic mutation or via the integration of exogenous genetic elements. The acquisition of resistance is known to be promoted by antimicrobial use, both at concentrations below the MIC and above the MIC. The former is more likely to select for a wider selection of resistance mutations (a larger mutational space) that confer smaller reductions in antimicrobial susceptibility while the latter will select for rarer pre-existing high level resistant mutants, (as the majority of the population will be killed)[188–190]. Like all evolutionary phenomena, resistance mechanisms are at the mercy of natural selection because they typically incur a fitness cost to the cell. In environments containing antimicrobial, the resistance mechanism will grant greater fitness than the wild type. Due to the increased use of antimicrobials, it is beneficial for bacteria to develop resistance mechanisms to maintain fitness. However, in the absence of selection, the resistance mechanisms will lower fitness, which may result in the eradication of the resistant phenotype[191,192]. Consequently, resistant mutations can often occur in a stepwise

manner, with incremental increases in resistance associated with smaller (usually beneficial) changes in bacterial fitness.

A publication by Baym *et al* (2016) successfully demonstrates the concept of stepwise evolution on the pathway to high resistance mutants[193]. The authors created a device called the microbial evolution and growth arena, (MEGA) plate, which consisted of a large agar substrate, loaded with increasing concentrations of either trimethoprim or ciprofloxacin. By using a strain of *E. coli* sensitive to the two antimicrobials, the authors showed that it would acquire resistance in a cumulative fashion, travelling across the agar from areas of low antimicrobial to areas with high antimicrobial concentrations. Crucially, they showed that resistance to higher concentrations could only be obtained if resistance to the preceding intermediate concentrations evolved; if the intermediate concentration was too high, the lineage would cease to advance further[193]. This is presented in Figure 8.

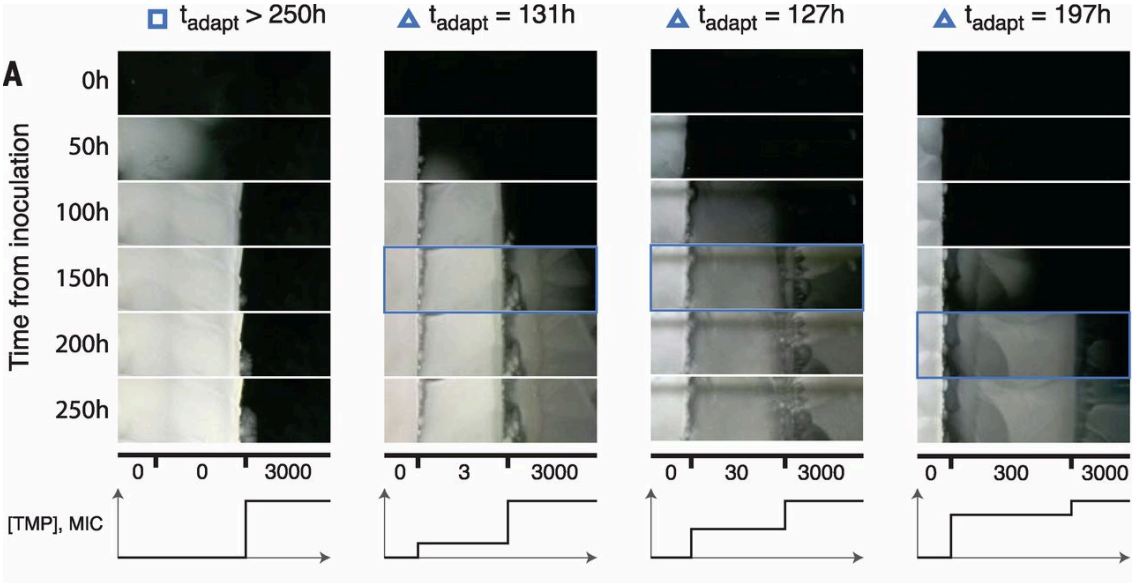

Figure 8: The MEGA plate experiment

(L-R) Layout of antimicrobial gradients between 0 and 3000 x the MIC of trimethoprim for *E. coli*. Resistance to the highest concentration of trimethoprim was only obtained after resistance had evolved to lower concentrations thus highlighting the stepwise evolutionary processes which can occur during the emergence of AMR. A one-step mutation resulting in high level resistance may be possible, but the associated fitness cost could be too high. In all cases, resistance mechanisms can be outcompeted due to natural selection. Reprinted with permission from The American Association for the Advancement of Science (AAAS):Science. Spatiotemporal microbial evolution on antibiotic landscapes. Baym M., Lieberman TD., Kelsic ED., Chait R., Gross R., Yelin I., Kishony R. Copyright 2016.

It should be obvious that the MEGA plate experiment is not representative of *in vivo* situations. However, the findings associated with stepwise evolution in the context of AMR have been documented on numerous occasions, such as in the case of fluoroquinolone resistance. Fluoroquinolones exert bactericidal activity by targeting DNA topoisomerases II and IV, (specifically the complex between the DNA and the protein), preventing the enzymes from relieving the stress associated with supercoiled DNA. The enzymes are modular; topoisomerase II, also called DNA gyrase, consists of two A and two B units, encoded by *gyrA* and *gyrB,* while topoisomerase IV, (which is homologous to DNA gyrase), consists of two C and two E units, encoded by *parC* and *parE*[194,195]. Fluoroquinolone resistance occurs due to the accumulation of stepwise amino acid substitutions in these subunits as a result of DNA point mutations. While mutations in any of these genes will contribute some degree of resistance, it has been shown that mutations in *gyrA* typically occur first (S83L, serine to leucine change at position 83), prior to the occurrence of any mutations in *parC* (S80I is overrepresented in clinical isolates). Additional mutations in *gyrA, parC* and genes associated with efflux (*acrR, marR* and *soxR*) can supplement resistance further[196]. In this example, the order of mutations was strongly associated with improvements to bacterial fitness in environments containing ciprofloxacin[196].

However, it is important to note that even though stepwise accumulation of mutational resistance is more likely to occur, (due to more frequent but lower impact fitness costs), high level resistance resulting from single genomic changes can still occur all at once. For example, single point mutations in *rpoB* can confer high level resistance to rifampicin. Sensitive strains of *Mycobacterium tuberculosis* can be inhibited at rifampicin concentrations less than 0.39 μg ml^{-1}. However, a single point mutation (TCG → TTG, S531L) has been linked to approximately a 500-fold increase in MIC (> 200 μg ml^{-1})[197].

Resistance traits can also be obtained from external sources via mechanisms such as transformation, transduction and conjugation. Transformation involves the incorporation of exogenous free DNA into the cellular genome and has been implicated in the emergence of β-lactam resistance in *S. pneumoniae*, via incorporation of alternative PBPs derived from *Streptococcus mitis*[198]. Transduction refers to the transfer of genetic elements from a bacteriophage. While theoretically possible, (numerous studies have demonstrated successful use of phage to transfer resistance elements to bacteria), the contribution of this form of HGT to the emergence of AMR is poorly understood[199]. Finally, conjugation

describes the transfer of plasmid-borne AMR elements between cells in direct contact with each other, irrespective of the phylogenetic kingdom[192]. A recent example of plasmid mediated resistance transfer involves the dissemination of MCR-1 polymyxin resistance among *Enterobacteriaceae*, including *E. coli* and *K. pneumoniae*[162].

1.6.3 Role of Stress Responses in the Emergence of Resistance

The mechanisms associated with promoting the evolution of resistance, such as increased mutagenesis and increased HGT have been attributed to activation of numerous bacterial stress responses, typically in response to antimicrobial treatment[188]. These systems include the SOS response, (activated in response to DNA damage), RpoS mediated stress response, (the global stress response) and the stringent response, (in response to nutrient starvation)[27-29].

The SOS response is a largely conserved bacterial stress response, regulated by the LexA repressor. Following DNA damage, RecA relieves LexA repression allowing for expression of genes associated with the SOS regulon including *recA* (to mediate recombination), *uvrABC* (for nucleotide excision repair) and various error-prone polymerase components, such as *dinAB* and *umuDC* (which act to rapidly repair DNA, sacrificing accuracy)[188]. Sub-inhibitory ciprofloxacin and tetracycline treatment of *A. baumannii* results in activation of its atypical SOS response, mediated by the UmuDAb regulon, leading to the expression of error prone polymerases and the introduction of point mutations across the genome[200]. SOS activation has also been associated with the dissemination of mobile elements that can harbour resistance genes between bacterial cells. For example, treatment of *E. coli* with mitomycin C or ciprofloxacin has been shown to liberate the SXT conjugative element, (responsible for sulfamethoxazole, trimethoprim and streptomycin resistance) and promote its transfer to *Vibrio cholerae*[201]. However, the SOS response does not appear to be universally responsible for adaptation. A conflicting study of *P. aeruginosa* by Torres-Barceló *et al* (2015) showed that while the SOS response increased bacterial fitness during growth in sub-inhibitory ciprofloxacin, it was not required for the evolution of resistance (as shown by the evolution of similar ciprofloxacin resistance in wild type and Δ*lexA* mutants)[202]. The authors predicted that SOS activation increased the competitive fitness of ciprofloxacin sensitive cells; as such the increase in fitness obtained by the resistant cells as a result of beneficial mutations is lessened. As the difference in fitness is lowered (selection for resistance is decreased), rate of adaptation is not increased[202].

RpoS is a stress induced sigma factor that can directly alter the expression profiles of bacterial cells. Antimicrobial treatment of *P. aeruginosa, E. coli* and *V. cholerae* has been shown to induce activation of the RpoS regulon, leading to a downregulation in DNA mismatch repair systems (e.g. *mutS*) and increased expression of error prone polymerase components (e.g. *dinB*). This culminates as increased mutagenesis which is associated with the emergence of novel genotypes. If fitness in the presence of an antimicrobial is increased compared to wild type cells, this could lead to fixation of *de novo* AMR mechanisms[203].

The bacterial stringent response is a conserved stress mechanism that is induced in response to nutrient deprivation and regulated via the synthesis of ppGpp and pppGpp alarmone second messengers[204]. The stringent response appears to strictly be associated with adaptive resistance mechanisms: AMR mechanisms associated with changes in gene expression. For example, activation of the stringent response in MRSA leads increased expression of *mecA,* resulting in high levels of resistance[205,206]. Populations of MRSA deficient in the stringent response are unable to achieve high levels of homogenous resistance, thereby emphasising its importance[206].

1.7 Connecting Tolerance and Resistance

While tolerance and resistance are distinct phenomena, there are links between the two. Recently, Levin-Reisman *et al* (2017) showed that tolerance was a requirement for the evolution of resistance in experimentally evolved populations of *E. coli*[207]. In this study, the authors evolved batch bacterial cultures in the presence of intermittent doses of ampicillin. By analysing isolates over the time course of the experiment, they found that bacterial lineages developed an increase lag phase (a form of tolerance to ampicillin, linked to mutations in known tolerance genes) prior to the development of resistance (linked to mutations in the *ampC* promoter region). The authors predicted that tolerance occurred first due to a higher rate of mutations (as tolerance can be caused by mutations in multiple genetic targets, the likelihood of it emerging as a phenotype is higher). The acquisition of tolerance improved bacterial fitness in the presence of ampicillin, extending the window for selection of mutations that could confer resistance[207]. The idea that tolerance facilitates the emergence of resistance is a worrying prospect and the theory is readily transferable to biofilm populations. This section will attempt to briefly summarise how certain aspects of biofilm mediated tolerance could result in the evolution of AMR.

Due to the overall heterogeneity of a biofilm, there is a possibility that following antimicrobial treatment, gradients of different antimicrobial concentrations will be set up throughout the population[208]. For some antimicrobials, this could be caused by limited diffusion through the EPS[111,112]. For others, diffusion may be unchanged but instead antimicrobials will be sequestered by extracellular components, (such as vancomycin and eDNA in biofilms of *S. epidermidis*, tobramycin and alginate and negatively charged phage components in biofilms of *P. aeruginosa*)[62,113,115] which may create foci of higher antimicrobial concentrations. The chemical heterogeneity of biofilms, such as decreased pH[119], may inactivate antimicrobials so that their effective concentration is lower and below the MIC in certain regions of the biofilm. As shown in the MEGA plate experiment[193], gradients of antimicrobial concentrations can facilitate the evolution of high level resistance and this concept could be applied to biofilms (Figure 9). Importantly, numerous stages of intermediate level resistance can also arise, increasing diversity. The graded concentrations of antimicrobial provides a large number of potential niches to adapt to via the accumulation of numerous small benefit, stepwise resistance mutations.

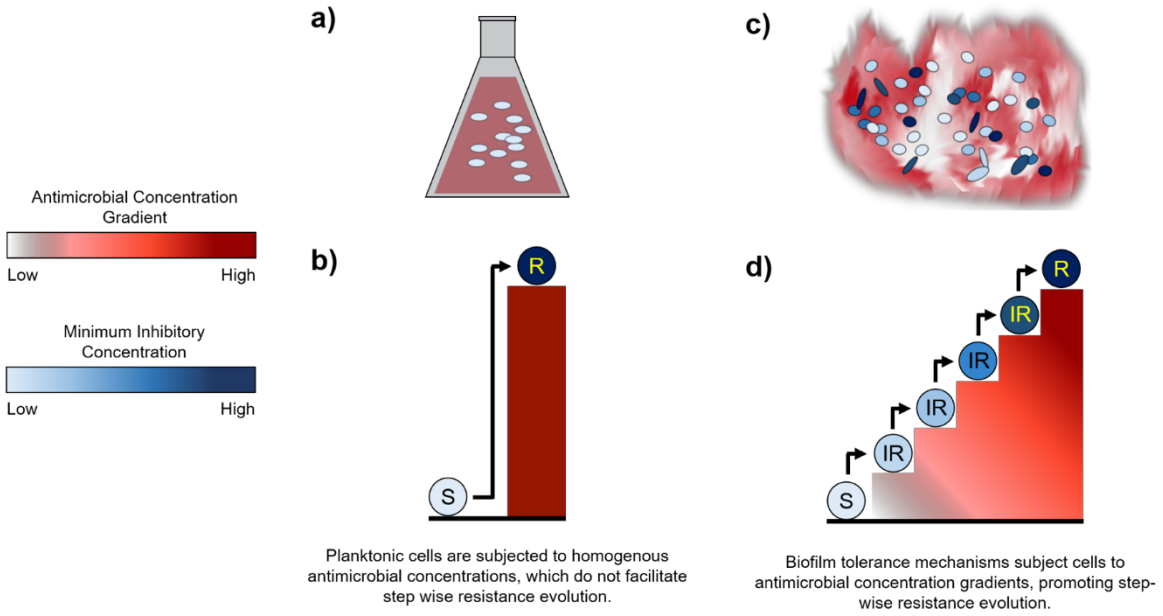

Figure 9: Antimicrobial concentration gradients can facilitate the emergence of resistance

Changes in antimicrobial concentration are depicted by shades of red and changes in bacterial resistance, quoted via alterations in the minimum inhibitory concentration, (MIC, the concentration required to inhibit bacterial growth), is depicted via shades of blue. Low concentrations are represented by lighter shades and higher concentrations by darker shades. Sensitive cells (S, light blue circle), Intermediate resistance (IR, graded blue circles), High level resistance (R, dark blue circle)

a) When a planktonic cell culture is treated with an antimicrobial, the cells are subjected to a homogenous concentration. b) When antimicrobial concentrations are homogenous, resistance acquisition is less likely. When the antimicrobial concentration is homogenous, it can kill every cell, selecting for rare pre-existing mutations. If multiple point mutations are required to fix for resistance to be obtained, this is unlikely. c) Biofilms can establish antimicrobial gradients throughout the structure. This leads to a cell population exhibiting a heterogenous resistant profile, with multiple bacterial lineages adapted to different concentrations of antimicrobials, (depicted by various shaded blue circles). d) The presence of antimicrobial concentration gradients allows resistance to be acquired in a stepwise fashion whereby the bacteria progressively adapt to the increasing concentrations of antibiotics, indicated by a gradual increase in their MIC. Combined with other biofilm characteristics (increased stress responses, predicted increases in mutation rate and HGT), novel AMR mechanisms can readily proliferate throughout a biofilm in ways that are not possible within a planktonic culture. Figure own work.

Furthermore, biofilms will frequently harbour non-dividing cells which are tolerant and survive in the presence of antimicrobials. This type of tolerance is similar to that observed by Levin-Reisman *et al* (2017), which was a pre-requisite for the evolution of resistance.[207] Similar dynamics could be implicated within biofilms, although it would be interesting to understand whether other mechanisms of tolerance and persistence, such as those mediated by the *hipA* toxin, are required in a similar manner prior to the emergence of resistance.

The predicted increased rate of mutation within biofilm populations could also increase the emergence of AMR. In isolation, increased rates of mutation do not necessarily mean that resistance will emerge as natural selection is still required for mutations to fix within the population. This is especially true if the mutational target (area of the genome where mutations could confer resistance to a particular compound) is small[101]. However, when combined with the heterogeneity of biofilms (particularly the numerous ecological and phenotypic niches), an increased rate of mutation may allow bacteria to "sample" pools of mutations more quickly. Resistant phenotypes will still only fix in the population if their fitness gains outweigh the fitness costs but an increased mutation rate may allow strains to converge onto these beneficial outcomes quicker and more effectively.

A large number of AMR mechanisms are harboured on mobile genetic elements, such as the *sccMec* cassette (encoding mecA, responsible for β-lactam resistance in *S. aureus*) and resistance encoding plasmids, such as MCR-1 responsible for polymyxin resistance in *Enterobacteriaceae*. As previously discussed, in certain instances HGT can be improved in biofilm populations. If this is the case, a bacterial species harbouring a resistance encoding plasmid could disseminate this to other sensitive species in the population, particularly if it would increase bacterial fitness (e.g. by containing a resistance gene against an antimicrobial being used toward the biofilm). Plasmid associated resistance mechanisms are often associated with a fitness cost. A study by Frost *et al* (2018) studied *P. aeruginosa* colony biofilms formed by an antimicrobial sensitive strain, and a strain resistant to both streptomycin and carbenicillin due to the presence of a resistance plasmid[209]. Despite the fitness cost linked to resistance, they found that the resistant strain was fitter than the sensitive strain in biofilms with a more defined spatial structure (lower cell density, no antimicrobial selection). When the colony was well mixed or the cell density was increased (increasing the numbers of fitter, sensitive cells), the resistant strain would decrease in fitness[209]. Crucially, this study shows that biofilm spatial structure (specifically social

interactions) can in certain situations increase the fitness of resistant strains and may be pivotal in promoting their survival.

The tolerance mechanisms of biofilms improve the chances of survival in the presence of antimicrobials. At its simplest, this improved survival would already be enough to increase the emergence of AMR: if bacteria are killed, they are unable to evolve. However, when paired with the vast amounts of heterogeneity, including the many clonal lineages within a biofilm, the generation of resistant genotypes, especially in response to antimicrobial treatment, is inevitable. Fitness landscapes can be used to describe how diversity within a biofilm may lead to the emergence of AMR. A fitness landscape summarises potential evolutionary routes that can be taken and displays them in terms of relative fitness to each other (Figure 10). Consider multiple lineages evolving resistance towards an antimicrobial. Due to the heterogeneity across a biofilm e.g. spatial partitioning, chemical heterogeneity, access to metabolites, etc, there are numerous fitness optima that could be acquired, depending on the actual environmental niche that a lineage occupies. For example, mutations that supply AMR but reduce a strains ability to survive in an acidic environment could decrease fitness if it occupied a low pH micro-environment. If this cost was higher than the fitness gain attributed to AMR, this lineage would be outcompeted.

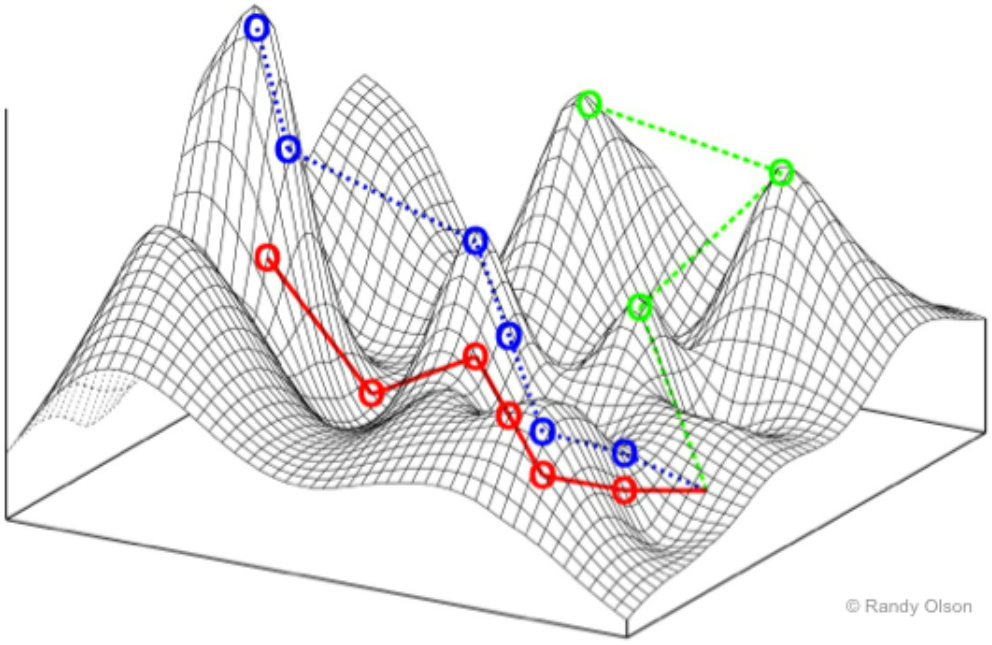

Figure 10: Theoretical fitness landscapes

The evolution of AMR among biofilms can be described in the context of a fitness landscape. Fitness is proportional to the height of the peaks and the different coloured lines represent the evolutionary pathways of different lineages. Via the accumulation of mutations and/or exogenous genetic elements such as plasmid, bacterial fitness can increase and decrease accordingly. In the context of biofilms, the heterogeneity of the population means that there is both a high number of independently evolving lineages as well as a high number of potential fitness peaks that can be evolved towards. As the micro-environment is diverse, this could allow for the evolution of diverse phenotypes may include novel AMR mechanisms. When a biofilm disperses, these novel genotypes, (of varying fitness) will be disseminated into a new environment, which can then diversify even further.

Theoretically, each sub-population within a biofilm could be evolving to completely different and unique fitness optima, generating high levels of within populaton diversity. Importantly, fitness landscapes are dynamic and as populations (and the surrounding environment) change and evolve, so will the fitness landscape. For example, one lineage may evolve to a fitness optima, X. However, a separate lineage may evolve and identify a new peak with improved fitness, Y. Those populations that have evolved to Y could be antagonistic to the X population. As such, evolving towards the X fitness peak may no longer confer fitness benefits, which in itself would also affect other possible peaks. Alternatively, the competition could select for mutations in the X population that increase fitness even further.

The concept of competition facilitating the evolution of AMR has been directly observed in *S. aureus* colony biofilms *in vitro*[210]. In this study, colony biofilms of *S. aureus* SC01 were grown for 5 days. Over the course of the experiment, the authors observed that

morphologically distinct sectors would form over time: initially the biofilm consisted of orange coloured variants, but following 48 hours of growth, white variants would emerge. Following 72 hours of growth yellow variants would subsequently appear. As the yellow variant emerged after the white variant, the authors hypothesised that the presence of the white variant was required for the selection of the yellow variant. Transcriptome analysis of the variants revealed that the white variant highly expressed a bacteriocin compound, Bsa. This compound could inhibit growth of the orange variant, but not the yellow, thereby suggesting that the competition levied by the white strain (resulting from Bsa bacteriocin production) facilitated the emergence of the yellow variant. Crucially, the yellow variant had evolved greater fitness in the presence of the Bsa bacteriocin, compared to the original orange variants. Further analysis of the yellow variant showed that it had also evolved intermediate resistance to vancomycin[210]. To summarise, this example illustrates how separate lineages can evolve within a biofilm and importantly, that bacterial competition can promote the emergence of variants with increased AMR.

The prospect of considering all possible adaptive routes is daunting, if not impossible. However, the take home message is that the structural and physiological nature of biofilms, plus factors which contribute to tolerance, thus generating antimicrobial gradients and other selective environments, make them a melting pot of diversity. When applied to AMR this means that there are many routes for adaptation that could be occurring simultaneosusly, enhanced by factors such as increased HGT or increased rates of mutation. The high levels of bacterial competition mean that natural selection is rife but ensures that only the highest fitness variants survive. It is plausible that this diversity can manifest as AMR mechanisms, especially when there is selection for those phenotypes (i.e. antimicrobial treatment). Once a biofilm disperses, novel genotypes, which may encompass AMR mechanisms, are disseminated into the environment. Only one lineage needs to survive to be able to repopulate another biofilm which could exacerbate chronic infections and may make treatment impossible, especially if further diversification and selection for resistance occurs.

1.8 Tackling Antimicrobial Resistance and Biofilms

This literature review has shown that both biofilm mediated tolerance and AMR can negatively impact the efficacy of antimicrobial treatment and that there is a need for novel therapeutic strategies. As there appears to be evidence linking tolerance to the development of resistance, there is a dire need for both novel antimicrobials and an improved understanding of how biofilms can contribute to the emergence of novel genotypes. Unfortunately, antimicrobial development by multi-national pharmaceutical companies has been somewhat limited; due to the rapid evolution of resistance, antimicrobial creation is currently not profitable in the long term.

However, strategies to combat bacterial infections are still being researched[10]. The ultimate goal would be the development of a compound that resistance cannot evolve to and is also effective at circumventing biofilm tolerance mechanisms. The antimicrobial, teixobactin, is an example of a compound that appears to be highly effective against Gram-positive bacterial species without any obtainable resistance[5]. Teixobactin functions by binding to lipid moieties of cell wall precursor components, thereby preventing cell wall biosynthesis. As the compound targets lipid components, the risk of mutation is lower[5]. However, that is not to say that resistance cannot evolve. Daptomycin also binds to the cell membrane lipids components and resistance soon developed once it was used within a clinical setting[211]. Importantly, and as is the case with many newer compounds, activity against Gram-negative bacteria is limited.

As for targeting biofilms, therapies that reduce attachment, disrupt maturation or induce dispersal are all in development. For example, a peptide, designated peptide 1018, has been shown to prevent biofilm formation and eradicate pre-existing biofilms formed by all members of the ESKAPE cohort by interfering with signals involved in biofilm formation. This occurs at concentrations below those required to have an effect on planktonic growth[212]. Agents that cause biofilm dispersal may be useful as they can cause a loss biofilm mediated tolerance. Low dose nitric oxide has been successfully used as an adjunctive therapy in chronic *P. aeruginosa* infection[213], while molecules that break down the EPS have also shown effectiveness[214]. An alternative approach to tackling biofilms is to prophylactically treat surfaces to reduce bacterial attachment. This can be achieved by adjusting the physicochemical properties (altered surface charge, roughness, hydrophobicity etc), or by coating the surface with bactericidal or bacteriostatic substance, (such as zinc, silver, copper, polymers or antimicrobials). However, antimicrobial coatings

may not be suitable for long term use as they could facilitate the emergence of additional resistance mechanisms[10].

1.9 Project Aims

Due to their increased tolerance, strategies to target non-dividing bacteria are also being investigated[11]. Helperby Therapeutics specialise in the development of antimicrobials that are effective against non-dividing cells. Their lead compound, a quinoline derivative called HT61, has shown to be highly effective against non-dividing cultures of *S. aureus.* Due to the presence of non-dividing cell populations within biofilms, compounds such as HT61 could prove to be a promising avenue of investigation.

Understanding the effect of antimicrobials on bacterial populations is crucial, especially when effective strategies are becoming more limited as a result of AMR. As such, the aim of this thesis was to investigate the action of HT61 on biofilms of clinically relevant pathogens.

By using standard phenotypic assays (Chapter 2) coupled with quantitative proteomics (Chapter 3), the first aim was to understand its mechanism of action and its level of effectiveness. Gaining insight into the mechanism of action of HT61 could inform the development of future antimicrobials.

Secondly, as tolerance is known to be important for the acquisition of AMR and interspecies interactions are important factors of biofilm physiology, it was important to understand how bacterial species would adapt to HT61. To achieve this, a co-culture biofilm model of *P. aeruginosa* and *S. aureus* was developed (Chapter 4) to investigate how interspecies interactions affected species evolvability. Whole genome sequencing was then used to analyse colonies derived from this model in order to understand how both interspecies interactions and HT61 treatment affected bacterial evolution (Chapter 5). Understanding evolution within the biofilms may grant insight into genomic regions that are under selection, and thus may be important targets for future therapies. Furthermore, by understanding the adaptive response to HT61, it may be possible to circumvent the acquisition of resistance and/or identify putative resistance elements to be aware of during the development of novel strategies in the future.

Chapter 2

Phenotypic Characterisation of Bacterial Biofilms Following Treatment with HT61

2 Phenotypic Characterisation of Bacterial Biofilms Following Treatment with HT61

2.1 Introduction

The majority of resistant, nosocomial infections are caused by a small cohort of bacterial species known as the ESKAPE pathogens, encompassing ***E****nterococcus faecium,* ***S****taphylococcus aureus,* ***K****lebsiella pneumoniae,* ***A****cinetobacter baumannii,* ***P****seudomonas aeruginosa* and ***E****nterobacter* species, respectively[20].

A further factor complicating treatment strategies is that bacteria readily form biofilms; surface attached multicellular communities that exhibit a phenotypic tolerance to antimicrobials and external stresses[108]. Unlike resistance mechanisms, which encompasses active efflux pumps, antibiotic degrading enzymes and antibiotic target alterations[186], biofilm associated tolerance mechanisms are linked to the unique environment granted to bacterial cells via biofilm formation. These mechanisms can include reduced antimicrobial penetration through the external matrix, heterogeneous microenvironments that affect the efficacy of antimicrobials and a high degree physiological heterogeneity[7]. Biofilms can also contain subpopulations of cells called persisters, which are no longer dividing and have become metabolically dormant[7]. These cells are particularly difficult to eradicate as the majority of conventional antimicrobials currently in use are only effective at killing rapidly dividing cells[117].

Consequently, there is a need for novel antimicrobial compounds that can successfully eradicate tolerant biofilm populations[10]. HT61 is a novel quinoline derivative that has demonstrated heightened efficacy towards stationary phase, non-dividing cultures of *S. aureus*[11] and has proven effective as a topical agent in an *in vivo* mouse model, both alone and in combination with other antimicrobials[11,12]. HT61 seems to exert its mechanism of action by disrupting the bacterial membrane and binding to negatively charged phospholipids[11,13]. However, despite the presence of a non-dividing cellular population, HT61 has not been tested on bacterial biofilms.

This chapter aimed to characterise the effect of HT61 on exponential phase and stationary phase planktonic cultures, as well as biofilm cultures of clinically relevant bacterial pathogens. Using *S. aureus* and *P. aeruginosa* as model Gram-positive and Gram-negative

organisms, the effect of HT61 on biofilm development and biofilm morphology was assessed using a combination of standard microbiological techniques, confocal laser scanning microscopy and scanning electron microscopy.

2.2 Materials and Methods

2.2.1 Bacterial Strains and Growth Media

Bacterial strains utilised in this chapter are presented in Table 2. All strains of *P. aeruginosa* were cultured in Luria-Bertani broth, (LB) (Formedium), while cultures of all other species were performed in tryptic soy broth, (TSB) (Oxoid). When plated onto solid media, *P. aeruginosa* was grown onto cetrimide agar (Formedium and Oxoid), supplemented with 1% glycerol (Sigma-Aldrich) while all other species were grown on tryptic soy agar, (TSA) (Oxoid). Biofilms of *P. aeruginosa* were grown in 1 X M9 Minimal Salts, (Formedium) supplemented with 20% glucose, (Sigma-Aldrich), 1M $CaCl_2$ (Sigma-Aldrich) and 1M $MgSO_4$ (Sigma-Aldrich, UK), (hereby referred to as M9 medium), while biofilms of all other species were grown in TSB.

Table 2: Bacterial strains utilised in Chapter 2.

Bacterial Species	Bacterial Strain	Comments	Source
Staphylococcus aureus	UAMS-1	Methicillin sensitive clinical isolate, originally isolated from a patient with osteomyelitis[215]. Proficient biofilm former.	LGC Standards
Klebsiella pneumoniae	ATCC 700831	Environmental isolate, utilised in previous biofilm studies	ATCC
Acinetobacter baumannii	ATCC 19606	Urine clinical isolate	ATCC
Pseudomonas aeruginosa	PAO1	Typical laboratory strain. Originally a wound isolate.	University of Washington.
	PA21	Non-mucoid, cystic fibrosis clinical isolate	Southampton General Hospital
Staphylococcus epidermidis	ATCC 35984	Catheter clinical isolate. Proficient biofilm former	ATCC

2.2.2 Growth Characteristics

To establish the growth kinetics of the different bacterial strains and species, 1 ml of overnight culture was diluted into 50 ml of appropriate fresh media. 200 µl of the inoculum was aliquoted into triplicate wells in a 96 well plate and the optical density at 680 nm (OD_{680}) was measured every 15 minutes for 18 hours with a microplate reader (BMG Omega). Additionally, 100 µl of the bacterial inoculum was serially diluted in Hanks Balanced Salt Solution (HBSS) (Sigma-Aldrich, UK) and plated onto appropriate agar plates every 2 hours, for 12 hours. The plates were incubated overnight at 37 °C and the number of CFUs were then counted. The number of CFUs was then corroborated with the OD_{680} values at each chosen time point.

2.2.3 Antimicrobial Susceptibility Testing

The effect of HT61 and other antimicrobials typically used in a clinical setting against each bacterial species was investigated. Susceptibility was determined against both planktonic cultures (log phase and stationary phase) and biofilm cultures. The antibiotics tested, and the bacterial species that they were utilised against are listed in Table 3.

It is critical to note that HT61 was poorly soluble in growth medium at concentrations higher than 64 µg ml^{-1}. As such, whenever the concentration of HT61 is quoted as 128 µg ml^{-1} or higher, the actual concentration (the concentration fully dissolved), will be lower because the majority of HT61 will have precipitated out of solution. Any effects observed at these higher concentrations could be attributed to physical interactions between the bacteria and the physical precipitate, alongside the antimicrobial mechanism of action.

Table 3: Antibiotic compounds utilised in Chapter 2.

Antibiotic Compound	**Antibiotic Class**	**Bacterial Species Treated**	**Source**
Ciprofloxacin	Fluoroquinolone	*K. pneumoniae*	Sigma-Aldrich
HT61	Novel quinoline derivative	*S. aureus,* *K. pneumoniae,* *A. baumannii,* *P. aeruginosa,* *S. epidermidis*	Helperby Therapeutics
Meropenem	Carbapenem	*A. baumannii*	Sigma-Aldrich
Tobramycin (tobramycin sulphate)	Aminoglycoside	*P. aeruginosa*	Sigma-Aldrich
Vancomycin (vancomycin hydrochloride)	Glycopeptide	*S. aureus,* *S. epidermidis*	Hospira Inc.

2.2.3.1 Determination of Minimum Inhibitory and Bactericidal Concentrations

The minimum inhibitory concentration, (MIC, the concentration of an antibiotic compound required to inhibit planktonic growth) was determined using the broth macro-dilution method. Briefly, overnight cultures of each bacterial species were diluted to 10^6 cells in appropriate liquid media and treated with a two-fold dilution series of each antibiotic, between 0.5 μg ml^{-1} and 1024 μg ml^{-1}, to a final volume of 10 ml. Following incubation for 24 hours at 37 °C, 120 rpm, 200 μl of each culture was loaded into a 96 well plate and the endpoint optical density at 680 nm (OD_{680}) measured with a microplate reader (BMG Omega).

The minimum bactericidal concentration (MBC, the concentration of antibiotic required to elicit a 3 log reduction in CFUs) of each antibiotic was subsequently determined by serially diluting 30 μl of each treatment group and plating onto appropriate agar. Plates were incubated for 24 hours at 37 °C and viable CFUs recorded to determine the MBC.

Due to the poor solubility of HT61, (128 μg ml^{-1} and above), use of HT61 at these concentrations would increase the turbidity of the solutions and interfere with the OD_{680} readings. In these instances, bacterial cultures were diluted to 10^6 cells and plated onto agar plates, (LB agar for *P. aeruginosa*, TSA for all other species), supplemented with either 32 μg ml^{-1}, 64 μg ml^{-1}, 128 μg ml^{-1}, 256 μg ml^{-1}, 512 μg ml^{-1} or 1024 μg ml^{-1} HT61. The MIC could then be defined as the antibiotic concentration that yielded no growth following incubation at 37 °C for 24 hours.

2.2.3.2 Determination of Minimum Stationary Phase-Cidal Concentration

Minimum stationary phase-cidal concentrations, ($MSC_{99.9}$, the concentration of antibiotic required to elicit a 3-log reduction in CFUs of stationary phase cultures) were determined as described by Hu *et al* (2010)[11]. The method was identical to determining the MBC of an antibiotic with two important differences. First, initial cultures were grown for 72 hours opposed to 24 hours, ensuring sufficient entry into stationary phase, (it has been suggested that at this point, the bacterial population is equally split into dividing and non-dividing cells)[11]. Secondly, the two-fold antibiotic dilution series was initiated in HBSS, opposed to fresh broth, preventing the bacterial inoculum from continuing exponential growth during incubation.

2.2.3.3 Determination of Minimum Bactericidal Concentrations for Biofilm Cultures.

To ascertain the MBC values for biofilm cultures, mature biofilms of each bacterial species were treated with antibiotic and the Biofilm MBC designated as the concentration that elicited a 3-log reduction in CFUs. Overnight cultures of each species were diluted to 10^6 cells in either M9 media (*P. aeruginosa*) or TSB (all other species) and 4ml was used to inoculate each well of a Nunclon coated 6 well polystyrene plates (Thermo-Scientific, UK).

Biofilms were grown for 72 hours at 37 °C, 50 rpm, with fresh media exchanges performed every 24 hours. Following 72 hours of growth, spent media was replaced with media supplemented with a twofold dilution series of each antibiotic compound (0.5 μg ml^{-1} to 1024 μg ml^{-1}, except for meropenem which was utilised at concentrations between 0.5 μg ml^{-1} and 128 μg ml^{-1}). Untreated samples underwent media replacement without antibiotic supplementation. Following a further 24 hour incubation, biofilms were rinsed twice with 4 ml of HBSS to remove non-attached planktonic cells and harvested from the surface of the well with a cell scraper. The cell suspension was serially diluted and plated onto appropriate agar. Plates were incubated at 37 °C for 24 hours and viable CFU's were counted.

2.2.4 Efficacy of Antimicrobial Combinations

2.2.4.1 Planktonic Cultures

The chequerboard method was utilised to assess possible combination effects of HT61 in conjunction with tobramycin or vancomycin, towards planktonic cultures of *P. aeruginosa* PAO1 and *S. aureus* UAMS-1, respectively.

Overnight bacterial cultures were diluted to 10^6 cells and treated with the selected antibiotic compounds both alone and in combination. Antibiotic dilution series were prepared in 96 well plates. For *P. aeruginosa,* a two-fold dilution series of HT61 was initiated between 1 μg ml^{-1} and 128 μg ml^{-1} in tandem with a dilution series of tobramycin between 0.063 μg ml^{-1} and 1 μg ml^{-1}. For *S. aureus,* the HT61 dilution series was between 0.5 μg ml^{-1} and 64 μg ml^{-1} and for vancomycin was between 0.5 μg ml^{-1} and 16 μg ml^{-1}. Plates were incubated at 37 °C for 24 hours and the endpoint optical density at 680 nm (OD_{680}) was measured with a microplate reader (BMG Omega).

The fractional inhibitory concentration index, (FICI), was calculated and used to characterise the effects of each drug combination as follows:

$$\frac{MIC\ of\ drug\ A, tested\ in\ combination}{MIC\ of\ drug\ A, tested\ in\ isolation} + \frac{MIC\ of\ drug\ B, tested\ in\ combination}{MIC\ of\ drug\ B, tested\ in\ isolation} = FICI$$

Synergistic interactions were defined by an FICI of ≤ 0.5, antagonistic interactions by an FICI of > 4.0 and a lack of interaction by an FICI between 0.5 and 4.0, as per guidelines recommended by The Journal of Antimicrobial Chemotherapy[216].

2.2.4.2 Biofilm Cultures

To evaluate the effect of antibiotic combinations on biofilms, the Minimum Biofilm Eradication Concentration, (MBEC), High-throughput Assay (Innovotech) was utilised. The MBEC system consists of two parts: a 96 well plate and a lid that incorporates 96 polystyrene pegs which sit into the wells of the plate, facilitating bacterial attachment and biofilm formation[217].

Overnight cultures of *P. aeruginosa* PAO1 and *S. aureus* UAMS-1 were diluted to 10^6 cells and 150 µl of the bacterial inoculum was added to each well of the 96 well plates. The MBEC lid was placed and the systems incubated for 72 hours at 37°C with media exchanges every 24 hours. Following incubation, biofilms of *P. aeruginosa* were treated with combinations of HT61 (between 1 µg ml^{-1} and 128 µg ml^{-1}) and tobramycin (between 1 µg ml^{-1} and 256 µg ml^{-1}) and biofilms of *S. aureus* were treated with combinations of HT61 (between 1 µg ml^{-1} and 1024 µg ml^{-1}) and vancomycin (between 1 µg ml^{-1} and 64 µg ml^{-1}).

Following a further 24-hour incubation at 37 °C, each MBEC lid was rinsed twice in HBSS and placed onto a recovery 96 well plate, where each well was loaded with 200 µl of either LB or TSB, dependent on the bacterial species. The biofilm biomass recovery plates were then individually sonicated using a U300 Ultrasonic Bath, (Ultrawave Limited), at full power for 30 minutes. The MBEC lid was discarded and recovery plates were incubated for 24 hours at 37°C. The endpoint optical density at 680 nm (OD_{680}) was measured with a microplate reader (BMG Omega). The formula to calculate the FICI value was altered to utilise the MBEC values instead, defining a fractional biofilm-cidal concentration index, (FBCI), to characterise the effect of the drug combinations on the biofilms.

2.2.5 Effect of HT61 on Early Biofilm Development of *P. aeruginosa* and *S. aureus*

To assess the effect of HT61 on early biofilm development, biofilms of *P. aeruginosa* PAO1 and *S. aureus* UAMS-1 were set up as previously described in Nunclon coated 6 well plates. However, the initial 10^6 inoculum contained a two-fold dilution series of HT61 at concentrations below the calculated biofilm MBC, ensuring a suitable antibiotic challenge throughout the entire biofilm growth period. For *P. aeruginosa* the concentrations chosen were 32 μg ml^{-1}, 64 μg ml^{-1} and 128 μg ml^{-1}. The concentrations for *S. aureus* were 1 μg ml^{-1}, 2 μg ml^{-1} and 4 μg ml^{-1}. Control treatment groups were grown in media without HT61 supplementation. Media exchanges were performed every 24 hours. Following 24, 72 and 120 hours, both the planktonic suspension and the attached cells, (harvested with a cell scraper, as described previously), were serially diluted in HBSS, plated onto appropriate agar and incubated overnight at 37 °C. CFUs were quantified and the effect of HT61 on both planktonic and biofilm populations was recorded.

Biofilms of each species were also inoculated in poly-D-lysine coated MatTek dishes and cultured for 24 hours in the presence and absence of HT61. Following incubation, the media was removed, and the biofilms rinsed with 4 ml of HBSS, prior to staining with a solution of 2 μl ml^{-1} of BacLight LIVE/DEAD (Life Technologies, UK). Biofilms were visualised using a Nikon Eclipse E800 episcopic differential interference contrast/epifluorescence (EDIC/EF) microscope (Best Scientific, UK).

2.2.6 Effect of Minimum Bactericidal Concentrations of HT61 on Biofilm Morphology of *P. aeruginosa* and *S. aureus*

Biofilms of *P. aeruginosa* PAO1 and *S. aureus* UAMS-1 were grown for 72 hours in MatTek dishes at 37°C and 50 rpm, with media replacement every 24 hours, as previously described. Following 72 hours of growth, the biofilms were separated into three treatment groups: a control group, subsequently treated with fresh media, an HT61 treatment group and a tobramycin/vancomycin group depending on the species. Antibiotics were utilised at a concentration equal to the calculated biofilm MBC. Following a further 24 hour incubation, biofilms were rinsed twice with 4 ml of HBSS and stained with a 2 μl ml^{-1} BacLight LIVE/DEAD (Life Technologies), solution for 20 minutes. Glycerol (80% v/v) was added to each biofilm prior to visualisation with an inverted Leica TCS SP8 confocal

laser scanning microscope (CLSM). Images were analysed using MatLab and the COMSTAT statistics program[218].

2.2.7 Effect of HT61 on Cell Morphology of Bacteria within Biofilms

Scanning electron microscopy, (SEM), was used to determine the effect of HT61 on the gross cell morphology of *S. aureus* UAMS-1 and *P. aeruginosa* PAO1. Biofilms of each bacterial species were cultured on glass cover slips for 72 hours, at 37 °C, 50 rpm, with fresh media replacements every 24 hours. Following 72 hours of growth, biofilms were treated with the calculated MBC values of HT61, (*S. aureus*: 32 μg ml^{-1}, *P. aeruginosa*: 512 μg ml^{-1}) and incubated for a further 24 hours.

Fixation was performed as per Allan *et al* (2014)[219]. Following media removal, biofilms were fixed in a solution of 3% glutaraldehyde, 0.1 M sodium cacodylate (pH 7.2) and 0.15% alcian blue for 24 hours at 4 °C. This solution was then replaced with 0.1 M sodium cacodylate (pH 7.2) and incubated for a further hour at room temperature. Following primary fixation, a secondary fixative consisting of 0.1 M sodium cacodylate (pH 7.2) and 0.1 M osmium tetroxide was utilised for 1 hour. The cover slips were then incubated for a final time in 0.1 M sodium cacodylate (pH 7.2) for 1 hour before dehydration via an ethanol series of 30%, 50%, 70%, 95% and twice at 100%. Finally, the dehydrated biofilms were critical point dried, sputter coated in a platinum-palladium alloy and visualised using a FEI Quanta 250 scanning electron microscope.

2.2.8 Statistical Analysis

All assays were performed with a minimum of three biological replicates. For quantitative analysis of CLSM data, three random fields of view were selected from each biological replicate. All statistical analyses were performed using GraphPad Prism version 7.0d for Mac and statistical significance was determined if $\alpha < 0.05$.

The effect of HT61 on the initial development of *P. aeruginosa* and *S. aureus* biofilms at each time point was analysed using a Kruskal-Wallis test with a post hoc Dunn's comparison to compare the treated groups with the untreated control. Analysis of CLSM data was performed using COMSTAT software and compared for significance using a Kruskal Wallis test with a post hoc Dunn's comparison between treatment groups. Error bars in all cases represent standard error of the mean.

2.3 Results

2.3.1 HT61 Efficacy Is Highly Variable Between Bacterial Species

Table 4: MIC, MSC and MBC Values for HT61 and a selection of clinically relevant antibiotic compounds

In cases where a value was not obtained, the > symbol is used to indicate that the value is higher than the stated concentration. For example, > 16 indicates the value is greater than 16 μg ml^{-1}.MIC: Minimum Inhibitory Concentration, MBC: Minimum Bactericidal Concentration, MSC_{99}: Minimum Stationary Phase-Cidal Concentration.

			MIC	**MBC**	**MSC**	**Biofilm MBC**
Gram	**Bacteria**	**Antimicrobial**	**μg ml^{-1}**			
Positive	*S. aureus*	HT61	16	32	8	32
		Vancomycin	4	4	> 16	64
	S. epidermidis	HT61	16	16	8	128
		Vancomycin	4	4	> 16	> 2048
Negative	*K. pneumoniae*	HT61	> 1024	> 1024	512	> 1024
		Ciprofloxacin	0.5	1	0.5	1
	A. baumannii	HT61	32	32	> 128	256
		Meropenem	2	2	8	64
	P. aeruginosa PAO1	HT61	> 1024	1024	> 1024	512
		Tobramycin	1	4	4	4
	P. aeruginosa PA21	HT61	> 1024	1024	1024	> 1024
		Tobramycin	2	2	2	4

HT61 was more effective against the Gram-positive species tested. Growth of *S. aureus* was inhibited following treatment with HT61, (MIC = 16 μg ml^{-1}) and at least a 3 log reduction in CFUs was observed following treatment at 32 μg ml^{-1}. Furthermore, HT61 was more effective towards stationary phase planktonic cultures (MSC = 8 μg ml^{-1}) and was more effective against biofilms than vancomycin (Biofilm MBC = 32 μg ml^{-1}, compared to 64 μg ml^{-1} for vancomycin). However, vancomycin was more effective against log phase planktonic cultures, (MIC = 4 μg ml^{-1}, MBC = 4 μg ml^{-1}).

As for *S. epidermidis,* HT61 was less effective than vancomycin at inhibiting growth and reducing bacterial viability (HT61 MIC and MBC = 16 μg ml^{-1} compared to vancomycin MIC and MBC = 4 μg ml^{-1}). However, HT61 was far more effective against stationary phase and biofilm cultures of *S. epidermidis* with MSC and Biofilm MBC values of 8 μg ml^{-1} and 128 μg ml^{-1}, compared to values obtained for vancomycin of > 16 μg ml^{-1} and > 2048 μg ml^{-1}, respectively.

HT61 was generally ineffective against the Gram-negative species tested, with no consistent pattern of action between species. Towards *K. pneumoniae,* HT61 was ineffective at inhibiting growth or viability of planktonic cultures when treated during log phase and biofilm cultures. However, against stationary phase cultures, HT61 was effective at a high concentration (MSC = 512 μg ml^{-1}).

Of the strains and species tested, *A. baumannii* was the only Gram-negative species for which both growth inhibition and bactericidal activity was observed following treatment with HT61 (MIC and MBC = 32 μg ml^{-1}). However, activity towards stationary cultures was reduced (MSC > 128 μg ml^{-1}) and biofilm mediated tolerance was observed, (Biofilm MBC = 256 μg ml^{-1}

No inhibitory effect was observed on the growth of either strain of *P. aeruginosa* following treatment with HT61 at the concentrations tested, (MIC > 1024 μg ml^{-1}). However, HT61 did confer a measurable bactericidal effect against log-phase cultures, (MBC = 1024 μg ml^{-1}), although an MSC was unable to be determined for either strain. The biofilm MBC for *P. aeruginosa* PAO1 was calculated as 512 μg ml^{-1}, suggesting improved activity against biofilms, although this finding was not replicated when biofilms of *P. aeruginosa* PA21 were treated (Biofilm MBC > 1024 μg ml^{-1})

Tobramycin was considerably more effective against *P. aeruginosa*, exerting its effect at far lower concentrations, (MIC = 1 μg ml^{-1}, MBC = 4 μg ml^{-1}, MSC = 4 μg ml^{-1}, Biofilm MBC = 4 μg ml^{-1}).

2.3.2 HT61 is an Ineffective Adjunct to Conventional Antibiotics

P. aeruginosa PAO1 and *S. aureus* UAMS-1 were utilised for all subsequent experiments as representative examples of Gram-negative and Gram-positive bacterial species, respectively.

The chequerboard method was used to assess whether HT61 demonstrated synergy alongside either tobramycin or vancomycin against planktonic and biofilm cultures of *P. aeruginosa* or *S. aureus*, respectively. For planktonic cultures the MIC of the antibiotics in isolation was compared to the MIC of the antibiotics in combination, whereas the MBEC value was utilised for the biofilm studies, both in isolation and in combination. These respective values were then used to calculate the FICI and FBCI's to determine the type of interaction between the antibiotic compounds. Synergistic interactions were defined by an FICI ≤ 0.5 represents synergy, an FICI between 0.5 and 4.0 represents no interaction, and an FICI > 4.0 represents an antagonistic interaction.

Results of the chequerboard studies with HT61 and tobramycin against *P. aeruginosa* are presented in Table 5, with the results of HT61 and vancomycin combinations towards *S. aureus* presented in Table 6. The combination of HT61 and tobramycin treatment against *P. aeruginosa* demonstrated no interactions, regardless of whether treatment was directed against planktonic or biofilm cultures, (FICI = 2.00 and FBCI = 2.00).

A similar relationship was identified with combinations of HT61 and vancomycin against *S. aureus,* with FICI and FBCI values of 1.00 and 0.504, respectively. While synergy was not detected, the required concentrations of HT61 and vancomycin were reduced when utilised in combination. Towards planktonic cultures, the MICs of HT61 and vancomycin were halved in combination (HT61: 8 μg ml^{-1} to 4 μg ml^{-1}; vancomycin: 4 μg ml^{-1} to 2 μg ml^{-1}. Towards biofilms, the MBEC of HT61 was halved (64 μg ml^{-1} to 32 μg ml^{-1}) and for vancomycin, an MBEC of 1 μg ml^{-1} was only obtained when used in combination with HT61 (no MBEC was obtained with vancomycin in isolation).

Table 5: Efficacy of HT61 in combination with tobramycin towards planktonic and biofilm cultures of *P. aeruginosa* PAO1.

In cases where a value was not obtained, the > symbol is used to indicate that the value is higher than the stated concentration. For example, > 256 indicates the value is greater than 256 μg ml^{-1}. FICI = Fractional Inhibitory Concentration Index, FBCI = Fractional Biofilm-Cidal Concentration Index, MIC = Minimum Inhibitory Concentration, MBEC = Minimum Biofilm Eradication Concentration.

		MIC (μg ml^{-1})					
		Lone Treatment		Combination Treatment			
P. aeruginosa PAO1	Growth State	HT61	Tobramycin	HT61	Tobramycin	FICI	Activity
	Planktonic	> 128	1	> 128	1	**2.00**	**No Interaction**

		MBEC (μg ml^{-1})					
		Lone Treatment		Combination Treatment			
	Growth State	HT61	Tobramycin	HT61	Tobramycin	FBCI	Activity
	Biofilm	> 2048	> 256	> 2048	> 256	**2.00**	**No Interaction**

Table 6: Efficacy of HT61 in combination with vancomycin towards planktonic and biofilm cultures of *S. aureus* UAMS-1.

In cases where a value was not obtained, the > symbol is used to indicate that the value is higher than the stated concentration. For example, > 64 indicates the value is greater than 64 μg ml^{-1}. FICI = Fractional Inhibitory Concentration Index, FBCI = Fractional Biofilm-Cidal Concentration Index, MIC = Minimum Inhibitory Concentration, MBEC = Minimum Biofilm Eradication Concentration.

		MIC (μg ml^{-1})					
		Lone Treatment		**Combination Treatment**			
	Growth State	**HT61**	**Vancomycin**	**HT61**	**Vancomycin**	**FICI**	**Activity**
S. aureus UAMS-1	Planktonic	8	4	4	2	**1.00**	**No Interaction**

		MBEC (μg ml^{-1})					
		Lone Treatment		**Combination Treatment**			
	Growth State	**HT61**	**Vancomycin**	**HT61**	**Vancomycin**	**FBCI**	**Activity**
S. aureus UAMS-1	Biofilm	64	> 64	32	1	**0.504**	**No Interaction**

2.3.3 Influence of HT61 on the Early Stages of *P. aeruginosa* PAO1 and *S. aureus* UAMS-1 Biofilm Development

The impact of HT61 treatment on the biofilm development of *P. aeruginosa* PAO1 biofilm morphology at 24 hours is shown in Figure 11, panels A-D, and the effect of differing HT61 concentrations on cell viability over the course of 120 hours is presented in Figure 11, panel E.

For *P. aeruginosa,* Kruskal-Wallis analysis of the data between HT61 treated and untreated at each time point suggests significant variation in the medians at 24 and 72 hours (p = 0.0009 and p = 0.0135, respectively) but no significant variation at 120 hours (p = 0.2974).

At 24 hours, incubation with 128 μg ml^{-1} HT61 resulted in a 0.88 log decrease in CFU cm^{-2} compared to the untreated control, although post-hoc comparison implies that this difference was not significant. However, there was a significant decrease in the viability of the planktonic suspension at this concentration and time point, corroborating the observed decrease in biofilm ($p < 0.0001$; see Appendices, Figure S1). The only significant change found following 24 hours of culture was between biofilms grown in 64 μg ml^{-1} and 128 μg ml^{-1} HT61, where there is a decrease in CFUs equal to 1.32 log at the higher concentration.

After 72 hours of growth, there was a significant decrease in biofilm CFU cm^{-2} following incubation with 128 μg ml^{-1} HT61 compared to the untreated control. There was no significant difference in biofilm growth following incubation with either 32 or 64 μg ml^{-1}. Despite this, comparisons of the planktonic suspensions showed a statistically significant decrease in viability (approximately 0.5 log) between each HT61 treated group and the untreated control group planktonic (32 μg ml^{-1}, $p < 0.05$; 64 μg ml^{-1}, $p < 0.05$; 128 μg ml^{-1}, $p < 0.01$; see Appendices, Figure S1).

However, by 120 hours of biofilm growth, there was no statistically significant variation between any treatment groups or the untreated control group. However, there was variation between CFU counts within the planktonic suspension between treated and untreated groups (Kruskal Wallis p = 0.0004, Dunn's comparisons Control compared to 32 and 64 μg ml^{-1}, $p < 0.01$ for each comparison, see Appendices, Figure S1).

Imaging of the *P. aeruginosa* biofilms formed following 24 hours growth revealed differences in biofilm morphology that were dependent on the concentration of HT61 utilised. Incubation with 32 and 64 μg ml^{-1}, (Figure 11, panels B and C), led to an increased frequency of microcolony type structures compared to the untreated control biofilm (Figure 11, panel A). Incubation with 128 μg ml^{-1}, (Figure 11, panel D), resulted in a lower cell density, which corroborates with the CFU data (Figure 11, panel E).

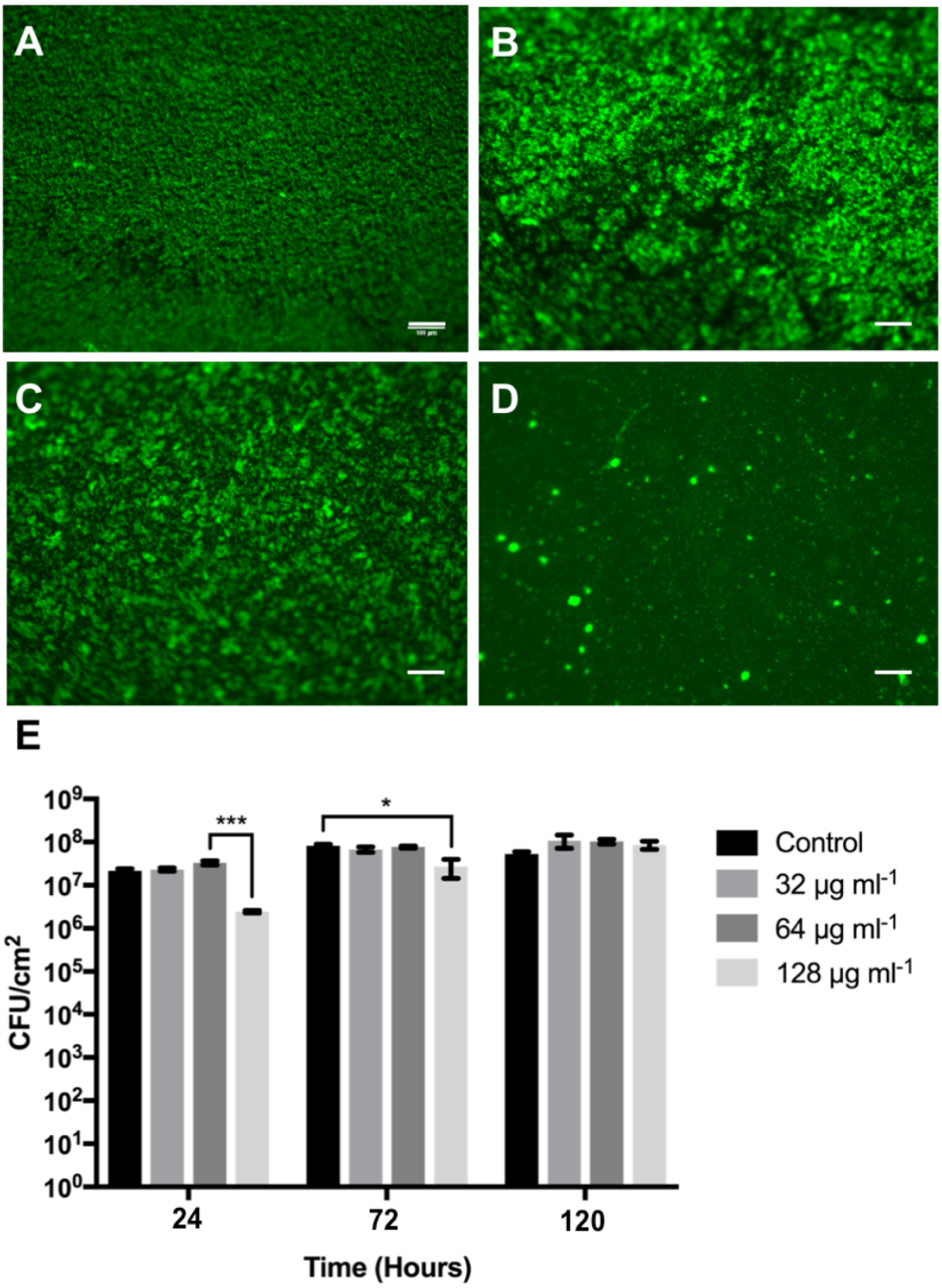

Figure 11: Effect of HT61 on initial attachment and biofilm maturation of *P. aeruginosa* PAO1.

(A-D) Representative epi-fluorescence images of *P. aeruginosa* biofilms, grown for 24 hours in either M9 (A), or M9 supplemented with either 32, 64 or 128 μg ml^{-1} HT61, (B-D, respectively), and stained with SYTO9. Scale bars = 100 *μ*m. (E) CFU cm^{-2} at 24, 72 and 120 hours following growth in either control media, (M9) or media supplemented with HT61. Error bars represent standard error of the mean, (n = 6, from 3 experimental repeats). Statistical significance calculated using Kruskal-Wallis test, with Dunn's multiple comparison within each time point. *, $p < 0.05$, ***, $p < 0.001$.

Regarding biofilms of *S. aureus*, Kruskal-Wallis analysis of each time point suggests significant variation in the median of the obtained CFU values (24 hour: $p = 0.0175$, 72 hour: $p = 0.0264$, 120 hour: $p = 0.0184$). However, post-hoc Dunn's multiple comparisons show that this variance is not associated with differences between the untreated control group and HT61 treated groups. In other words, pre-incubation with HT61 did not have a significant effect on viability. By 120 hours, there was a slight decrease in CFUs correlating with increased concentrations of HT61, although these differences were not significant when compared to the untreated control group. These results, paired with the consistency observed across the images of the *S. aureus* biofilms at 24 hours (Figure 12, panels A to D) suggests that HT61 has no effect on the development of *S. aureus* biofilms at the concentrations tested.

The variance within each time point appears to be associated with differences among the treated groups, specifically at 24 hours between biofilms grown in 1 and 2 μg ml^{-1} HT61 and at 120 hours between biofilms grown in 1 and 4 μg ml^{-1} HT61. However, these differences are slight and all biofilms, regardless of growth time or media composition returned counts of approximately 10^8 CFU cm^{-2}.

The effects of HT61 on the planktonic suspension during biofilm formation of *S. aureus* is slight (see Appendices, figure S2). At 24 hours, no variation in the medians is found between untreated and treated groups ($p = 0.1262$) and at 72 hours, while variation between medians is statistically significant ($p = 0.154$), the differences are slight and no significance is found with post-hoc comparisons. Following 120 hours of growth, there is a small decrease in the viability of the planktonic suspension when grown in 4 μg ml^{-1} HT61, but the difference is only significant between the other treated groups (1 μg ml^{-1} comparison $p < 0.05$; 2 μg ml^{-1} comparison $p < 0.001$) and not the untreated control.

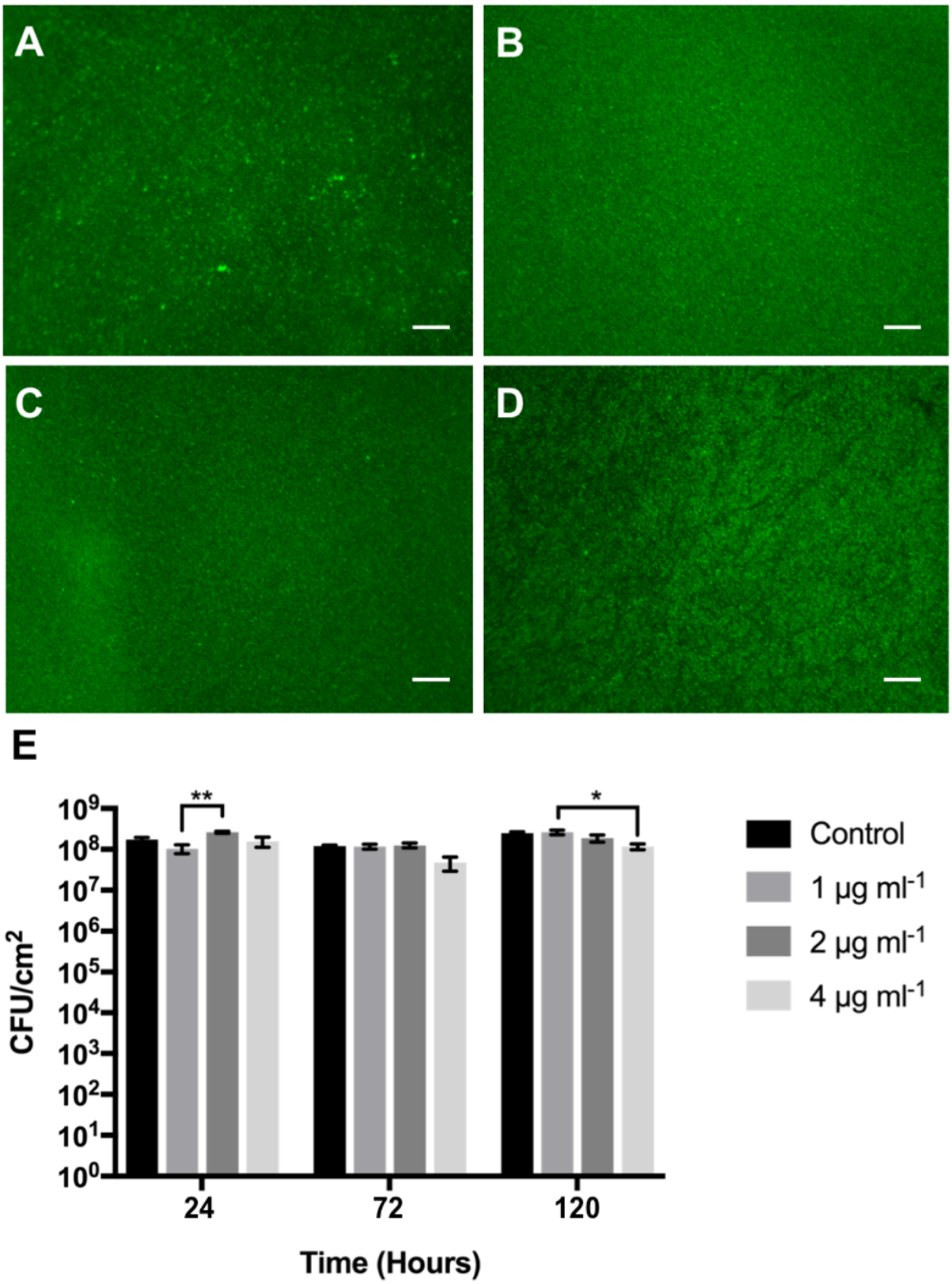

Figure 12: Effect of HT61 on initial attachment and biofilm maturation of *S. aureus* UAMS-1

(A-D) Representative epi-fluorescence images of *S. aureus* biofilms, grown for 24 hours in either TSB (A), or TSB supplemented with either 1, 2 or 4 μg ml^{-1} HT61, (B-D, respectively), and stained with SYTO9. Scale bars = 100 *μ*m. (E) CFU cm^{-2} at 24, 72 and 120 hours following growth in either control media, (TSB) or media supplemented with HT61. Error bars represent standard error of the mean, (n = 6, from 3 experimental repeats). Statistical significance calculated using Kruskal-Wallis test, with Dunn's multiple comparison within each time point. *, $p < 0.05$, **, $p < 0.01$.

2.3.4 Effect of Minimum Bactericidal Concentrations of HT61 on Biofilm Morphology of *P. aeruginosa* PAO1 and *S. aureus* UAMS-1

The effect of HT61 on the biofilm morphology of *P. aeruginosa* PAO1 and *S. aureus* UAMS-1 was determined using CLSM. The effects of HT61 were compared to the effects of tobramycin or vancomycin at their respective biofilm MBCs for either *P. aeruginosa* PAO1 (Figure 13) or *S. aureus* UAMS1 (Figure 14).

Following treatment of a 72-hour biofilm of *P. aeruginosa* with HT61 or tobramycin, highly significant changes in maximum biofilm thickness and the volume of live biomass were observed (Kruskal Wallis $p = 0.0001$ and $p < 0.0001$, respectively). HT61 treatment (Figure 13**,** panel D) reduced the maximum biofilm thickness from an average of 13.2 μm (untreated control) to an average of 2.78 μm ($p < 0.01$). Following tobramycin treatment, maximum biofilm thickness increased slightly to 13.67 μm, however this change was not statistically significant ($p > 0.05$).

HT61 treatment at the biofilm MBC resulted in a significant decrease in *P. aeruginosa* live biomass compared to the untreated control, (Figure 13**,** panel E, $p \leq 0.0001$). Equivalent treatment with tobramycin also caused a decrease in live biomass, however this was not statistically significant according to post-hoc comparisons. Comparing biofilms treated with HT61 and tobramycin shows significant reductions in terms of both maximum thickness and live biomass ($p < 0.01$ and $p < 0.05$, respectively).

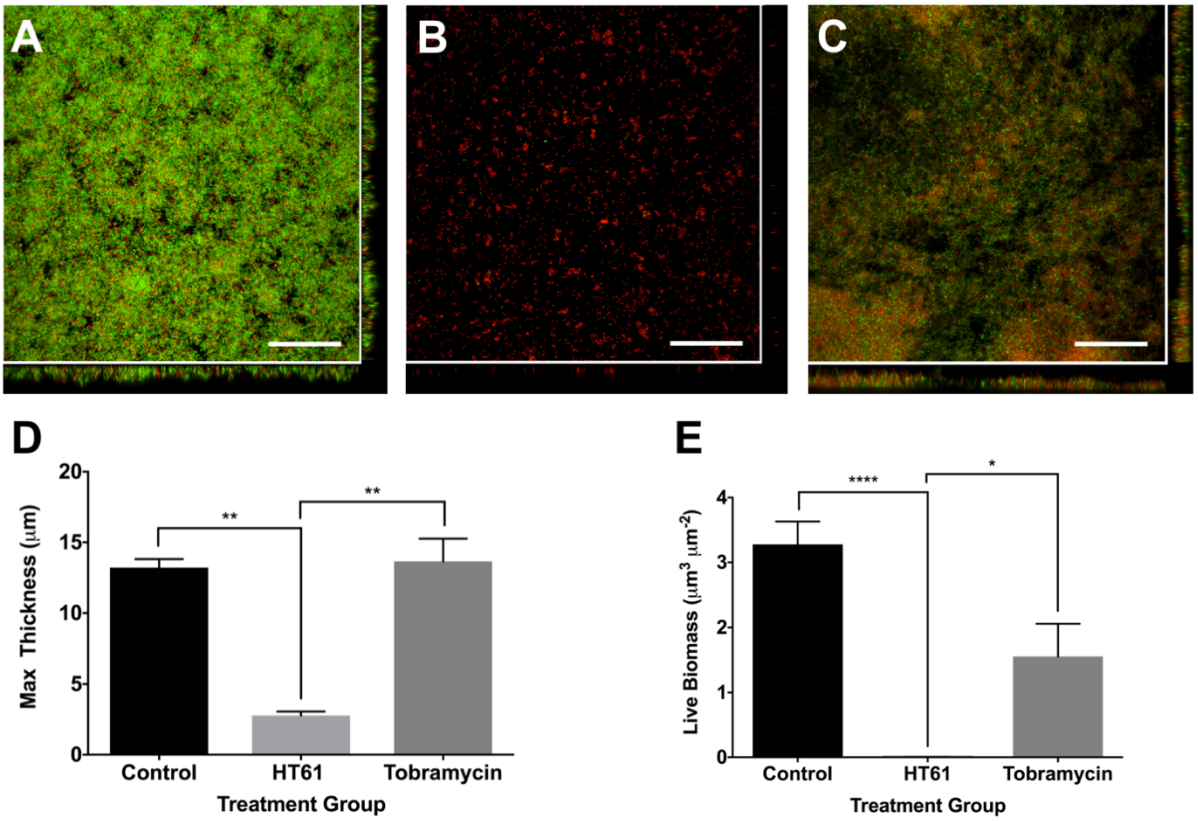

Figure 13: Effect of MBC HT61 and tobramycin treatment on 72-hour biofilms of *P. aeruginosa*

Representative images of (A) 96 hour control biofilm, (B), 96 hour biofilm, treated with 512 μg ml^{-1} HT61 at 72 hours of growth and (C) 96 hour biofilm, treated with 4 μg ml^{-1} tobramycin at 72 hours of growth. Scale bars = 50 μm. (D) Effect of antibiotic treatment on maximum biofilm thickness. (E) Effect of antibiotic treatment on live biofilm biomass. Error bars represent standard error of the mean, (n = 9 from 3 experimental repeats.) Asterisks indicate statistically significant results: * ($P \leq 0.05$), ** ($P \leq 0.01$), **** ($P \leq 0.0001$), as determined by Kruskal-Wallis Test and post-hoc Dunn's comparisons.

The effects of HT61 and vancomycin against 72 hour *S. aureus* biofilms were more comparable. Kruskal-Wallis analysis suggested significant variance in the acquired medians for both maximum biofilm thickness and levels of live biomass ($p = 0.0022$, $p = 0.0003$, respectively). In terms of maximum biofilm thickness, shown in Figure 14**,** panel D, HT61 treatment reduced the average maximum biofilm thickness from 12.98 μm, (untreated control), to 4.67 μm ($p < 0.01$). Treatment with vancomycin resulted in a smaller, but still statistically significant reduction, with an average maximum biofilm thickness after treatment of 9.8 μm ($p < 0.05$). Both HT61 and vancomycin treatments caused significant reductions in the amount of detectable live biomass compared to the untreated control biofilm, illustrated in Figure 14**,** panel E ($p < 0.001$ and $p < 0.05$ for HT61 and vancomycin treatments, respectively). No statistically significant differences was identified directly between HT61 and vancomycin treated groups.

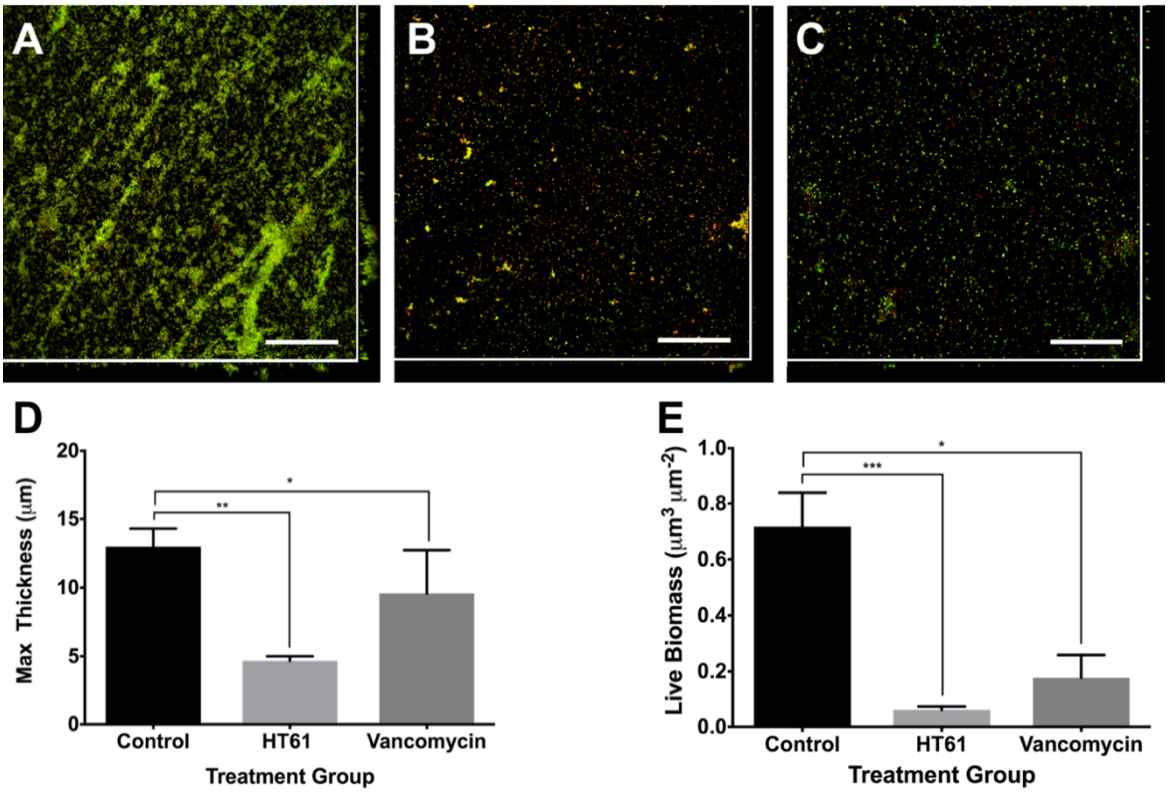

Figure 14: Effect of MBC HT61 and vancomycin on 72-hour biofilms of *S. aureus*

Representative images of (A) 96 hour control biofilm, (B), 96 hour biofilm, treated with 32 μg ml-1 HT61 at 72 hours of growth and (C) 96 hour biofilm, treated with 64 μg ml-1 vancomycin at 72 hours of growth. Scale bars = 50 μm. (D) Effect of antibiotic treatment on maximum biofilm thickness. (E) Effect of antibiotic treatment on live biofilm biomass. Error bars represent standard error of the mean, (n = 12 from 3 experimental repeats). Asterisks indicate statistically significant results: * ($P \leq 0.05$), ** ($P \leq 0.01$), *** ($P \leq 0.001$), as determined by Kruskal-Wallis Test and post-hoc Dunn's comparisons.

2.3.5 Assessment of the Action of HT61 on Bacterial Biofilms Using Scanning Electron Microscopy

Biofilms of *P. aeruginosa* PAO1 and *S. aureus* UAMS-1 were grown for 72 hours and treated with HT61 at a concentration equal to the calculated biofilm MBC, prior to fixation and visualisation using SEM.

Control biofilms of *P. aeruginosa* demonstrated high levels of attachment along with large, cell dense microcolony type structures and a large amount of EPS production (Figure 15, panels A, B and C). Following treatment with HT61 at 512 μg ml^{-1}, both surface attachment and the size of the cellular aggregates was reduced, (Figure 15, panel D), corroborating with the previously obtained CSLM data (Figure 13, panel B). On closer examination of the *P. aeruginosa* cell surfaces following HT61 treatment, surface blebbing occurred suggesting disruption to the cell membrane. However due to the presence of EPS artefacts, it is difficult to say this with certainty. (Figure 15, panels E and F)

Prior to HT61 treatment, biofilms of *S. aureus* were formed of large cellular aggregates, with a relatively high cell density and low production of EPS. (Figure 16, panels A, B and C). Following treatment with 32 μg ml^{-1} HT61, the overall number of cell numbers was reduced, (Figure 16, Panel D), and the actual cell surfaces were majorly disrupted, (Figure 16, panels E and F).

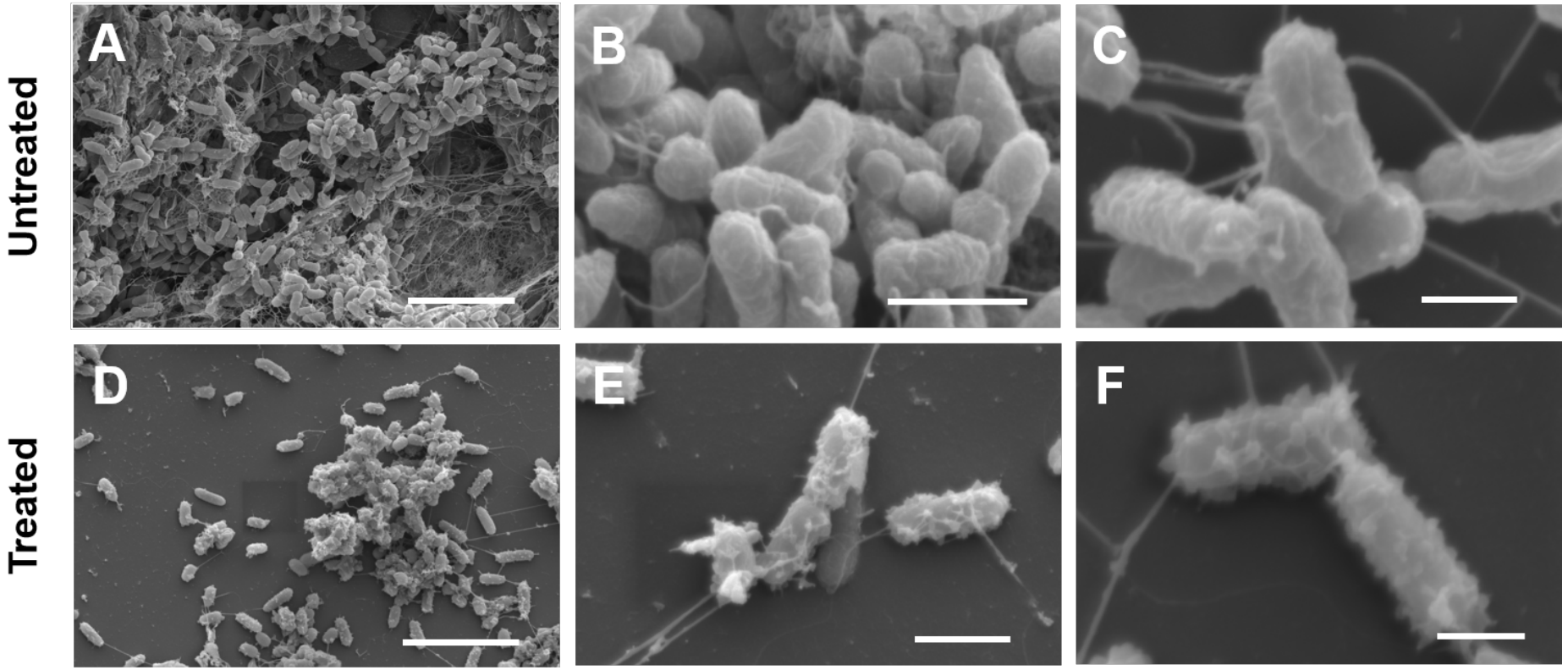

Figure 15: SEM micrographs of *P. aeruginosa* PAO1 biofilms, before and after treatment with 512 μg ml^{-1} HT61

Untreated (panels A-C), treated (panels D-F). Scale bars: Panels A and D = 5 *μ*m, B and E = 1 *μ*m, C and F = 0.5 *μ*m).

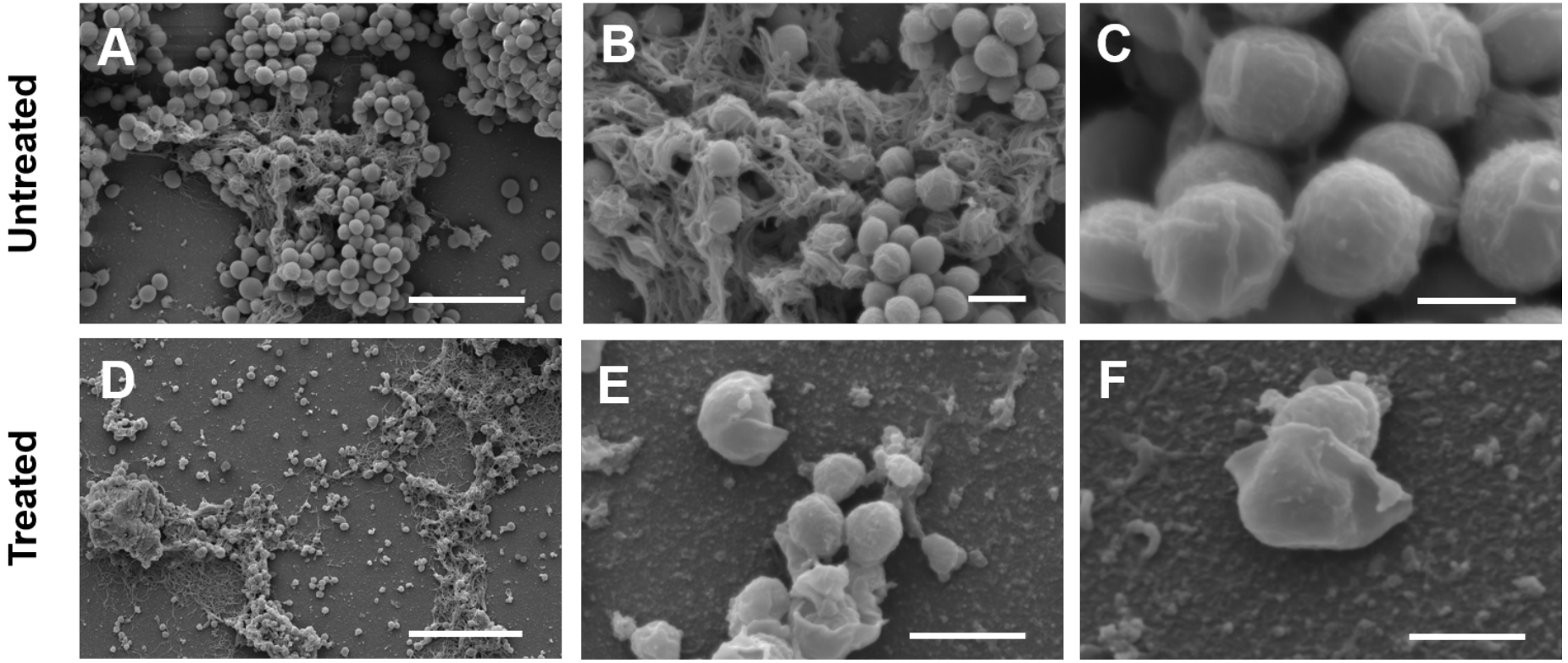

Figure 16: SEM micrographs of *S. aureus* UAMS-1 biofilms, before and after treatment with 32 μg ml^{-1} HT61

Untreated (panels A-C), treated (panels D-F). Scale bars: Panels A and D = 5 *μ*m, B and E = 1 *μ*m, C and F = 0.5 *μ*m

2.4 Discussion

A direct consequence of the increased levels of AMR bacterial infections is that the number of effective antimicrobials is dwindling. As such, development and characterisation of novel compounds is of paramount importance. Metabolically inactive cells exhibit tolerance to antibiotic treatment so the creation of antimicrobials that are more effective against these populations would be highly desirable[117]. Biofilms often contain metabolically inactive cellular sub-populations[72], so compounds that target non-dividing cells have the potential to be important anti-biofilm agents. The aim of this chapter was to investigate the effects of a novel quinoline derivative, HT61, against biofilm cultures of clinically relevant bacterial species using a combination of standard antimicrobial susceptibility testing and high-resolution imaging techniques. These approaches have improved our understanding of this novel antimicrobial, although more work needs to be performed to fully understand its mechanism of action.

2.4.1 HT61 is Most Effective Against Stationary Phase Gram-positive Bacterial Species

HT61 treatment of planktonic cultures of *S. aureus* and *S. epidermidis* demonstrated similar findings to previously published data[11], with the highest efficacy found towards stationary phase planktonic cultures. Compared to vancomycin, HT61 was less effective at inhibiting growth and killing dividing cultures but was more effective against stationary phase cultures and biofilms. Of note was the marked improvement against biofilms of *S. epidermidis*, which were unaffected even by very high concentrations of vancomycin. The ability of HT61 to successfully treat these biofilms could be a result of its improved efficacy against non-dividing subpopulations. However, for both antimicrobials, biofilm tolerance was observed, indicated by increased MBCs towards biofilms compared to planktonic cultures. Vancomycin tolerance in *S. epidermidis* biofilms has been linked to the production of eDNA which impedes vancomycin transport, contributing to bacterial survival[115]. However, the mechanisms of HT61 tolerance have not been explored. Recent work by Hubbard *et al* (2017) shows that HT61 preferentially binds to negatively charged phospholipids[13]. If *S. epidermidis* is producing negatively charged phospholipids as a component of its EPS, these could sequester HT61 in a similar fashion to the sequestration of vancomycin by eDNA. Tagging HT61 with a fluorophore would allow it to be tracked through the biofilm architecture and could show if it is impeded in any way.

Activity of HT61 against planktonic cultures of Gram-negative species was more varied. Interestingly, HT61 demonstrated improved efficacy towards stationary phase cultures of *K. pneumoniae*, although the required concentration was extremely high. Similarly, high concentrations were also required for the eradication of planktonic and biofilm cultures of both *P. aeruginosa* PAO1 and PA21. A curious observation was the finding that HT61 appeared to be more effective against biofilms of *P. aeruginosa* PAO1, compared to planktonic cultures (Biofilm MBC = 512 μg ml^{-1}, Planktonic MBC = 1024 μg ml^{-1}). This effectiveness was also demonstrated in the accompanying CLSM and COMSTAT analysis. Unfortunately, this pattern of activity was not replicated against *P. aeruginosa* PA21, suggesting a strain specific effect rather than a *Pseudomonas spp.* specific effect.

Curiously, *A. baumannii* was the only Gram-negative species tested where an MIC could be obtained (MIC = 32 μg ml^{-1}), although stationary phase and biofilm cultures exhibited increased HT61 tolerance (MSC > 128 μg ml^{-1}, Biofilm MBC = 256 μg ml^{-1}). While the increased survivability of Gram-negative species to HT61 is likely a result of intrinsic resistance thanks to the presence of the protective outer membrane[220], the differing profile presented towards *A. baumannii* also provides evidence suggesting that species specific factors may also be important.

Recent work by Hubbard *et al* (2017) has suggested that HT61 preferentially exerts its action by binding to anionic phospholipids in the membrane of *S. aureus*[13]. The outer membrane of Gram-negative bacteria does not typically contain phospholipids in the outer leaflet of the bilayer[17], possibly explaining why HT61 is not as effective against them. However, it is possible that differences in the membrane composition between Gram-negative species will also influence the efficacy of HT61 on a species by species basis.

2.4.2 HT61 is an Ineffective Adjunct to Tobramycin or Vancomycin Against *P. aeruginosa* and *S. aureus*

In an effort to prevent evolution of antibiotic resistance, combination therapies utilising two or more antibiotic compounds are often implemented in clinical practice, especially if MDR pathogens are implicated[221–223]. A recent study by Gifford *et al* (2018) demonstrates this in the context of β lactamase expression in *P. aeruginosa*[224]. The authors found that presence of the AmpR transcriptional regulator potentiated the accumulation of mutations within peptidoglycan biosynthesis genes. These mutations resulted in increased expression

of β lactamases and concurrently, a highly resistant phenotype. However, by co-administering ceftazidime with avibactam (a β lactamase inhibitor), the authors were able to kill entire populations of *P. aeruginosa* before resistance could evolve[224]. This study perfectly illustrates why identifying effective combinations of antimicrobials is an attractive concept. HT61 has previously demonstrated synergistic interactions with neomycin, gentamicin and chlorhexidine towards planktonic cultures of MSSA and MRSA, both *in vitro* and *in vivo*[12], but its effect on biofilms has not been explored.

No interactions were observed between HT61 and tobramycin against either planktonic or biofilm cultures of *P. aeruginosa*. Furthermore, no interaction was identified between HT61 and vancomycin against planktonic or biofilm cultures of *S. aureus.* However, analysis using a less conservative set of published parameters, (synergy ≤ 0.5; partial synergy $> 0.5, < 1$; additive $= 1$; no interaction $> 1, < 2$; antagonistic ≥ 2)[225] suggests that combinations of HT61 and vancomycin are additive against *S. aureus* planktonic cultures and partially synergistic against *S. aureus* biofilms.

The observed additive effect of HT61 in combination with vancomycin towards planktonic cultures could be a result of HT61 improving the accessibility of vancomycin to the *S. aureus* cell wall. The further improved efficacy towards biofilms could be due to HT61 preferentially targeting the non-dividing cell population and vancomycin effectively targeting the dividing population, although further work would be required to confirm this.

These types of additive and partially synergistic effects, (where the MIC/MBEC of an antimicrobial decrease when utilised in combination), are highly desirable in a clinical setting. Firstly, a combinatorial approach will reduce the selection for antibiotic resistance mechanisms within the bacterial population. Secondly, a lower effective concentration will reduce the antimicrobial load administered to a patient, reducing toxic side effects. Finally, by using lower antimicrobial concentrations, hospitals and healthcare facilities will inherently save money.

However, use of these less stringent antimicrobial interaction parameters is open to debate as it has been suggested they can be misused to "over interpret" data[216]. To investigate antimicrobial interactions further, alternative methodologies could be used such as time-kill assays, whereby the cellular viability following treatment with different antimicrobial

combinations is determined over a time course; synergistic combinations will reduce viability quicker and/or at a higher degree.

It is worth noting a disadvantage that was identified during the use of the MBEC system. As the system requires total biofilm eradication, opposed to the typically utilised 3-log reduction in CFUs, an antimicrobial has to be extremely effective and/or used at a higher concentration to prevent growth in the recovery plate. Consequently, the effectiveness of an antimicrobial combination may be underestimated if it is anything less than 100% effective. This may have occurred in the case of HT61 and tobramycin towards biofilms of *P. aeruginosa* PAO1.

2.4.3 HT61 Has No Effect on Initial Biofilm Development of *S. aureus* and *P. aeruginosa*

The effect of HT61 on biofilm development was analysed further using *P. aeruginosa* PAO1 and *S. aureus* UAMS-1. It has been shown previously that growth of bacterial cultures with sub-inhibitory concentrations of antibiotic compounds can reduce biofilm attachment and maturation. For example, sub-inhibitory concentrations of azithromycin has been shown to reduce biofilm formation of *P. aeruginosa*[226,227]. Understanding whether novel antibiotic compounds such as HT61 can exert similar effects is important for biofilm control.

Broadly, sub-inhibitory concentrations of HT61 did not impact the initial development of biofilms of *S. aureus* and *P. aeruginosa,* although slight perturbations in viability were recorded. For *S. aureus,* there was no significant change in CFUs at any time point across any population. Slight differences were seen in biofilms of *P. aeruginosa* but CFU counts normalised to the same level following 120 hours of growth, regardless of HT61 concentration. Interestingly the planktonic CFU counts obtained for *P. aeruginosa* showed that HT61 reduced planktonic viability by approximately 1 log (see Appendices, figure S1). Consequently, the slight differences that were seen during *P. aeruginosa* biofilm growth, both statistically significant and otherwise, could be explained by a toxic effect on cellular viability, rather than an actual mechanism that inhibited biofilm development.

These findings are not necessarily surprising. HT61 is predicted to exert its mechanism of action by causing membrane depolarisation[11,13], and as such is likely to have an “all or nothing” type mechanism. In other words, sub-MIC levels may have limited effect, while

effective concentrations will result in membrane permeabilization and cell death. This would lead to a reduction in pre-attached biofilm rather than a reduction in biofilm formation.

2.4.4 Scanning Electron Microscopy Provides Evidence Towards a Mechanism of Action Targeted to the Bacterial Membrane of *S. aureus*

Previous work has suggested that HT61 exerts its bactericidal effect by interfering with the cell membrane, preferentially interacting with anionic lipids to cause rapid depolarisation, resulting in cell death[11,13]. To investigate whether the same mechanism was responsible for the killing effect observed against biofilm cultures, SEM was used to directly visualise the biofilm cells.

The SEM data obtained following treatment of *S. aureus* biofilms with HT61 appears to confirm this mechanism, not only revealing a stark reduction in biomass but also catastrophic disruption of the outer cell layers, as depicted in panels E and F of Figure 16, corroborating the previous findings in the literature[11,13].

Despite requiring a much higher concentration of HT61, similar effects were seen in the treated *P. aeruginosa* biofilms, resulting in a considerably sparser population. In addition, HT61 appeared to cause blebbing of the *P. aeruginosa* membrane, which has not previously been documented following HT61 treatment. Blebbing refers to the production of outer membrane vesicles which are used to eject accumulated proteins from the cell, especially in response to stress focused on the cell envelope[228]. Atomic force microscopy of *E. coli* after treatment with a membrane permeabilising antimicrobial peptide revealed similar cellular disruption[229] and SEM imaging of *P. aeruginosa* following treatment with a macrocyclic peptidomimetic antibiotic called L27-11, revealed cells with an altered morphology[230]. Moreover, the cells treated with L27-11 appear to be morphologically similar in appearance to the HT61 treated cells presented in this chapter (Figure 15). The authors in this study also note that the cellular response to L27-11 was supportive of a mechanism that inhibited the incorporation of lipopolysaccharide, (LPS), into the outer membrane[230] and it is plausible that HT61 could also cause similar effects.

2.4.5 Conclusions, Experimental Limitations and Future Work

The findings of this chapter demonstrate that while HT61 is highly effective against non-dividing cultures of *S. aureus* and *S. epidermidis*, this is not the case with other bacterial species. Moreover, while HT61 demonstrated significant *in vitro* activity towards biofilms of *S. aureus*, *A. baumannii, P. aeruginosa* and *S. epidermidis*, the large range of effective concentrations, (32 μg ml^{-1} to 512 μg ml^{-1}), means that it is not clear whether the mechanism of action is identical across species. In addition, for many of the species tested, HT61 needed to be utilised at a concentration higher than 128 μg ml^{-1}. This is an important limitation to be aware of, primarily because these concentrations would be unattainable in a clinical setting. Secondly, it was found over the course of this chapter that HT61 would precipitate out of solution at these concentrations. This means that that bacteria were likely being treated with concentrations lower than intended. The only way to address this would be to alter the chemical structure of HT61 to increase its solubility and this would potentially alter its efficacy, possibly for the worse.

A further limitation of the antimicrobial susceptibility testing performed within this chapter is that it focuses on relatively naïve biofilms. Chronic infections are defined as those that last longer than three months[231], and subsequently the population dynamics of biofilms found in these cases will be different to those of a biofilm grown for 72 hours. If the metabolic inactivity of susceptible cells is higher in these chronic infections, the efficacy of HT61 could be higher, particularly when compared to more typical treatments. A related limitation is that clinical infections are polymicrobial. Polymicrobial biofilms exhibit markedly different phenotypic characteristics, including reduced antimicrobial susceptibility when compared to single species counterparts[145,148]. To address this concern, Chapter 4 describes the development and phenotypic characterisation of a dual-species biofilm model of *P. aeruginosa* and *S. aureus*.

Furthermore, there is no common theme that can be used to identify whether HT61 will be effective against certain bacterial species, although it does seem to be generally less effective against Gram-negative species. With this in mind it would be interesting to characterise HT61 against other species of bacteria, such as the other members of the ESKAPE cohort, *E. faecium* and a member of the *Enterobacter spp.*, such as *E. cloacae,* as well as other clinically relevant pathogens such as *S. pneumoniae*, implicated in pneumonia and otitis media[66], or *M. tuberculosis*, the causative agent in tuberculosis[232]. As

an addition, testing HT61 against isolated persister cell populations, which are defined by metabolic dormancy[121], would be a useful future point of investigation.

Additionally, the cellular response to HT61 is not yet fully understood. This is partly because the antibacterial mechanism of quinoline compounds in general is poorly understood. For example, quinoline compounds have shown efficacy as dispersal agents of *S. aureus* and *S. epidermidis* biofilms[233], as well as antimalarial[234], anti-inflammatory[235], and even anti-viral agents[236]. The highly broad-spectrum nature of quinoline activity suggests that their mechanism of action is likely specific to the various sub-groups and derivations attached to the quinoline backbone and not the result of a general mechanism. In an attempt to characterise the cellular response to HT61, a comparative proteomic analysis is detailed in Chapter 3 of this thesis.

In conclusion, the effectiveness of HT61 towards biofilm cultures is incredibly varied and depends on both growth phase and bacterial species. It was most effective against biofilm cultures of *S. aureus* but demonstrated significant *in vitro* activity towards biofilms of *A. baumannii* and *P. aeruginosa*, albeit when utilised at a high concentration. However, this variability simply highlights the difficulties faced during treatment of biofilm associated infections and the need for increased antibiotic development.

Chapter 3

Proteomic Response of Planktonic and Biofilm Cultures of *S. aureus* to HT61

3 Proteomic Response of Planktonic and Biofilm Cultures of *S. aureus* to HT61

3.1. Introduction

Antimicrobials exert their function by interfering with cellular processes, leading to either the inhibition of cell growth or the death of the cell. HT61 has been shown to exert its action by causing permeabilisation of the cell membrane[11,12]. However, an interesting facet of its activity is that it appears to be most effective against stationary phase cultures of *S. aureus* and *S. epidermidis*, as demonstrated in the published literature and the previous chapter[11–13]. The increased efficacy against stationary phase bacteria has been linked to the composition of the bacterial cell membrane: specifically, that HT61 preferentially interacts with membranes containing a greater proportion of anionic phospholipids[13]. However, the exact cellular response to HT61 has not been investigated. Understanding which cellular processes change following treatment, and ultimately how these process link to membrane permeabilisation, is extremely important. Firstly, the information could be useful for the development of future antimicrobials. Secondly, it could highlight processes and genes that are important for the evolution of resistance mechanisms. Understanding both of these factors would facilitate the creation and development of optimal future antimicrobial compounds.

One possible approach to this problem is to employ a proteomic based method that can quantify the expression of individual proteins within a cell. By calculating differences in protein expression following antimicrobial treatment, changes in cellular pathways and processes can be identified and the information can be used to infer a mechanism of action[237]. The gold standard for protein quantification is mass spectrometry. In liquid chromatography mass spectrometry, (LC/MS), peptide fragments suspended in a liquid are separated from each other and ionised using a method such as electrospray ionisation. The mass to charge ratio of the ionised fragments is then measured[238]. While samples can be labelled, for example with stable isotopes such as ^{15}N, or isobaric tags for relative and absolute quantitation (iTRAQ)[239], label-free technologies are also available. Label-free methodologies reduce the number of sample preparation steps, which in theory, reduces the introduction and likelihood of downstream errors, resulting in accurate proteome coverage and quantitation. Both labelled and label-free LC/MS methods are frequently used in bacterial proteomic investigations. A selection of successful examples include

determining the proteomic profiles of fluoroquinolone resistant *S. aureus*[240], understanding how biofilm growth[219] and nitric oxide treatment[241] influence the proteome of *S. pneumoniae,* and evaluating the effect of oxacillin treatment on cultures of MSSA and MRSA[242].

The goal of this chapter was to use label-free ultra-performance liquid chromatography-mass spectrometry$^{\text{Elevated Energy}}$, UPLC/$MS_E$, to address two specific aims. The first aim was to identify the proteomic differences separating planktonic cultures (early and late stationary phase) of *S. aureus* UAMS-1 from biofilm cultures. The second aim was to understand how HT61 treatment influenced the proteome of *S. aureus* UAMS-1, depending on whether it was treated planktonically (both early and late stationary phase) or as a biofilm culture. By combining the results of these two separate investigations, it was hoped that a more in depth understanding of HT61's mechanism of action could be obtained that informed whether there is a proteomic based explanation for the compounds improved efficacy towards stationary phase planktonic cultures.

3.2. Materials and Methods

3.2.1. Selection of Appropriate Reference Proteome

3.2.1.1. Short Read Whole Genome Sequencing

An overnight culture of *S. aureus* UAMS-1 was grown as previously described and streaked onto a TSA plate, which was incubated for 24 hours at 37 °C. A single colony was isolated and streaked onto a second TSA plate and incubated at 37 °C for 24 hours. Following confirmation that the growth was pure and free of contamination, the entire plate growth was collected into a tube and sent for DNA extraction and short read whole genome sequencing, courtesy of MicrobesNG (University of Birmingham). Sequencing was performed using an Illumina HiSeq 2500, with a target coverage of 60X using 2 x 250 bp paired end reads.

3.2.1.2. DNA Extraction and Purification

Genomic DNA of *S. aureus* was extracted using the PureLink Genomic DNA Mini Kit (Thermo-Fisher, UK). Briefly, an overnight culture of *S. aureus* UAMS-1 was centrifuged at 2500 *x g* for 15 minutes to pellet the cells. The cell pellet was resuspended in 200µl Hanks Balanced Salt Solution (HBSS), supplemented with Lysostaphin (Sigma-Aldrich, UK) at a final concentration of 100 µg ml^{-1}. The culture was incubated at 37 °C for 1 hour. 20 µl Proteinase K and 200 µl of PureLink Genomic Lysis/Binding Buffer was added to continue the cell lysis and gently mixed via inversion to prevent shearing of genomic DNA. The lysate was incubated at 55 °C for 1 hour. Following incubation, 20 µl of RNase A was added, mixed by inversion and incubated at room temperature for 2 minutes. Finally, 200 µl of 100% ethanol was added and mixed by inversion. The lysate was then added to a PureLink Spin Column and centrifuged at 10, 000 *x g* for 1 minute to bind the DNA to the column. 500 µl of Wash Buffer 1 was added, followed by a second centrifugation at 10, 000 *x g* for 1 minute. 500 µl of Wash Buffer 2 was added and the sample centrifuged at 16, 000 *x g* for 3 minutes. The collection tube was placed in a clean microcentrifuge tube and 200 µl PureLink Genomic Elution Buffer was added. The sample was incubated at room temperature for 1 minute, prior to centrifugation at 16, 000 *x g* for 1 minute. The elution step was then repeated with an additional 200 µl PureLink Genomic Elution Buffer.

The DNA was then further purified using a phenol chloroform extraction and ethanol precipitation stage. 400 µl of phenol:chloroform:isoamyl alcohol (25:24:1) (Thermo-Fisher, UK) was added and mixed gently by inversion for 5 minutes. The sample was centrifuged for 5 minutes at 16, 000 *x g* and the upper aqueous phase removed and transferred to a fresh tube. 20 µg glycogen, 100 µl 7.5 M NH_4OAc and 750 µl 100% ethanol was added and the sample placed at -20 °C overnight. Following ethanol precipitation, the sample was centrifuged for 30 minutes at 16, 000 *x g* to pellet the DNA and carefully rinsed with 150 µl of 70% ethanol. Following a second centrifugation at 16 000 *x g* for 2 minutes, the supernatant was removed and a final centrifugation step performed at 16, 000 *x g* for 30 minutes. The gDNA pellet was dried at room temperature for 15 minutes and resuspended in 30 µl 10 mM Tris-HCl with 50 mM NaCl. Isolated DNA was quantified using a Nano-Drop 2000 spectrophotometer.

3.2.1.3. Long Read Whole Genome Sequencing

In addition to short read sequencing, long read sequencing was performed using the Oxford Nanopore MinION Sequencer (Oxford Nanopore Technologies, UK).
400 ng of DNA was adjusted to a final volume of 7.5 µl with nuclease free water and gently mixed. 2.5 µl Fragmentation Mix was added and incubated at 30 °C for 1 minute and 80 °C for 1 minute in two separate heat blocks. 1 µl of rapid adapters was added to the sample mixture and incubated at room temperature for 5 minutes. The prepared library was stored on ice until ready to sequence.

In a separate microcentrifuge tube, 34 µl sequencing buffer, 25.5 µl Library Loading Beads, 4.5 µl Nuclease free water was thoroughly mixed. The entire 11 µl of the DNA library was added and gently mixed by inversion, ready for loading onto the sequencer.

To prime the flow cell, bubbles were removed from the priming port. 800 µl of priming mixture (consisting of 30 µl Flush Tether and 1000 µl Flush Buffer) was added to the flow cell via the priming port and incubated at room temperature for 5 minutes. The DNA library was loaded into the SpotON sample port in a dropwise fashion.

Sequencing was performed for 12 hours using the Rapid Sequencing MinKNOW protocol. Albacore 2.0 was used for live basecalling. Following sequencing, adapter sequences were trimmed using Porechop (https://github.com/rrwick/Porechop) with default settings.

3.2.1.4. Genome Assembly, Annotation and Genome Comparison

A *de novo* hybrid assembly of *S. aureus* UAMS-1 was performed using Unicycler with default settings[243] and annotated using PROKKA[244]. The assembled genome was aligned and compared to several published *S. aureus* genomes (see Table 7) using RAST[245–247]. A visualisation of this comparison is presented in the appendices for this chapter. Based on this information and evidence from the published literature[248], *S. aureus* MN8 was chosen as the most suitable reference for proteome analysis.

Table 7: Published *S. aureus* genomes and accession numbers.

Strain	Accession Number
NCTC 8325	GCA_000013425.1
MRSA252	GCA_000011505.1
MN8	GCF_000160195.1
Newman	GCA_000010465.1

3.2.2. Lysis Optimisation and Preliminary Proteome Quantification

A selection of lysis buffers were tested to maximise protein yield from cultures of *S. aureus* UAMS-1. Overnight cultures were grown in 15 ml TSB and 1 ml was aliquoted to 3 separate microcentrifuge tubes. Cultures were centrifuged at 2500 *x g* to pellet the cells, rinsed twice with 0.1M triethylammonium bicarbonate (TEAB) and re-suspended in either 0.1M TEAB, 0.1M TEAB and 4 M guanidine hydrochloride (G-HCl) or 0.1 M TEAB and 4 M G-HCl and 100 μg lysostaphin (Sigma-Aldrich). Suspensions were incubated at 37 °C for 30 minutes and mechanically lysed using a TissueLyser LT (Qiagen) (50 Hz, 20 cycles x 30 seconds, 30 seconds on ice between sessions).

The extracted protein was quantified using a Bradford Assay. Briefly, a set of bovine serum albumen (BSA) standards were prepared in each cell lysis buffer at concentrations of 0, 25, 125, 250, 500, 750, 1000, 1500 and 2000 μg ml^{-1}. 10 μl of each protein standard

was combined with 300 µl of the detergent compatible Bradford Assay reagent (Thermo Fisher) and the absorbance measured at 584 nm using a spectrophotometer (BMG Omega) to construct a standard curve of protein concentrations. 10 µl of each unknown protein fraction, as well as 1/10 and 1/100 dilutions of each fraction, was then mixed with the Bradford Assay reagent and the absorbance at 584 nm recorded. To calculate the concentration of protein, each absorbance value was substituted into the equation of the standard curve.

3.2.3. Bulk Bacterial Culture for Staphylococcal Proteome Isolation

The effect of HT61 on the proteome of planktonic, (early stationary and late stationary phase) and biofilm cultures of *S. aureus* UAMS-1 was assessed using label-free ultra-performance liquid chromatography-mass spectrometry$^{\text{Elevated Energy}}$, UPLC/$MS_E$. To ensure sufficient yields of protein, the bacterial cultures were performed in larger volumes than previously described. For the early stationary phase treatment groups, 3 overnight cultures of *S. aureus* UAMS-1 were initiated in 15 ml of TSB for 24 hrs at 37 °C, 120 rpm. 1 ml of each culture used to inoculate a separate 40 ml of fresh TSB. HT61 was supplemented directly for a final concentration of either 4 µg ml^{-1}, (Sub-MIC) or 16 µg ml^{-1}, (MIC). Cultures were incubated for a further 12 hours at 37 °C, 120 rpm. To maximise the protein yield for the MIC treatment group, the entire 15 ml of each biological replicate overnight culture was distributed to 15 sets of fresh TSB, supplemented with 16 µg ml^{-1} HT61 and following incubation, each biological replicate was pooled together for analysis.

For the late stationary phase treatment group, nine overnight cultures of *S. aureus* were initiated in 40 ml of TSB and incubated for 120 hrs at 37 °C, 120 rpm. The cultures were then centrifuged at 2500 x *g* for 15 minutes and the cell pellet was re-suspended in 40 ml of HBSS, or HBSS supplemented with HT61 at a final concentration of either 4 µg ml^{-1} or 16 µg ml^{-1}. Cultures were incubated for a further 12 hours at 37 °C, 120 rpm.

Biofilms were cultured as previously described. Briefly, nine overnight cultures were used to inoculate fresh TSB with 10^6 CFU ml^{-1} of *S. aureus*. Each inoculum was used to inoculate 6 wells of a 6 well plate, (Thermo-Scientific) with 4 ml each, for a total of 9 x 6 well plates. Biofilms were grown for 72 hours at 37 °C, 50 rpm, with fresh media replacements every 24 hours. Following 72 hours of incubation, media was replaced with

either fresh TSB or TSB supplemented with either 4 μg ml^{-1} or 16 μg ml^{-1} HT61 and grown for a further 12 hours at 37 °C, 50 rpm.

3.2.4. Proteome Isolation

To harvest the bacterial cultures, planktonic suspensions (log phase and stationary phase cultures), were centrifuged at 2500 x *g* for 15 minutes. Biofilms were rinsed twice with 4 ml HBSS and harvested with a cell scraper into 1 ml of HBSS. Biofilm suspensions from 6 wells were pooled and also centrifuged at 2500 x *g* for 15 minutes.

Following centrifugation, cell pellets were rinsed twice with 0.1 M (TEAB) prior to resuspension in 1 ml of 0.1 M TEAB and 4 M G-HCl and incubation at 37°C for 30 minutes. Cell suspensions were added to Lysing Matrix B tubes (MP Biomedicals) and mechanically lysed using a TissueLyser LT (Qiagen) (50 Hz, 20 cycles x 30 seconds, 30 seconds on ice between sessions). Following mechanical lysis, proteins were purified by adding the cell lysates to 9 ml of ice cold ethanol and incubated overnight at -20 °C. Samples were centrifuged at 12, 000 x *g* for 10 minutes and the pellet containing the cellular protein fraction resuspended in 100 μl 0.1 M TEAB and 0.1% Rapigest SF Surfactant (Waters).

3.2.5. Fluorometric Protein Quantification

Samples were quantified with a Qubit fluorometer (Thermo Fisher). After calibration with a set of known standards, each protein lysate was diluted 1:100 with Qubit working solution and the total concentration of protein determined. Samples with a protein concentration higher than 26 μg ml^{-1} (the detectable limit of the device), were diluted 1:10 in 0.1M TEAB and re-analysed.

3.2.6. Validation of Proteome Extraction using SDS-PAGE

To validate each protein sample, 40 μg of each proteins in each sample were separated according to size using SDS-Gel Electrophoresis. Samples were mixed with NuPAGE LDS Sample Buffer (4 X) and NuPAGE Reducing Agent (10X) to a final volume of 10 μl and heated at 70 °C for 10 minutes. The X Cell SureLock Mini Cell (Thermo Fisher) was used for electrophoresis. A NuPAGE 4-12% Bis-Tris Protein Gel was fitted into the cell system and the inner and outer chambers filled with MOPS Running Buffer (Thermo

Fisher). 500 µl of NuPAGE Antioxidant was added to the inner chamber buffer. Samples were loaded into the gel and run for 50 minutes at 200V. Following electrophoresis, gels were stained with Coomassie Blue (Bio-Rad) for 24 hours and destained with Destaining Solution (Bio-Rad) overnight.

3.2.7. Sample Preparation for Mass Spectrometry

3.2.7.1. Protein Reduction, Alkylation and Digestion

Volume of sample equivalent to 40 µg of protein was made up to a final volume of 300 µl with additional 0.1 M TEAB and briefly vortexed. Dithiothreitol, (DTT) was added to each sample at a final concentration of 2.5 nM (0.8 µg per sample) and incubated at 56 °C for 1 hour to allow for complete reduction of the protein structure and disassembly of disulphide bridges. Samples were then alkylated to prevent disulphide reformation via the addition of iodoacetamide at a final concentration of 7.5 mM. Samples were incubated at room temperature in the dark for 30 minutes. Enzymatic protein digestion was performed by the addition of 0.5 µg trypsin per sample and incubated overnight at 37°C. Following enzymatic digestion, trifluoroacetic acid was added to a final concentration of 0.5% prior to a final 37 °C incubation for 30 minutes. Samples were centrifuged at 13, 000 *x g* for 10 minutes and lyophilised overnight using a Thermo SpeedVac (Thermo-Fisher). Lyophilised samples were resuspended in 100 µl 0.5% acetic acid in preparation for C18 Solid Phase Extraction.

3.2.7.2. C18 Solid Phase Extraction

C18 solid phase extraction plates (Thermo-Fisher) were prepped with 100 µl of methanol and left for 30 seconds. This was followed by the addition of 100 µl of 80% acetonitrile and 0.5% acetic acid. Plates were centrifuged at 100 x *g* for 1 minute. Two rinses of 100 µl of 0.5% acetic acid were performed on each well, with a further 2 minutes of centrifugation at 100 x *g* following each rinse. Samples were concentrated using a Thermo Speed Vac until the liquid phase had evaporated fully and the sample was resuspended in 100 µl of 0.5% acetic acid. The total volume of each sample was added to individual wells of the SPE plate and peptides were bound to the solid phase extraction disks by centrifugation at 150 x *g* for 2 minutes. Contaminants were removed with 2 rinses of 200 µl 0.5% acetic acid, with each rinse followed by centrifugation of 2 minutes at 150 x *g*. Finally, peptides were eluted from the C_{18} disks by addition of 75 µl of 80% acetonitrile

and 0.5% acetic acid, which was allowed to wet the disks for 30 seconds prior. Eluent was flowed through using a vacuum pump. A second elution of 75 µl of 80% acetonitrile and 0.5% acetic acid was performed for a final total sample volume of 150 µl.

Prior to sample analysis, each sample was concentrated using the Thermo SpeedVac Concentrator and sent to the Centre for Proteomic Research (University of Southampton) for final sample preparation and UPLC/MS_E, using a Waters Synapt HDMS Mass Spectrometer.

3.2.8. Data Analysis

Each protein data set was normalised to the total concentration of the top 200 most abundant proteins. For quantitative analysis, identified proteins were filtered using the following criteria: protein must be present in all three biological replicates of a treatment group, false discovery rate (FDR) ≤ 1%, sequence coverage ≥ 5%. For qualitative analysis, proteins were filtered with the following criteria: protein must be present in at least two of three biological replicates, FDR between 1% and 4%. Proteins were categorised using a combination of UniProt database searches (www.uniprot.org, accessed between 01/05/18 and 07/07/18) and gene ontologies obtained from the GeoPANTHER tool[249]. Pathway analysis and interaction networks were determined using the STRING database, version 10.5[250].

To identify if a protein was differentially expressed, ratios between the normalised protein quantities were calculated. Proteins were classed as differentially expressed if the ratio was ≥ 1.5 for increased expression or ≤ 0.667 for decreased expression, as per previous label free proteomic studies[240]. Statistical significance between protein abundances for control and treated groups was calculated using a one-way student t-test in Microsoft Excel ($\alpha \leq 0.05$). A one tailed t-test was chosen as the differential expression on a per protein basis is by definition, in one direction. Therefore, a one tailed test would calculate the significance of the data occurring in the predicted direction i.e. increased or decreased expression.

Comparisons were made between untreated early stationary phase planktonic cultures and untreated biofilm, untreated late stationary phase planktonic cultures and untreated biofilm and untreated early and late stationary phase planktonic cultures. To discern the effect of

HT61, comparisons were made between treated and untreated populations of like growth conditions.

3.3. Results

3.3.1. Optimisation of *Staphylococcal* Whole Proteome Extraction

To optimise the extraction protocol, 3 extraction buffers were tested on a 10 ml overnight planktonic culture of *S. aureus* UAMS-1 and the extracted protein was quantified using Bradford's Assay. The buffers utilised were 1) 0.1M TEAB, 2) 0.1M TEAB + 4 M G-HCl and 3) 0.1M TEAB + 4 M G-HCl + 100 μg ml^{-1} lysostaphin. Addition of 4 M G-HCl resulted in a slight decrease in protein yield (0.1 M TEAB: 0.447 μg μl^{-1}; 0.1 M TEAB + 4 M G-HCl: 0.395 μg μl^{-1}). However, the addition of 100 μg μl^{-1} lysostaphin reduced protein yield even further. This seems counterintuitive but it is possible that the protein concentration was actually so high that the Bradford reagent could not be completely re-solubilised, leading to an underestimation. For validation, 10 μg of each sample was analysed using SDS-PAGE, as per Figure 17. Similar banding patterns were observed across all sample preparations indicating a range of protein weights. The only exception is the presence of a high intensity band just below the 30 kDa marker, which likely represents the added lysostaphin. While 0.1 M TEAB in isolation gave slightly higher yields than when supplemented with 4 M G-HCl, as banding patterns were clean across both conditions, the buffer was used with 4 M G-HCl was chosen as the additional denaturant would likely be beneficial for lysis of the biofilm cultures.

Table 8: Impact of lysis buffer on the yield of extracted protein from plankonic cultures of *S. aureus* UAMS-1

Extraction Buffer	Protein (μg μl^{-1})
0.1M TEAB	0.447
0.1M TEAB + 4 M Guanidine HCl	0.395
0.1M TEAB + 4 M Guanidine HCl + 100μg ml^{-1} Lysostaphin	0.086

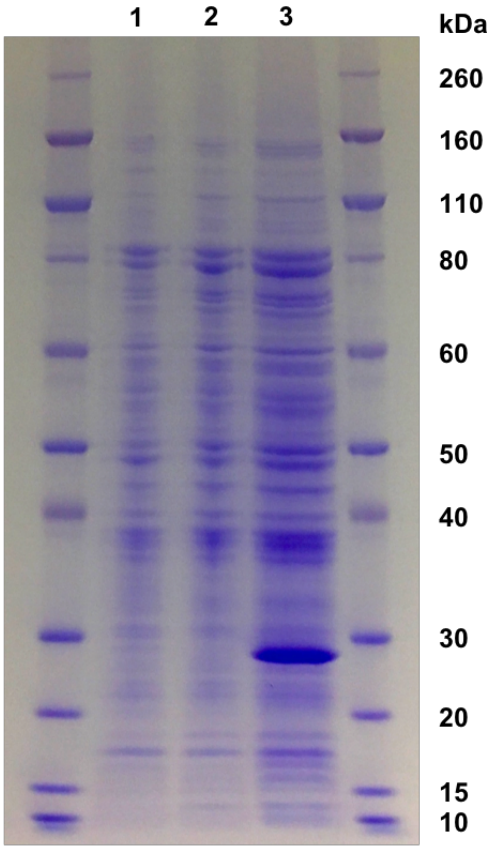

Figure 17: SDS PAGE of *S. aureus* UAMS-1 cell lysates, following extraction with 3 different buffers

1) 0.1 M TEAB, 2) 0.1 M TEAB + 4 M G-HCl, 3) 0.1 M TEAB + 4 M G-HCl + 100 μg ml^{-1} lysostaphin. 10 μg loaded in each sample lane. Stained with Coomassie Blue (Bio-Rad, UK). Outside lanes contain Novex Sharp Prestained Protein Standards (Thermo Scientific). The addition of lysostaphin can be identified by the high intensity band in lane 3, below 30 kDa.

3.3.2. Extraction of Planktonic and Biofilm Proteomes of *Staphylococcus aureus* Following Treatment with HT61

Following optimisation of the extraction procedure, larger cultures were utilised for the actual extraction. Planktonic cultures were cultured in 40 ml, while each biofilm sample consisted of 6 pooled biofilms from a 6 well plate. In total, 27 proteomes were isolated consisting of untreated, sub-MIC HT61 treated and MIC HT61 treated early stationary, late stationary and biofilm cultures, with 3 biological replicates for each.

Following extraction, protein concentrations were determined fluorometrically using a Qubit fluorometer, which grants higher degrees of accuracy than spectrophotometric methods (Table 9). To validate the extraction and confirm sufficient quantities of protein for downstream analysis, 40 μg of each sample was analysed using SDS-PAGE. Images of gels for early stationary samples, late stationary phase samples and biofilm samples are depicted in Figure 18, Figure 19 and Figure 20, respectively.

All gels showed sufficient quantities of protein and banding patterns that encompassed a wide range of molecular weights. No differences in expression were visible between any groups using this data, although due to the resolution of this method, only very large changes would be noticeable. For the early stationary phase samples, Figure 18, samples treated with 16 μg ml^{-1} HT61 formed a smear pattern across the entirety of the gel. Due to the predicted membrane specific action of HT61, this smear could be explained by lipid contamination as a result of membrane permeabilization. Similar banding patterns were also observed in the late stationary samples, Figure 19, even across samples not treated with HT61. Stationary phase samples could contain a higher proportion of dead (i.e. lysed) cells, which would explain increased lipid contamination within the sample.

A general observation is that the gels containing the planktonic samples are overloaded with protein. This suggests that their concentration was greatly underestimated. Reducing the protein concentration loaded into each well may have clarified the banding pattern for these samples but due to time constraints, this was not possible. If more time had been available, the gel running conditions could have been optimised using different sample dilutions. Furthermore, while these gels served the purpose of confirming the presence of protein, they yield little quantitative value. Protein samples could have been normalised

between certain groups (e.g. planktonic and biofilm), which would have allowed for clearer visualisation of proteins that were altered in expression.

After validation, samples were further processed and subjected to UPLC/MS_E analysis.

Table 9: Protein concentration of samples for mass spectrometry, as determined via Qubit

Protein concentrations are given in μg $μl^{-1}$

Sample		**Protein Concentration (μg $μl^{-1}$)**		
		Biological Replicate 1	Biological Replicate 2	Biological Replicate 3
Early Stationary	Untreated	0.803	0.806	0.793
	4 μg ml^{-1} HT61	0.776	0.786	0.787
	16 μg ml^{-1} HT61	0.824	0.857	0.917
Late Stationary	Untreated	0.927	0.805	0.897
	4 μg ml^{-1} HT61	1.017	1.067	0.823
	16 μg ml^{-1} HT61	0.947	0.857	0.788
Biofilm	Untreated	1.697	1.060	1.157
	4 μg ml^{-1} HT61	2.287	1.060	1.417
	16 μg ml^{-1} HT61	1.407	1.18	2.037

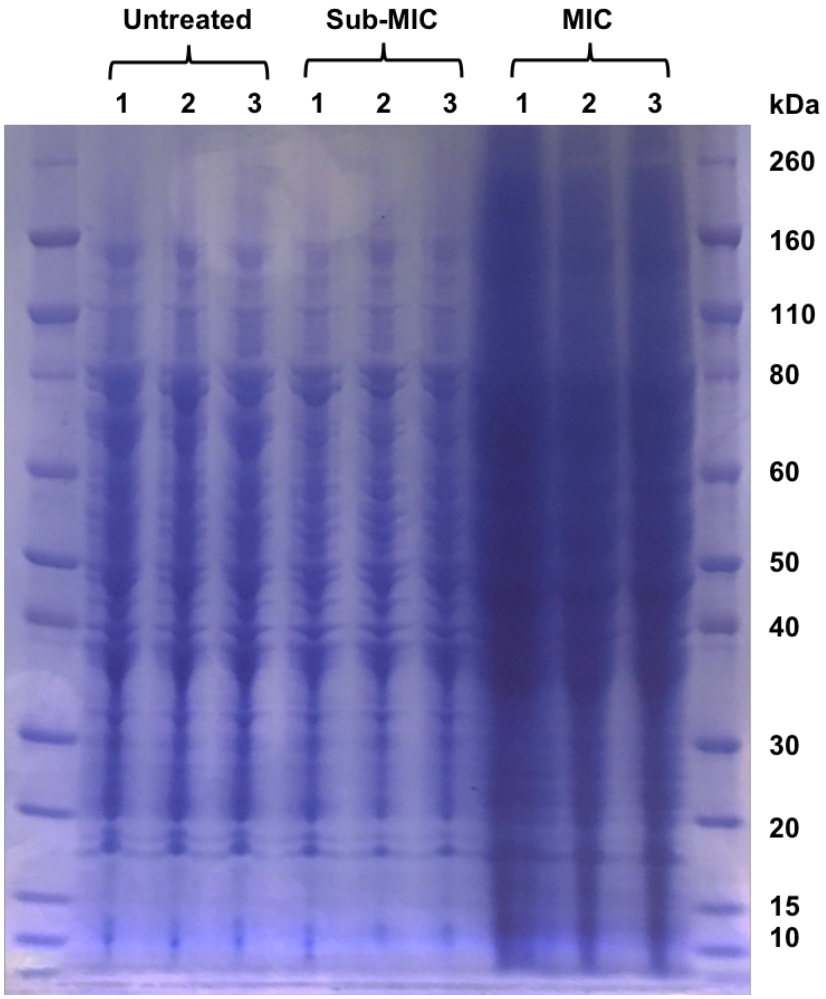

Figure 18: SDS PAGE of *S. aureus* UAMS-1 early stationary phase planktonic cell lysates

40 μg loaded in each sample lane. Stained with Coomassie Blue (Bio-Rad, UK). Outside lanes contain Novex Sharp Prestained Protein Standards (Thermo Scientific). Sub-MIC = 4 μg ml^{-1} HT61, MIC = 16 μg ml^{-1}.

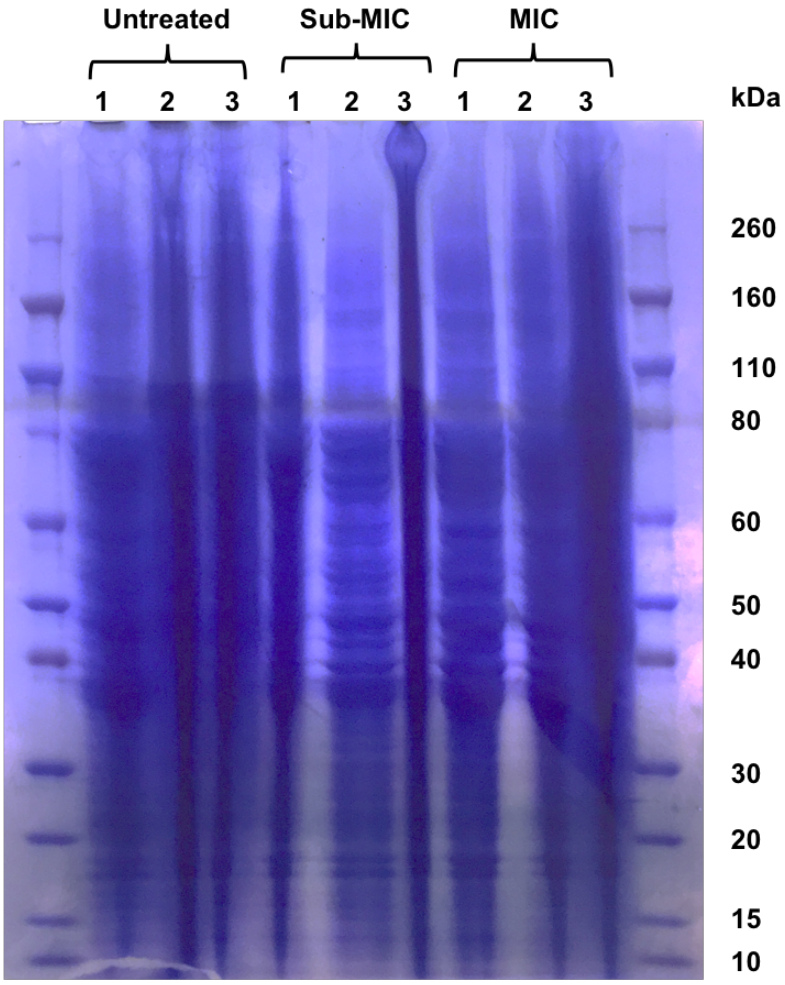

Figure 19: SDS PAGE of *S. aureus* UAMS-1 late stationary phase planktonic cell lysates

40 μg loaded in each sample lane. Stained with Coomassie Blue (Bio-Rad, UK). Outside lanes contain Novex Sharp Prestained Protein Standards (Thermo Scientific). Sub-MIC = 4 μg ml^{-1} HT61, MIC = 16 μg ml^{-1}.

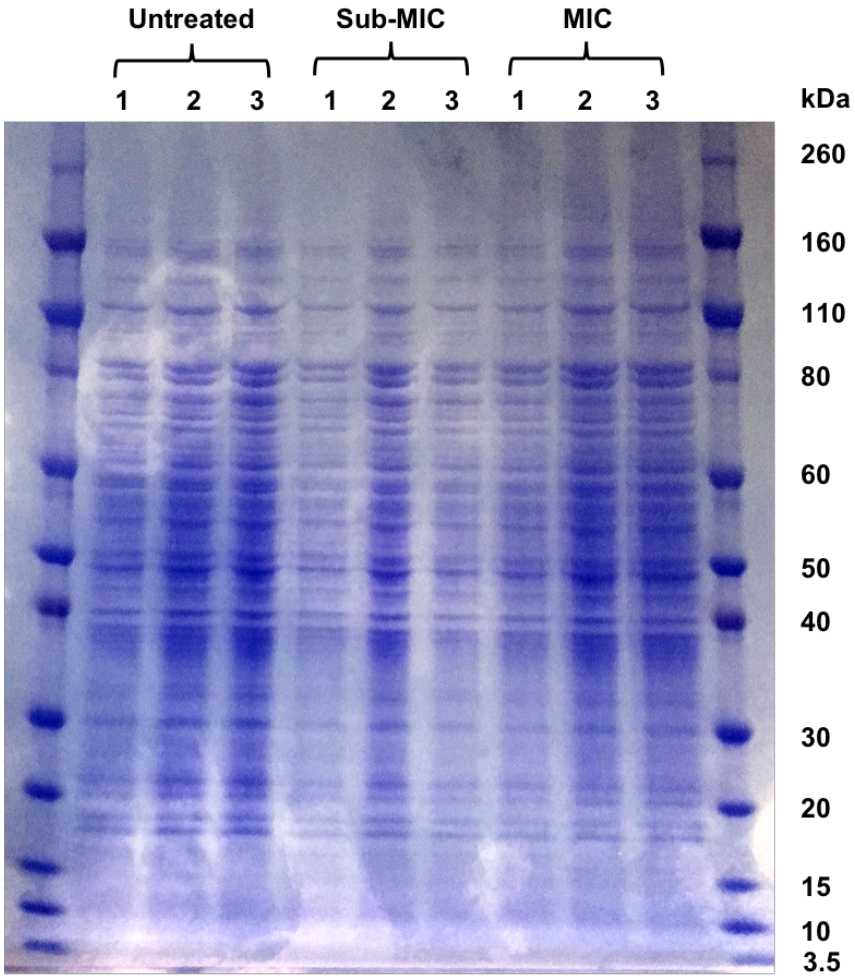

Figure 20: SDS PAGE of *S. aureus* UAMS-1 biofilm lysates

40 μg loaded in each sample lane. Stained with Coomassie Blue (Bio-Rad, UK). Outside lanes contain Novex Sharp Prestained Protein Standards (Thermo Scientific). Sub-MIC = 4 μg ml^{-1} HT61, MIC = 16 μg ml^{-1}.

3.3.3. Mass Spectrometry Results

Detected proteins were compared between early stationary planktonic, late stationary planktonic and biofilm cultures both with and without HT61 treatment. Samples were normalised by dividing the detected mass in ng by the total mass of the top 200 most abundant proteins within each group. Proteins were included for quantitative analysis if they were identified in all three biological replicates of a treatment group, with an FDR ≤ 1% and sequence coverage ≥ 5%. Fold changes were calculated between groups of interest and a protein was classed as differentially expressed if this ratio was ≤ 0.667 (down-regulation) or ≥ 1.5 (up regulation). A one tailed student's t-test was used to ascribe statistical significance to each comparison. Unless explicitly stated in the text, $p \leq 0.05$. Where appropriate, qualitative data was used to inform quantitative findings, with more lenient inclusion criteria (present in two of three biological replicates, FDR between 1% and 4%). Proteins utilised in quantitative analysis are included in the supplementary information of this chapter.

3.3.3.1. Proteomic Comparison of Early and Late Stationary Planktonic with Biofilm Cultures Demonstrates Large Scale Metabolic Changes

Proteomic profiles of untreated planktonic and biofilm populations were compared to identify differences between these modes of growth. Three comparisons were made: early stationary planktonic vs biofilm, early stationary planktonic vs late stationary planktonic and late stationary planktonic vs biofilm. Of these data, the only comparisons that were immediately valid were between early stationary planktonic and biofilm cultures as these were both grown in TSB opposed to HBSS for the late stationary phase planktonic cultures.

To briefly summarise the following mass spectrometry results sections, comparisons between the different growth states revealed distinct proteomic profiles. Biofilm growth of *S. aureus* was associated with the increased use carbohydrates and amino acids as sources of energy, implicated via upregulation of proteins associated with the tricarboxylic acid, (TCA) cycle, the arginine deiminase, (ADI), pathway and glycolysis/gluconeogenesis pathways. Protein synthesis appeared to be downregulated in biofilms compared to early stationary phase cultures, suggesting the adoption of a more dormant lifestyle. However, when compared to biofilms, late stationary phase cultures exhibited further reduced

expression of protein biosynthesis components, likely as a result of reduced nutrient availability. Finally, late stationary phase planktonic cultures appeared to show higher expression of proteins associated with cell wall biosynthesis and turnover when compared to both early stationary phase planktonic cultures and biofilm cultures, which could be implicated in cell survival.

3.3.3.2. Early Stationary Phase Planktonic vs Biofilm Cultures

Comparison between early stationary planktonic and biofilm cultures identified 500 proteins suitable for quantitative analysis, with 70 proteins upregulated and 117 proteins downregulated in biofilm cultures, (37.2 % of proteins differentially expressed) encompassing a wide range of cellular functions.

Expression of metabolic proteins was affected the most encompassing 34 (6.8%) upregulated proteins, and 30 (6%) downregulated proteins, suggesting large changes in the utilisation of specific metabolic pathways as a result of biofilm growth. Additional upregulated proteins of note included 8 miscellaneous proteins (2%), as well as 10 proteins (2%) that were uncharacterised.

For downregulated proteins, the second and third most abundant protein categories were associated with protein biosynthesis (28 proteins, 5.6%, including ribosomal proteins and elongation factors), suggesting greatly reduced translational capacity, and miscellaneous proteins (13 proteins, 2.6%, including various domains and other functional enzymes such as hydrolases), respectively.

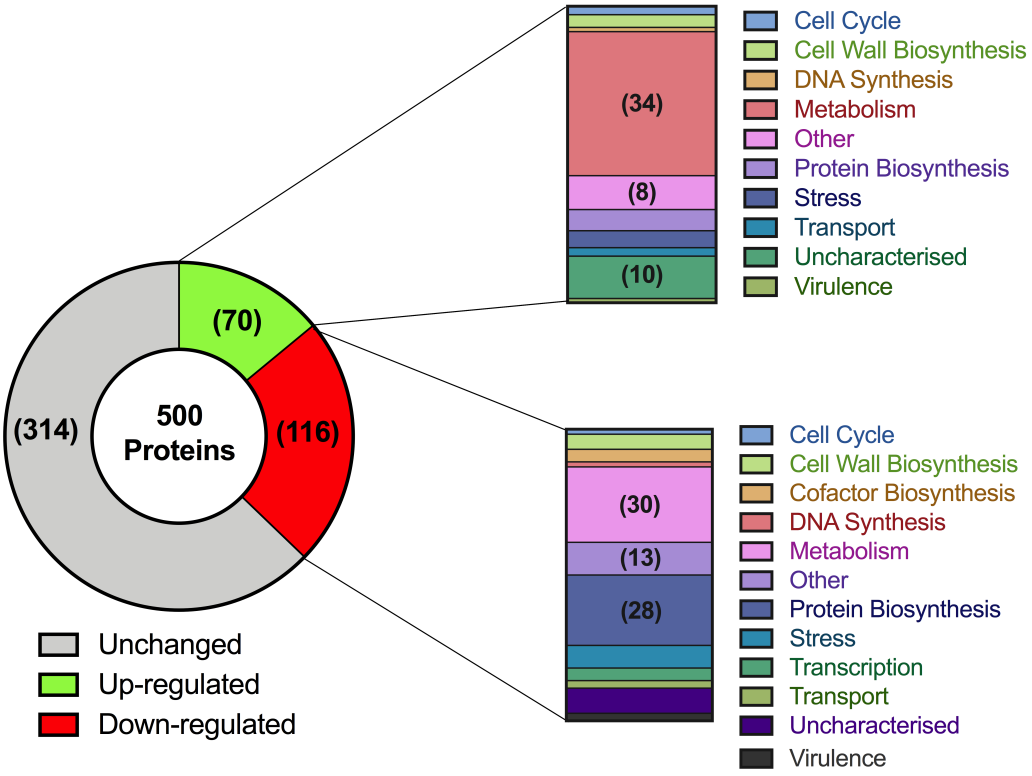

Figure 21: Summary of proteins identified for quantitative analysis between early stationary phase planktonic and biofilm cultures of *S. aureus* UAMS-1

Number of proteins identified for each category is displayed in brackets. For quantitative analysis, protein must satisfy the following selection criteria: present in all three biological replicates, FDR ≤ 1%, sequence coverage ≥ 5%. Proteins were classed as differentially expressed in Biofilm cultures if the ratio was ≥ 1.5 for increased expression or ≤ 0.667 for decreased expression. Functional categories assigned using GeoPANTHER and UniProt database searches.

Network analysis of the differentially expressed metabolic proteins revealed a number of protein-protein interactions, including enrichments of certain metabolic pathways.

For the upregulated proteins, these pathways included increased expression of proteins involved in the TCA cycle, glycolysis/gluconeogenesis and amino acid metabolism (Figure 22)**.** Proteins involved with the TCA cycle in particular were very highly upregulated, (average 5.85 fold increase) with the lowest increase occurring for 2-oxoglutarate dehydrogenase, SucA/OdhA (3.03 fold increase in biofilm) and the highest occurring for citrate synthase, CitZ (11.95 fold increase in biofilm). Increased expression of Aldehyde-Alcohol dehydrogenase, AdhE (1.58 fold increase) is indicative of either aerobic ethanol catabolism, producing acetyl-CoA, which could directly enter the TCA cycle, or anaerobic catabolism of acetyl-CoA. Aldehyde dehydrogenases, AldA and AldH, were upregulated 8.66 and 1.52 fold respectively, suggesting increased aldehyde stress[251], which could be a result of increased AdhE expression. Upregulation of AldA and AldH could also be

important for fuelling the TCA cycle as AldA expression has been associated with the conversion of L-lactaldehyde to pyruvate, (via lactate dehydrogenase), which can then be converted to Acetyl CoA to supply the TCA cycle[252]. Of proteins associated with amino acid metabolism, the upregulation of arginine deiminase *(*ArcA, 2.22 fold increase, facilitates conversion of L -arginine to carbamoyl phosphate), carbamate kinase (ArcC, 1.67 fold increase, synthesises carbamate and ATP from carbamoyl phosphate and ADP) and arginine repressor (ArgR, 1.76 fold increase, binds to upstream promoter regions), suggests activation of the ADI pathway, which is responsible for the creation of ATP via the catabolism of arginine and is a requirement during anaerobic growth[219,253].

An ornithine carbamoyltransferase was also upregulated 1.8 fold. Based on the initial protein annotations, this was identified as ArgF. However, ArgF is anabolic (facilitates the conversion of L-ornithine to L-citrulline during L-arginine biosynthesis), therefore its upregulation does not make sense when considered alongside upregulated proteins associated with arginine catabolism[253]. However, it does share high sequence similarity with the catabolic ornithine carbamoyltransferase, ArcB, so it is possible that it has been misidentified based on the peptides sequenced.

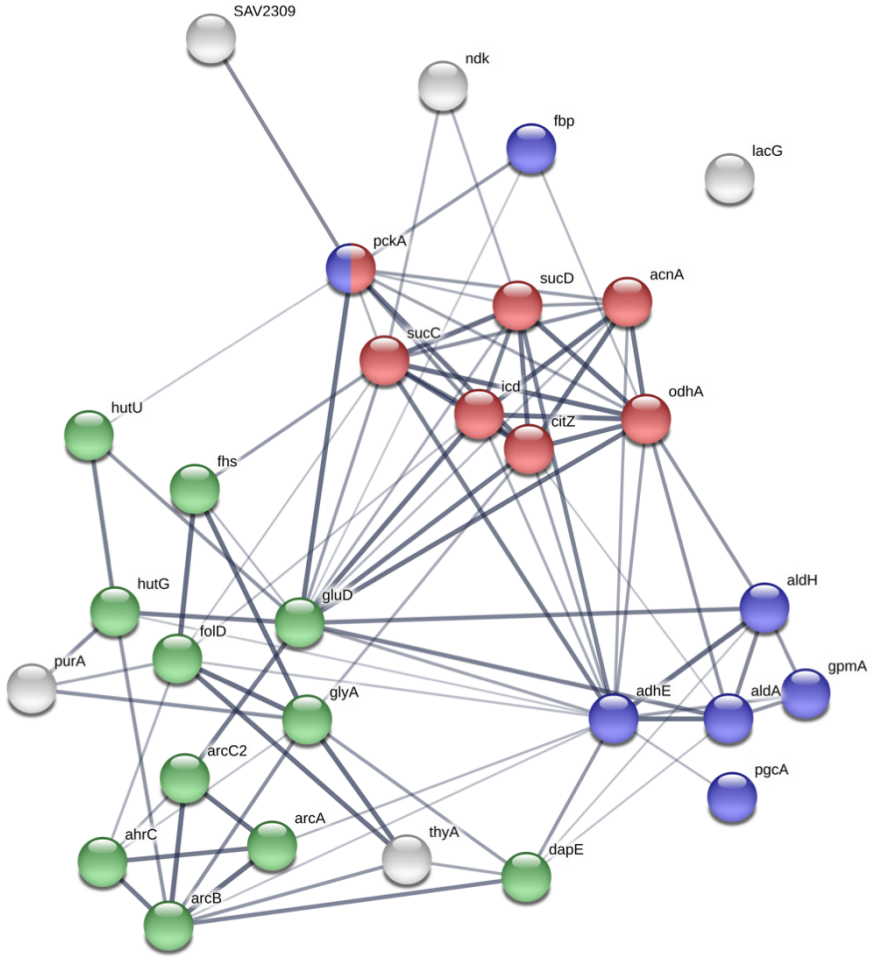

	Protein	Gene	Expression Ratio
Amino Acid Metabolism	Succinyl-diaminopimelate desuccinylase	HMPREF0769_1 1160 (dapE)	1.57
	Ornithine carbamoyltransferase	argF (arcB)	1.8
	Formimidoylglutamase	hutG	5.05
	Urocanate hydratase	hutU	1.82
	Arginine deiminase	arcA	2.22
	Arginine repressor	argR/ahrC	1.76
	Carbamate kinase	arcC	1.67
	Glutamate dehydrogenase	gluD	1.51
	Bifunctional protein FolD	folD	3.43
	Serine hydroxymethyltransferase	glyA	2.59
	Formate--tetrahydrofolate ligase	fhs	2.44
Glycolysis/Gluconeogenesis	Aldehyde dehydrogenase (NAD) family protein	aldA	8.66
	Phosphoglucomutase/phospho mannomutase_ alpha/beta/alpha domain II	HMPREF0769_1 0657 (pgcA)	1.74
	Aldehyde-alcohol dehydrogenase	adhE	1.58
	Aldehyde dehydrogenase	aldH	1.52
	Fructose-1_6-bisphosphatase class 3	fbp	2.91
	2_3-bisphosphoglycerate-dependent phosphoglycerate mutase	gpmA	2.24
TCA Cycle	Citrate synthase	citZ	11.95
	Phosphoenolpyruvate carboxykinase (ATP)	pckA	2.18
	Succinate--CoA ligase [ADP-forming] subunit beta	sucC	5.46
	Succinate--CoA ligase [ADP-forming] subunit alpha	sucD	5.07
	Aconitate hydratase	acnA	6.21
	Isocitrate dehydrogenase [NADP]	icd	3.36
	2-oxoglutarate dehydrogenase E1 component	sucA/odhA	3.03
Other Metabolic Processes	6-phospho-beta-galactosidase	lacG	2.93
	Probable malate:quinone oxidoreductase	mqo	1.65
	Formate dehydrogenase_ alpha subunit	HMPREF0769_1 0845 (SAV2309)	1.96
	Adenylosuccinate synthetase	purA	3.28
	Thymidylate synthase	thyA	1.56
	Nucleoside diphosphate kinase	ndk	4.74

Figure 22: STRING interaction network of upregulated metabolic proteins in biofilm cultures of *S. aureus* UAMS-1, compared to early stationary phase planktonic cultures

A number of proteins are present from amino acid metabolism pathways (green), Alcohol Metabolism and Gluconeogenesis pathways (blue) and the TCA cycle (red).

Network analysis of the downregulated metabolic proteins identified a decrease in expression of proteins associated with fatty acid and lipid metabolism (acyl carrier proteins, FabD, FabG, FabI and FabH, average 0.61 fold decrease, $p \leq 0.05$ for all comparisons except FabD, where $p = 0.104$) as well as decreased expression of other proteins associated with amino acid biosynthesis, such as the aforementioned ornithine carbamoyltransferase ArgF (0.53 fold decrease, $p = 0.179$). As ArgF is anabolic for arginine, this provides further evidence for activation of the ADI pathway in *S. aureus* UAMS-1 biofilms.

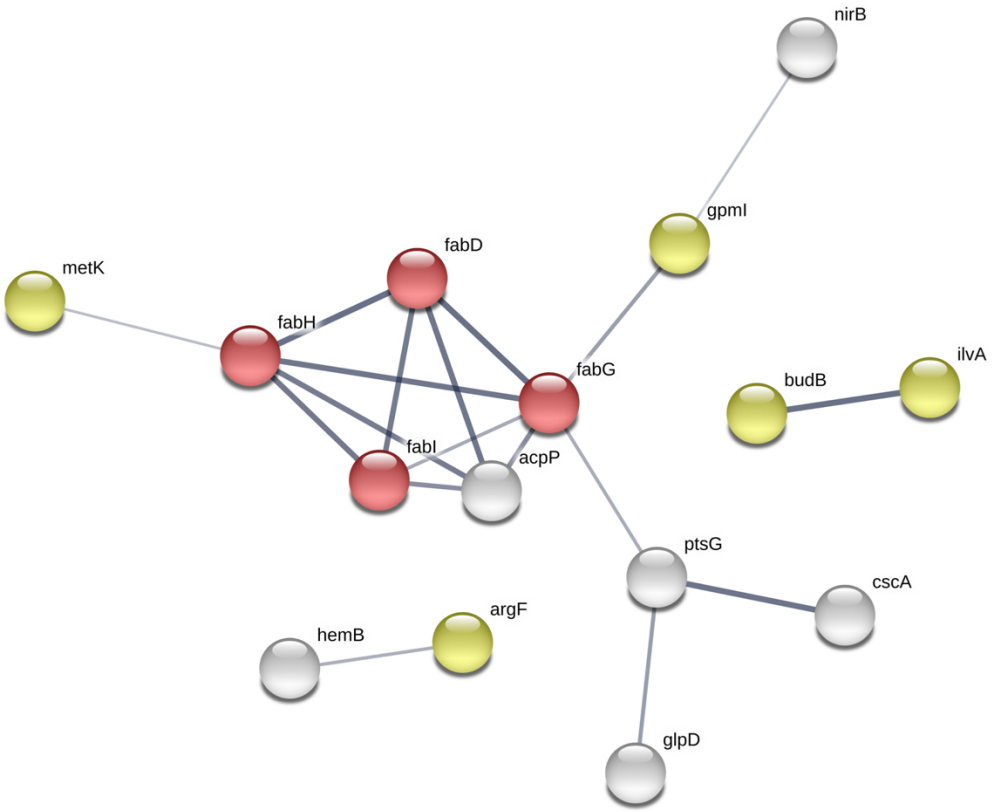

	Protein	Gene	Expression Ratio
Biosynthesis of Amino Acids	S-adenosylmethionine synthase	metK	0.58
	2_3-bisphosphoglycerate-independent phosphoglycerate mutase	gpmI	0.47
	Acetolactate synthase_ catabolic	alsS (budb)	0.41
	L-threonine dehydratase catabolic TdcB	ilvA	0.33
	Ornithine carbamoyltransferase	argF	0.53
Fatty Acid Metabolism	3-oxoacyl-[acyl-carrier-protein] synthase 3	fabH	0.62
	Enoyl-[acyl-carrier-protein] reductase [NADPH]	fabI	0.66
	3-oxoacyl-[acyl-carrier-protein] reductase	fabG	0.60
	Malonyl CoA-acyl carrier protein transacylase	fabD	0.54
Other Metabolic Processes	Nitrite reductase [NAD(P)H]_ large subunit	nirB	0.58
	Acyl carrier protein	acpP	0.59
	Delta-aminolevulinic acid dehydratase	hemB	0.65
	Glycerol-3-phosphate dehydrogenase	HMPREF0769_ 12478 (glpD)	0.66
	Invertase	HMPREF0769_ 11122 (cscA)	0.66
	PTS system_ glucose-specific IIBC component	ptsG	0.56

Figure 23: STRING interaction network of downregulated metabolic proteins in biofilm cultures of *S. aureus* UAMS-1, compared to early stationary phase planktonic cultures

A number of proteins are present from amino acid biosynthesis pathways (yellow) and fatty acid metabolic pathways (red).

3.3.3.3. Late Stationary Phase Planktonic vs Biofilm Cultures

Comparison of late stationary phase planktonic cultures to biofilm cultures identified 493 proteins suitable for quantitative analysis. Compared to early stationary phase planktonic cultures, a higher percentage of proteins in biofilm cultures were differentially expressed when compared to late stationary planktonic cultures (57.2%) equal to 119 proteins upregulated (24.1%) and 163 downregulated (33.1%) in biofilms (Figure 24). Differentially expressed proteins were again predominantly associated with metabolic functions and protein biosynthesis. Upregulated proteins included 46 (9.3%) metabolic proteins and 31 (6.3%) proteins associated with protein biosynthesis. Of the proteins associated with protein biosynthesis, upregulated proteins were mainly ribosomal proteins (22/31), whereas downregulated proteins were associated with tRNA modification and ligation of specific amino acids to tRNA molecules (10/21). Down regulated proteins also included 63 (12.8%) metabolic proteins and 21 (4.3%) proteins linked to protein biosynthesis).

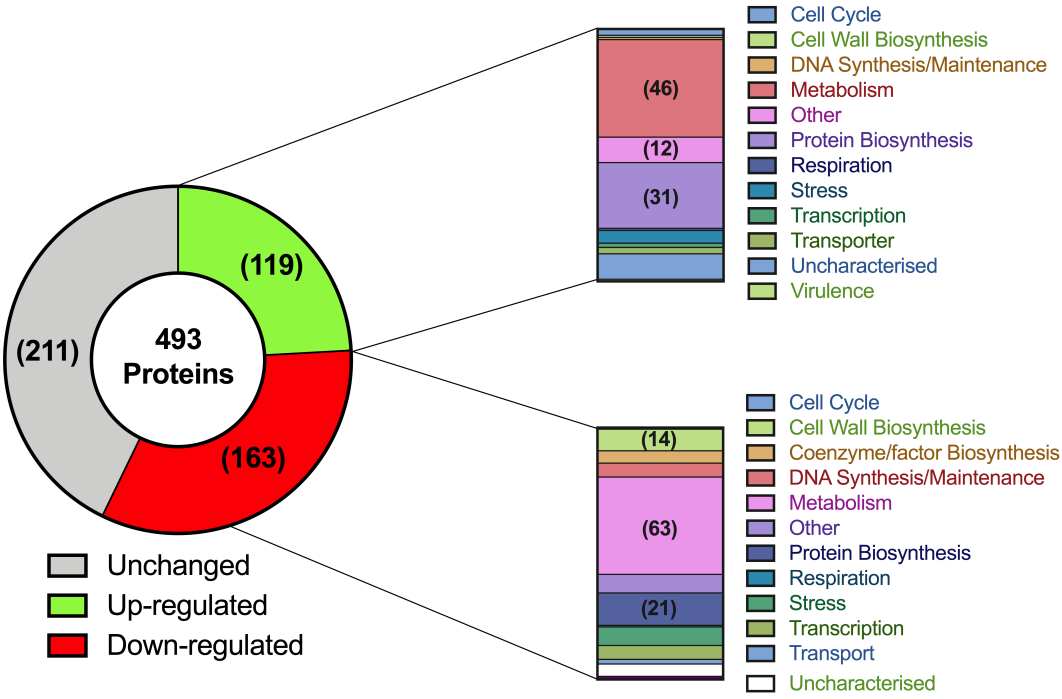

Figure 24: Summary of proteins identified for quantitative analysis between late stationary phase planktonic and biofilm cultures of *S. aureus* UAMS-1

Number of proteins identified for each category is displayed in brackets. For quantitative analysis, protein must satisfy the following selection criteria: present in all three biological replicates, FDR ≤ 1%, sequence coverage ≥ 5%. Proteins were classed as differentially expressed in Biofilm cultures if the ratio was ≥ 1.5 for increased expression or ≤ 0.667 for decreased expression. Functional categories assigned using GeoPANTHER and UniProt database searches.

When upregulated metabolic proteins were compared to late stationary phase planktonic cultures, similar findings as those found between early stationary phase planktonic cultures were identified. Specifically, biofilms of *S. aureus* presented increased expression of proteins associated with amino acid metabolism, gluconeogenesis and the TCA cycle (Figure 25). The ADI pathway was also increased in biofilms compared to late stationary planktonic cultures, with large fold increases in ornithine carbamoyltransferases, (both annotated as ArgF, with 8.53 and 4.78 fold increases, respectively) and arginine deiminase (ArcA, 2.16 fold change).

The instance of ArgF that increased 8.53 fold is the same that was previously suggested to be misidentified and is actually predicted to be ArcB. However, increased expression of both ArgF and ArcB would seem counterintuitive because they are anabolic and catabolic in regards to arginine, respectively. It is possible that due to the heterogeneous nature of a biofilm, separate sub-populations could be concurrently anabolic and catabolic for arginine. Comparatively, during late stationary phase planktonic growth, the cells are homogenously nutrient limited and will have exhausted both their intracellular supply of arginine as well as environmental nitrogen and carbon sources. Hence, late stationary phase planktonic cells would present with reduced expression of both anabolic and catabolic arginine focused enzymes (limited carbon and nitrogen means that no arginine can be produced, and lack of intracellular arginine means there is no need for catabolic processes). These reasons could explain why both ArgF and ArcB appear to be increased in expression during biofilm growth. This problem would not be unique to arginine metabolism; biofilms also exhibited increased expression of Glutamine synthetase, GlnA (2.20 fold increase), suggesting that late stationary phase cells are less able to produce amino acids in general.

Activation of the TCA cycle in biofilms was associated with upregulation of citrate synthase (CitZ, 2.61 fold change), all 4 subunits of 2-oxoglutarate dehydrogenase (SucABCD, average 2.43 fold increase), isocitrate dehydrogenase (Icd, 3.36 fold increase, $p = 0.112$) and aconitate hydratase (AcnA, 3.42 fold increase). Reduced activation of the TCA cycle in late stationary phase cultures would limit the supply of amino acid metabolic intermediates and may provide another reason as to why proteins associated with amino acid biosynthesis were comparatively upregulated in biofilms[254].

Furthermore, increased levels of glycolysis/gluconeogenesis can be associated with large fold changes in aldehyde dehydrogenase family protein, AldA (3.32 fold increase) alongside increases in fructose-1-6-bisphosphatase Fbp (2.90 fold increase). The increase in Fbp expression alongside decreased expression of phosphofructokinase (PfkA, 0.51 fold decrease) provides evidence that the balance of the pathway is shifted towards gluconeogenesis rather than glycolysis within biofilms, when compared to late stationary phase planktonic cultures. The latter are unlikely to have the necessary nutrient availability that is necessary for gluconeogenesis.

As per comparisons with early stationary phase planktonic cultures, comparisons with late stationary phase planktonic cultures suggest that biofilms of *S. aureus* UAMS-1 harbour decreased expression of proteins involved in fatty acid biosynthesis such as FabH, FabI, FabG, and FabD, (0.59, 0.49, 0.52 and 0.43 fold decreases, respectively, $p < 0.05$ in all instances except for FabH, where $p = 0.093$) and acetyl-coenzyme A carboxylase carboxyl transferase subunit beta, AccD (0.67 fold decrease, $p = 0.215$). 14 proteins (2.8%) associated with cell wall biosynthesis including numerous components of the Mur pathway (MurD, MurE, MurG, MurI, 0.63, 0.38, 0.44 and 0.36 fold decrease, respectively) and D-alanine-D-alanine ligase (Ddl, 0.35 fold decrease) were identified as downregulated in biofilms, suggesting a higher degree of cell wall turnover in late stationary phase planktonic cells.

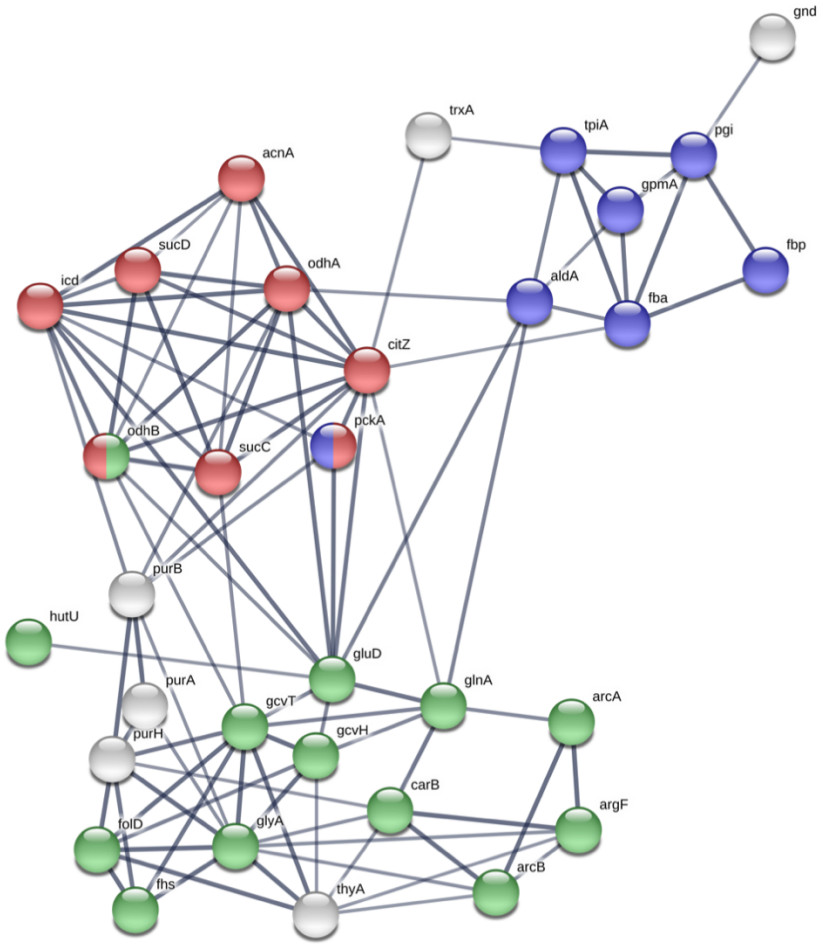

	Protein	Gene	Expression Ratio
Amino Acid Metabolism	Urocanate hydratase	hutU	2.69
	Serine hydroxymethyltransferase	glyA	3.05
	Aminomethyltransferase	gcvT	2.25
	Bifunctional protein FolD	folD	1.71
	Formate--tetrahydrofolate ligase	fhs	2.23
	Ornithine carbamoyltransferase	argF (arcB)	8.53
	Ornithine carbamoyltransferase	argF	4.78
	Arginine deiminase	arcA	2.16
	Glutamine synthetase	glnA	2.20
	Glutamate dehydrogenase	gluD	3.05
	Aldehyde dehydrogenase (NAD) family protein	aldA	3.32
	Carbamoyl-phosphate synthase large chain	carB	1.86
	Glycine cleavage system H protein	gcvH	4.93
	Dihydrolipoyllysine-residue succinyltransferase component of 2-oxoglutarate dehydrogenase complex	odhB/sucB	2.11
Gluconeogenesis	Aldehyde dehydrogenase (NAD) family protein	aldA	3.32
	Triosephosphate isomerase	tpiA	2.05
	Glucose-6-phosphate isomerase	pgi	1.74
	Fructose-1_6-bisphosphatase class 3	fbp	2.90
	Fructose-1_6-bisphosphate aldolase_ class II	fba	3.25
	2_3-bisphosphoglycerate-dependent phosphoglycerate mutase	gpmA	6.51
TCA Cycle	Citrate synthase	citZ	2.61
	2-oxoglutarate dehydrogenase E1 component	odhA/sucA	3.32
	Dihydrolipoyllysine-residue succinyltransferase component of 2-oxoglutarate dehydrogenase complex	odhB/sucB	2.11
	Succinate--CoA ligase [ADP-forming] subunit beta	sucC	1.94
	Succinate--CoA ligase [ADP-forming] subunit alpha	sucD	2.36
	Isocitrate dehydrogenase [NADP]	icd	1.53
	Phosphoenolpyruvate carboxykinase (ATP)	pckA	1.98
	Aconitate hydratase	acnA	3.42
Other Metabolic Proteins	Adenylosuccinate synthetase	purA	2.68
	Adenylosuccinate lyase	purB	1.55
	Thioredoxin	trxA	2.46
	6-phosphogluconate dehydrogenase_ decarboxylating	gnd	1.80
	Bifunctional purine biosynthesis protein PurH	purH	3.34
	Thymidylate synthase	thyA	1.86

Figure 25: STRING interaction network of upregulated metabolic proteins in biofilm cultures of *S. aureus* UAMS-1, compared to late stationary phase planktonic cultures

A number of proteins are present from amino acid metabolism pathways (green), glycolysis/gluconeogenesis pathways (blue) and the TCA cycle (red).

3.3.3.4. Early Stationary vs Late Stationary Planktonic Cultures

Comparison of early and late stationary phase planktonic cultures identified 547 proteins suitable for quantitative analysis, with 154 (28.2%) increased in expression and 112 (20.5%) decreased in expression in late stationary planktonic cultures (Figure 26). Changes in metabolic proteins were the most prevalent with 59 (10.8%) upregulated and 25 (4.6%) downregulated. 14 proteins (2.6%) associated with cell wall biosynthesis were also upregulated in late stationary phase planktonic cultures, compared to early stationary phase cultures. These proteins covered the majority of the cytoplasmic Mur ligase peptidoglycan biosynthesis pathway and are depicted in Figure 27[255]**.** It is worth noting that while not all comparisons were deemed statistically significant ($p > 0.05$, see Figure 27 for full breakdown), the simultaneous upregulation of several proteins within the pathway, as defined by an expression ratio ≥ 1.5, provides evidence that the proteins are likely upregulated, despite p values exceeding the threshold for significance. Interestingly, MurB was the only identified component of the pathway to not satisfy the criteria for differential expression (1.18 fold increase). Alanine racemase, Alr, responsible for the interconversion of alanine stereoisomers was decreased in expression 0.38 fold, possibly to prevent the conversion of D-alanine, (which during cell wall biosynthesis is further processed by Ddl), back to L-alanine, which is not used during cell wall synthesis. Finally, 17 (3.1%) miscellaneous proteins were also upregulated, predominantly encompassing domains of assorted types (9/17).

Regarding downregulated proteins, 29, (5.3%) were associated with protein biosynthesis, (25 ribosomal proteins, elongation factors P and Tf, and initiation factor IF-3, 19 statistically significant, $p > 0.05$ for 10 of 29 proteins). These were expressed an average of 0.35 fold lower than early stationary planktonic cultures, suggesting markedly lower translational capacity in late stationary phase cultures compared to early stationary phase cultures.

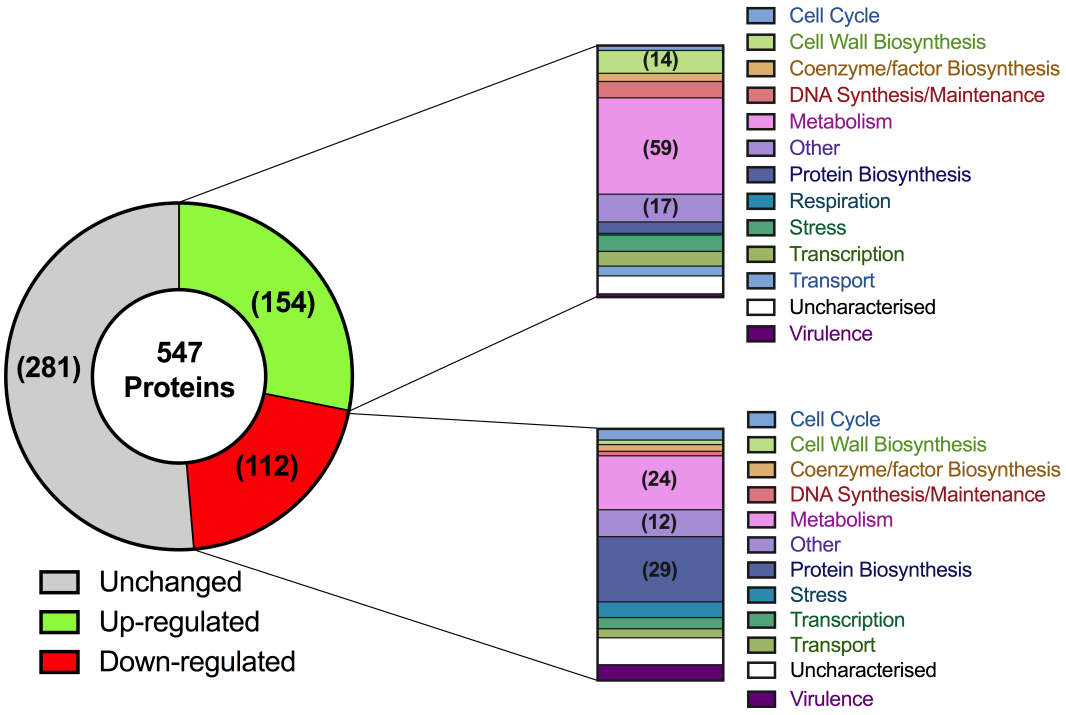

Figure 26: Summary of proteins identified for quantitative analysis between early and late stationary phase planktonic cultures of *S. aureus* UAMS-1

Number of proteins identified for each category is displayed in brackets. For quantitative analysis, protein must satisfy the following selection criteria: present in all three biological replicates, FDR ≤ 1%, sequence coverage ≥ 5%. Proteins were classed as differentially expressed in Late Stationary Planktonic Cultures if the ratio was ≥ 1.5 for increased expression or ≤ 0.667 for decreased expression. Functional categories assigned using GeoPANTHER and UniProt database searches

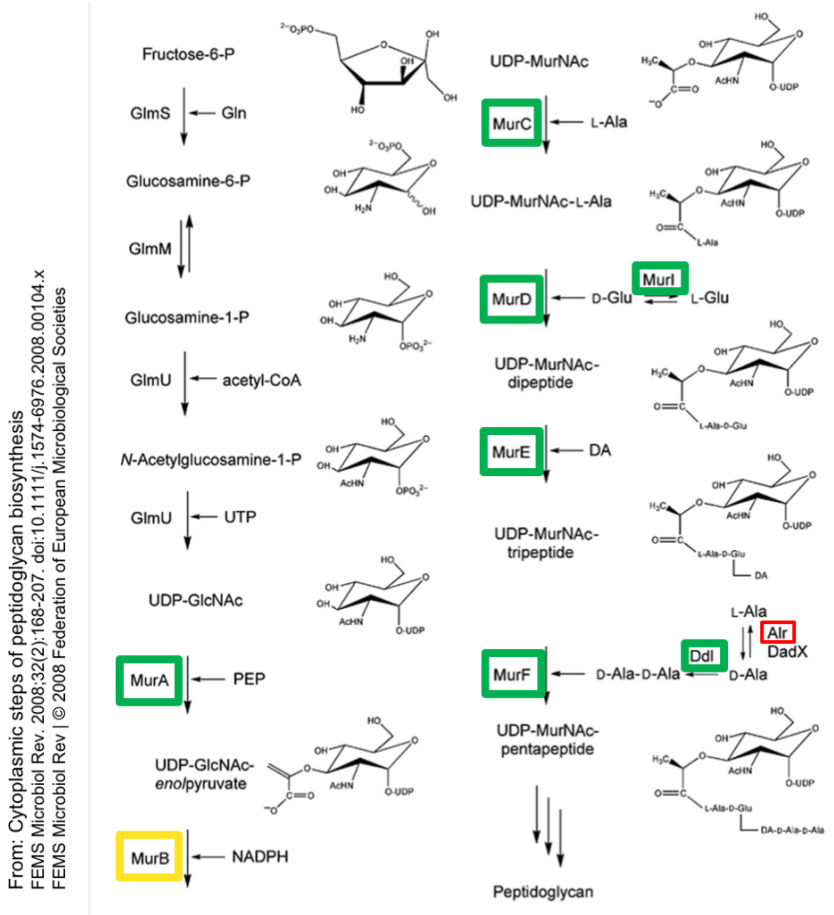

Protein Name	*Gene*	Expression Ratio	*p* value
UDP-N-acetylglucosamine 1-carboxyvinyltransferase	*murA1*	1.75	0.161
UDP-N-acetylglucosamine 1-carboxyvinyltransferase	*murA2*	1.57	0.178
UDP-N-acetylenolpyruvoylglucosamine reductase	*murB*	1.18	**0.05**
UDP-N-acetylmuramate--L-alanine ligase	*murC*	1.52	0.113
UDP-N-acetylmuramoylalanine--D-glutamate ligase	*murD*	2.54	**0.031**
UDP-N-acetylmuramoyl-L-alanyl-D-glutamate--L-lysine ligase	*murE*	1.66	0.078
UDP-N-acetylmuramoyl-tripeptide--D-alanyl-D-alanine ligase	*murF*	2.24	**0.011**
UDP-N-acetylglucosamine--N-acetylmuramyl-(pentapeptide) pyrophosphoryl-undecaprenol N-acetylglucosamine transferase	*murG*	1.68	0.061
Glutamate racemase	*murI*	3.82	**0.0005**
D-alanine--D-alanine ligase	*ddl*	1.53	0.194
Alanine Racemase	*alr*	0.38	0.233

Figure 27: Differential expression of Mur ligase peptidoglycan biosynthesis associated proteins in planktonic cultures of *S. aureus* UAMS-1 late stationary phase, compared to early stationary phase planktonic cultures

Identified proteins are highlighted on pathway using green squares if upregulated and red squares if downregulated. All Mur proteins were upregulated except for MurB which did not satisfy the ≥ 1.5 fold change in expression to be defined as increased in expression. *p* values calculated using a one tailed students t-test. Pathway figure taken from Barreteau et al (2008)

Analysis of the upregulated metabolic proteins in late stationary phase cultures showed increased expression of proteins associated with amino acid biosynthesis, porphyrin metabolism and the TCA cycle (Figure 28, A). Iron, in particular heme, is an important cofactor for the function of many bacterial proteins and processes, including *S. aureus* survival and virulence[256,257]. Upregulated proteins associated with porphyrin metabolism, (specifically heme biosynthesis via upregulation of HemE, HemH, $p = 0.261$ and 0.167, respectively, and HemG, and HemL: average fold increase of 2.55) suggests environmental iron is decreased in late stationary cultures and/or increased heme synthesis was required for survival.

Downregulated metabolic processes appear to be associated with amino acid metabolism, including proteins the aforementioned alanine racemase Alr1, and glycine cleavage system H protein GcvH, which catalyses glycine degradation. Decreased expression of glutamate dehydrogenase GluD (0.50 fold decrease, $p = 0.115$) and glutamine synthetase GlnA (0.53 fold decrease, $p = 0.058$) suggests less reliance on glutamine during late stationary phase, which is typically utilised as a major source of intracellular nitrogen for *S. aureus*[254].

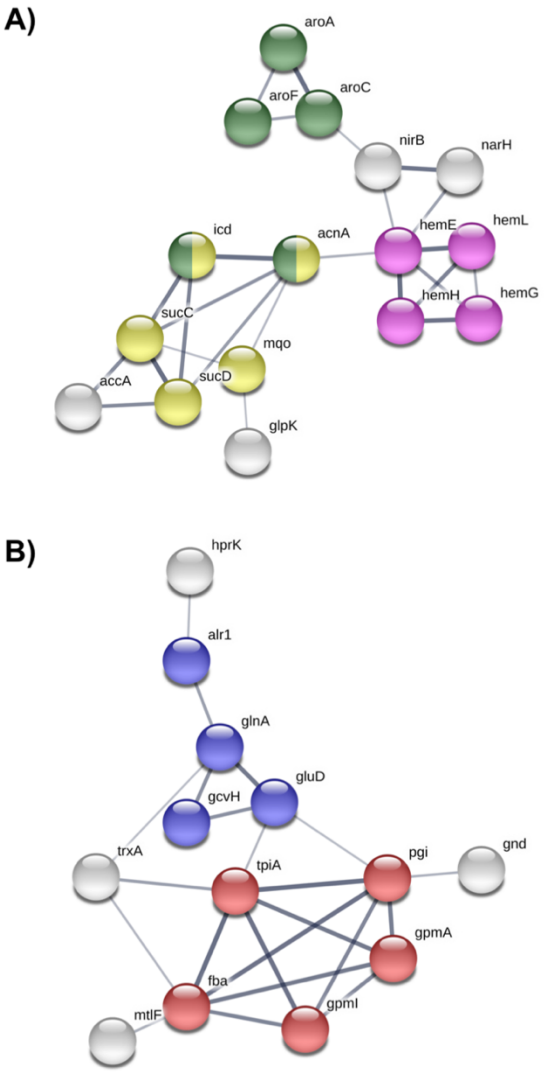

	Protein	Gene	Expression Ratio
Biosynthesis of Amino Acids	3-phosphoshikimate 1-carboxyvinyltransferase	aroA	3.49
	3-deoxy-7-phosphoheptulonate synthase	aroF	1.61
	Chorismate synthase	aroC	2.11
	Isocitrate dehydrogenase [NADP]	icd	2.20
	Aconitate hydratase	acnA	1.82
Porphyrin Metabolism	Glutamate-1-semialdehyde 2_1-aminomutase	hemL	1.91
	Ferrochelatase	hemH	2.90
	Uroporphyrinogen decarboxylase	hemE	2.82
	Protoporphyrinogen oxidase	hemG	2.56
TCA Cycle	Isocitrate dehydrogenase [NADP]	icd	2.20
	Aconitate hydratase	acnA	1.82
	Succinate--CoA ligase [ADP-forming] subunit beta	sucC	2.82
	Succinate--CoA ligase [ADP-forming] subunit alpha	sucD	2.15
	Probable malate:quinone oxidoreductase	mqo	1.83
Other Metabolic Processes	Acetyl-coenzyme A carboxylase carboxyl transferase subunit alpha	accA	1.89
	Glycerol kinase	glpK	1.85
	Nitrite reductase [NAD(P)H]_ large subunit	nirB	1.56
	Nitrate reductase_ beta subunit	narH	1.83

	Protein	Gene	Expression Ratio
Amino Acid Metabolism	Alanine racemase	alr	0.38
	Glutamine synthetase	glnA	0.53
	Glutamate dehydrogenase	gluD	0.50
	Glycine cleavage system H protein	gcvH	0.26
Glycolysis/ Gluconeogenesis	Triosephosphate isomerase	tpiA	0.33
	Glucose-6-phosphate isomerase	pgi	0.41
	Fructose-1_6-bisphosphate aldolase_ class II	fba	0.34
	2_3-bisphosphoglycerate-dependent phosphoglycerate mutase	gpmA	0.34
	2_3-bisphosphoglycerate-independent phosphoglycerate mutase	gpmI	0.47
Other Metabolic Proteins	Mannitol-specific phosphotransferase enzyme IIA component	mtlF	0.39
	Thioredoxin	trxA	0.29
	6-phosphogluconate dehydrogenase_ decarboxylating	gnd	0.56
	HPr kinase/phosphorylase	hprK	0.42

Figure 28: STRING interaction network of differentially expressed metabolic proteins between early and late stationary phase planktonic cultures of *S. aureus* UAMS-1

A) Upregulated metabolic proteins in late stationary phase cultures. Protein clusters of interest include those associated with amino acid biosynthesis (green), TCA cycle (yellow) and porphyrin metabolism (pink).

B) Downregulated metabolic proteins in late stationary phase planktonic cultures. Amino acid metabolism and Glycolysis/Gluconeogenesis pathways appeared to be decreased (blue and red, respectively).

3.3.3.4 Planktonic and Biofilm Cultures of *S. aureus* Present with Altered Proteomic Responses to HT61

Proteomic profiles of early stationary and late stationary phase planktonic cultures, as well as biofilm cultures of *S. aureus* UAMS-1 were analysed following treatment with sub-inhibitory (4 μg ml^{-1}) and inhibitory (16 μg ml^{-1}) concentrations of HT61 and compared to untreated control populations. A quantitative summary of the differentially expressed proteins for sub-inhibitory and inhibitory treatments of each bacterial growth state is shown in Table 10. A breakdown of the differentially expressed protein categories following treatment with both sub-MIC and MIC HT61 is shown in Figure 29, Figure 30 and Figure 31 (early stationary phase planktonic, biofilm and late stationary phase planktonic, respectively).

Table 10: Summary of differentially expressed proteins in *S. aureus* UAMS-1 following treatment with sub-inhibitory and inhibitory concentrations of HT61

For quantitative analysis, protein must satisfy the following selection criteria: present in all three biological replicates, FDR ≤ 1%, sequence coverage ≥ 5%. Proteins were classed as differentially expressed in Late Stationary Planktonic Cultures if the ratio was ≥ 1.5 for increased expression or ≤ 0.667 for decreased expression.

	4 μg ml^{-1} HT61			
	Unchanged	**Up Regulated**	**Down Regulated**	**Total**
Early Stationary Phase	**540** (89.4%)	**39** (6.5%)	**25** (4.1%)	604
Late Stationary Phase	**527** (83.7%)	**25** (4.0%)	**78** (12.4%)	630
Biofilm	**436** (94.6%)	**5** (1.1%)	**20** (4.3%)	461

	16 μg ml^{-1} HT61			
	Unchanged	**Up**	**Down**	**Total**
Early Stationary Phase	**270** (49.8%)	**135** (24.9%)	**137** (25.3%)	542
Late Stationary Phase	**505** (83.7%)	**31** (5.1%)	**67** (11.1%)	603
Biofilm	**472** (92.0%)	**15** (2.9%)	**26** (5.1%)	513

Initial findings show that in response to HT61 treatment, a higher proportion of proteins were decreased, rather than increased in expression. In addition, a greater number of proteins were differentially expressed when cultures were treated with a higher concentration of HT61. The proteomic response of biofilm cultures is considerably lower than either of the planktonic cultures, suggesting some degree of tolerance to the action of HT61.

For all culture types and treatment concentrations, differentially expressed proteins were responsible for a wide range of cellular functions, including cell wall biosynthesis, DNA synthesis, metabolism, translation, stress and virulence. While there are trends, there is no clear class of proteins that are specifically increased or decreased as a response to treatment with HT61.

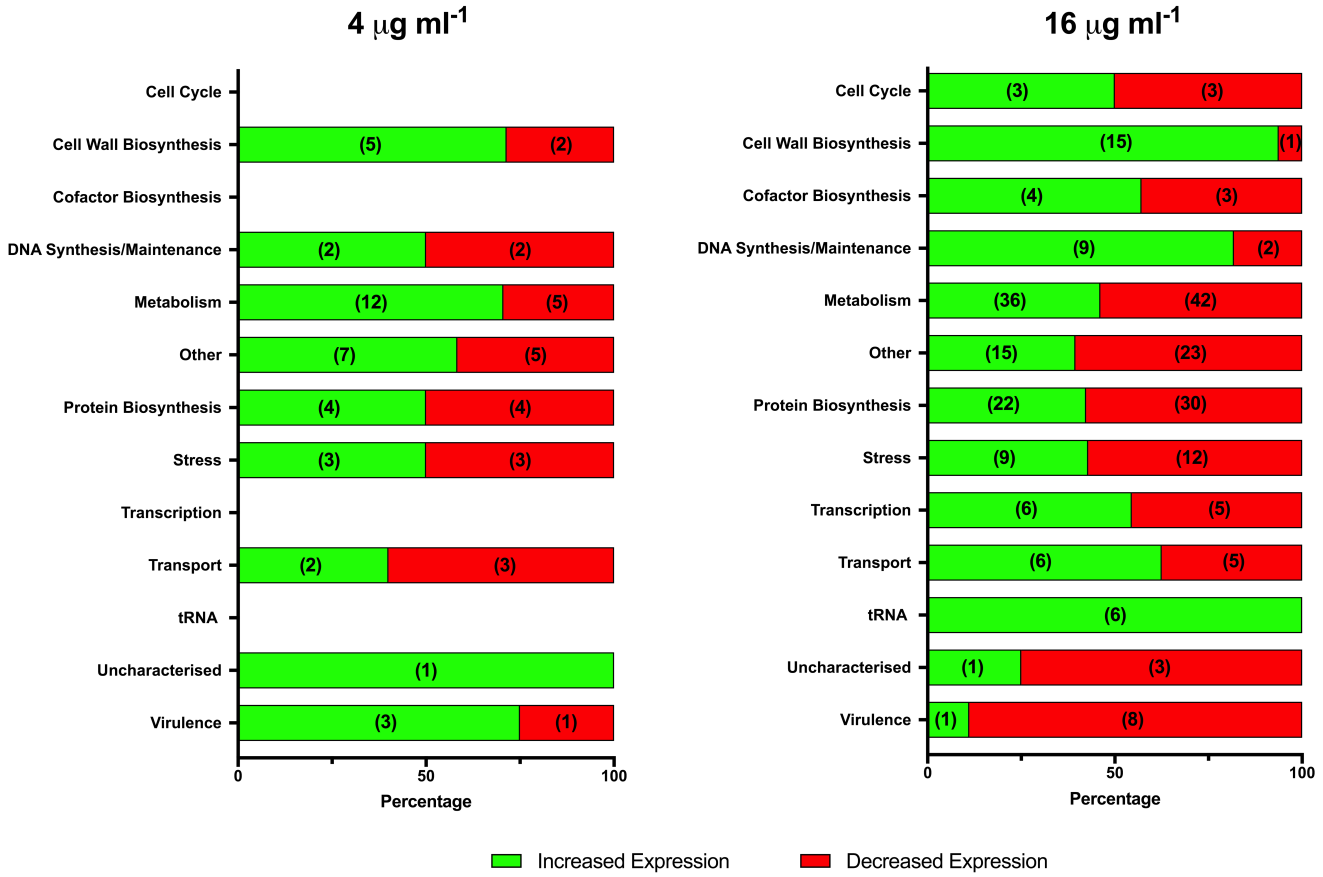

Figure 29: Summary of differentially expressed proteins in early stationary phase planktonic cultures of *S. aureus* UAMS-1 following treatment with sub-inhibitory and inhibitory concentrations of HT61

Proteins are categorised based on uniprot and GeoPANTHER database searches. Percentage dictates the percentage of the differentially expressed proteins for a certain category. Numbers in brackets refer to the actual numbers of proteins identified. Green indicates increased expression, red indicates decrease expression. Concentration of HT61 is utilised is presented at the top of the figure.

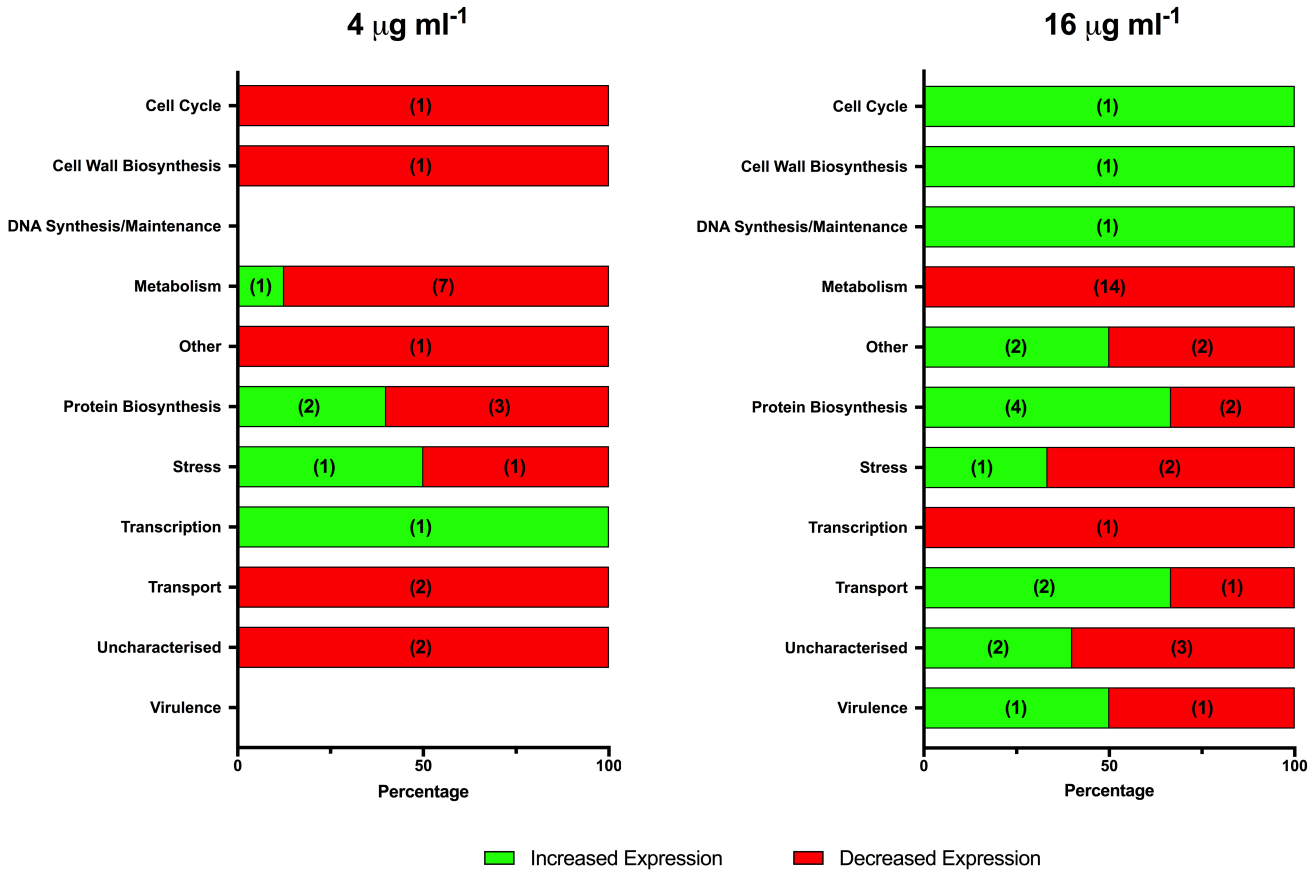

Figure 30: Summary of differentially expressed proteins biofilm cultures of *S. aureus* UAMS-1 following treatment with sub-inhibitory and inhibitory concentrations of HT61

Proteins are categorised based on uniprot and GeoPANTHER database searches. Percentage dictates the percentage of the differentially expressed proteins for a certain category. Numbers in brackets refer to the actual numbers of proteins identified. Green indicates increased expression, red indicates decrease expression. Concentration of HT61 is utilised is presented at the top of the figure.

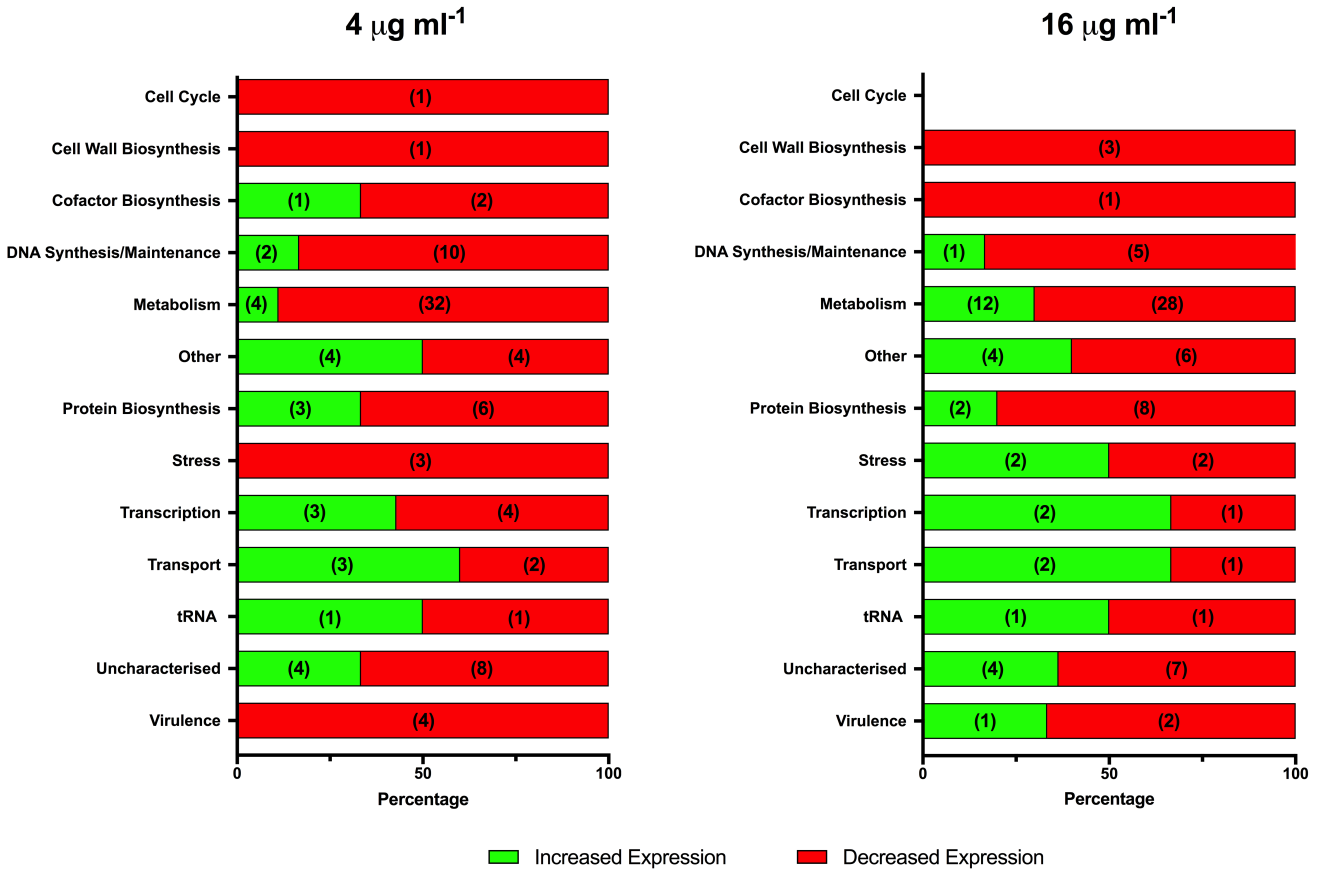

Figure 31: Summary of differentially expressed proteins in late stationary phase planktonic cultures of *S. aureus* UAMS-1 following treatment with sub-inhibitory and inhibitory concentrations of HT61

Proteins are categorised based on uniprot and GeoPANTHER database searches. Percentage dictates the percentage of the differentially expressed proteins for a certain category. Numbers in brackets refer to the actual numbers of proteins identified. Green indicates increased expression, red indicates decrease expression. Concentration of HT61 is utilised is presented at the top of the figure.

3.3.3.5. HT61 Causes an Upregulation of Cell Wall Associated Proteins, and Differential Expression of Cell Cycle, DNA Maintenance and Metabolic Proteins in Early Stationary Phase Planktonic Cultures of *S. aureus*

Analysis of early stationary phase planktonic cultures following HT61 treatment identified an upregulation of proteins associated with cell wall biosynthesis, including the central region of DltD (HMPREF0769_11446, 1.78 fold increase), three components of the Mur operon (MurC, MurD and MurI, 1.59, 1.84 and 1.52 fold increases, respectively; MurC, $p = 0.096$) and the response regulator VraR (1.54 fold increase, $p = 0.167$). Metabolic changes were linked to activation of the ADI pathway with upregulation of arginine deiminase ArcA (2.01 fold), carbamate kinase ArcC (2.04 fold) and ornithine carbamoyltransferase ArgF (1.73 fold). Proteins associated with the metabolism and biosynthesis of alternative amino acids were decreased in expression, including alanine dehydrogenase Ald (0.62 fold), Alanine racemase Alr (0.34 fold, $p = 0.097$) and L-threonine dehydratase catabolic TdcB/IlvA (0.61 fold). Alanine and threonine catabolism results in the production of pyruvate[258]. As pyruvate can be used to enter the TCA cycle, decreased amino acid catabolism could be linked to decreased activation of the TCA cycle. Qualitative evidence supporting this includes predicted downregulation of SucB (0.63 fold decrease, only identified in 2/3 untreated control populations). Sub-inhibitory treatment with HT61 also induced the upregulation of two putative transporters, HMPREF0769_12399 and HMPREF0769_10174 (1.58 and 1.72 fold increases, respectively), which may be involved in the efflux of HT61 or associated toxic metabolites. Virulence factors were also upregulated in response to sub-inhibitory HT61 treatment. 2 leukocidin-like β-channel forming cytolysins, HMPREF0769_11161 and HMPREF0769_11162, were upregulated 1.61 and 1.76 fold, respectively, alongside HMPREF0769_10200, a WXG100 family type secretion target, which was upregulated 2.75 fold. A negative regulator of virulence factors, SrrB was decreased in expression 0.28 fold. As virulence factors can be pro-inflammatory during an infection it is possible that HT61 may exacerbate an infection if utilised at a sub-inhibitory concentration[259].

Increasing the concentration of HT61 to 16 μg ml^{-1} resulted in the differential expression of a greater number of proteins. Noticeably, 15 upregulated proteins were involved in cell wall biosynthesis including MurA, MurC, MurD, MurE, MurF and MurI (average 2.63 fold increase), aminoacyltransferase FemB (3.24 fold increase) and VraR (2.19 fold

increase). Qualitative analysis also identified a 2.27 fold increase in the teichoic acid export ATP binding protein TagH, suggesting increased cell wall turnover. The only cell wall associated protein that was decreased in expression was the putative mannosyl-glycoprotein endo-beta-*N*-acetylglucosaminidase (HMPREF0769_12730, greater than 90% identity to the bifunctional autolysin Atl, 0.63 fold change), which is involved in cell wall degradation. These data suggest that cell wall maintenance and synthesis is important for survival during HT61 treatment.

A number of cell cycle proteins were also differentially expressed, with 3 increased and 3 decreased in expression. Upregulated proteins included the GTPase Era, (1.71 fold increase, $p = 0.063$), cell division protein FtsA, (1.66 fold increase) and GTPase Obg, (3.04 fold increase). Downregulated proteins included the 60 kDa chaperone GroL (0.29 fold decrease), cell cycle protein GpsB (0.20 fold decrease), trigger factor Tig (0.34 fold decrease) and DivlVA domain protein (0.29 fold decrease). The combined expression of cell wall biosynthesis proteins and cell cycle proteins, specifically MurD and FtsA, could also indicate expression of the divison cell wall, *dcw*, cluster, which is important for maintaining cell shape and integrity[260,261].

In addition, a number of proteins associated with the relaxation of DNA supercoiling were upregulated including DNA topoisomerase 1 TopA (2.62 fold change, $p = 0.095$) DNA gyrase GyrA (1.55 fold change) and DNA topoisomerase 4 (ParC and ParE subunits, 1.89 and 3.34 fold increases, respectively. ParC: $p = 0.051$), which suggests that HT61 could be affecting the integrity of the bacterial chromosome. The putative transporter HMPREF0769_12399 was also upregulated following MIC HT61 treatment (2.41 fold increase), along with 4 further transporters (2 transporters $p > 0.05$), suggesting a potential mechanism for HT61 efflux.

Virulence factor expression was also affected by the use of HT61 at an inhibitory concentration. While the conserved virulence factor, CvfB was upregulated 1.67 fold, 5 other virulence factors were decreased in expression. These were SrrB (0.55 fold decrease, $p = 0.149$), Gram-positive signal peptide, YSIRK family HMPREF0769_10369 (0.43 fold decrease), putative immunodominant antigen B HMPREF0769_10508 (0.44 fold decrease), fibronectin binding protein A FbpA (0.57 fold decrease, $p = 0.104$) and RNAIII-activating protein TRAP HMPREF0769_11844 (0.25 fold decrease). This suggests that when HT61 is utilised at an inhibitory concentration, *S. aureus* virulence factor production

is lowered, which is in stark contrast to the effect observed following sub-inhibitory HT61 treatment.

A large number of metabolic proteins were differentially expressed in response to an inhibitory concentration of HT61, most likely the result of altered metabolic requirements during cellular stress. Decreased expression was observed for proteins involved in the TCA cycle and gluconeogenesis/glycolytic pathways, including PTS system transporters, but increased expression was observed for proteins associated with fatty acid and porphyrin metabolism. Interestingly and unlike sub-inhibitory treatment, the ADI pathway appears to be downregulated, with a 0.30 fold reduction in carbamate kinase ArcC, although the *p* value does not meet the criteria for statistical significance ($p = 0.337$). However, qualitative analysis provides further evidence to downregulation of the ADI pathways, with downregulation of both ArgF (0.06 fold) and ArgF (predicted ArcB) (0.04 fold). However, both of these proteins were only identified in 2 of 3 untreated control populations. Decreased expression of all of these proteins could simply be indicative of a general reduction in metabolic function due to cell death.

Finally, increased expression was noted for 6 proteins that modify tRNA following treatment with HT61 at 16 μg ml^{-1} (4 of 6; $p \leq 0.05$). tRNA modifications are important as they can affect the specificity and interaction strength of tRNA codon:anticodon pairs[262]. A particular example, yqeV, a tRNA methylthiotransferase, was highly upregulated, with a 7.32 fold increase and this is likely to have a significant effect on the overall protein output.

3.3.3.6. Biofilm Tolerance Limits the Proteomic Response to HT61 but Cell Wall and *dcw* Cluster Components are Implicated

Compared to either early or late stationary phase planktonic cultures, the proteomic changes observed in *S. aureus* UAMS-1 biofilms following HT61 treatment was minimal, suggesting a degree of biofilm tolerance. Sub-inhibitory treatment with HT61 resulted in only 5 upregulated proteins: UvrA, of the UvrABC endonuclease system, part of the SOS response and involved in repairing DNA damage[258] (1.53 fold increase, $p = 0.289$), ribosomal RNA small subunit methyltransferase H MraW, (2.07 fold increase, $p = 0.225$), 50S ribosomal protein L27 (1.59 fold increase), phosphate binding protein PstS, (1.80 fold increase) and DNA-directed RNA polymerase subunit Ω (RpoZ, 2.07 fold increase), which

is important for RNA polymerase specificity and *S. aureus* biofilm formation[263]. The increased upregulation of RpoZ and UvrA implies a generalised stress response, rather than a specific response towards HT61. However, MraW is part of the *S. aureus dcw* cluster, which may indicate a more focussed response[261].

20 proteins were found to be decreased in expression. Of interest was the decreased expression of Ribulose-5-phosphate reductase, TarJ (0.65 fold decrease), which is associated with the synthesis of teichoic acid, a component of the bacterial cell wall. Metabolic changes were minimal, although a reduction in amino acid metabolism, specifically glycine, via decreased expression of glycine dehydrogenase (GcvPA and GcvPB subunits, 0.58 and 0.62 fold changes, respectively) was noted alongside potentially reduced biosynthesis of aromatic amino acids, resulting from decreased expression of 3-deoxy-7-phosphoheptulonate synthase AroF (0.53 fold decrease, $p = 0.101$).

Treatment of *S. aureus* UAMS-1 biofilms with 16 μg ml $^{-1}$ HT61 resulted in a modest increase in the number of differentially expressed proteins. Similar to the response of early stationary phase planktonic cultures, proteins associated with cell wall biosynthesis were upregulated, namely *N*-acetylmuramoyl-L-alanine amidase, Sle1 (1.95 fold increase, $p = 0.065$) and MurD (1.59 fold increase). Upregulation of MraW was also consistent with sub-MIC treatment (1.85 fold increase), which alongside upregulation of MurD, provides further evidence for upregulation of the *dcw* cluster. The putative transporter, HMPREF0769_12399 was also upregulated (1.56 fold). The only virulence factor to be altered in expression in biofilm cultures was the Gram-positive signal peptide protein, YSIRK family HMPREF0769_10369 (1.82 fold increase). The increased concentration of HT61 also caused decreased expression of citrate synthase, (citZ 0.65 fold decrease) and further decreases in proteins associated with amino acid metabolism such as the putative proline dehydrogenase HMPREF0769_111919 (90% identity to FadM, 0.63 fold change, $p = 0.210$).

3.3.3.7. Treatment of Late Stationary Phase Planktonic Cultures with HT61 Affects Cell Metabolism and Protein Biosynthesis

The proteomic profile of late stationary phase planktonic cultures following treatment with HT61 was distinct from those of HT61 treated early stationary phase planktonic cultures and biofilm cultures. However, it should be noted that the treatment conditions were also slightly different: early stationary phase planktonic and biofilm cultures were treated with

HT61 suspended in TSB, whereas the late stationary phase cultures were treated with HT61 suspended in HBSS.

Treatment of late stationary phase cultures with 4 μg ml^{-1} HT61 resulted in the upregulation of 25 proteins. Proteins of interest included three putative transporters (average 2.04 fold increase, $p > 0.05$ for each transporter), a putative helicase C-terminal domain protein HMPREF0769_10659 (4.06 fold increase, $p = 0.187$) and the DNA mismatch repair protein MutL (1.56 fold increase). In combination, increased expression of these enzymes suggests that HT61 treatment affected the integrity of the bacterial DNA. Similar to early stationary phase cultures, biofilm cell wall synthesis was also affected by HT61 treatment, but in a subtler manner. Expression of the autolytic *N*-acetylmuramoyl-L-alanine amidase, Sle1 was decreased 0.55 fold ($p = 0.173$), indicating efforts to maintain cell wall integrity[264]. However, the teichoic acids export ATP-binding protein, TagH was also decreased in expression 0.61 fold ($p = 0.118$), suggesting reduced export of teichoic acids, possibly restricting cell wall turnover, which could be lethal to the cell[265].

Transcriptional and translational output is also likely to have been significantly altered following HT61 treatment, as inferred by the differential expression of numerous transcription factors and other translational machinery. For example, two transcription factors, MgrA and MalR were upregulated (1.59 and 1.60 fold, respectively. $p > 0.168$ and 0.098), alongside a queuine tRNA-ribosyltransferase Tgt (2.68 fold increase). In general, there is likely to have been a reduction in translational capacity, thanks to the upregulation (2.62 fold increase) of peptide chain release factor 2, a translation termination factor, and the concurrent decreased expression of several ribosomal proteins. Metabolic processes associated with amino acid, carbohydrate, porphyrin, nitrogen, pyrimidine and folate metabolism were all downregulated, which could be indicative of cellular quiescence. Furthermore, virulence factors were also downregulated, although none of the observed changes were statistically significant. These included histidine protein kinase SaeS, (0.64 fold decrease, $p = 0.114$), the Gram-positive signal peptide protein, YSIRK family HMPREF0769_10369, (0.48 fold decrease, $p = 0.054$) and Fibronectin binding protein A FbpA (0.59 fold decrease, $p = 0.184$)

When utilised against late stationary phase cultures of *S. aureus* at a concentration of 16 μg ml^{-1}, HT61 is highly bactericidal. As such, the proteomic profile may incorporate proteins isolated from a high number of dead cells and consequently, may be more general, without

emphasis on a particular protein class or pathway. Metabolic pathways associated with amino acid biosynthesis, carbohydrate/glycolysis/gluconeogenesis and the TCA cycle were all largely decreased in expression, although certain proteins such as alanine dehydrogenase, Ald, alanine racemase, Alr and 3-phosphoskikimate 1-carboxyvinyltransferase, AroA were upregulated 1.62, 2.08 and 2.79 fold, respectively (p = 0.017, 0.204, 0.200, respectively). Furthermore, uridine kinase, Udk, associated with pyrimidine metabolism was highly upregulated with a 4.76 fold increase (p = 0.237). The Gamma-hemolysin component B, a virulence factor, was also upregulated 2.58 fold (p = 0.060), suggesting that HT61 treatment could lead to a pro-inflammatory response at the site of *S. aureus* infection. However, 2 virulence factors were also decreased in expression, which may contradict this theory. These were histidine protein kinase SaeS (0.65 fold decrease, p = 0.104) and the putative immunodominant antigen B HMPREF0769_10508 (0.67 fold decrease, p = 0.115).

Decreased expression of proteins involved in cell wall biosynthesis were also identified, including downregulation of the VraR response regulator (0.65 fold, p = 0.199), MurC (0.52 fold) and a putative glycoprotein aminidase (0.59 fold, p = 0.194). Further evidence suggesting that HT61 treatment also results in damage to DNA is provided by the upregulation of the DNA repair protein, RadA (2.06 fold increase, p = 0.159). In addition, qualitative analysis also suggests upregulation of the putative helicase C-terminal domain protein HMPREF0769_10659, similar to the response observed following treatment with 4 $\mu g\ ml^{-1}$ HT61, with a predicted 3.09 fold increase. However, the FDR values for this protein do not meet the criteria for strict quantitative analysis. Furthermore, the predicted increase in DNA damage could simply be a result of increased cell death.

Unlike early stationary phase planktonic cultures and biofilm cultures, the cell wall stimulon and *dcw* clusters did not appear to be influenced by HT61 treatment. This is likely because these procedures are already basally upregulated in late stationary phase cultures.

3.4. Discussion

HT61 has demonstrated efficacy against *S. aureus* as shown in both the previous chapter as well as the published literature[11,12]. While membrane composition is predicted to be important for its mechanism of action[13], the cellular response to HT61 treatment has not been investigated. The aim of this chapter was to use a quantitative label-free proteomic approach to determine the effect of HT61 treatment on early and late stationary phase planktonic and biofilm cultures of *S. aureus*, to identify proteins or pathways that are implicated during treatment. In addition, quantitative proteomics was used to determine differences in the basal proteome of planktonic (early and late stationary) and biofilms, to identify whether these differences could be attributed to a differential proteomic response to HT61 treatment.

3.4.1. Metabolic Changes Dominate the Differences Between the *S. aureus* Proteome of Planktonic and Biofilm Growth

Comparisons between untreated planktonic and biofilm populations identified a large number of proteins that were associated with cellular metabolism. Noticeably, *S. aureus* biofilm growth was linked to upregulation of TCA cycle, glycolytic/gluconeogenesis and amino acid metabolic proteins, including the ADI pathway. This suggests that biofilms utilise carbohydrates such as glucose and lactate, as well as amino acids as their primary source of energy. Exponential planktonic cultures would likely present with similar carbohydrate utilisation, however, the cultures studied in this chapter were entering/had entered stationary phase, therefore carbohydrate utilisation was decreased[266].

Upregulation of the TCA cycle (particularly of genes encoding succinate dehydrogenase) has been implicated in improved *S. aureus* survival during biofilm development[267]. In addition, activation of the ADI pathway has been shown to be important during biofilm growth and maturation in numerous bacterial species including *S. pneumoniae*[219], *S. epidermidis*[264] and *S. aureus*[267]. While concurrent activation of these metabolic processes has been observed in previous proteomic and transcriptomic studies of *S. aureus* biofilms[268,269] the work presented here is, as far as I am aware, the first to demonstrate these responses using a label-free proteomic method.

However, the TCA and ADI pathways are typically activated during aerobic and anaerobic metabolism, respectively. As such, their concurrent upregulation appears counterintuitive.

Additionally, while glycolysis/gluconeogenesis was upregulated in biofilms, it is difficult to ascertain the direction of the reaction as many of the enzymes involved catalyse both processes. Despite these observations, this chapter provides evidence for the simultaneous activation of all of these processes in biofilms of *S. aureus*. This is most likely due to the physiological heterogeneity found across a biofilm. These data highlight that by as little as 84 hours growth, distinct sub-populations of *S. aureus* may have arisen with markedly different metabolic demands. Unfortunately, these nuances are lost when analysed using a population level proteomic method, as per this chapter. In order to investigate this, the biofilm would need to be fixed and sectioned, for example at different depths. These sub-populations could then be independently analysed.

When early stationary phase cultures were compared to biofilms, a number of proteins linked to protein biosynthesis were also decreased in expression. This suggests that biofilms have become quiescent and exhibit reduced translational capacity. However, comparison of biofilms to late stationary phase planktonic cultures suggests that the biofilms cells are more translationally active. This could be explained by a combination of reasons. Firstly, the late stationary phase planktonic cells will have exhausted the available nutrients. This problem is compounded by the use of HBSS as a medium, because it does not supply exogenous carbon or nitrogen. Thus, amino acid and protein synthesis will be greatly inhibited resulting in lower translational capacity. Further evidence for this scenario can be seen by the increased expression of proteins associated with amino acid anabolism, such as glutamine synthetase, in biofilms. Secondly, it is possible that upon adopting the biofilm phenotype, the cells have adapted to their new micro-environments and altered their metabolic processes accordingly, facilitating increased protein synthesis.

Comparison of early and late stationary phase planktonic cultures identified numerous differences, but of note was the increased expression of cell wall biosynthesis associated proteins in late stationary phase planktonic cultures. In stationary phase *E. coli*, cell wall biosynthesis is upregulated, increasing cell wall thickness in order to withstand external stressors[270]. A thicker cell wall has also been linked to vancomycin resistance in *S. aureus*[271] and the recycling of cell wall components has recently been demonstrated to be important for the survival of *S. aureus* and *B. subtilis* during stationary phase[272]. It is possible that the upregulation of cell wall biosynthesis associated proteins observed in this chapter is the result of a similar stress response of the *S. aureus* cells in late stationary phase.

3.4.2. HT61 Activates Component of the *S. aureus* Cell Wall Stress Stimulon, but the Exact Response Depends on Bacterial Growth State

In order to understand the cellular response to HT61, the proteomic response of early stationary phase planktonic, late stationary phase planktonic and biofilm cultures was analysed following treatment with sub-inhibitory and inhibitory concentrations (4 and 16 μg ml^{-1}) of HT61 respectively.

Alongside numerous metabolic changes and the differential expression of components involved in protein biosynthesis, analysis of early stationary phase cultures following treatment with HT61 identified the upregulation of a number of cell wall associated proteins as well as components of the *dcw* cluster, necessary for the maintenance of cell structure[261]. This response was mimicked by biofilm cultures following HT61 treatment, albeit to a lesser extent. The reduced response of biofilms to HT61 suggests a degree of biofilm tolerance, although the precise mechanisms of this cannot be determined using the data acquired in this chapter. In contrast, treatment of late stationary phase planktonic cultures with HT61 appeared to decrease the expression cell wall biosynthesis components. When compared to early stationary phase or biofilm cultures, late stationary phase cultures it was found that the basal expression of cell wall biosynthesis components was already increased, even without HT61 treatment. As discussed, this could be due to increased stress during stationary phase so it is possible that the response of early stationary and biofilm cultures to HT61 treatment is a more general stress response that is already activated in stationary phase cultures prior to treatment, rather than the result of a certain mechanism of action.

Previous functional studies on the interactions of antimicrobials with *S. aureus* have also implicated differential expression of the cell wall biosynthesis machinery. This response network is known as the cell wall stress stimulon[273]. Daptomycin is a lipopeptide antimicrobial and functions in a membrane dependent manner, similar to the predicted mechanism of HT61, whereby interactions with the bacterial membrane result in rapid depolarisation and ultimately cell death[274]. Transcriptomic studies of investigating the action of daptomycin towards *S. aureus* revealed the upregulation of 32 cell envelope related genes including genes such as *murAB, murI* and *vraR*[275], all of which were linked to HT61 treatment in this chapter.

Treatment of *Haemophilus influenzae* biofilms with D-methionine resulted in a cellular response similar to that of *S. aureus* and HT61[276]. In this study the authors found that D-methionine caused a dramatic increase in cell size as well as shape. Using a quantitative, labelled proteomic approach they found that this was caused by the upregulation of several components of the Mur ligase pathway, and several cell division and transcriptional regulators. All 9 of the upregulated proteins were part of the *dcw* cluster[276]. As HT61 dramatically alters *S. aureus* cell morphology, it makes sense that components of the *S. aureus dcw* cluster were also differentially expressed following treatment.

Recent reports have shown that HT61 preferentially interacts with negatively charged phospholipids, which are typically enriched in the membrane of stationary phase bacterial cells[13]. Ultimately, this leads to membrane depolarisation and cell death[11–13], however the cellular mechanisms leading to this are not understood. The results presented in this chapter suggest that upon binding to the cell membrane, HT61 applies stress to the cell that may interfere with cell wall biosynthesis and cell division. The exact response depends on the growth state of the cell. Following treatment, in early stationary phase and biofilm cultures, this translates to activation of the cell wall stress stimulon and *dcw* cluster, potentially mitigating the action of HT61, which may directly interfere with the cell wall or inhibit the function of the cell wall machinery. However, when HT61 is utilised against late stationary phase cultures, proteins such as autolysins and export pathways are downregulated to preserve cell wall integrity. The increased efficacy of HT61 against late stationary phase cells is likely a consequence of increased membrane interactions and increased intra-membrane concentrations of HT61, with a higher concentration leading to improved killing. Ultimately, the cells of *S. aureus* seem to respond in a manner that protects the structural stability of the cell wall either by increasing production, or reducing degradation.

It was also shown that when HT61 was utilised at a sub-inhibitory concentration, *S. aureus* virulence factor expression increased in both early and late stationary phase planktonic cultures. However, by increasing the concentration of HT61 to 16 μg ml^{-1}, virulence factor production was reduced. For biofilms, virulence factor production was only affected by the use of HT61 at 16 μg ml^{-1}; however, as discussed, this reduced proteomic response could be the result of biofilm mediated tolerance. This observation illustrates the importance of understanding the bacterial response to antibiotics. In the case of HT61, it implies that if it is used at an ineffective (i.e. non-lethal) concentration, bacterial virulence factor

production may increase. Within a clinical setting, this could promote a pro-inflammatory response within a patient, exacerbating their condition. As such, the concentration of HT61 should be chosen carefully to limit any negative side effects.

A final insight into the mechanism of action for HT61 was the interesting observation that following treatment, analysis of early stationary phase cultures identified upregulated topoisomerases including *gyrA, parC* and *parE*. HT61 is a quinoline derived compound[11] and structurally similar to quinolone antimicrobials such as ciprofloxacin, which inhibit topoisomerase function[194]. Consequently, HT61 may also be interfering with these enzymes, either by directly interacting with them, or by influencing their expression, which could explain their upregulation in this body of work. However, identifying secondary interactions would require further investigation.

3.4.3. Conclusions, Experimental Limitations and Future Work

In this chapter, a quantitative proteomic approach was used to understand the differences between early stationary phase, late stationary phase and biofilm cultures of *S. aureus*, as well as investigate the cellular response to HT61 in order to understand its mechanism of action. Axiomatically, comparison between the different states of growth revealed a high number of differentially expressed proteins, encompassing transporters, metabolic processes, transcription, translation, virulence and structural functions. Of particular interest was the identification that biofilm growth was associated with upregulation of the ADI pathway and TCA cycle, and that a defining feature of late stationary planktonic cultures compared to early stationary phase and biofilm cultures was the heightened upregulation of proteins associated with cell wall biosynthesis. Proteomic analysis of HT61 treated cultures suggested that, similar to other membrane active antimicrobials, it may exert its mechanism of action by interfering and stimulating the *S. aureus* cell wall stress stimulon and *dcw* operon, in conjunction with its known membrane associated mechanism.

However, there are limitations to the work described in this chapter and further investigation would be beneficial to understanding the mechanism of action of HT61. Firstly, while activation of the cell wall stimulon appears to be important, this response was most apparent in the analysis of early stationary phase cultures. The response was limited in biofilm cultures and even less so in late stationary phase cultures. For the

biofilm cultures, this could be because a biofilm-mediated tolerance mechanism is actively inhibiting the action of, and consequently the cellular response to HT61. Repeating the experiment with a higher concentration of HT61 against biofilm cultures may allow for more insight and investigation into whether components of the cell wall stimulon are affected. As for the late stationary phase cultures, the opposite effect could be true. Due to its increased effectiveness, the concentrations of HT61 that were used may have been too high, resulting in the generation of a less nuanced, more generic cellular stress response that makes discerning a precise mechanism more difficult. In this instance using a lower range of HT61 concentrations could address the problem.

A related point is that biofilms and stationary phase cultures can contain a significant portion of dead cells. These proteins will still be detected even though the cells are dead, which may distort the measured cellular response. A similar issue was alluded to earlier in regards to the presence of different metabolic sub-populations within biofilms. However, the only way to address this would be to selectively sample these sub-populations, although separating live from dead cells would be almost impossible. As such, whole proteome studies would ideally be followed up with more targeted analyses, such as western blots of specific sub-populations to identify the presence of certain proteins.

Assuming the cell wall stimulon is important for the action of HT61, the data presented in this study do not provide enough resolution to understand the exact cellular interactions HT61 is making. Is HT61 directly interacting with cell wall biosynthesis components? Or does it exert its effect via other interactions, either with other proteins or indirectly via its interactions with the cell membrane, compromising cell envelope functionality? An alternative approach to expression-based proteomics called thermal proteome profiling, (TPP) could be used to investigate this[277]. TPP relies on the principle that proteins become more thermostable upon interacting with a ligand; in other words, an antimicrobial target will become more thermostable when interacting with the antimicrobial. This interaction can be detected by a systematic screen of proteome melting curves. If there is a thermal shift depicting an increase in melting temperature for a particular protein ion peak, then it can be inferred that the protein is directly interacting with the antimicrobial[277]. Applying this technique to HT61 treated cells would enable identification of the proteins that it is directly interacting with.

A larger limitation of the work performed in this chapter was that populations were analysed 12 hours after treatment with HT61. If cells were harvested sooner after treatment, there would be less chance of proteins degrading/returning to basal levels prior to analysis, allowing for the identification of a higher number of differentially expressed proteins. It would also enable proteins associated with the immediate response to HT61 to be identified. If this study was to be repeated or expanded, it would be highly beneficial to analyse cultures during mid-exponential phase, for example by harvesting at a specific optical density measurement[219,242].

There are some more general issues with the work performed within this chapter. Firstly, due to the limitations of proteomic methods in 2018, the quality of the data relies on the use of a suitable, high quality, annotated reference genome. While a number of *S. aureus* genomes are available for use, the strain used in this study (*S. aureus* UAMS-1) was not. This meant that the reference genome chosen (*S. aureus* MN8) did not share 100% homology, leaving scope for proteins to be annotated incorrectly. For example, two proteins were identified as the anabolic ornithine carbamoyltransferase ArgF. Further investigation revealed that one of the proteins was more similar to the catabolic ornithine carbamoyltransferase, ArcB. These annotation discrepancies between highly homologous proteins, could result in the misinterpretation of results. Additionally, this issue highlights a clear disadvantage regarding the use of "non-reference" species and/or strain for proteomic based investigations. A related issue was that in this study, a number of uncharacterised proteins were found to be differentially expressed. However, the impact of these proteins on the cellular phenotype is not possible to determine until further investigation, characterisation and curation of the genome and proteome are performed.

Secondly, to ensure the late stationary phase cells remained in stationary phase during HT61 treatment (rather than enter and leave exponential phase, as per the cultures which were analysed during early stationary phase), the cells were treated using HT61 suspended in HBSS. This means that the results obtained for the late stationary phase groups are not immediately comparable to early stationary phase or biofilm treatment groups, which were treated using fresh TSB. Unfortunately, financial limitations meant that additional treatment groups (early stationary phase and biofilm treatment groups treated with HT61 suspended in HBSS), could not be performed. However, it should be noted that the data itself is not worthless and does provide insight into the proteomic profile of late stationary phase planktonic cells.

Furthermore, the number of biological replicates limits the statistical power available. Biological variants naturally present with higher levels of variation than technical replicates. In terms of protein concentrations, this can manifest as different basal protein levels, or different degrees of differential expression per sample. As only three biological replicates were utilised per treatment condition, there is potential for values to be skewed, particularly during the calculation of statistical significance. For example, when considering upregulation of the peptidoglycan biosynthesis pathway in late stationary phase cultures compared to early stationary phase cultures, 8 of the 9 proteins identified were upregulated according to the selection criteria employed in this chapter (Expression ratio ≥ 1.5). While these criteria are more than adequate to account for the accuracy of the mass spectrometer (previous studies have defined upregulation with an expression ratio ≥ 1.3)[219,241], only 3 of the 8 proteins were upregulated in a statistically significant manner, according to a one tailed student's t-test, $p \leq 0.05$.

To illustrate this problem, consider the protein, murA1. murA1 was upregulated 1.75 fold but was not deemed to be significantly altered ($p = 0.161$). However, another protein in the same dataset, the GTPase Era, was upregulated to a lesser degree and was considered significantly changed (1.73 fold, $p = 0.016$). An examination of the raw data behind murA1, (displayed in Table 11) shows that while 2 of 3 biological replicates demonstrated clear upregulation, one replicate did not satisfy the criteria for increased expression. Hence, even though the upwards trend is clear, there was no statistical significance. The only way to reduce the occurrence of instances like this is to increase the number of biological replicates. Data sets utilising three biological replicates are particularly sensitive to these types of analysis difficulties. However, it is also important to not automatically discount data that does not satisfy an arbitrary threshold for significance. When the expression of murA1 is examined alongside the entire dataset, there is strong evidence supporting its upregulation because other members of the *mur* operon are also upregulated.

Table 11: Expression dataset for the protein MurA1 following comparison of early and late stationary phase planktonic cultures of *S. aureus* UAMS-1

Numbers in bold describe the replicate. Data is presented as ng, normalised to the top 200 most abundant proteins per biological replicate. Expression ratios between the corresponding numbered replicates are displayed in brackets. Despite 2 of 3 late stationary samples presenting with clear upregulation of murA (Expression ratio ≥ 1.5), the remaining replicate is not differentially expressed, resulting in calculation of a p value that suggests the change is statistically insignificant (p = 0.161, one tailed students t-test)

Protein Concentration (ng)					
Early Stationary			**Late Stationary**		
1	**2**	**3**	**1**	**2**	**3**
0.001297	0.001954	0.001274	0.003104 (2.39 fold change)	0.002065 (1.06 fold change)	0.002764 (2.17 fold change)

Finally, the proteome extraction method utilised in this chapter was not optimised for the extraction of membrane proteins. As HT61 interacts with the membrane, understanding the impact of treatment on the composition of membrane proteins would have been a useful addition to the dataset. However, these types of extractions typically require the use of additives in the lysis buffer such as deoxycholic acid and high concentrations of SDS[278]. The addition of deoxycholic acid to the lysis buffers was tested, however it was not soluble in 0.1M TEAB and 4M G-HCl (data not shown). SDS could not be used as restrictions were placed on the mass-spectrometer, whereby samples containing high quantities of SDS were not able to be analysed.

In conclusion, this chapter has shown that planktonic and biofilm cultures of *S. aureus* present with diverse proteomic profiles and that biofilms can be highly heterogenous in regards to their metabolism. Treatment with the novel antimicrobial, HT61, suggests activation of the cell wall stress stimulon and *dcw* cluster, which are important regulators of cell integrity. However, no clear proteomic reason was identified which could explain why HT61 is more effective at treating late stationary phase cultures than biofilm or exponential phase planktonic cultures. Future work should aim to investigate the interactions of HT61 on the cell wall biosynthesis machinery using techniques such as TPP.

The remaining chapters of this thesis will investigate the effectiveness of HT61 towards a dual species biofilm model of *S. aureus* and *P. aeruginosa.* By applying NGS technologies to HT61 treated biofilm isolates, potential adaptive mechanisms, and the influence of interspecies interactions on bacterial evolution are explored.

Chapter 4

Development and Characterisation of a Stable Co-Culture Biofilm Model of *Pseudomonas aeruginosa and Staphylococcus aureus*

4 Development and Characterisation of a Stable Co-Culture Biofilm Model of *P. aeruginosa* and *S. aureus*

4.1 Introduction

The rise in AMR poses one of the greatest threats to modern medicine and treatment of bacterial infections is complicated by the presence of biofilms; surface attached communities of bacteria characterised by a highly heterogeneous composition and tolerance to antimicrobial treatment[10]. Tolerance to antimicrobial treatment has been directly associated with increased emergence of AMR in planktonic cultures[207]. It is possible that biofilm mediated tolerance mechanisms could contribute in a similar manner. Therefore, the development of relevant biofilm models is vital to understanding the interplay between biofilm tolerance mechanisms and the emergence of AMR.

Two bacterial species that are commonly implicated in biofilm infections are *P. aeruginosa* and *S. aureus.* In cystic fibrosis, co-infection with *P. aeruginosa* and *S. aureus* is associated with increased inflammation and reduced therapeutic outcomes for patients[144]. In chronic wounds, *P. aeruginosa* and *S. aureus* are the most commonly co-isolated bacterial species linked to poorer clinical outcomes[279]. However, whether the two species are co-localised or spatially partitioned remains a point of contention because *in vitro* studies suggest that the relationship of these two bacteria is often antagonistic in nature[149,150].

Although it is widely recognised that *in vivo* biofilms are composed of a multispecies consortium, the majority of *in vitro* biofilm studies fail to reflect this, focusing on single species biofilms. Previous models investigating co-culture of *P. aeruginosa* and *S. aureus in vitro* have frequently observed that *P. aeruginosa* rapidly outcompetes and reduces the viable numbers of *S. aureus* within 24 hours[149,150]. Consequently, use of these species within *in vitro* co-culture biofilm models is often restricted to short incubation periods, such as 24 or 48 hours[146,149–151], which is not representative of long-term biofilm colonisation associated with chronic infection. Furthermore, use of these short-term *in vitro* models does not address or investigate factors that could improve the viability of *S. aureus* within a co-culture population.

There is a dire need to explore the impact of biofilm associated interspecies interactions on bacterial viability, virulence and evolvability in order to develop novel treatment strategies and to even circumvent the emergence of adaptive mechanisms, such as those associated with AMR. In order to investigate bacterial evolvability, the mutation rate of a population can be estimated. Mutation rate can be defined as "the expected number of mutations that a cell will sustain during its lifetime" and is a more useful measurement than mutation frequency, which is simply a measure of the fraction of mutants within a population[280,281]. The generation of mutations is a stochastic process and results in the production of numerous mutant clonal lineages. If a low probability mutation occurs early on during growth, (jackpot mutations), mutant frequency can be distorted due to the expansion of these lineages. On the other hand, calculations of rate can account for these discrepancies[280,281].

There are two main methodologies to calculate rate: mutant accumulation studies and fluctuation analysis. In a mutant accumulation experiment, the change in mutant frequency is determined over time by measuring the increase in mutant fraction (*de novo* mutants as well as proliferation of pre-existing mutants) within a population. However, mutant accumulation experiments are arduous to perform, requiring large cell numbers, long timeframes and numerous sampling stages (which can introduce errors) which can limit their effectiveness[280,281].

The alternative approach is the fluctuation test, originally described in 1943 by Luria and Delbrück[282]. In this paper, the authors wanted to investigate the occurrence of phage resistance in *E. coli*. They showed that a random number of resistant colonies would occur following viral treatment, suggesting spontaneous and independent mutation, rather than adaptive evolution (which would result in identical mutant counts following treatment)[282]. The principles of the fluctuation test are simple: numerous parallel cultures, inoculated with a low cell number (to limit the occurrence of pre-existing mutants, approx. $10^2 – 10^3$ CFU), are plated onto a media that selects for mutants. These mutants are then counted and used to calculate a parameter defined as *m*, the number of mutations per culture. *m* is then divided by a function of the population size, N_t, to calculate the mutation rate, μ[280,281]. As of writing, the most accurate method for calculating *m* from the number of mutants, *r,* is the Ma-Sandri-Sarkar Maximum Likelihood Method and is utilised in the automated FALCOR calculator[283].

Analysis of the evolvability of biofilms has been limited, although calculation of mutation frequencies has linked biofilm growth of *P. aeruginosa* and *S. aureus* in mono-culture to increased mutation frequencies for each species, respectively[91,92]. However, the impact of interspecies interactions has not been evaluated. This is likely because, until recently, comparison of mutation rates derived from populations with differing cell densities has not been statistically validated[280,281]. However, it has recently been demonstrated that comparison of confidence intervals is a statistically valid approach to comparing mutation rates from experiments with different terminal population sizes[284].

The aim of this chapter was to develop and characterise an *in vitro* dual-species biofilm formed by *S. aureus* and *P. aeruginosa* that was more representative of chronic infection. To achieve this, the impact of strain selection and media composition (specifically iron content) was studied in order to identify the conditions that would facilitate growth of both species for 10 days. The effect of iron was examined because iron availability has been shown to be important for the growth of these bacteria; *P. aeruginosa* will even lyse *S. aureus* to utilise it as an iron source[149,153]. The effect of biofilm co-culture on the antimicrobial susceptibility of each species was also tested and biofilm morphology studied using CLSM. In addition, the effect of biofilm mono- and co-culture growth on the mutation rates of the *S. aureus* and *P. aeruginosa* populations was determined. To our knowledge, this is the first documented approach that uses the fluctuation assay to assess short-term biofilm evolvability. Finally, using next generation sequencing techniques, we compared two strains of *P. aeruginosa* to identify important genomic areas that may be important to consider when developing future co-culture models with this species and *S. aureus*.

4.2 Materials and Methods

4.2.1 Bacterial Strains and Growth Conditions

Table 12: Bacterial strains utilised in Chapter 4

Bacterial Species	Strain	Comments	Source
Staphylococcus aureus	UAMS-1	Methicillin sensitive clinical isolate, originally isolated from a patient with osteomyelitis[215]. Proficient biofilm former.	LGC Standards
	LAC AH1279	Methicillin resistant isolate, harbouring pCM11 plasmid, allowing for constitutive superGFP expression via sarA promoter.	Kind gift from Blaise Boles and Alex Horswill[285]
Pseudomonas aeruginosa	PAO1	Typical laboratory strain, non-mucoid. Originally a wound isolate. Proficient biofilm former.	University of Washington
	PA21	Non-mucoid, cystic fibrosis clinical isolate	Southampton CF Trust

The strains of *P. aeruginosa* and *S. aureus* utilised in this chapter are described in Table 1. Overnight planktonic cultures of *P. aeruginosa* and *S. aureus* were grown in LB broth, (ForMedium, UK) and TSB, (Oxoid, UK), respectively. Biofilm culture was performed in either Nunc Coated 6 well polystyrene plates (Thermo-Scientific, UK) to harvest biomass or in poly-L-lysine coated glass bottomed dishes (MatTek, USA), for imaging experiments, each utilising a total culture volume of 4 ml per well/dish.

Brain heart infusion (BHI, Oxoid, UK) was chosen as a medium for planktonic competition assays as well as biofilm mono and co-culture assays. BHI is a mixture of dehydrated brain and heart homogenates and is rich in physiologically sourced amino acids and proteins. The medium is also supplemented with salt and glucose, which acts as a source of carbon. The richness of the medium means that it is able to support the growth of a wide variety of bacterial species. However, this richness means that it is not indicative of conditions found in infection sites such as the CF lung, where the bacteria can be nutrient limited. Consequently, BHI was utilised at 50 % and 20 % strength to somewhat mimic nutrient limitation. Hemin was chosen as a physiologically relevant source of ferric iron and was supplemented to reduce competition for exogenous iron between *P. aeruginosa* and *S. aureus.*

Despite using BHI at a lower concentration, the overall richness of the medium, paired with the addition of hemin, means that it does not resemble a specific infection environment. Instead, it is more suited for basic science investigations, (such as

investigating the interactions of *P. aeruginosa* and *S. aureus*), in environments where competition for nutrients is limited.

All cultures were grown aerobically at 37 °C, with agitation at 120 rpm for planktonic cultures and 50 rpm for biofilms, unless otherwise stated.

For enumeration and differentiation between *P. aeruginosa* and *S. aureus,* planktonic and biofilm cultures were plated onto either cetrimide agar (Oxoid, UK) supplemented with 1% glycerol (Sigma-Aldrich, UK) and Baird Parker agar, (BPA), supplemented with 5% egg yolk tellurite emulsion (Oxoid, UK). Cetrimide agar contains several quaternary ammonium salts that are toxic to bacteria other than *P. aeruginosa*. In addition, cetrimide will increase the production of *P. aeruginosa* pigments. BPA contains potassium salts and tellurite which inhibit the growth of contaminants, while the addition of pyruvate and glycine enhance Staphylococcal growth.

4.2.2 Growth Kinetics

Overnight cultures were diluted to approximately 10^6 CFU ml^{-1} in either LB or TSB as appropriate and incubated for 24 hours at 37 °C with optical density measurements at 560 nm (OD_{560}) taken every 15 minutes for 15 hours.

4.2.3 Crystal Violet Assay

S. aureus UAMS-1 and LAC AH1279, (referred to as *S. aureus* LAC from this point forward), biofilms were grown using TSB in 6 well Nunc Coated 6 well plates at 37 °C, 50 rpm for 72 hours, with media exchanges every 24 hours. *P. aeruginosa* PAO1 and PA21 biofilms were grown in an identical fashion with LB. Crystal violet staining was performed at 24, 48 and 72 hours. Spent media was removed and biofilms stained with 0.1% (v/v in dH_2O) crystal violet for 10 minutes at room temperature. The stain was removed and biofilms rinsed 3 times with dH_2O to remove excess crystal violet. 30% acetic acid was then added to each biofilm and incubated for 10 minutes at room temperature with light shaking. The suspended crystal violet was removed and the OD_{584} measured using a spectrophotometer (Jenway 6300), with 30% acetic acid used as a blank.

4.2.4 Planktonic Competition Assays

The relative fitness of *S. aureus* UAMS-1 and LAC was determined when cultured in competition with either *P. aeruginosa* PAO1 or PA21 in either 20 % strength BHI (Oxoid, UK) or 20% BHI supplemented with hemin (Sigma-Aldrich, UK) at a final concentration of 2 μM, 20 μM or 100 μM. Iron availability is important for these two species, particularly *in vivo*[153]. Hemin was chosen as a ferric iron donor, as it bears more *in vivo* relevance, rather than direct supplementation with $FeCl_3$. Following initial overnight culture in LB or TSB as previously stated, all strains were diluted to 10^6 CFU ml^{-1} in the selected liquid media and set up in competition so that each strain of *P. aeruginosa* was cultured with each strain of *S. aureus*. A sample of each starting competition inoculum was serially diluted in Hanks Balanced Salt Solution (HBSS, Sigma-Aldrich UK) and plated onto cetrimide agar and BPA to obtain initial cell counts, prior to incubation at 37 °C, 120 rpm for 24 hours. Final counts of each bacterial species were obtained by diluting samples in HBSS from the completed assays onto cetrimide agar and BPA.

The relative fitness of each bacterial species and strain in competition with the other was obtained by comparing the ratio of their Malthusian parameters ($M_{P.\ aeruginosa}$ and $M_{S.\ aureus}$) whereby:

$$M_{P.aeruginosa} = {}^{N_i}\!/_{N_f}$$

$$M_{S.aureus} = {}^{N_i}\!/_{N_f}$$

$$W = {}^{\log M_{P.aeruginosa}}\!/_{\log M_{S.aureus}}$$

$N_i =$ Initial cell number

$N_f =$ Final cell number

$W =$ Relative fitness

4.2.5 Biofilm Co-Culture Optimisation

The ability for *P. aeruginosa* and *S. aureus* to form dual species biofilms was assessed over 240 hours and was adapted from a previously used method[286]. Briefly, overnight cultures of *P. aeruginosa* PAO1 or *P. aeruginosa* PA21 and *S. aureus* UAMS-1 or *S. aureus* LAC were diluted to 10^5 CFU ml $^{-1}$ in ½ strength BHI at a 1:1 ratio of each species. 1 ml was used to inoculate each well of a Nunclon coated 6 well plate (Thermo Scientific, UK) and incubated for 6 hours at 37 °C, 50 rpm to facilitate bacterial attachment. Media was then replaced with 4 ml of 20% BHI or 20% BHI supplemented with hemin (Sigma-Aldrich, UK) at a final concentration of 2 μM, 20 μM or 100 μM. Fresh media replacements occurred after a further 18 hours and every 24 hours thereafter. After 24, 72, 168 and 240 hours, biofilms were rinsed twice with HBSS to remove non-adherent cells and harvested using a cell scraper. Cell suspensions were serially diluted and plated onto cetrimide agar and BPA for selective enumeration of *P. aeruginosa* and *S. aureus,* respectively.

4.2.6 Confocal Laser Scanning Microscopy of *P. aeruginosa* and *S. aureus* co-culture

Mono- and co-culture biofilms of *P. aeruginosa* PA21 with *S. aureus* UAMS-1 or *S. aureus* LAC were cultured to assess biofilm architecture. Biofilms were grown as previously described using 20% BHI supplemented with 20 μM hemin in MatTek dishes. Biofilms were assessed at 24, 72, 168 and 240 hours of growth. To prepare biofilms for imaging, spent media was removed and the biofilms rinsed twice with HBSS prior to staining for 15 minutes with 1 ml of LIVE BacLight Bacterial Gram stain (Life Technologies), (3 μl ml^{-1} SYTO9, 2 μl ml^{-1} hexidium iodide). Imaging was performed using an inverted Leica TCS SP8 confocal laser scanning microscope and a 63x glycerol immersion lens, with 1 μm vertical sections. Fluorescent dyes were excited using concurrent 514 nm and 561 nm lasers.

4.2.7 Antimicrobial Susceptibility Testing

The MIC of rifampicin (Sigma-Aldrich, UK) was determined for both *P. aeruginosa* PA21 and *S. aureus* UAMS-1 using the broth microdilution method. Briefly, overnight cultures of each strain were diluted to approximately 10^6 cells and treated with a two-fold dilution series of rifampicin (0 to 128 μg ml^{-1}). Following incubation at 37 °C for 24 hours, the endpoint optical density at 680 nm (OD_{680}) was measured with a microplate reader (BMG Omega) and the MIC determined as the antimicrobial concentration that resulted in no bacterial growth within the wells.

The biofilm MBCs of several antimicrobials was also determined for mono- and co-culture biofilms of *P. aeruginosa* PA21 and *S. aureus* UAMS-1. Biofilms were cultured in Nunclon coated 6 well polystyrene plates as previously described, with a 6 hour attachment phase in 50% BHI prior to media replacement with 20% BHI supplemented with 20 μM hemin. Incubation was performed at 37 °C, 50 rpm. Following 72 hours of culture, spent media was replaced with media, supplemented with a twofold dilution series of either tobramycin, vancomycin or HT61 (0 to 128 μg ml^{-1}). After an additional 24 hours of incubation, biofilms were rinsed twice with HBSS, harvested with a cell scraper and serially diluted and plated onto cetrimide agar and BPA. Plates were incubated at 37 °C for 24 hours and viable CFUs were counted. The biofilm MBCs were identified as the antimicrobial concentration resulting in a 3-log reduction in CFU's compared to the untreated control group.

4.2.8 Estimation of Planktonic and Biofilm Mutation Rates

Fluctuation tests were performed for planktonic cultures as previously described in Foster (2006)[281] and adapted for use with biofilm cultures grown in 6 well plates. Both planktonic and biofilm assays were adjusted to be as comparable as possible.

Overnight cultures of *P. aeruginosa* PA21 and *S. aureus* UAMS-1 were diluted to 10^3 CFU ml^{-1} in 50% BHI, either in isolation, or in a 1:1 co-culture. 30 parallel planktonic or biofilm cultures were initiated using 1 ml of the inoculum in 20 ml universal containers or Nunclon coated 6 well plates, respectively. All cultures were incubated at 37 °C, 50 rpm for 6 hours, with planktonic cultures tilted at approximately 45° to allow for movement of the media.

Following incubation, planktonic cultures were centrifuged at 4000 x *g* for 15 minutes. The cell pellet was re-suspended in 4 ml of 20% BHI supplemented with 20 μM hemin. For biofilm cultures, spent media was removed and replaced with 4 ml of 20% BHI supplemented with 20 μM hemin. All cultures were incubated at 37 °C, 50 rpm for a further 18 hours. Following incubation, planktonic cultures were centrifuged at 4000 x *g* and the cell pellet rinsed twice with 4 ml HBSS. The pellet was re-suspended in 500 μl HBSS. Biofilm cultures were rinsed twice as previously described and harvested using a cell scraper into 500 μl HBSS.

As all cultures were grown equally and grown to saturation, the final cell count was determined by taking a sample from 5 random cultures, which was serially diluted and plated onto cetrimide agar and BPA. Limiting the number of cultures used to calculate final cell density maximises the total volume available for the subsequent detection of spontaneous mutants. Half of each remaining planktonic and biofilm suspension was then plated onto cetrimide agar and BPA supplemented with 64 μg ml^{-1} or 0.25 μg ml^{-1} rifampicin for selection of spontaneous rifampicin resistant *P. aeruginosa* or *S. aureus* mutants, respectively. These concentrations were determined to be 4 X the calculated MIC of each species. All plates were incubated at 37 °C. Plates without antibiotics were counted following 24 hours of incubation to determine the total cell counts. Plates containing rifampicin were incubated for 48 hours prior to CFU enumeration.

Mutation rates were calculated using the online calculator FALCOR and the Ma-Sandri-Sarkar Maximum Likelihood Estimator[283]. Fluctuation tests were performed with 2 biological replicates (for a total of 60 technical replicates).

4.2.9 Genomic Comparison of *P. aeruginosa* PAO1 and PA21

To determine if there were any large-scale genetic differences that could explain the differing ability of *P. aeruginosa* PAO1 and PA21 to form dual species biofilms with *S. aureus*, the entire genomes of each *P. aeruginosa* strain were sequenced and compared. Short read sequencing was performed by MicrobesNG on Illumina MiSeq and HiSeq platforms using 250 bp paired end reads. Long read sequencing of *P. aeruginosa* PAO1 and *P. aeruginosa* PA21 was performed using the MinIon sequencing platform (Oxford Nanopore, UK and the rapid barcoding kit as per manufacturer's instructions (refer to Chapter 3 for full methodology). Long read data was basecalled using albacore and trimmed and demultiplexed using PoreChop (https://github.com/rrwick/Porechop) with default settings.

Sequence data was assembled *de novo* using Unicycler[287] in normal mode resulting in a hybrid assembly for both strains. Genomes were annotated using PROKKA[244]. Annotations were preserved and genomes compared using RAST[245,246]. ResFinder 3.0 (https://cge.cbs.dtu.dk/services/ResFinder/, last accessed 14/02/18) and PHASTER[288,289] (http://phaster.ca/ , last accessed 07/02/18) were used to identify genes associated with antimicrobial resistance and bacteriophages, respectively.

4.2.10 Statistical Analysis

Statistical significance was calculated using a variety of tests. Crystal violet data and comparisons between single species biofilms were made using multiple t-tests with the Holm-Sidak correction, the effects of media composition and bacterial competition on fitness was analysed using a 2-way ANOVA and Kruskal-Wallis test with Dunn's multiple comparisons was used to analyse within time point comparisons of biofilm co-culture and for comparison of biofilm maximum thickness, derived from microscopy data. (within time point comparisons of bacterial growth following biofilm co-culture in different media compositions). For all of the above statistical tests, $\alpha < 0.05$.

Statistical significance was determined between fluctuation tests by comparing 94 % confidence intervals. Comparison of 94% confidence intervals has been demonstrated to mimic statistical tests for $p \leq 0.01$ and has also been shown to be a valid statistical approach when comparing fluctuation test data with differing terminal cell population sizes[284,290].

The majority of statistical analyses were performed using GraphPad Prism version 7.0d for Mac. The R package, RSalvador[291], was used to calculate 94% confidence intervals for the fluctuation test data. Confocal image z-stacks were analysed using the COMSTAT 2 plug in for ImageJ (downloadable at www.comstat.dk)[218].

4.3 Results

4.3.1 Planktonic Co-Culture of *P. aeruginosa* and *S. aureus* Did Not Affect Relative Fitness of Either Species, Despite Differences in Growth Kinetics or Biofilm Formation

Basic phenotyping of each strain of *P. aeruginosa* and *S. aureus* was performed, comparing growth kinetics, (Figure 32A), capacity to form and grow biofilms (Figure 32B), and the relative fitness of each strain when grown as planktonic co-cultures in a selection of defined media (Figure 33).

No difference in growth kinetics was observed for either strain of *S. aureus*, and both exhibited similar biofilm-forming capacities with no statistically significant differences at any time point (multiple t-tests, Holm-Sidak correction: 24 hr $p = 0.505$, 48 hr $p = 0.615$, 72 hr $p = 0.893$).

For *P. aeruginosa*, the exponential phase of growth for PAO1 was approximately 2 hours longer than that of PA21, although final cell density was equal between cultures (data not shown). PAO1 formed biofilms with considerably more biomass at each measured time point compared to PA21, (multiple t-tests, Holm-Sidak correction: 24 hr $p = 0.0001$, 48 hr $p < 0.0001$, 72 hr $p = 0.0002$). Both strains formed more biofilm biomass than either strain of *S. aureus*.

Finally, the relative fitness of each *S. aureus* strain in planktonic co-culture with each *P. aeruginosa* strain was calculated following 24 hours of growth in 20% BHI, and 20% BHI supplemented with hemin to a final concentration of either 2 μM, 20 μM or 100 μM (Figure 2). Iron availability is known to be important for bacterial growth *in vivo*[153,292] and has been implicated as an important factor for the survival of these two bacterial species in co-culture[149]. Hemin, an iron containing porphyrin, was chosen as a ferric iron donor to mimic *in vivo* iron delivery mechanisms that would be available to the bacteria during host infection[286,293]. Understanding planktonic fitness in these media was important as they were to be used for co-culture biofilm assays.

Relative fitness values for each combination was approximately equal to 1 in all permutations, with no statistical differences between any calculated values (2-way

ANOVA, Interaction $p = 0.0538$, Bacterial Combinations $p = 0.1960$, Media choice $p = 0.5100$). This suggests that there was no decrease in *Staphylococcal* fitness when co-cultured with either strain of *P. aeruginosa* (and vice versa).

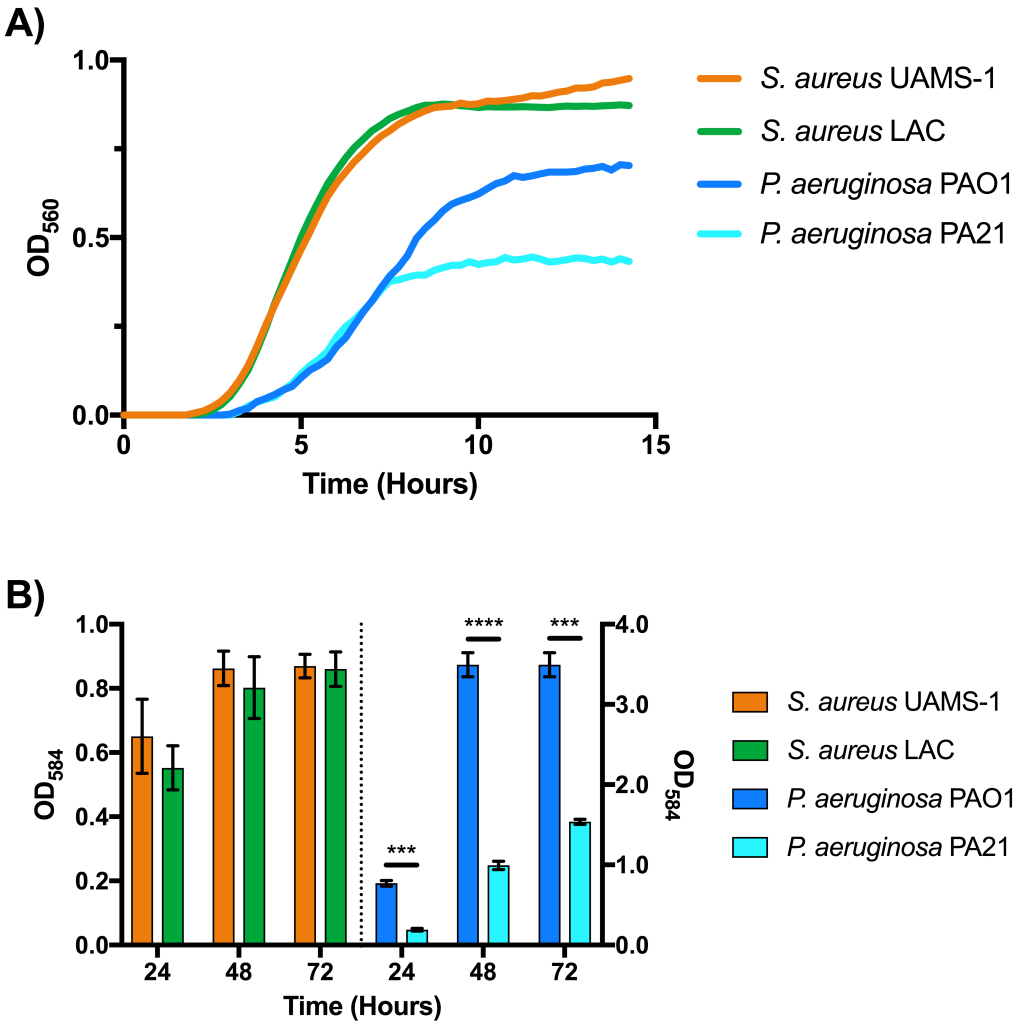

Figure 32: Growth kinetics and biofilm formation ability of *P. aeruginosa* PAO1, PA21 and *S. aureus* UAMS-1 and LAC

A) S. aureus UAMS-1 and LAC exhibit near identical growth kinetics and biofilm formation whereas P. aeruginosa PAO1 and PA21 differ on both accounts. Both enter exponential phase at the same point in time, but PA21 enters stationary earlier resulting in a considerably less dense culture. B) Biofilm formation of PA21 is also less than that measured for PAO1 at all time points.
Growth curves: n = 12 for S. aureus, n = 3 for P. aeruginosa, Crystal violet assays: n = 3. Error bars represent standard error of the mean. **** $p \leq 0.0001$, *** $p \leq 0.001$. P values calculated using multiple unpaired student t-tests, corrected using the Holm-Sidak method.

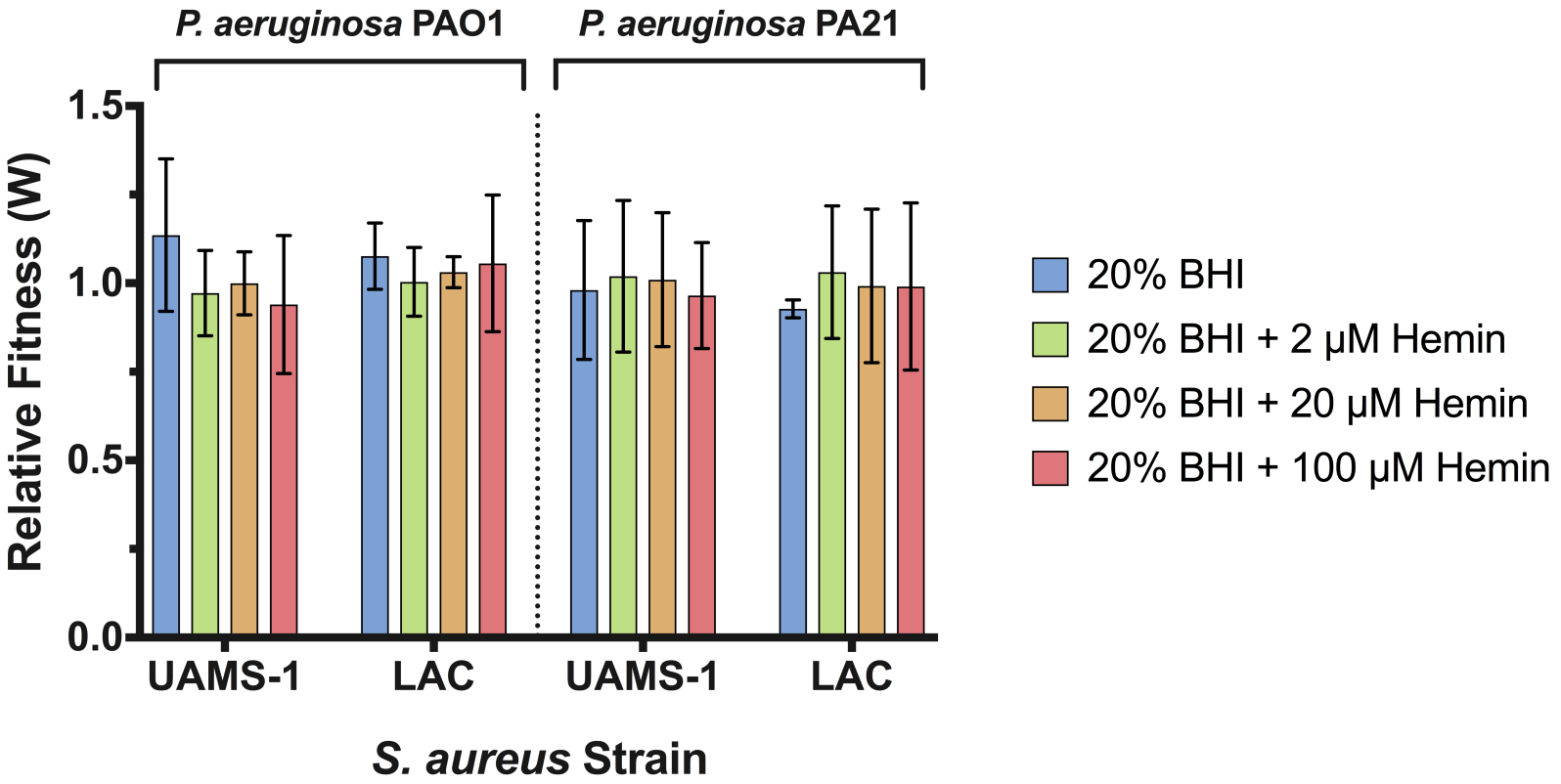

Figure 33: Relative fitness of *P. aeruginosa* and *S. aureus* strains in planktonic co-culture

Relative Fitness of *S. aureus* UAMS-1 and *S. aureus* LAC following planktonic co-culture with *P. aeruginosa* PAO1 and *P. aeruginosa* PA21 in either 20% BHI or 20% BHI supplemented with hemin to a final concentration of 2, 20 or 100 μM. There is no statistically significant difference in relative fitness when either media or strain combination is considered, in combination ($p = 0.0538$) or in isolation (strain combination $p = 0.1960$, media $p = 0.5100$ as calculated from a 2-way ANOVA). As all values of relative fitness are approximately 1, there is no change in fitness of *S. aureus* compared to *P. aeruginosa*. Neither species has a competitive advantage over the other in planktonic culture. $n = 9$, from 3 biological replicates for each competition. Error bars represent 95% confidence intervals.

4.3.2 Addition of Hemin Does Not Affect Viability of *S. aureus* or *P. aeruginosa* During Growth as a Single Species Biofilm

Prior to biofilm co-culture, the effects of hemin on the growth of each species and strain as single species biofilms was determined (Figure 34). By 24 hours, *P. aeruginosa* PA21 formed biofilms with a lower cell density compared to those formed by *P. aeruginosa* PAO1 at 24 hours in all media tested (multiple unpaired t-tests with Holm-Sidak Correction for each media combination, $p \leq 1.34 \times 10^{-6}$ for all conditions, see Appendices for data). Cell densities for each *P. aeruginosa* strain remained largely consistent at approximately 10^8 CFU cm^{-2} across the time course of the experiment, with only slight discrepancies. Specifically, *P. aeruginosa* PA21 was slightly lower in density in 20% BHI + 2μM hemin at 72 hours, ($p = 0.0218$) and in 20% BHI + 100 μM hemin at 168 hours ($p = 0.0005$). However, by 240 hours, both strains of *P. aeruginosa* were of equal density with no statistically significant differences between them, in any media.

Regarding the two strains of *S. aureus*, both strains formed biofilms with equal cell densities at 24 and 72 hours, regardless of the hemin concentration in the media. By 168 hours, regardless of hemin supplementation, *S. aureus* LAC biofilms exhibited approximately a 1 log lower cell density compared to *S. aureus* UAMS-1, indicating reduced viability or increased antagonism with *P. aeruginosa* ($p \leq 0.0203$, see Appendices for full statistics). This 1 log difference in viability remained between the strains following 240 hours of growth ($p \leq 2.6 \times 10^{-6}$, see Appendices for full statistics).

Fundamentally, this assay demonstrates that altering the hemin concentration of the media does not alter the viability or growth patterns of *P. aeruginosa* or *S. aureus* as a single species biofilm, as any inter-strain differences are maintained across all media, regardless of hemin concentration.

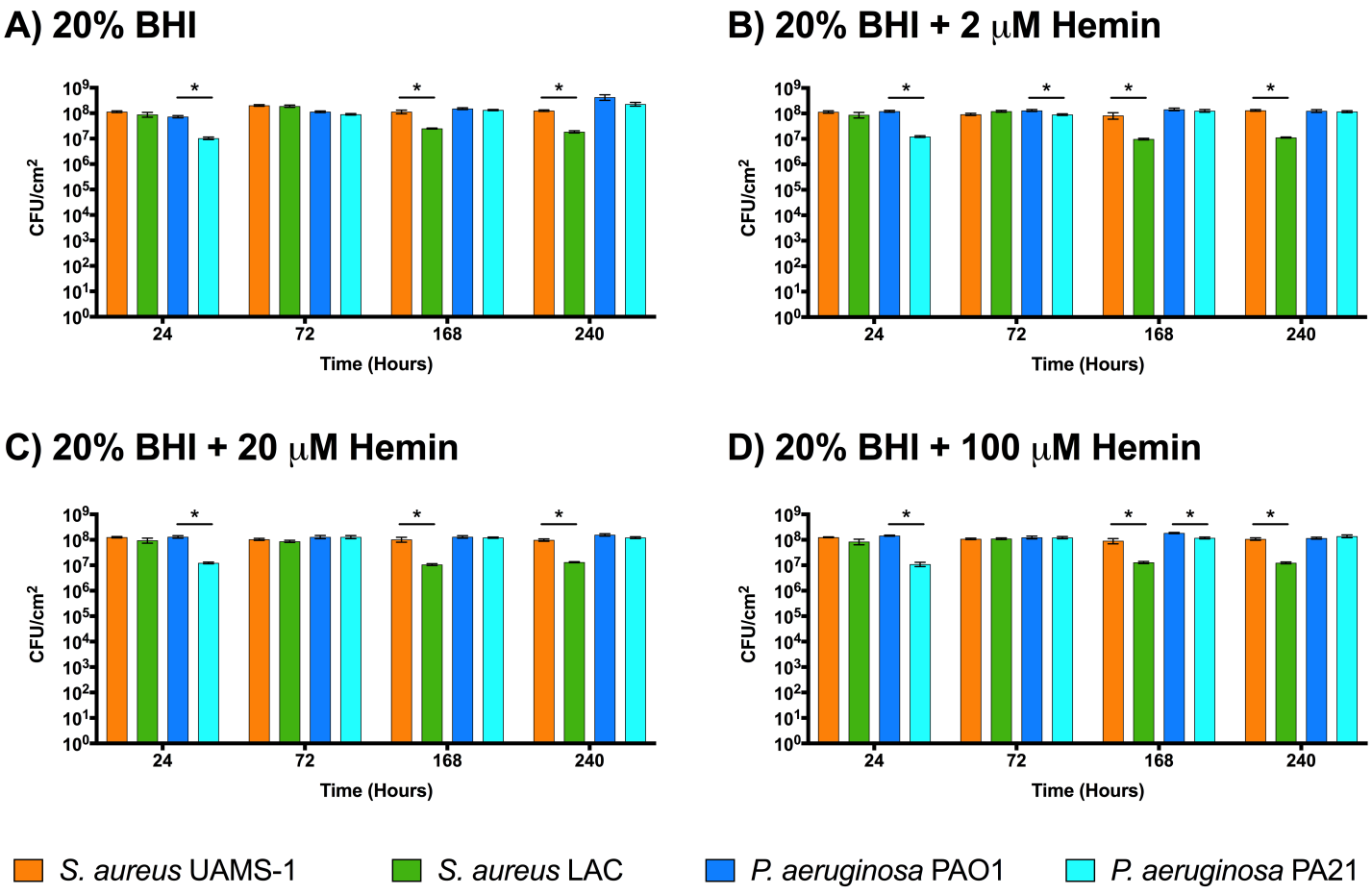

Figure 34: Effect of altering hemin concentration on biofilm mono-culture of *P. aeruginosa* and *S. aureus*

Altering the concentration of hemin within the media does not alter the viability or ability of any of the species and strains tested to form a single species biofilm. Differences between strains of the same species are highlighted if deemed statistically significant: * $p \leq 0.05$, based on student t-tests, corrected with the Holm-Sidak method. n = 9, from 3 biological replicates.

4.3.3 *P. aeruginosa* Strain Selection and Increased Hemin Concentrations Facilitate the Survival of *S. aureus* During Biofilm Co-Culture

Co-culture biofilms of *P. aeruginosa* PAO1 or PA21 with *S. aureus* UAMS-1 and LAC were cultured for 10 days (240 hours) and the impact of different hemin concentrations on the viability of the co-culture was assessed (Figure 35). *P. aeruginosa* viability was not affected by the addition of hemin to the media. In all co-cultures, *S. aureus* was present at a lower abundance compared to *P. aeruginosa*. Furthermore the *S. aureus* cell densities identified during co-culture were considerably lower than the associated *S. aureus* densities following growth within a single species biofilm (as per Figure 34).

For the co-culture of *P. aeruginosa* PAO1 and *S. aureus* UAMS-1, (Figure 35, panel A), addition of hemin reduced *S. aureus* viability at 24 hours, although the reduction was not statistically significant in BHI supplemented with 20 μM hemin (No hemin vs 2 μM: $p = 0.0167$, No hemin vs 20 μM: $p > 0.999$, No hemin vs 100 μM: $p = 0.0006$).

S. aureus LAC was not detectable following 72 hours of growth with *P. aeruginosa* PAO1. Hemin supplementation improved *S. aureus* viability so that it was detectable at 72 hours, although due to a number of zero counts in 2 μM hemin, the improved viability was only significant in 20 or 100 μM hemin (72 hour *p* values: No hemin vs 2 μM = 0.7089, No hemin vs 20 μM = 0.0015, No hemin vs 100 μM = 0.0241). However, similar to *S. aureus* UAMS-1, *S. aureus* LAC was not detectable after 168 hours regardless of hemin supplementation.

Conversely, both strains of *S. aureus* were detectable after 240 hours of co-culture with *P. aeruginosa* PA21 (Figure 2, panels B and D). Hemin supplementation improved viability further, although for both strains, *S. aureus* counts in 2 μM hemin were statistically identical to counts in non-supplemented media at all time points ($p > 0.9999$). In the non-supplemented and 2 μM hemin supplemented media *S. aureus* UAMS-1 viability decreased over 240 hours from approx. 10^5 CFU cm^{-2} to 10^2 CFU cm^{-2}, whereas *S. aureus* LAC remained at a density between approximately 10^2 and 10^3 CFU cm^{-2}. Supplementation of media with 20 and 100 μM hemin increased *S. aureus* viability compared to non-supplemented media with final counts at 240 hours approximately 10^5

CFU cm^{-2} for both strains (*S. aureus* No hemin vs 20 μM *p* values: UAMS-1 240 hour < 0.0001, LAC 240 hour = 0.0033). *S. aureus* viability in media supplemented with 100 μM hemin was similar to that in media supplemented with 20 μM hemin, with the exception of *S. aureus* UAMS-1 at 24 hours, which was 1 log lower in density ($p < 0.0001$). All other differences were statistically insignificant (20 μM vs 100 μM *S. aureus* UAMS-1 *p* values: 72 hour > 0.9999, 168 hour > 0.9999, 240 hour = 0.5851 and 20 μM vs 100 μM *S. aureus* LAC *p* values: 24 hour = 0.0753, 72 hour > 0.9999, 168 hour = 0.4190, 240 hour > 0.9999)

Addition of 100 μM hemin did not discernibly improve viability of *S. aureus* or *P. aeruginosa* compared to supplementation with 20 μM hemin. In addition, it was observed that use of a higher concentration resulted in heavy deposition of hemin within the biofilm culture wells. For this reason, subsequent assays utilised hemin at a concentration of 20 μM in 20% BHI.

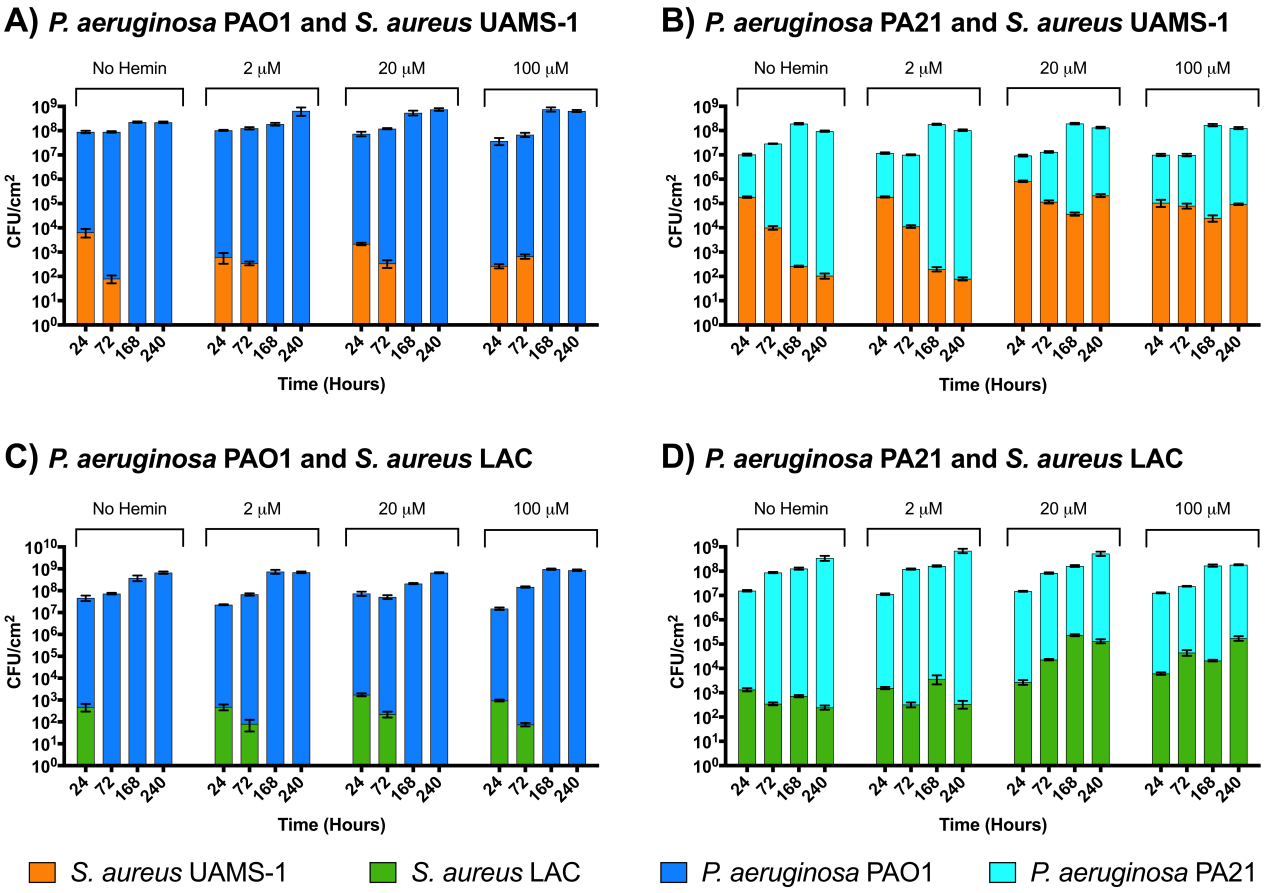

Figure 35: Effects of hemin supplementation on the dynamics of *P. aeruginosa* and *S. aureus* biofilm co-culture

The ability of *S. aureus* to survive in co-culture depends on a combination of the *P. aeruginosa* strain and the hemin concentration of the media. Both strains of *S. aureus* were less successful in co-culture with *P. aeruginosa* PAO1, compared to *P. aeruginosa* PA21. Kruskal Wallis with Dunn's multiple comparison performed to determine significance between different media compositions. Points of note are mentioned in the text. Due to the large number of comparisons, significance levels are not presented on chart and are instead compiled in the supplementary information. n = 9 from 3 biological replicates

4.3.4 Visualisation of *P. aeruginosa* and *S. aureus* Biofilm Co-Cultures

To visualise changes in biofilm morphology, *P. aeruginosa* PA21 was co-cultured using 20% BHI supplemented with 20 μM hemin, with either *S. aureus* UAMS-1 or *S. aureus* LAC in MatTek glass bottom dishes and harvested at 24, 72, 168 and 240 hours. Biofilms were stained using a fluorescent Gram stain (Thermo-Fisher) and visualised using CLSM. Differences in maximum thickness of the biofilms was calculated using COMSTAT 2. Representative images at each time point are presented in Figure 36, for biofilms of *P. aeruginosa* PA21 and *S. aureus* UAMS-1 and in Figure 37, for biofilms of *P. aeruginosa* PA21 and *S. aureus* LAC.

When cultured in isolation, *P. aeruginosa* PA21 began to form microcolony structures after 24 hours of growth. These structures expanded after 72 hours and by 168 hours of growth had formed a confluent layer. By 240 hours of growth, the overall density of the biofilm appeared to reduce, possibly due to biofilm dispersal, although microcolony-esque clumps of cells were still visible, contributing to increased maximum biofilm thickness (Figure 38). Both *S. aureus* UAMS-1 and *S. aureus* LAC underwent a near identical biofilm development cycle, corroborating the previously obtained crystal violet and CFU data (Figure 32 and Figure 34, respectively), forming a uniform sheet of biomass without any significant changes in maximum biofilm thickness over 240 hours (Figure 38, $p > 0.05$).

As for the *P. aeruginosa* PA21 and *S. aureus* UAMS-1 co-culture, *S. aureus* was distributed uniformly throughout the biofilm for the first 72 hours. By 168 hours of growth, *S. aureus* appeared to become more abundant around cellular aggregates, (indicated by the yellow colour within the image, indicative of a high number of green and red (*P. aeruginosa* and *S. aureus*) cells in close proximity), similar to the observation made

by DeLeon *et al*[151]. By 240 hours, the dense areas of *Staphylococcal* cells appeared to have lessened, although clumps of red cells were still apparent (indicated by the white arrows).

When the co-culture of *P. aeruginosa* PA21 and *S. aureus* LAC is considered, (Figure 37), a similar observation was seen apparent over the first 72 hours of growth, with *S. aureus* evenly distributed across the biofilm. Unlike *S. aureus* UAMS-1, this uniform distribution was more apparent at 168 and 240 hours, with far fewer localised clumps of *S. aureus* AH1278, suggesting altered propensity for microcolony formation and/or different interactions with *P. aeruginosa* PA21.

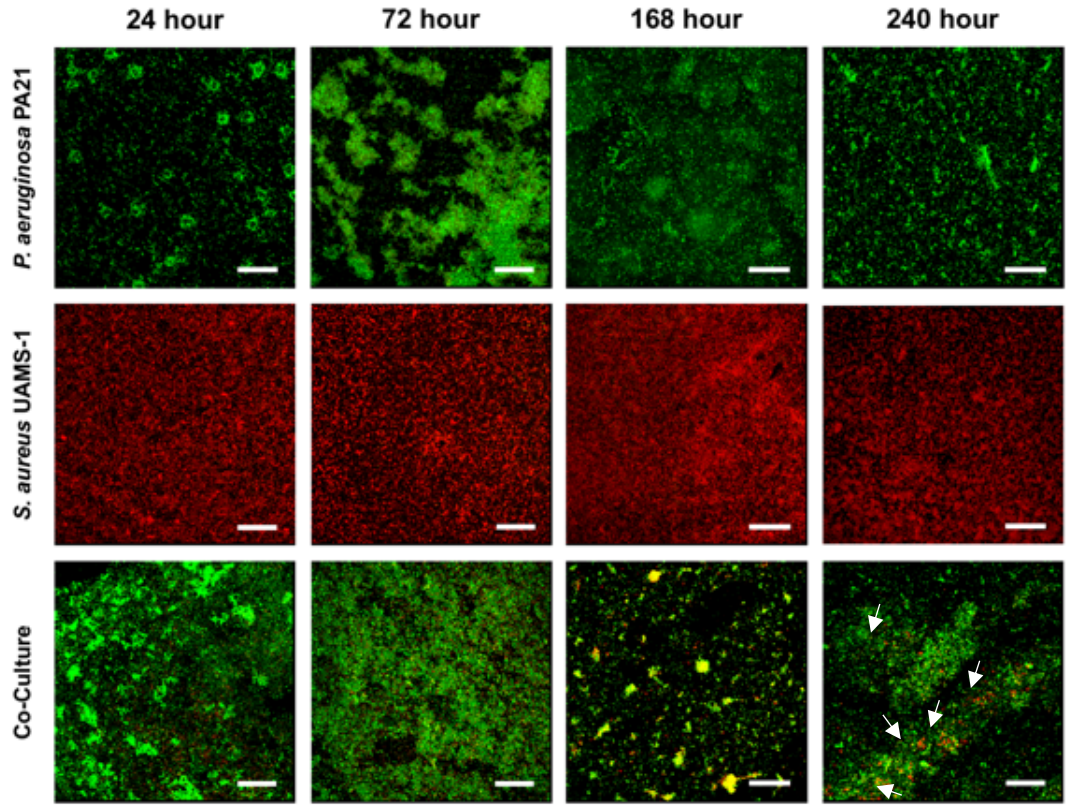

Figure 36: Representative confocal laser scanning microscopy images of a single and dual species biofilms of *P. aeruginosa* PA21 and *S. aureus* UAMS-1 over 240 hours

Biofilms were stained with a fluorescent Gram stain for differentiation between species. Hexidium iodide stains Gram-positive bacteria to fluoresce red, (*S. aureus*), while SYTO9 counterstains the remaining Gram-negative bacteria (*P. aeruginosa*) and fluoresces green. White arrows point to clumps of *S. aureus* UAMS-1 within the biofilm as mentioned in the text. Scale bars represent 25 μm.

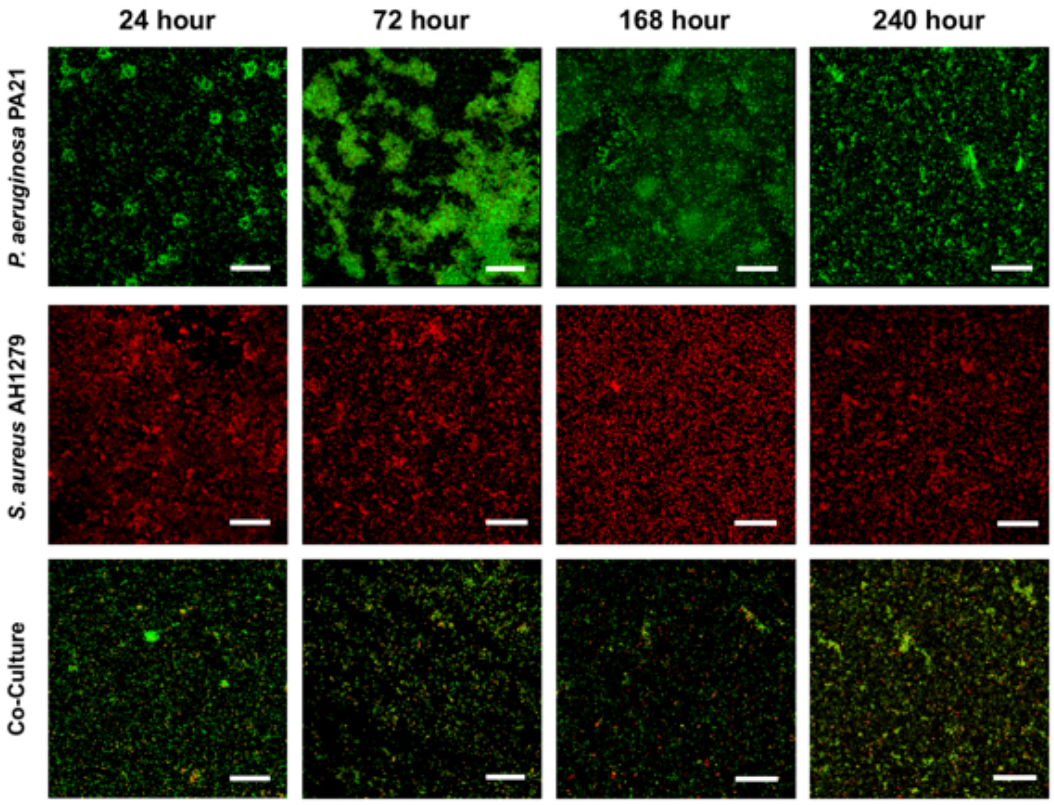

Figure 37: Representative confocal laser scanning microscopy images of a single and dual species biofilms of *P. aeruginosa* PA21 and *S. aureus* LAC over 240 hours

Biofilms were stained with a fluorescent Gram stain for differentiation between species. Hexidium iodide stains Gram-positive bacteria to fluoresce red, (*S. aureus*), while SYTO9 counterstain the remaining Gram-negative bacteria (*P. aeruginosa*). Scale bars represent 25 μm

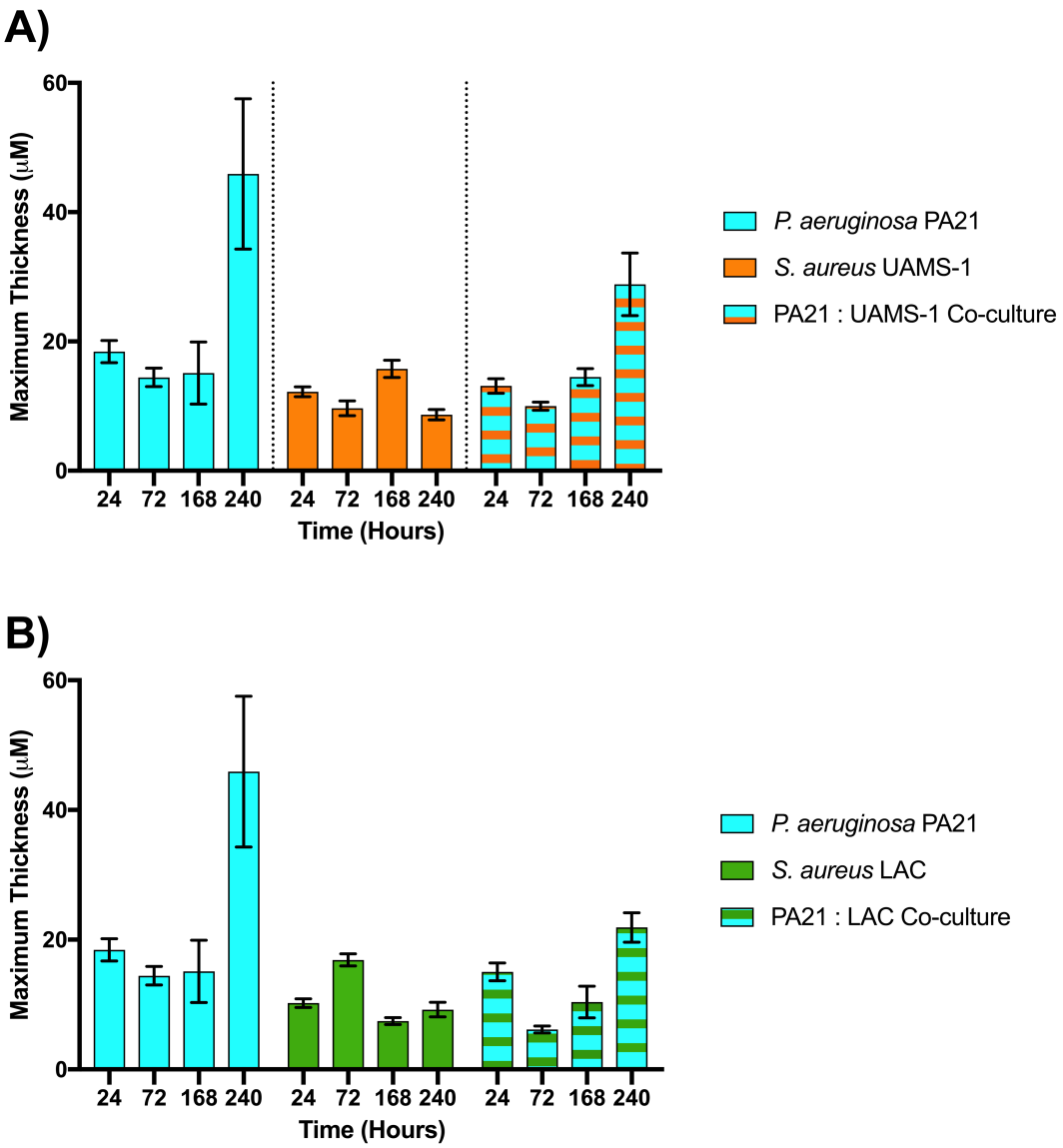

Figure 38: Maximum thickness of single and co-culture biofilms of *P. aeruginosa* PA21 and A) *S. aureus* UAMS-1 or B) *S. aureus* LAC

Maximum biofilm thickness was similar between all species, strains and co-cultures for the first 168 hours. By 240 hours, co-culture of *P. aeruginosa* PA21 with either strain of *S. aureus* caused a reduction in maximum biofilm thickness compared to a biofilm of *P. aeruginosa* PA21 in isolation. Kruskall-Wallis with Dunn's multiple comparisons used to compare differences between single species and co-culture within time points, but no differences were deemed significant ($p > 0.05$). n = 9 for single species biofilms, using only images from the SYTO9 or hexidium iodide channels, to exclusively quantify P. aeruginosa or S. aureus, respectively. n = 18 for dual species biofilms to account for the analysis of both separate fluorescent channels (n=9 SYTO9, n=9 hexidium iodide). Error bars represent standard error of the mean.

S. aureus LAC constitutively expresses sGFP so imaging was attempted using a red counterstain (SYTO59) with *P. aeruginosa* PA21. If successful, *S. aureus* cells would fluoresce green while all cells would be stained red; as such the *S. aureus* would be able to be distinguished. However, *S. aureus* fluorescence decreased over the course of the assay, suggesting plasmid loss. For optimal plasmid maintenance, it is recommended that *S. aureus* LAC is cultured in media containing 10 μg ml^{-1} spectinomycin[285]. Plasmids typically confer a fitness cost to a bacterial species and unless they are maintained with an appropriate selective condition, they can be lost[294]. However, it was decided not to co-culture these biofilms in media containing antimicrobials as antimicrobial pressure is known to influence biofilm formation[44,295]. The lack of plasmid selection, paired with the possibility of reduced fitness due to negative interactions with *P. aeruginosa*, meant that plasmid loss occurred over the course of the assay, to such an extent that no *S. aureus* was visible at 168 hours (despite CFU counts and fluorescent Gram stains confirming its presence.

As a proof of concept, *P. aeruginosa* PA21 and *S. aureus* UAMS-1 were exclusively used for further phenotyping experiments.

4.3.5 Biofilm Co-Culture Alters the Antimicrobial Susceptibility of *P. aeruginosa* and *S. aureus*

Table 13: Antimicrobial susceptibility of *P. aeruginosa* PA21 and *S. aureus* UAMS-1 in single and dual species biofilms

Biofilm minimum bactericidal concentrations (MBCs) of tobramycin, vancomycin and HT61 defined as the concentration of antimicrobial that reduced the viable counts of each species by 3 log or more. Values in table represent antimicrobial concentration in μg ml^{-1} n = 9 for tobramycin and vancomycin, n = 6 for HT61. Biofilm co-culture increased the tobramycin MBC for *P. aeruginosa* from 2 μg ml^{-1} to 4 μg ml^{-1} but did not alter susceptibilities to vancomycin or HT61. The susceptibility of *S. aureus* to vancomycin was not altered during co-culture but decreased from 16 μg ml^{-1} to 2 μg ml^{-1} for tobramycin and from 64 μg ml^{-1} to 16 μg ml^{-1} for HT61.

	***P. aeruginosa* PA21**		***S. aureus* UAMS-1**	
Antimicrobial	Single Species	Dual Species	Single Species	Dual Species
Tobramycin	2	4	16	2
Vancomycin	> 128	> 128	> 128	> 128
HT61	> 128	> 128	64	16

To prove that the biofilm model could be utilised in phenotyping experiments, *P. aeruginosa* PA21 and *S. aureus* UAMS-1 were used exclusively as a proof of concept. The antimicrobial susceptibility of established mono- and co-culture biofilms of *S. aureus* UAMS-1 and *P. aeruginosa* PA21 was determined using two antimicrobials in clinical use (tobramycin and vancomycin) and a novel antimicrobial compound currently in development (HT61).

Biofilm co-culture increased the biofilm MBC of *P. aeruginosa* to tobramycin, from 2 to 4 μg ml^{-1}. Vancomycin and HT61 had no effect at the concentrations tested and this was not altered by co-culture. However, co-culture increased *S. aureus* susceptibility to tobramycin and HT61 with an eightfold (16 to 2 μg ml^{-1}) and fourfold (64 to 16 μg ml^{-1}) reduction in biofilm MBC, respectively. Vancomycin susceptibility was not affected at the concentrations tested.

4.3.6 Biofilm Co-Culture of *P. aeruginosa* and *S. aureus* Significantly Increases the Mutation Rate of Each Species

Understanding whether interspecies interactions can alter bacterial evolvability is incredibly relevant, considering the rapid emergence of AMR. The Luria-Delbrück fluctuation test was applied to both single species and dual species co-cultures of *P. aeruginosa* PA21 and *S. aureus* UAMS-1, both in planktonic and biofilm culture to measure the spontaneous mutation rate (via the development of rifampicin resistance) of each species (Figure 5).

In planktonic mono-culture, the mutation rates of *P. aeruginosa* PA21 and *S. aureus* UAMS-1 were low, at 2.84 x 10^{-9} and 1.37 10^{-9} mutations per cell division, respectively. Planktonic co-culture led to an increase in mutation rate for both species to 8.90 x 10^{-9} mutations per cell division. Biofilm mono-culture resulted in a similar increase to 1.03 x 10^{-8} and 1.32 x 10^{-8} mutations per cell division for *P. aeruginosa* PA21 and *S. aureus* UAMS-1, respectively. Following biofilm co-culture, the mutation rate of *P. aeruginosa* remained at a similar level (1.05 x 10^{-8} mutations per cell division). However, the mutation rate of *S. aureus* increased to 7.44 x 10^{-7} mutations per cell divisions, which is an approximately 500-fold relative increase compared to the rate during planktonic mono-culture.

Due to differences in terminal population sizes, statistical significance was determined by comparison of 94% confidence intervals to mimic a 0.01 statistical test[290]. This method is a valid comparison as calculation of confidence intervals accounts for differences in the terminal population density[284]. With these thresholds in place, the change in mutation rate of *P. aeruginosa* following planktonic co-culture and biofilm mono- and co-culture are all significant increases compared to planktonic mono-culture. The same is also true for *S. aureus*, but the increase in mutation rate observed following co-culture is also statistically significant compared to values obtained following planktonic co-culture and biofilm mono-culture.

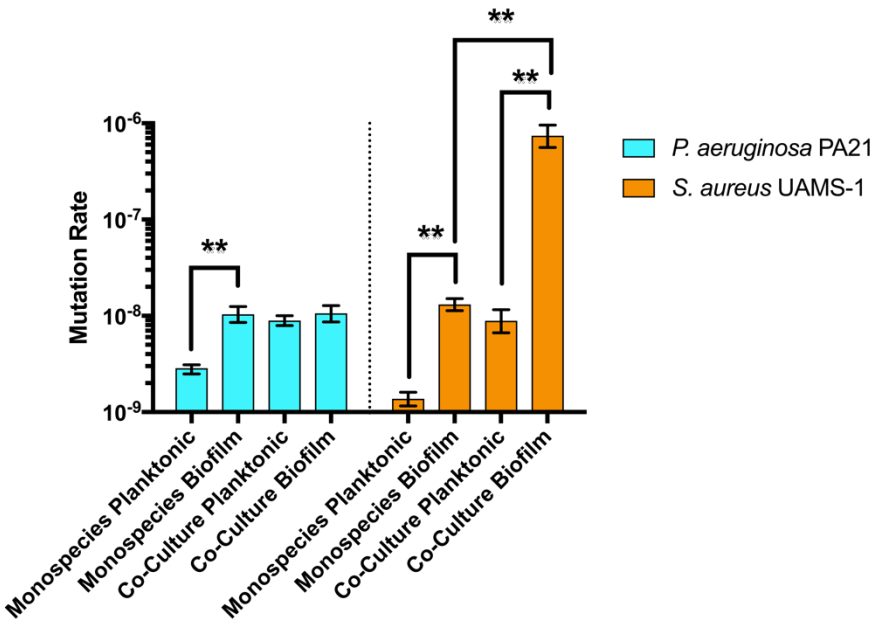

Species	Culture Type		CFUs Plated (Nt)	Mutation Rate (mutations per cell division)
P. aeruginosa	Planktonic	Mono-culture	9.83×10^{9}	2.84×10^{-9}
		Co-culture	3.40×10^{9}	8.90×10^{-9}
	Biofilm	Mono-culture	3.21×10^{8}	1.03×10^{-8}
		Co-culture	2.73×10^{8}	1.05×10^{-8}
S. aureus	Planktonic	Mono-culture	3.44×10^{9}	1.37×10^{-9}
		Co-culture	2.58×10^{8}	8.90×10^{-9}
	Biofilm	Mono-culture	5.60×10^{8}	1.32×10^{-8}
		Co-culture	2.62×10^{6}	7.44×10^{-7}

Figure 39: Effect of Biofilm Growth on Mutation Rate of *P. aeruginosa* PA21 and *S. aureus* UAMS-1

Mutations rates are given as the number of mutations per cell division.

Following biofilm mono-culture, both species are shown to have an increased rate of mutation, (*P. aeruginosa*: 1.03×10^{-8}, *S. aureus*: 1.32×10^{-8}). The rate of mutation for *P. aeruginosa* stays at this level following planktonic and biofilm co-culture, which suggests that the species interactions between *P. aeruginosa* and *S. aureus* do not impact the evolvability of *P. aeruginosa* more than the conditions associated with biofilm growth. The mutation rate of *S. aureus* following planktonic co-culture is approximately the same as that following biofilm mono-culture (Planktonic co-culture: 8.90×10^{-9}, biofilm mono-culture: 1.32×10^{-8}), suggesting that the pressures associated with the presence of planktonic *P. aeruginosa* on staphylococcal evolvability is similar to those associated with mono-culture biofilm growth. However, following biofilm co-culture, the mutation rate of *S. aureus* is highly elevated to 7.44×10^{-7}. This suggests that both biofilm growth and the interspecies interactions present during biofilm co-culture with *P. aeruginosa* may influence the evolvability of *S. aureus*. Error bars represent 94% confidence intervals. ** represents $p \leq 0.01$, obtained by comparing overlap of confidence intervals.

4.3.7 Whole Genome Comparison of *P. aeruginosa* PAO1 and *P. aeruginosa* PA21 Reveal Major Genetic Differences Associated with Iron Metabolism, Phage Proteins, Resistance and Virulence Genes

Table 14: *De novo* assembly evaluation of *P. aeruginosa* PAO1 and *P. aeruginosa* PA21 Information derived from RAST, QUAST and PHAST. CDS: Coding Sequences.

Strain	Contigs	Bases	N50	CDS	RNAs	Bacteriophages
PAO1	1	6275216	6275216	5815	76	3 intact
PA21	3	6781785	2692404	6206	87	3 intact, 1 incomplete, 2 questionable

Due to the dramatically differing abilities of *P. aeruginosa* PAO1 and *P. aeruginosa* PA21 to form co-culture biofilms, the genomes of these two strains were sequenced and compared to identify whether any obvious genetic differences might explain the different co-culture phenotypes.

Genomes of both *P. aeruginosa* PAO1 and PA21 were sequenced and assembled *de novo* (details in Table 4). By performing a hybrid assembly combining both short read and long read datasets, the assembly of *P. aeruginosa* PAO1 was consolidated into 1 complete contig, comprising 6.27 Mb and 5683 coding sequence (CDS) regions. The *de novo* assembly of *P. aeruginosa* PA21 consisted of 3 contigs made up of 6.78 Mb and 6206 CDS regions suggesting that there are a considerable number of additional genomic features which are only present in the clinical isolate compared to *P. aeruginosa* PAO1.

The following sections summarise genomic differences worthy of discussion in the context of biofilm co-culture, hemin and iron uptake, virulence and antimicrobial resistance. See Appendices for a complete list of the large scale genetic differences observed between *P. aeruginosa* PAO1 and PA21.

4.3.7.1 Genes Absent in *P. aeruginosa* PA21 compared to *P. aeruginosa* PAO1

Following annotation and comparison of the two strains of *P. aeruginosa*, 77 genes were identified that were present only in *P. aeruginosa* PAO1. Of these, 41 were hypothetical, resulting in 36 annotated genes (see Appendices).

Genes not present in *P. aeruginosa* PA21 include various unspecified mobile element proteins and integrases, S-adenosyl methionine-dependent methyltransferases, nucleic acid helicases, phage proteins, (particularly those associated with the Pf1 phage such as coat proteins and the 10.1 kDa protein), as well as number of genes associated with lipopolysaccharide production and maintenance of the cell membrane. Absence of unspecified phospholipases, LPS biosynthesis proteins alongside the O-antigen flippase Wzx, and the associated polymerase Wzy, suggests differences in the lipopolysaccharide of *P. aeruginosa* PA21 compared to *P. aeruginosa* PAO1, which could be important for evasion of the host immune system[296].

P. aeruginosa PA21 appears to lack manganese catalase. Manganese catalases utilise manganese within their active site opposed to the more typical heme containing catalases. Manganese catalase enzymes are typically found in bacteria predicted to occupy environmental niches low in iron or possess ineffective iron uptake mechanisms[297]. As *P. aeruginosa* PA21 appears to lack manganese catalase, it could mean that it previously occupied an iron rich niche and/or is better suited to take advantage of exogenous iron than *P. aeruginosa* PAO1.

Filkins *et al* suggest that *P. aeruginosa* mediated killing of *S. aureus* requires the presence of both *pvdA* and *pchE* genes, encoding the pyoverdine and pyochelin siderophores, respectively[146]. In their study, Δ*pvdA* and Δ*pchE* single and double knockout mutants of *P. aeruginosa* PA14 exhibit markedly reduced killing of *S. aureus,* facilitating successful co-culture with all *S. aureus* strains tested[146].

As *P. aeruginosa* PA21 was less lethal to *S. aureus* than *P. aeruginosa* PAO1, these genes may not be present. However, genomic comparison of the strains shows that both *pvdA* and *pchE* are conserved between them. This means that the improved viability of *S. aureus* in biofilm co-culture with *P. aeruginosa* PA21 is independent of these genes and associated with a hitherto unexplored mechanism.

4.3.7.2 Additional Genes in *P. aeruginosa* PA21 compared to *P. aeruginosa* PAO1

Comparison of the two *P. aeruginosa* genomes identified the presence of 500 genes unique to *P. aeruginosa* PA21. Of these genes, 234 coded for hypothetical proteins without a defined annotation. 266 genes were annotated across multiple categories including virulence factors, resistance genes, cell signalling, metabolism, as well as extensive phage associated proteins and proteins associated with DNA recombination, such as integrases and recombinases (complete list in S2).

While there are no specific genes that appear to be directly associated with the improved ability of *P. aeruginosa* PA21 to form a stable co-culture biofilm with *S. aureus,* there are numerous proteins of interest.

For example, *P. aeruginosa* PA21 harbours the phd-doc toxin antitoxin (TA) system. TA systems have been implicated in bacterial survival and persistence, with this particular example shown to be important in the inhibition of translation elongation[298]. If this module is activated during biofilm co-culture, it could possibly inhibit *P. aeruginosa* growth, allowing *S. aureus* to survive. Presence of this module could also be useful for increased survival of *P. aeruginosa* during colonisation of the CF lung.

P. aeruginosa PA21 also has genes encoding additional proteins associated with iron and heme metabolism compared to PAO1. Examples of these include periplasmic TonB components, important for siderophore transport and uptake[299]. While expression data is not available within this study, it could be possible that an increased selection of iron transport machinery improves the uptake of environmental iron. In the context of the dual species biofilm model with *S. aureus*, more efficient iron uptake by *P. aeruginosa* could negatively regulate the production of molecules that are produced to lyse *S. aureus* and utilise it as an iron source[149]. Heightened efficiency of iron uptake may also explain the deletion of a manganese catalase, highlighted in the previous section.

Other additional genes identified in *P. aeruginosa* PA21 include those coding for unspecified nitric oxide dioxygenase flavohemoproteins which are known to link cellular responses to NO and iron transport[300], and nreA like proteins, which in Staphylococci, are crucial components in nitrate regulation[301].

Numerous genes associated with DNA secretion and recombination were identified in PA21 compared to PAO1, including various unspecified integrases, mobile genetic elements and the ISPsy6 transposase. Components of the VirB/VirD4 Type IV secretion system, (named after the system isolated from the rod shaped Gram-negative bacterium, *Agrobacterium tumefaciens*) which can facilitate the transfer of novel DNA elements via conjugation[302] were also identified.

4.3.7.3 Prophage and Antimicrobial Resistance Genes

As previously mentioned, numerous phage proteins were also identified within the PA21 genome. Following PHASTER analysis, this corresponded to 3 intact prophages, 1 incomplete prophage and 2 questionable prophages. For comparison, the strain of PAO1 used in this study harbours 3 intact prophage (see Appendices). The higher number of prophages in PA21 has been seen in similar cystic fibrosis derived isolates such as the Liverpool epidemic strain, LES, which harbours 5 known inducible prophages important for regulating the cell density of *P. aeruginosa* during infection[303]. Genes encoding proteins associated with prophages are also present including RusA, an endonuclease that can resolve Holliday junctions during DNA recombination[304].

Both strains shared identical genes conferring antimicrobial resistance as identified using the ResFinder database. These include *aph(3')-lib* conferring aminoglycoside resistance, *blaOXA-50* and *blaPAO*, conferring β-lactam resistance, *fosA* conferring fosfomycin resistance and *catB7* conferring phenicol resistance (full information in supplementary information). However, *P. aeruginosa* PA21 also harboured genes associated with arsenic resistance (*acr3* and an arsenical ATPase pump), chromate resistance (*chrB*), cobalt-zinc-cadmium resistance (*czcD)* and mercury resistance (*merF, mere, merT,* mercuric resistance operon coregulatory). These additional protective mechanisms may have evolved as a response to the increased evolutionary pressures associated with host infection, including the presence of host immune proteins, other bacterial species and possible antimicrobial treatment.

4.4 Discussion

This chapter described an *in vitro* biofilm co-culture of *P. aeruginosa* and *S. aureus* that could be utilised for at least 10 days to allow for phenotyping experiments to be performed on both early-stage and established biofilms. Following optimisation, the impact of co-culture on bacterial evolvability was determined by applying the Luria-Delbrück fluctuation test, revealing heightened rates of mutation. Finally, using a genomic based approach, the genomes of *P. aeruginosa* PAO1 and PA21 were compared to identify features that could be implicated in sustaining a biofilm co-culture.

4.4.1 Strain and Media Composition Alter the Dynamics of Biofilm Co-Culture

When comparing planktonic and biofilm co-culture of *P. aeruginosa* and *S. aureus,* the viability of *S. aureus* was only negatively affected during biofilm growth. This was interesting as numerous studies have shown that the viability of *S. aureus* is negatively affected by *P. aeruginosa* even in planktonic culture[133,151,305,306]. However, Miller *et al* (2017) found that use of a more nutrient rich medium improved *S. aureus* survival[306]. This suggests, consistent with the findings of this chapter, that media composition is an important consideration for the development of a co-culture model.

In particular, the effect of increasing ferric iron availability on biofilm co-culture was investigated. It was found that increasing the concentration of hemin, improved the viability of *S. aureus* within biofilm co-culture but had no effect on either species or strain when grown as single species biofilms or when competed within a planktonic culture. Iron availability is known to be extremely important for bacterial survival within the CF lung[153,292]. In terms of the relationship between *P. aeruginosa, S. aureus* and iron, it has been hypothesised that the latter is lysed and used as an iron source for *P. aeruginosa* to facilitate its growth[149]. Growth suppression of *S. aureus* in this manner is likely mediated by the *Pseudomonas* quinolone signal, PQS, and in an iron rich environment, PQS expression is decreased[307]. Increased iron availability has been shown to decrease the production of anti-Staphylococcal antimicrobials by *P. aeruginosa* PAO1[308]. Hence it is possible that the increased iron availability during biofilm co-culture leads to reduce *P. aeruginosa* PA21 PQS expression and favours co-existence with *S. aureus.* Measuring the changes in expression of associated genes, (using qPCR or for a global analysis, RNA-

seq) in *P. aeruginosa* PA21 such as *pqsA* and *pqsH,* with differing concentrations of hemin may provide insight into this scenario.

The differences observed in this chapter could also be due to the combination and selection of bacterial strains. Altered levels of killing of *S. aureus* by different *P. aeruginosa* strains has already been observed in previous publications and this has been linked to the ability of *P. aeruginosa* to form biofilms, specifically, that strains which form less biofilm are less able to induce killing of *S. aureus*[149]. Similar observations were made in this chapter. Based on crystal violet staining, *P. aeruginosa* PAO1 formed more robust single species biofilms compared to *P. aeruginosa* PA21 and also caused more killing of *S. aureus* when in a co-culture biofilm. It has been demonstrated that *P. aeruginosa* isolates taken from patients co-infected with *P. aeruginosa* and *S. aureus* are less competitive towards *S. aureus,* presumable because they have already adapted to co-exist[133,150]. While the exact clinical background of *P. aeruginosa* PA21 is not available, this could be a factor that favours its co-culture with *S. aureus*.

A study by Limoli *et al* (2017) showed that alginate production, associated with CF conversion to a mucoid phenotype was linked to improved co-existence with *S. aureus*[150]. *P. aeruginosa* PA21 does not possess a mucoid phenotype. Its successful coexistence with *S. aureus* could be mediated by increased alginate production during co-culture, however the culture did not appear to become more mucoidy in this study. More in depth analysis would be required to measure the expression of alginate producing genes.

Whole genome comparison of *P. aeruginosa* PA21 with *P. aeruginosa* PAO1 revealed large genetic differences, encompassing a large number of bacteriophage proteins, genes associated with cellular metabolism and virulence factors. However, narrowing down the relevance of these differences in regards to infection and biofilm co-culture is difficult and aside from hypothesising possible roles, further investigation of specific targets was beyond the scope of this study.

As far as I am aware, the model described here is the first *in vitro* co-culture that maintains populations of *P. aeruginosa* and *S. aureus* for at least 10 days. As such, it is more representative of a chronic clinical infection than *in vitro* models that are cultured for only 24 or 48 hours. When supplemented with 20 μM or 100 μM hemin, the *in vitro* model described here mimics viability counts found in *in vivo* models, where following 10 days

of infection, *P. aeruginosa* is the dominant pathogen and *S. aureus* exists approximately 2-3 log lower in abundance[140]. Interestingly, in this study the authors utilised *P. aeruginosa* PAO1 alongside *S. aureus* UAMS-1; as we were unsuccessful at *in vitro* co-culture of these strains for longer than 72 hours, it suggests that the *in vivo* environment harbours other important factors that modulate the dynamics of polymicrobial infection.

Curiously, during development of the co-culture, no small colony variants (SCVs) of either *S. aureus* strain were identified. This is contrary to well documented observations that *S. aureus* enters a small colony state as a protective mechanism towards *P. aeruginosa*[87,309]. Assay dependent emergence of SCVs has been documented before, suggesting that very specific stressors and exogenous compounds may be required[145]. *S. aureus* SCVs are often auxotrophic (they cannot synthesise) hemin[87]. It is possible that the addition of exogenous hemin complements and reverts the SCV phenotype.

4.4.2 Planktonic and Biofilm Co-Culture of *P. aeruginosa* and *S. aureus* Can Increase Short Term Rates of Genomic Mutation

As of writing, this chapter describes the first parallel application of the fluctuation assay to planktonic and biofilm cultures, in mono- and co-culture. The results suggest that planktonic co-culture and biofilm mono- and co-culture can increase the mutation rate of bacterial species, to varying degrees, which may have important implications in the emergence of AMR. The general increase in mutation rate following planktonic co-culture of *P. aeruginosa* and *S. aureus* provides evidence that the presence of additional bacterial species and associated exoproducts within a population is important when considering bacterial evolution. It has recently been demonstrated that planktonic cultures of *P. aeruginosa* undergo a different evolutionary trajectory when cultured in the presence of *S. aureus*, obtaining mutations in lipopolysaccharide biosynthesis genes, leading to increased resistance to β-lactam antimicrobials[154].

Previous work has suggested that single species biofilms have an elevated mutation rate based on increased mutation frequencies[91,92]. By applying the fluctuation assay to biofilm cultures, additional evidence is provided to support this claim and moreover, suggest that biofilm co-culture can modulate mutation rate of certain bacterial species even further. The mechanisms associated with the increased mutation rates of *S. aureus* following biofilm

co-culture with *P. aeruginosa* are yet to be explored but I hypothesise that it is likely stress mediated, as per the mechanism previously discussed by Mashburn *et al*[149]. The increased levels of external stress, paired with potential increases in reactive oxygen species during biofilm culture (implicated in increased *Staphylococcal* mutation frequency by Ryder *et al*[92]*),* could result in higher rates of mutation. It is well known that biofilms can act as harbours of genetic diversity, facilitating evolution of novel lineages, even in parallel across independent populations[8,82,84,104]. Understanding how biofilm growth, and in particular, how co-culture within biofilms, modulates evolution and possibly mutation rate is of paramount importance, particularly when the emergence of AMR is considered.

Regarding the fluctuation test data, it is worth noting that the total plated cell population of *S. aureus* was lower than that of *P. aeruginosa* (2.62×10^6 CFU opposed to 2.58×10^8 CFU). If considered in isolation, the larger increase in mutation rate of *S. aureus* compared to *P. aeruginosa* could be a product of the decreased cell density. A recent systematic study of fluctuation assay data by Krašovec *et al* suggests an inverse correlation between population density and mutation rate, with low densities being associated with higher mutation rates[310]. However, this finding does not necessarily apply to the work performed here because while the individual population of *S. aureus* plated is lower, the overall cell density found within the co-culture biofilm during growth would be the sum of both species population sizes (i.e. $2.62 \times 10^6 + 2.58 \times 10^8 = 2.61 \times 10^8$ CFU) and not that of each individual species in isolation.

4.4.3 *P. aeruginosa* and *S. aureus* Exhibit Altered Antimicrobial Susceptibilities in a Co-Culture Biofilm

Biofilm co-culture of *P. aeruginosa* and *S. aureus* caused the two species to present with different levels of susceptibility compared to growth as a single species biofilm. For this investigation, the efficacy of tobramycin, vancomycin and HT61 was tested.

Biofilm co-culture of the two species caused *P. aeruginosa* to become less susceptible to tobramycin treatment, and *S. aureus* to become more susceptible. These effects have both been documented in the literature. Beaudoin *et al* (2017), showed that interactions between *P. aeruginosa* derived Psl polysaccharide and *S. aureus* derived Staphylococcal protein A caused aggregates of *P. aeruginosa* to form, decreasing overall susceptibility to tobramycin[148]. Conversely, increased *S. aureus* susceptibility to tobramycin has been

attributed to the presence of *P. aeruginosa* produced rhamnolipids that potentiate tobramycin uptake within the *S. aureus* cells[147]. Interestingly, within the same study, the authors also found that the presence of the *P. aeruginosa* exoproduct, LasA, an endopeptidase, would increase the effectiveness of vancomycin against *S. aureus,* an observation that was not seen in this chapter.

As for HT61, *P. aeruginosa* PA21 susceptibility was not altered, although as it has proven ineffective against *P. aeruginosa* PA21 in previous work (see Chapter 2), this is not necessarily surprising. However, *S. aureus* susceptibility to HT61 was increased during biofilm co-culture, with a 4 fold decrease in biofilm MBC. A recent study found that co-culture of *S. aureus* with *P. aeruginosa* reduced the susceptibility of *S. aureus* to vancomycin via the production of 2-heptyl-4-hydroxyquinoline *N*-oxide (HQNO), causing it to switch to fermentative metabolism and decrease its growth rate, subsequently reducing the effectiveness of antimicrobial compounds that act on the bacterial cell wall[145,146]. While *S. aureus* susceptibility to vancomycin did not appear to be altered in this work, this decrease in growth rate could be associated with changes in membrane composition (namely increased anionic charge) which may explain the improved activity of HT61[12]. It is worth noting that susceptibility to vancomycin may have changed but was simply not detected because the concentration of vancomycin was not high enough.

4.4.4 Conclusions, Experimental Limitations and Future Work

However, there are limitations with the work described herein. To begin, the co-culture biofilm model still only utilises two bacterial species. During an *in vivo* situation, many more factors are influential including additional bacterial species, coagulating factors and host derived factors such as immune cells and cytokines, all of which can affect the dynamics within a polymicrobial environment[311]. As such, further host derived elements and/or more bacterial species could be introduced to try and improve the accuracy and relevance of the model. This logic is the basis of why hemin was chosen as the ferric iron donor for use in this chapter. However, that specific choice also has issues as it has been shown that in the CF lung, ferrous (Fe^{2+}) iron is also incredibly important in terms of iron bioavailability[153]. Ultimately, to optimise the model further, changes to media selection and media supplementation need to be carefully considered to justify their biological relevance.

The counterargument is that if media composition becomes too complicated, the accessibility and potentially, reproducibility of a model is limited. For example, as a growth medium, BHI does not accurately replicate conditions found during bacterial infection, unlike artificial human serum (such as artificial urine or mucus). However, BHI has the advantage of being well defined, easy to prepare and readily available regardless of laboratory facilities. These factors are important when designing a model that can be easily replicated. Notably, the issues associated with the use of BHI means that the model described within this chapter is not suitable for use as a specific infection model and caution should be asserted when applying findings to an *in vivo* situation. Instead, the value of the model described in this chapter lies in its reproducibility and its ease of application to answer basic science questions.

A more general issue with the model is that it was performed on abiotic plastic. The use of *in vivo* models naturally circumvents this issue but, they are generally not as well defined nor are they available to the majority of researchers, due to a lack of suitable facilities. A compromise would be to perform *in vitro* models utilising more *ex vivo* factors, particularly alternative substrata for growth. For example, recent models of primary ciliary dyskinesia include *H. influenzae* and diseased ciliated epithelial cells[312], while a model of *P. aeruginosa* has been developed that utilises pig bronchioles as a growth environment[313,314]. A final example is a dual species wound model of *P. aeruginosa* and *S. aureus,* which utilises immortalised keratinocytes as a substratum[315].

Furthermore, the genomic comparisons between *P. aeruginosa* PAO1 and PA21 only focus on large scale genomic changes and fail to explain why *P. aeruginosa* PA21 was more suitable for extended co-culture with *S. aureus*, compared to *P. aeruginosa* PAO1. Future work could investigate these differences in more detail via analysis of SNPs and if appropriate, the generation and characterisation of appropriate knockout mutants. For example, understanding whether there is a role for the Phd-doc TA system in *P. aeruginosa* PA21 in co-culture may provide insight into bacterial survival and could reveal possible targets for therapeutic manipulation.

To summarise, this chapter describes a stable, co-culture model of *P. aeruginosa* and *S. aureus* that is suitable and accessible for use by laboratories that wish to study the interactions of these two species, regardless of their capabilities for animal models. It has shown that factors such as iron availability can be adjusted for the benefit of the co-culture

and that biofilm culture can increases the rate of bacterial mutation, which could have important implications when studying bacterial evolution. Finally, by using next generation sequencing, candidate genes are identified that may be important in *P. aeruginosa* for successful biofilm co-culture with *S. aureus.* Understanding how biofilms and species interaction affect the evolution of bacteria is of paramount importance and the results in this chapter can help inform the creation of co-culture infection models in the future.

Chapter 5

Genotypic and Phenotypic Characterisation of Variants Derived from Single and Dual Species Biofilms of *P. aeruginosa* and *S. aureus*

5 Genotypic and Phenotypic Characterisation of Variants Derived from Single and Dual Species Biofilms of *P. aeruginosa* and *S. aureus*

5.1 Introduction

Biofilms can act as hubs for bacterial diversification, facilitating the emergence of numerous genetic lineages[8,9]. These bacterial lineages can present with altered phenotypes compared to their wild types ancestors, with differences in colony morphology, biofilm formation, virulence, growth rate and antimicrobial susceptibility all being observed[78,81,83,86]. Moreover, identical genomic changes (both at the gene and nucleotide level) can occur in independent bacterial lineages: a process known as parallel evolution, which infers a genetic region is under strong evolutionary selection[82,84,89,90,316].

Biofilms have been linked to increased mutation frequencies in single species cultures of *P. aeruginosa* and *S. aureus*[91,92]. However as of writing, no co-culture biofilm experiments specifically focusing on evolution have been performed. A recent planktonic experiment suggests that co-culture of *P. aeruginosa* and *S. aureus* results in differential evolutionary trajectories compared to single species planktonic cultures[154]. This finding, paired with the results described in Chapter 4 showing that biofilm co-culture can influence the genomic mutation rate, suggests that further investigation into the evolution within a co-culture biofilm is warranted. In particular, an increased rate of mutation may facilitate the emergence of novel genotypes more quickly and could accelerate the emergence of AMR.

Evolution in biofilms is often studied under flow for an extended period of time to allow for bacterial adaptation. Flow systems have the advantage of supplying systems with a constant supply of media and nutrients. In the bead transfer system, biofilms are grown on plastic beads. These beads are then transferred to fresh media, with fresh beads that can be colonised by the dispersed biofilm population. The process is repeated, allowing for multiple rounds of biofilm dispersal and attachment[102,104]. The alternative flow system is conceptually simpler: biofilms are grown within a chamber and media is flowed through. This allows for the study of biofilms over an extended period of time, although it is limited

because it does not account for dispersal and reformation events, which can be measured with the bead transfer system[89,102].

There were two main aims in this chapter. Firstly, to understand whether isolates of *P. aeruginosa* and *S. aureus* possessed differing evolutionary trajectories when grown in single or co-culture biofilms. The second aim was to identify whether HT61 resistance or adaptation mechanisms (which have not been identified in planktonic experiments)[11], could be identified in biofilm derived isolates. As biofilms are predicted to possess increased rates of mutation, these adaptive mechanisms may be more likely to emerge.

To test these hypotheses, a 14-day flow model was initiated and both single and dual species biofilms of *P. aeruginosa* and *S. aureus* were cultured. These populations were also subjected to sub-inhibitory antimicrobial pressure. Following growth, a selection of colony isolates were characterised in terms of morphology, growth rate, antimicrobial susceptibility and ability to form biofilms. Finally, using whole genome sequencing, the genome of each colony isolate was sequenced in full to determine which genes were under selection during single and dual species biofilm growth, both with and without sub-inhibitory antimicrobial supplementation.

5.2 Materials and Methods

5.2.1 Continuous Biofilm Culture

5.2.1.1 Media Composition and Bacterial Inocula

Single and dual species biofilms of *P. aeruginosa* PA21 and *S. aureus* UAMS-1 were cultured in a flow cell system for 14 days, with and without antimicrobial pressure. Biofilms were grown using either 20 % BHI supplemented with 20 μM hemin, or 20 % BHI supplemented with 20 μM hemin and either HT61 at a final concentration of 4 μg ml^{-1} or ciprofloxacin at a final concentration of 0.063 μg ml^{-1}. Ciprofloxacin was chosen as its resistance mechanisms and associated genomic mutations are well characterised[194]. Sub-MIC antimicrobials were chosen because they have been shown previously to be suitable at selecting for *de novo* resistance mechanisms[188–190]. The exact concentrations were a quarter of the MIC of whichever bacterial species was most susceptible. In the case of HT61 the chosen concentration was a quarter of the *S. aureus* MIC as HT61 had no effect against *P. aeruginosa*. For ciprofloxacin, *P. aeruginosa* was more susceptible than *S. aureus,* so the chosen concentration was a quarter of the *P. aeruginosa* MIC.

Inocula for each individual flow cell population were prepared by diluting overnight cultures of *P. aeruginosa* and *S. aureus* (prepared in LB and TSB, as described in previous chapters), in 50% BHI to 10^5 CFU ml^{-1}, either alone or in a 1:1 co-culture. Each biofilm inocula was comprised of separate overnight cultures. This ensured that any observed genomic similarities could not be attributed to the biofilms being initiated from identical inocula. For each treatment group e.g. single and dual species, untreated, HT61 or ciprofloxacin supplemented, 2 biological replicates were performed.

5.2.1.2 Flow Cell Construction

Single channel flow cells with a total chamber volume of 6 ml were utilised. The setup is depicted in Figure 40. To set up flow cells, glass microscope slides (75 mm x 25 mm) were attached to each flow cell using silicone sealant and cured for 24 hours at room temperature. To supply media, hollow glass tubes were inserted into bungs that would be used to stopper the fresh media. Each bung contained 3 tubes: 2 for media delivery to each flow cell, and a third shorter tube to act as an air inlet. A mixture of silastic tubing and 2-stop tubing (for use with a Bio-Rad peristaltic pump system) was used to connect each flow cell to a glass tube for media delivery. A final piece of silastic tubing was attached to the opposite side of a flow cell to function as a waste outlet. Water was then pumped

through the flow cell setup, tubing ends were wrapped in tin foil, and the system was autoclaved at 121°C for 30 minutes. Following sterilisation, the flow cell was connected and the inlet tubes aseptically inserted into a sterile bottle of media. A 0.2 μm filter was attached to the air inlet.

Once the flow cell was connected, it was flushed with the appropriate media for 10 minutes. Tubing immediately upstream of the flow cell was clamped off and using a hypodermic needle, 6 ml of bacterial inoculum was injected directly into the flow cell, via the silastic tubing. Silicone sealant was used to plug the puncture site and the tubing immediately downstream of the flow cell was clamped off. The flow cell was inverted to facilitate bacterial attachment to the glass slide. After 1 hour, the flow cell was put upright and the peristaltic pump started. Flow rate was set to 200 ml per flow cell per day, equivalent to a peristaltic pump speed of 10 rpm. This rate was chosen because it was the lowest flow rate that still prevented biofilm formation back along the tubing, which would risk contamination of the sterile media.

Flow cell biofilms were cultured for a total of 14 days at room temperature, with media changes every day. To change media, the peristaltic pump was stopped, and the glass rods and bung aseptically moved to a fresh bottle of media.

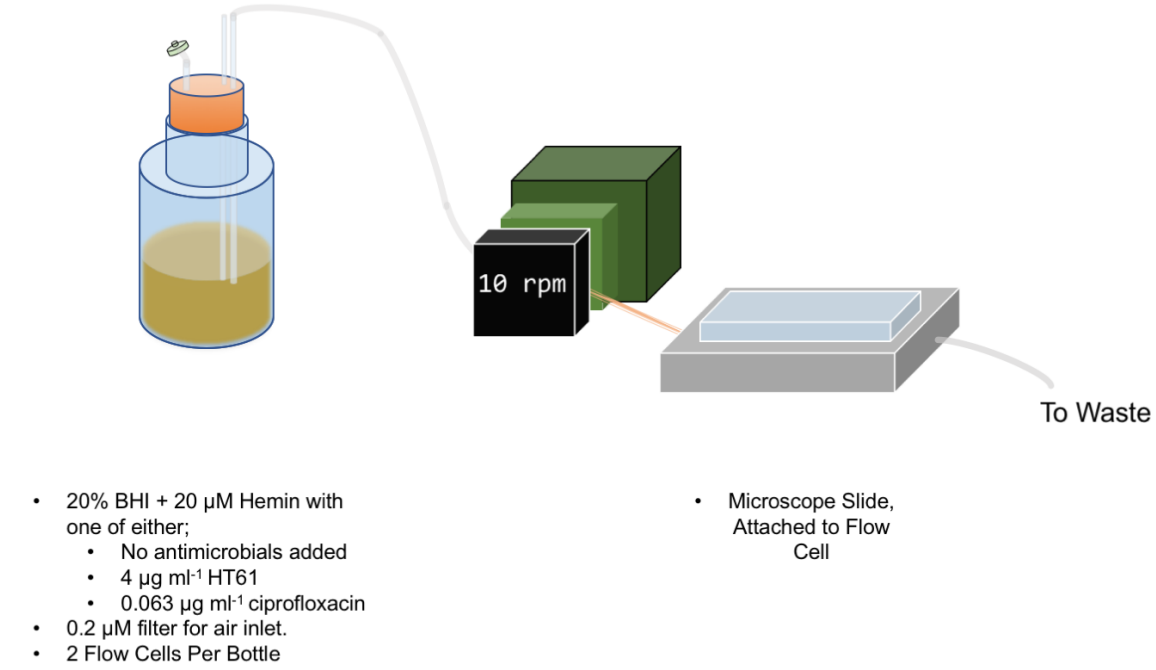

Figure 40: Setup of continuous flow culture system

Single and Dual Species Biofilms of *P. aeruginosa* PA21 and *S. aureus* UAMS-1 were cultured for 14 days in 20% BHI supplemented with 20 µM hemin and either no antimicrobial, 4 µg ml^{-1} HT61 or 0.063 µg ml^{-1} ciprofloxacin. Biofilms would form on the underside of the glass microscope slide. Upon removal, the biofilm populations were plated onto baird parker agar and cetrimide agar plates to differentiate between *S. aureus* and *P. aeruginosa*, respectively. Colonies were isolated and stored at -80°C for future phenotyping and genotyping.

5.2.1.3 Flow Cell Biofilm Harvesting

Following 14 days of continuous culture, the peristaltic pump was stopped and the entire system was transported into a sterile cell-culture safety cabinet. The entire flow cell system was surface sterilised with 100% EtOH and allowed to air dry. Using a sterile scalpel and forceps, each slide was detached from the flow cell and placed into a sterile dish of HBSS to rinse off non-attached cells and biomass. Forceps were used to move the slide into a separate dish containing 15 ml HBSS. Both scalpel and forceps were frequently soaked in 100% EtOH and flamed to ensure sterility. Using a cell scraper, the biomass was removed from the slide. A sample was then serially diluted in HBSS and plated onto cetrimide agar and BPA to select for *P. aeruginosa* and *S. aureus*, respectively. Plates were incubated at 37 °C for 24 hours.

Following incubation, a random selection of *S. aureus* and *P. aeruginosa* colonies were passaged twice onto non-selective TSA plates and incubated at 37°C. Two successive

passages ensured that any mutations present had come to fixation and, in the case of colony phenotypes, determined if the phenotype was maintained. A single colony was then used to inoculate a CryoBead vial (Thermo-Fisher) and stored at -80 °C for future phenotyping and whole genome sequencing.

5.2.2 Variant Phenotyping

From each biofilm population, 10 colonies (in the case of dual species biofilms, 10 colonies of each species) were isolated and frozen down (a total of 120 colonies of each species). All variants were assessed in terms of colony morphology.

36 colonies of each species were isolated for additional analysis including whole genome sequencing, antimicrobial susceptibility testing, assessment of biofilm formation and growth kinetics. This equated to 12 colonies from each treatment group (6 single species and 6 dual species, with 3 per biological population), for a total of 36 variants of *P. aeruginosa* and 36 variants of *S. aureus.*

5.2.2.1 Colony Morphology

To determine colony morphology, overnight cultures of all variant isolates were performed at 37°C in either LB or TSB, for *P. aeruginosa* and *S. aureus*, respectively. 100 µl of culture was streaked onto a TSA plate and single colonies imaged using a Nikon Eclipse ME600 microscope and camera attachment.

5.2.2.2 Antimicrobial Susceptibility

Antimicrobial susceptibility to HT61 and ciprofloxacin was determined for wild type and the 72 subset variant colonies using the broth microdilution method as per previous chapters.

5.2.2.3 Early Biofilm Development

Biofilm formation at 24 hours was determined for the 72 subset variant colonies using a crystal violet-based assay, as per previous chapters. However, 96 well plates were used to facilitate high throughput. Biofilms of *P. aeruginosa* were cultured in LB and *S. aureus* was cultured in TSB. Following 24 hours of static incubation at 37 °C, media was removed and biofilms stained with 0.1% (v/v in dH_2O) crystal violet for 10 minutes at room temperature. Biofilms were rinsed 3 times with dH_2O and crystal violet resolubilised in 30

% acetic acid. The suspended crystal violet was transferred to a fresh 96 well plate and the OD_{550} measured using a plate reader (BMG Omega).

5.2.2.4 Growth Kinetics

Growth kinetics were determined for the 72 biofilm derived colonies. Overnight cultures of each were diluted to approximately 10^6 CFU ml^{-1} in either LB, for *P. aeruginosa* or TSB, for *S. aureus* and incubated for 24 hours at 37 °C with optical density measurements at 560 nm (OD_{560}) taken every 15 minutes for 15 hours.

Growth rates were calculated within the exponential phase of the growth using the following formula:

$$\mu = \frac{\ln OD_2 - \ln OD_1}{(t_2 - t_1)}$$

Where:

μ = Growth rate

OD_1 = Optical density reading at earlier first time point of exponential phase

OD_2 = Optical density reading at later second time point of exponential phase

t_1 = first time point, corresponding with OD_1

t_2 = second time point, corresponding with OD_2

5.2.3 Whole Genome Sequencing and Bioinformatic Analysis

5.2.3.1 Reference Genomes

Prior to analysis of variants, reference genomes of wild type *S. aureus* UAMS-1 and *P. aeruginosa* PA21 were assembled. The methods used for each species are described in chapters 3 and 4, respectively. Briefly, to obtain the most complete reference genome, both species underwent short and long read sequencing.

For short read sequencing, an overnight culture of each species was grown as previously described and streaked onto a TSA plate, prior to incubation for 24 hours at 37 °C. A single colony was restreaked onto a fresh TSA plate and following an additional incubation, the entirety of plate growth was sent for DNA extraction and sequencing, courtesy of MicrobesNG (University of Birmingham). Sequencing was performed using an Illumina HiSeq 2500, with a target coverage of 60 X using 2 x 250 bp paired end reads.

For long read sequencing, DNA was extracted using a PureLink Genomic DNA Mini Kit (Thermo-Fisher) according to manufacturer's instructions and purified using a phenol chloroform extraction and ethanol precipitation. Libraries for long read sequencing were prepared and sequenced using a MinION sequencer for 6 hours.

Genomes were assembled using Unicycler[243] and annotated with PROKKA[244]. Coverage of long and short read sequence data was assessed further by aligning the raw sequencing reads to the assemblies with bwa mem[317], and coverage calculated with samtools depth[318,319]. QUAST was used for additional assembly metrics[320].

5.2.3.2 Variant Analysis

All variants underwent short-read sequencing courtesy of MicrobesNG (University of Birmingham) to a target coverage of at least 30 X. Achieved coverage compared to the assembled reference genomes was assessed using a combination of bwa mem and samtools depth[317–319]. Genome assemblies were performed *de novo* using Unicycler[243] and annotated using PROKKA[244]. Core and pan genomes were compared using ROARY[321] while single nucleotide polymorphisms, (SNPs) and small insertions or deletions, (INDELS) were identified using breseq[322,323]. Mutations were manually curated by visualising the aligned reads in the Integrated Genomics Viewer 2.4.10[324,325]. Annotations of variant genes were manually curated by running the amino acid sequences through the NCBI BLASTP algorithm[326–328]. Annotations for variants of *P. aeruginosa* were also manually curated by utilising the NCBI BLASTP algorithm, in conjunction with the Pseudomonas database[329].

5.2.4 Statistical Analysis

Statistical significance was determined using one-way ANOVA's with either Tukey's or Dunnet's post-hoc comparisons. The threshold for significance was designated $\alpha < 0.05$. All statistical analyses were performed using GraphPad Prism version 7.0d for Mac.

5.3 Results

5.3.1 Biofilm Culture of *P. aeruginosa* and *S. aureus* Results in Notable Phenotypic Diversity in Colony Morphology

Following biofilm growth, (single and dual species, with and without antimicrobial pressure), numerous colonies of *S. aureus* and *P. aeruginosa* were isolated and characterised in terms of their morphology and colony size (Figure 41). For each biofilm type (single species or dual species, with no antimicrobial, HT61 or ciprofloxacin), 20 colonies were randomly chosen, equally split between the two biological replicates. A plot depicting the average sizes of the sampled biofilm derived colonies is shown in Figure 41A and Figure 41B, for *P. aeruginosa* and *S. aureus,* respectively.

For single species biofilms of *P. aeruginosa,* one-way ANOVA suggests differences between the mean colony sizes of each group ($p < 0.0001$). When examining all of the derived colonies, there is considerable variation in colony size (minimum diameter : 0.449 mm, maximum diameter: 2.6 mm, median diameter: 1.47 mm, interquartile range: 0.801 mm). For the single species biofilms, without antimicrobial supplementation, mean colony size was 0.88 mm. Co-culture with *S. aureus* led to an increase in mean colony size to 1.23 mm, although this difference was not significant ($p = 0.0571$). Colonies of *P. aeruginosa* isolated from antimicrobial treated biofilm cultures were on average, larger than those sampled from biofilms cultured without antimicrobials. Untreated single species derived variants were significantly smaller than variants derived from single and dual species biofilms treated with either HT61 or ciprofloxacin. (Tukey's post-hoc comparison of untreated single species variants against HT61 single and dual species: $p < 0.0001$ and $p = 0.0074$ and against ciprofloxacin single and dual species: $p < 0.0001$ and $p < 0.0001$). Variants derived from untreated dual species biofilms were only significantly smaller than variants derived from ciprofloxacin treated single species biofilms (Tukey's post-hoc test $p = 0.0301$).

Biofilm derived colonies of *S. aureus* also exhibited variation in mean colony diameter between groups, as determined by one-way ANOVA ($p = 0.0011$), although to a lesser extent than that observed with colonies of *P. aeruginosa* (minimum diameter: 0.698 mm, maximum diameter: 2.02 mm, median diameter: 1.06 mm, interquartile range: 0.3 mm). No difference in mean colony size was determined between variants derived from non-

antimicrobial treated single or dual species biofilms (mean diameters: 1.019 mm and 1.015 mm, respectively, Tukey's post-hoc comparison $p = 0.9798$).

S. aureus variants derived from dual species biofilms treated with HT61 (mean diameter: 1.28 mm), and single and dual species biofilms treated with ciprofloxacin (mean diameters: 1.19 mm and 1.07 mm, respectively), were larger than variants from untreated biofilms. However, according to post-hoc comparisons, the only statistically significant difference was between colonies derived from non-antibiotic supplemented biofilms (single and dual species) and colonies derived from HT61 treated dual species biofilms ($p = 0.0042$ and $p = 0.0074$, respectively).

36 colonies of each species were randomly selected for further phenotyping experiments. The morphologies of these colonies are presented in Figure 42 to Figure 47. Imaging of these colonies demonstrates the observed variation seen in colony diameter, but also reveals differences in gross colony morphology, particularly within colonies of *P. aeruginosa* (Figure 42 to Figure 44), with some colonies resembling the planktonic wild type (e.g. Figure 42, panel 3), others with more "ruffled" edges, (e.g. Figure 43, panel 19) others that are considerably smaller and more round (e.g. Figure 42, panel 2) and others that are very large, rugose type colonies (e.g. Figure 44, panel 27 and 29). Aside from differences in diameter, the morphology of the *S. aureus* colonies does not appear altered from the planktonic derived wild type colonies (Figure 45 to Figure 47).

Fundamentally these results show that it is not possible to identify the origin of a biofilm derived variant based on its morphology alone.

For conciseness, colonies will from this point onwards be referred to using the ID numbers shown in Figure 42 to Figure 47, prefaced with either SAV or PAV, for *S. aureus* or *P. aeruginosa* variant, as appropriate. A summary of this numbering scheme, and the origin of each colony is supplied for reference in Table 15**.**

Table 15: Naming scheme for flow cell biofilm derived variants

Species	Prefix	ID Number	Biofilm Replicate Population	Single or Dual Species	Antimicrobial
S. aureus	SAV	1-3	1	Single	None
		4-6	2		
		7-9	1	Dual	
		10-12	2		
		13-15	1	Single	HT61
		16-18	2		
		19-21	1	Dual	
		22-24	2		
		25-27	1	Single	Ciprofloxacin
		28-30	2		
		31-33	1	Dual	
		34-36	2		
P. aeruginosa	PAV	1-3	1	Single	None
		4-6	2		
		7-9	1	Dual	
		10-12	2		
		13-15	1	Single	HT61
		16-18	2		
		19-21	1	Dual	
		22-24	2		
		25-27	1	Single	Ciprofloxacin
		28-30	2		
		31-33	1	Dual	
		34-36	2		

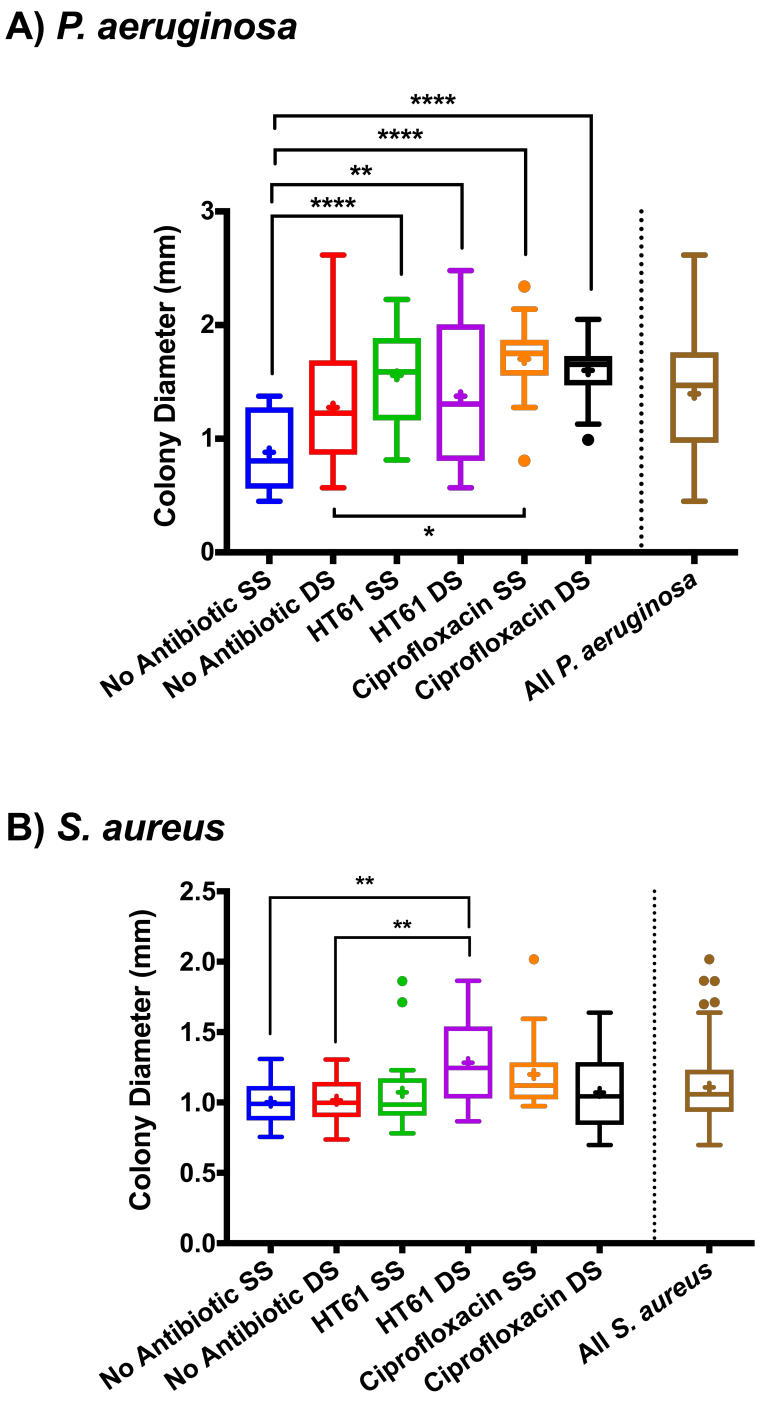

Figure 41: Variation in size of sampled biofilm derived colonies from single and dual species biofilms of *P. aeruginosa* PA21 and *S. aureus* UAMS-1

Colonies imaged using a Nikon Eclipse ME600 and diameter assessed with ImageJ. Diameters from each biofilm group plotted as a box and whisker plot, where the box represents the interquartile range (25th to 75th percentile) and the whiskers represent the Tukey calculated fences. Individual dotted points are outside of the Tukey calculated fences (greater or less than the 25th or 75th percentile + 1.5 x the interquartile range) are outliers. Horizontal line within each box plot represents the median diameter and the cross within each box plot represents the mean diameter. n = 20 for all subsets, except for summary dataset (far right), whereby all values are incorporated therefore n = 120. Statistical comparisons performed using a one-way ANOVA with post-hoc Tukey's comparisons. * $p < 0.05$, ** $p < 0.01$, *** $p < 0.001$, **** $p < 0.0001$. SS = single species, DS = dual species.

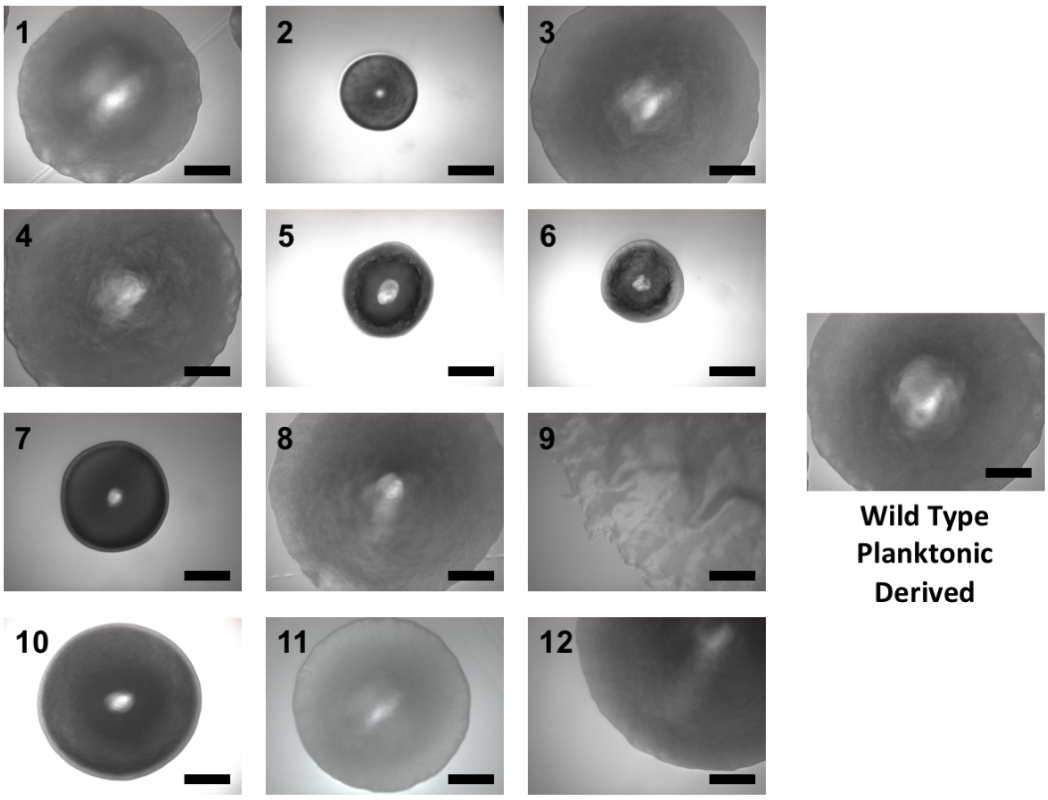

Figure 42: Colony variants of *P. aeruginosa* PA21 derived from 14-day continuous culture flow cell biofilms

1-3 Derived from single species biofilm, replicate population 1. 4-6: Derived from single species biofilm, replicate population 2. 7-9 Derived from dual species biofilm, with *S. aureus* UAMS-1, replicate population 1. 10-12 Derived from dual species biofilm, with *S. aureus* UAMS-1, replicate population 2. Colony derived from a 24-hour wild type *P. aeruginosa* PA21 planktonic culture displayed on right, for comparison. Scale bar = 0.25 mm.

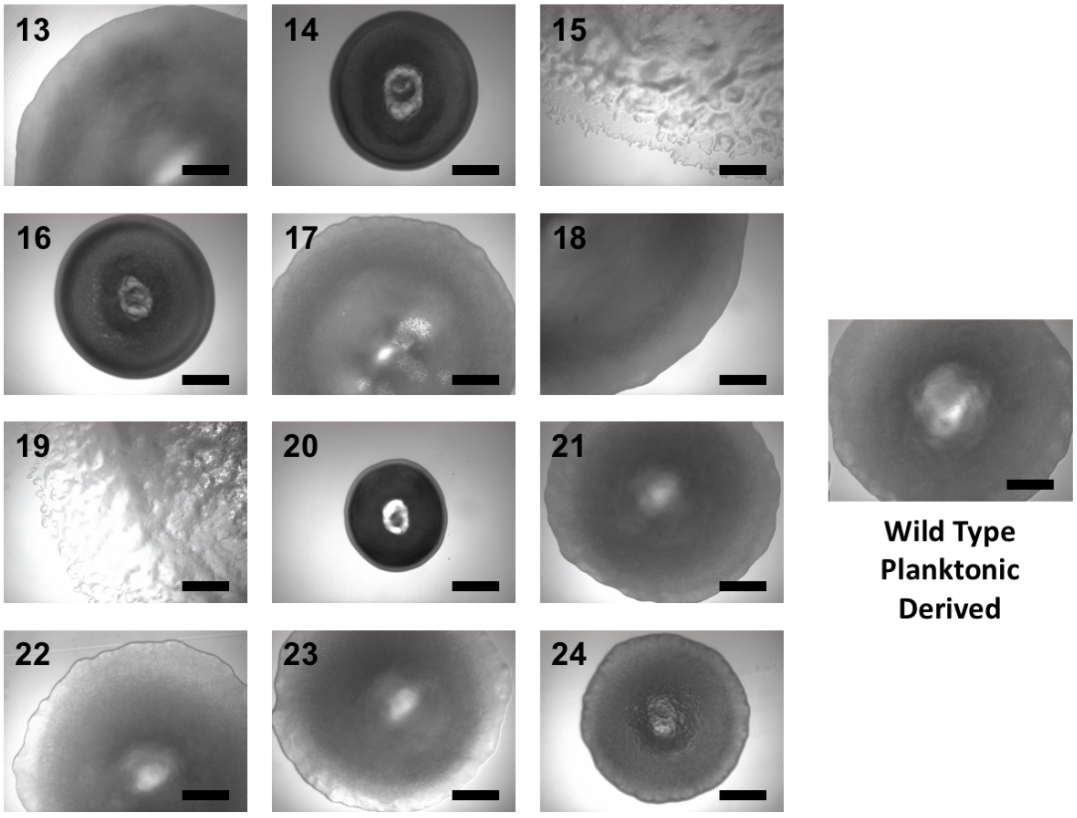

Figure 43: Colony variants of *P. aeruginosa* PA21 derived from 14-day continuous culture flow cell biofilms grown with 4 μg ml^{-1} HT61

13-15 Derived from single species biofilm, replicate population 1. 16-18: Derived from single species biofilm, replicate population 2. 19-21 Derived from dual species biofilm, with *S. aureus* UAMS-1, replicate population 1. 22-24 Derived from dual species biofilm, with *S. aureus* UAMS-1, replicate population 2. Colony derived from a 24-hour wild type *P. aeruginosa* PA21 planktonic culture displayed on right, for comparison. Scale bar = 0.25 mm.

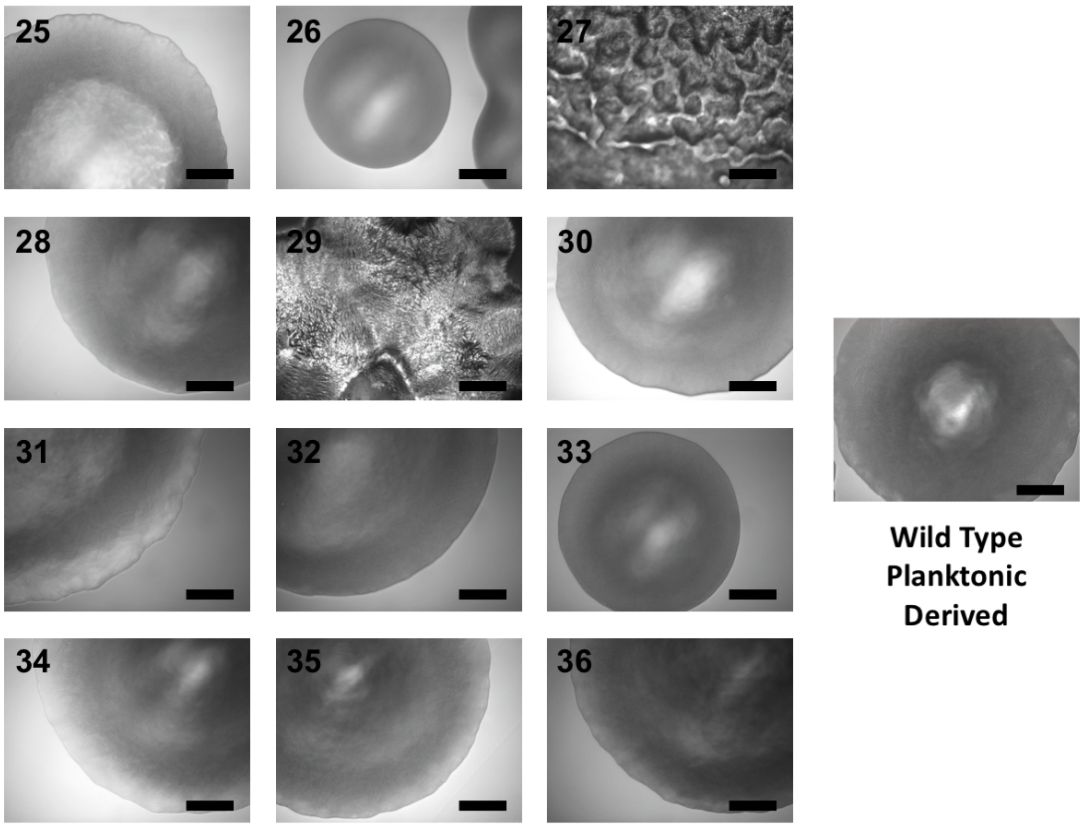

Figure 44: Colony variants of *P. aeruginosa* PA21 derived from 14-day continuous culture flow cell biofilms grown with 0.063 μg ml^{-1} ciprofloxacin

25-27 Derived from single species biofilm, replicate population 1. 28-30: Derived from single species biofilm, replicate population 2. 31-33 Derived from dual species biofilm, with *S. aureus* UAMS-1, replicate population 1. 34-36 Derived from dual species biofilm, with *S. aureus* UAMS-1, replicate population 2. Colony derived from a 24-hour wild type *P. aeruginosa* PA21 planktonic culture displayed on right, for comparison. Scale bar = 0.25 mm.

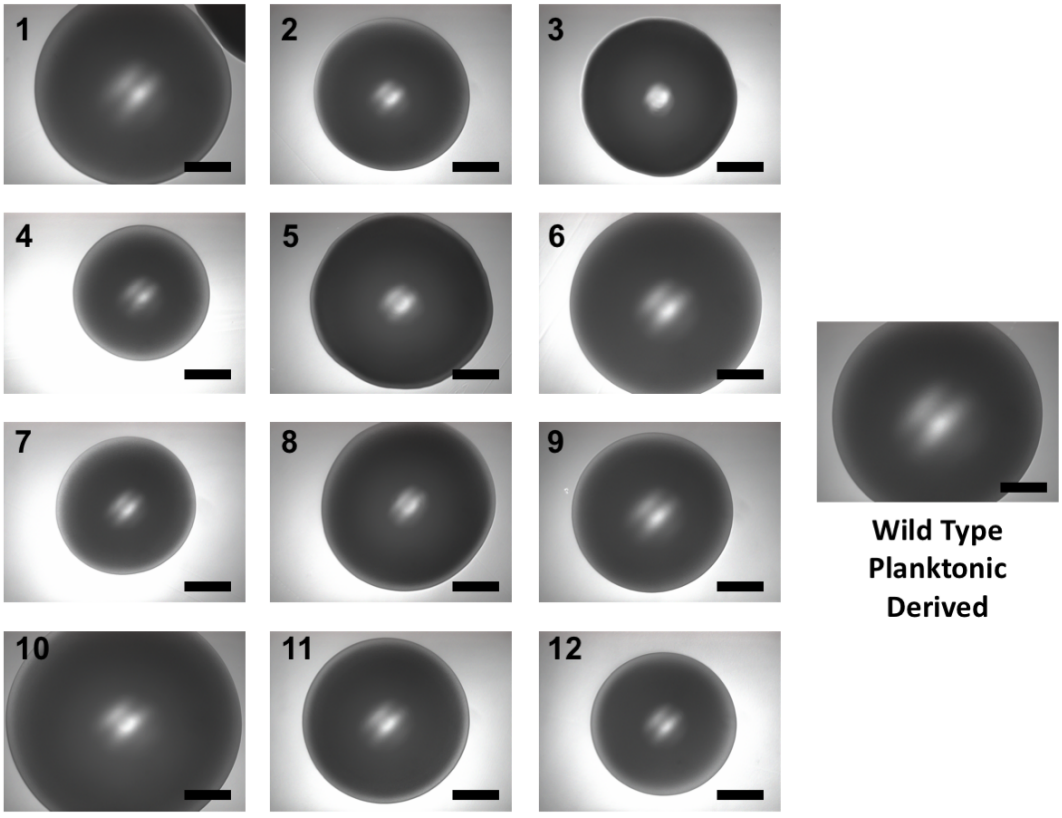

Figure 45: Colony variants of *S. aureus* UAMS-1 derived from 14-day continuous culture flow cell biofilms

1-3 Derived from single species biofilm, replicate population 1. 4-6: Derived from single species biofilm, replicate population 2. 7-9 Derived from dual species biofilm, with *P. aeruginosa* PA21, replicate population 1. 10-12 Derived from dual species biofilm, with *P. aeruginosa* PA21, replicate population 2. Colony derived from a 24-hour wild type *S. aureus* UAMS-1 planktonic culture displayed on right, for comparison. Scale bar = 0.25 mm.

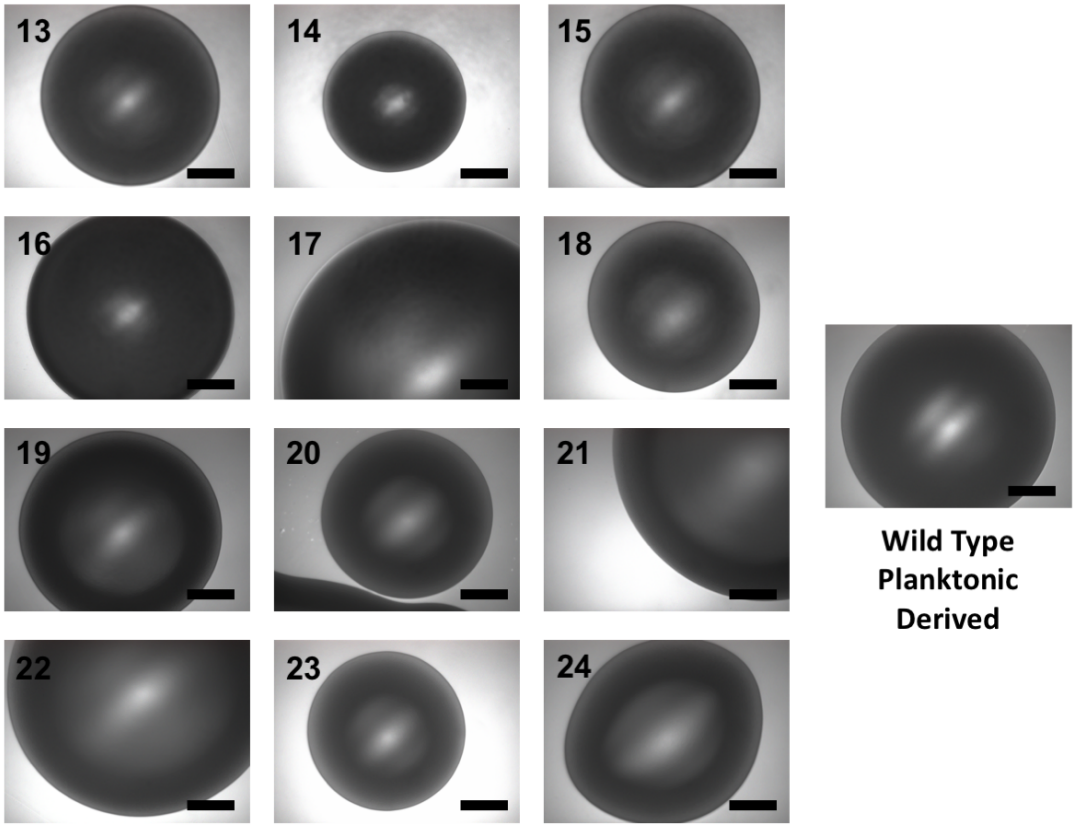

Figure 46: Colony variants of *S. aureus* UAMS-1 derived from 14-day continuous culture flow cell biofilms grown with 4 μg ml^{-1} HT61

13-15 Derived from single species biofilm, replicate population 1. 16-18: Derived from single species biofilm, replicate population 2. 19-21 Derived from dual species biofilm, with *P. aeruginosa* PA21, replicate population 1. 22-24 Derived from dual species biofilm, with *P. aeruginosa* PA21, replicate population 2. Colony derived from a 24-hour wild type *S. aureus* UAMS-1 planktonic culture displayed on right, for comparison. Scale bar = 0.25 mm.

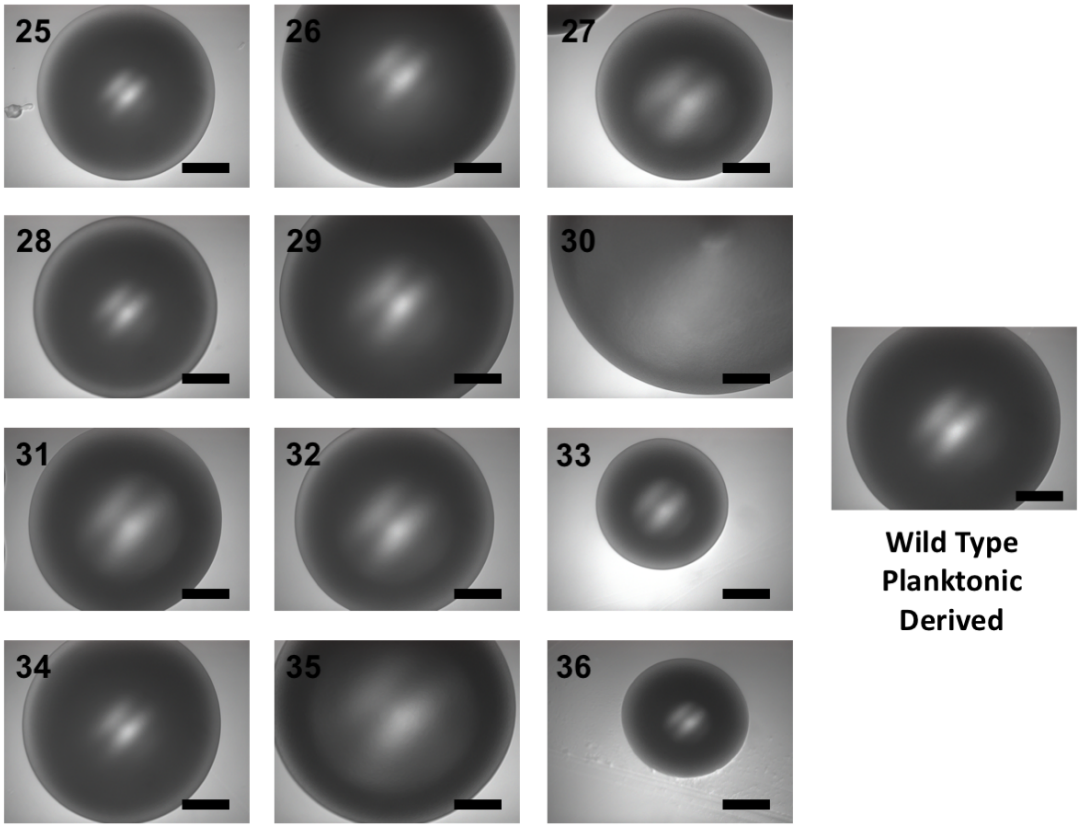

Figure 47: Colony variants of *S. aureus* UAMS-1 derived from 14-day continuous culture flow cell biofilms grown with 0.063 μg ml^{-1} ciprofloxacin

25-27 Derived from single species biofilm, replicate population 1. 28-30: Derived from single species biofilm, replicate population 2. 31-33 Derived from dual species biofilm, with *P. aeruginosa* PA21, replicate population 1. 34-36 Derived from dual species biofilm, with *P. aeruginosa* PA21, replicate population 2. Colony derived from a 24-hour wild type *S. aureus* UAMS-1 planktonic culture displayed on right, for comparison. Scale bar = 0.25 mm.

5.3.2 Antimicrobial Susceptibility to HT61 and Ciprofloxacin is Altered in Biofilm Derived Variants

Biofilm derived colony variants SAV1-36 and PAV1-36 underwent antimicrobial susceptibility testing to determine whether their susceptibilities to HT61 or ciprofloxacin had altered compared to the wild type of each species.

For *P. aeruginosa,* (Table 16), susceptibility to HT61 was not altered in any of the biofilm derived colonies, with no MIC obtained at the concentrations tested (MIC > 128 μg ml^{-1}). In terms of susceptibility to ciprofloxacin, 32 colonies presented with no altered susceptibility compared to the wild type (MIC = 0.25 μg ml^{-1}). 4 colonies presented with reduced susceptibility: 3 exhibited an MIC of 0.5 μg ml^{-1} (PAV2, PAV31, PAV34) and for PAV26, an MIC was not identified at the concentration tested, suggesting at least a 4-fold increase in MIC compared to the wild type (MIC > 1 μg ml^{-1}). With the exception of PAV2, which was derived from a single species *P. aeruginosa* biofilm, without antimicrobial pressure, all of the other implicated variants were derived from ciprofloxacin treated biofilms, both single species (PAV26) and dual species (PAV31 and PAV34).

The antimicrobial susceptibility of *S. aureus* variants to HT61 and ciprofloxacin was also evaluated, (Table 17). 30 variants exhibited no change in susceptibility compared to the wild type ancestor. Curiously, 6 variants (SAV4, SAV6, SAV8, SAV21, SAV30 and SAV36), from differing backgrounds in terms of the biofilm they were derived from, presented with increased susceptibility to HT61 (MIC = 8 μg ml^{-1}). *S. aureus* susceptibility to ciprofloxacin was also altered in a number of examples. While 21 variants shared susceptibility with the wild type ancestor (MIC = 1 μg ml^{-1}), 15 variants (SAV1, SAV6, SAV12, SAV18, SAV19, SAV22, SAV25, SAV28, SAV29 and SAV31-36), presented with reduced susceptibility to ciprofloxacin (MIC = 2 μg ml^{-1}). 9 of these variants (SAV12, SAV19, SAV22 and SAV31-36) were derived from dual species biofilms.

Table 16: Antimicrobial susceptibility of biofilm derived variants of *P. aeruginosa* PA21 to HT61 and ciprofloxacin

In cases where a value was not obtained, the > symbol is used to indicate that the value is higher than the stated concentration. For example, > 1 indicates the value is greater than 1 μg ml^{-1}
MIC = minimum inhibitory concentration. Antimicrobial susceptibility was largely unchanged in *P. aeruginosa* isolates. HT61 susceptibility was not altered in any isolate, while susceptibility to ciprofloxacin decreased for 4 isolates, as shown. n = 2

Antimicrobial	Ancestral MIC	Variant MIC	Frequency	Implicated Variants
HT61	> 128 μg ml^{-1}	> 128 μg ml^{-1}	36	-----
Ciprofloxacin	0.25 μg ml^{-1}	> 1 μg ml^{-1}	1	PAV26
		0.5 μg ml^{-1}	3	PAV2, PAV31, PAV34
		0.25 μg ml^{-1}	32	-----

Table 17: Antimicrobial susceptibility of biofilm derived variants of *S. aureus* UAMS-1 to HT61 and ciprofloxacin

MIC = minimum inhibitory concentration. Antimicrobial susceptibility was largely unchanged in *S. aureus* isolates. However, HT61 susceptibility increased for in 6 isolates, while susceptibility to ciprofloxacin decreased for 15 isolates, as shown. n = 2

Antimicrobial	Ancestral MIC	Variant MIC	Frequency	Implicated Variants
HT61	16 μg ml^{-1}	8 μg ml^{-1}	6	SAV4, SAV6, SAV8, SAV21, SAV30, SAV36
		16 μg ml^{-1}	30	-----
Ciprofloxacin	1 μg ml^{-1}	2 μg ml^{-1}	15	SAV1, SAV6, SAV12, SAV18, SAV19, SAV22, SAV25, SAV28, SAV29, SAV31-36
		1 μg ml^{-1}	21	-----

5.3.3 Biofilm Derived Variants Exhibit Altered Propensity for Early Stage Biofilm Formation

The ability of each biofilm derived variant to form biofilms was determined using a crystal violet based assay (Figure 48 and Figure 49, for *P. aeruginosa* and *S. aureus,* respectively). Significant variation in the mean levels of detected biomass was found for variants of both *P. aeruginosa* and *S. aureus* (one-way ANOVA $p < 0.0001$ for each species).

Compared to the ancestral wild type of each species, all 36 variants of *P. aeruginosa* presented with increased biofilm formation after 24 hours, although according to Dunnet's post-hoc comparison, this was only statistically significant for 32 variants. While all biofilm derived variants presented with increased biofilm formation, the 4 variants that were not significantly different compared to the wild type control were all derived from biofilms treated with HT61 (PAV13, PAV16, PAV21, PAV24).

The mean and median fold increases in produced biomass were 4.24 and 3.77 fold respectively, if only variants with statistically significant levels of variation are considered. If all samples are considered, the mean and median fold changes decrease slightly to 4.04 and 3.71-fold, respectively. Interestingly, PAV26, derived from a single species biofilm treated with ciprofloxacin, presented with an extremely large fold increase compared to the ancestral wild type (15.81-fold change). If this value is excluded, the mean and median fold change of all samples are both equal to a 3.70-fold increase.

For the biofilm derived variants of *S. aureus*, all 36 variants exhibited increased biofilm formation compared to the ancestral wild type. According to Dunnet's post-hoc comparison, these differences were significant in 25 of the variants. When only these variants are considered, mean and median fold increases in biomass were calculated to 8.76 and 9.11, respectively. However, if all samples are considered, these average fold changes are lowered to a mean increase of 6.70-fold and a median increase of 4.94 fold.

A number of *S. aureus* variants formed biofilms with a 4-fold increase in biomass compared to the ancestral wild type (SAV14 to 17, SAV19, SAV20, SAV26, SAV27, SAV29 and SAV32). These were exclusively derived from antimicrobial treated biofilms. Furthermore, the majority of these samples, (7 of 10), were derived from single species biofilms of *S. aureus* (SAV14 to 17, SAV26, SAV27 and SAV29). A further observation is that the variants exhibiting no significant change in their ability to form biofilms were

predominantly isolated from the HT61 and ciprofloxacin treated dual species biofilms (8 of 12 non-significantly different variants). These observations could imply that antimicrobial pressure is an important selector of phenotypes associated with increased biofilm formation, although this effect can be altered if the population dynamics, i.e. species composition of a biofilm, are altered.

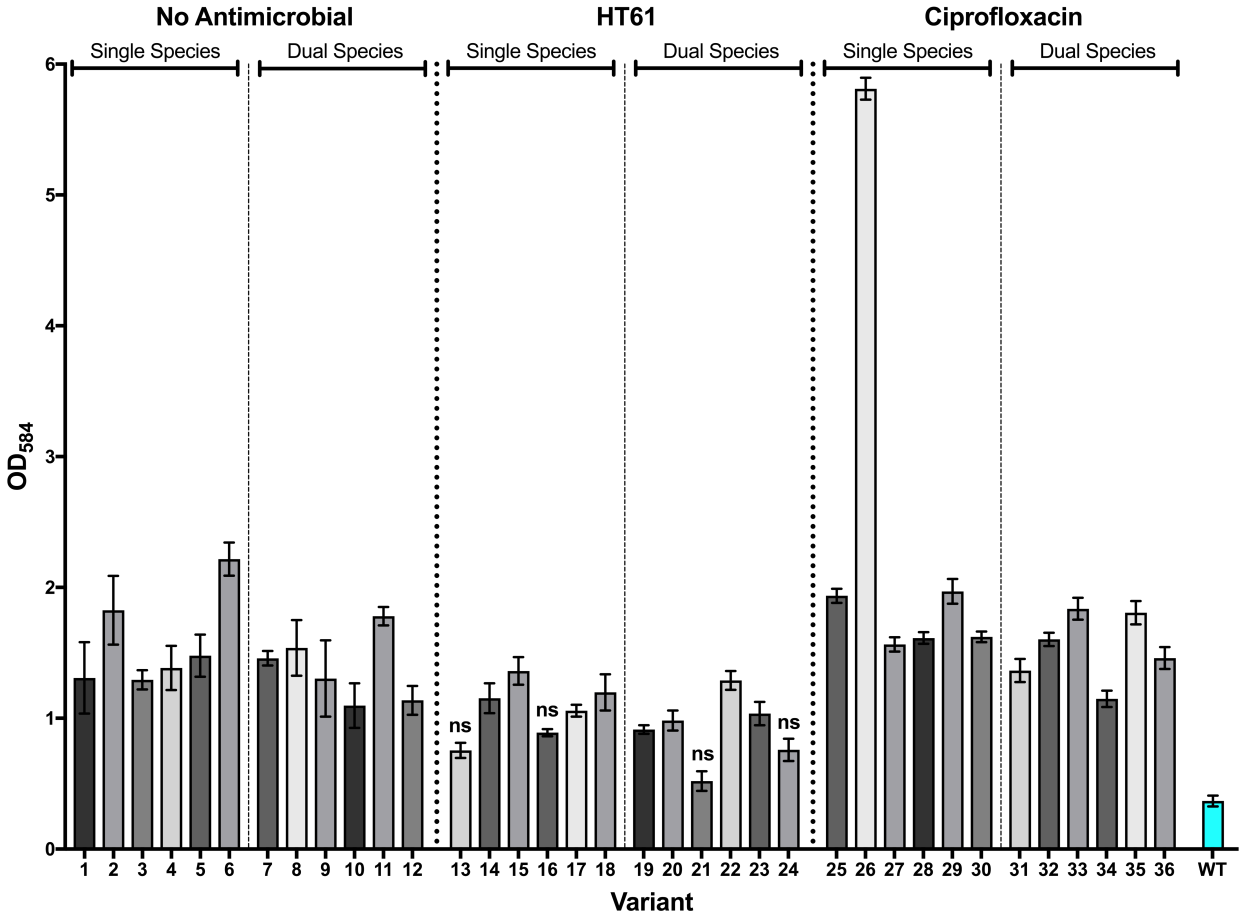

Figure 48: Early biofilm formation of biofilm derived colony variants of *P. aeruginosa* determined as a product of crystal violet staining

The majority of variants exhibit a statistically significant increase in biofilm formation compared to the wild type ancestor (WT, blue bar at right of graph, $p < 0.05$) ns = no statistical significance, compared to wild type ancestor ($p \geq 0.05$), as determined by one-way ANOVA with Dunnet's post-hoc comparison. Error bars represent standard error of the mean, n = 6.

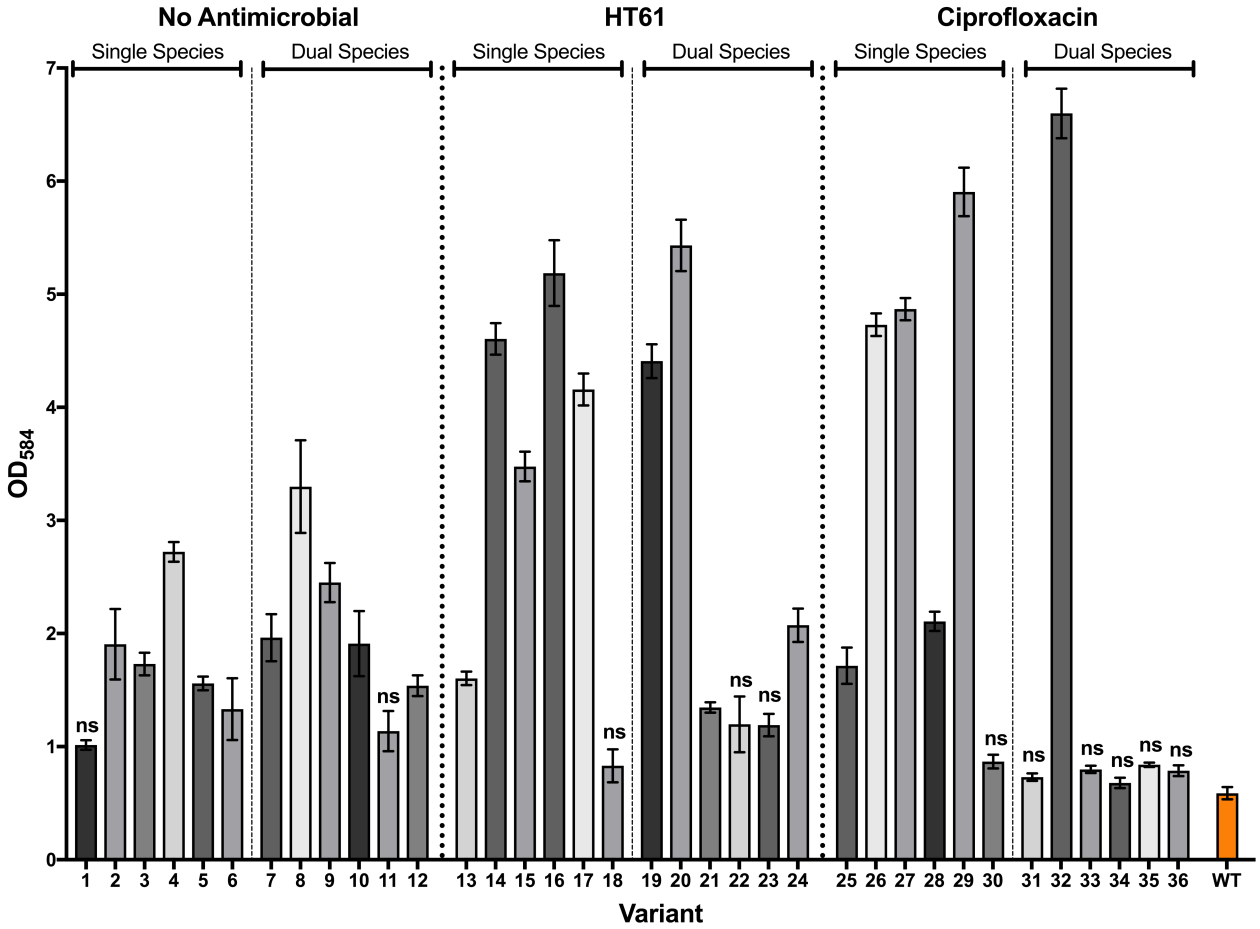

Figure 49: Early biofilm formation of biofilm derived colony variants of *S. aureus* determined as a product of crystal violet staining

The majority of variants exhibit a statistically significant increase in biofilm formation compared to the wild type ancestor (WT, orange bar at right of graph, $p < 0.05$) ns = no statistical significance, compared to wild type ancestor ($p \geq 0.05$), as determined by one-way ANOVA with Dunnet's post-hoc comparison. Error bars represent standard error of the mean, n = 6.

5.3.4 Growth Kinetics of Biofilm Derived Colonies

The growth rates of biofilm derived variants were calculated within the exponential phase of growth and compared to that of the ancestral wild type of *P. aeruginosa* or *S. aureus* (Figure 50 and Figure 51, respectively). Variation in the mean growth rate was statistically significant for both bacterial species (one-way ANOVA, $p < 0.0001$ for each). The actual growth curves are presented in the supplementary data.

P. aeruginosa variants presented both increased and decreased growth rates. Dunnet's post-hoc comparisons suggested that 3 variants, (PAV5, PAV6 and PAV23) had a statistically significant increased growth rate ($p = 0.0009$, < 0.0001 and < 0.0001, compared to ancestral wild type, respectively). PAV5 and PAV6 were both derived from single species biofilms with no antimicrobial treatment whereas PAV23 was derived from a dual species biofilm treated with HT61.

Decreased growth rates were far more abundant, identified in 21 variants compared to the ancestral wild type. 3 isolates were from single species non-antimicrobial supplemented biofilms, while 2 were derived from the equivalent dual species biofilm. PAV13 was the only variant derived from an HT61 treated, single species biofilm to present with a decreased growth rate. However, 4 variants were isolated from the HT61 treated dual species biofilm, suggesting an impact of the biofilm co-culture in this instance.

Interestingly, for ciprofloxacin treated biofilms, all isolates, except for PAV26, (which was identical to the wild type), exhibited a statistically significant reduction in growth rate. This occurred regardless of whether the variants were derived from a single or dual species biofilm, suggesting that ciprofloxacin treatment exerted stronger selection for phenotypes associated with slower growth, than the presence of HT61 or *S. aureus* during co-culture. It should be noted that PAV26 formed biofilms with considerably more biomass than the wild type (15.81 fold increase, see Section 5.3.3, Figure 48) and was the only variant to present with a ciprofloxacin MIC > 1 μg ml^{-1}, (5.3.2, Table 16), which implies that it has followed a different evolutionary trajectory compared with the other variants.

Unlike variants of *P. aeruginosa,* no biofilm derived *S. aureus* variants presented with decreased rates of growth. However, according to Dunnet's post-hoc comparisons, 22 variants presented with increased growth rates compared to the ancestral wild type ($p < 0.05$).

4 variants with increased growth rates were isolated from single and dual species biofilms without antimicrobial supplementation. In addition, 5 variants with increased growth rates were derived from HT61 treated single species biofilms, (SAV14, SAV15, SAV16, SAV17 and SAV18). Growth rate had increased in all colonies derived from HT61 treated dual species biofilms, however these differences were only statistically significant for one isolate (SAV23). A similar observation was made in variants derived from biofilms treated with ciprofloxacin. All 6 isolates from single species biofilms exhibited increased rates of growth, whereas only occurred in 2 isolates from the dual species biofilm (PAV31 and PAV36).

In these cases, it suggests that in the presence of antimicrobial, *P. aeruginosa* will limit the selection of faster growing phenotypes in *S. aureus* (or promote selection of phenotypes that do not alter growth rate).

To summarise the previous phenotyping data, these results collectively demonstrate that while significant variation from the wild type can occur during biofilm growth, it is not possible to identify whether a colony was derived from a particular biofilm population based on any combination of growth rate, antimicrobial susceptibility or ability to form biofilms. This is because none of the identified phenotypes were exclusive/more prevalent in variants from a certain origin. The remainder of this chapter will explore whether genomic differences can be used as an alternative identifier, and explore adaptation to HT61 and ciprofloxacin.

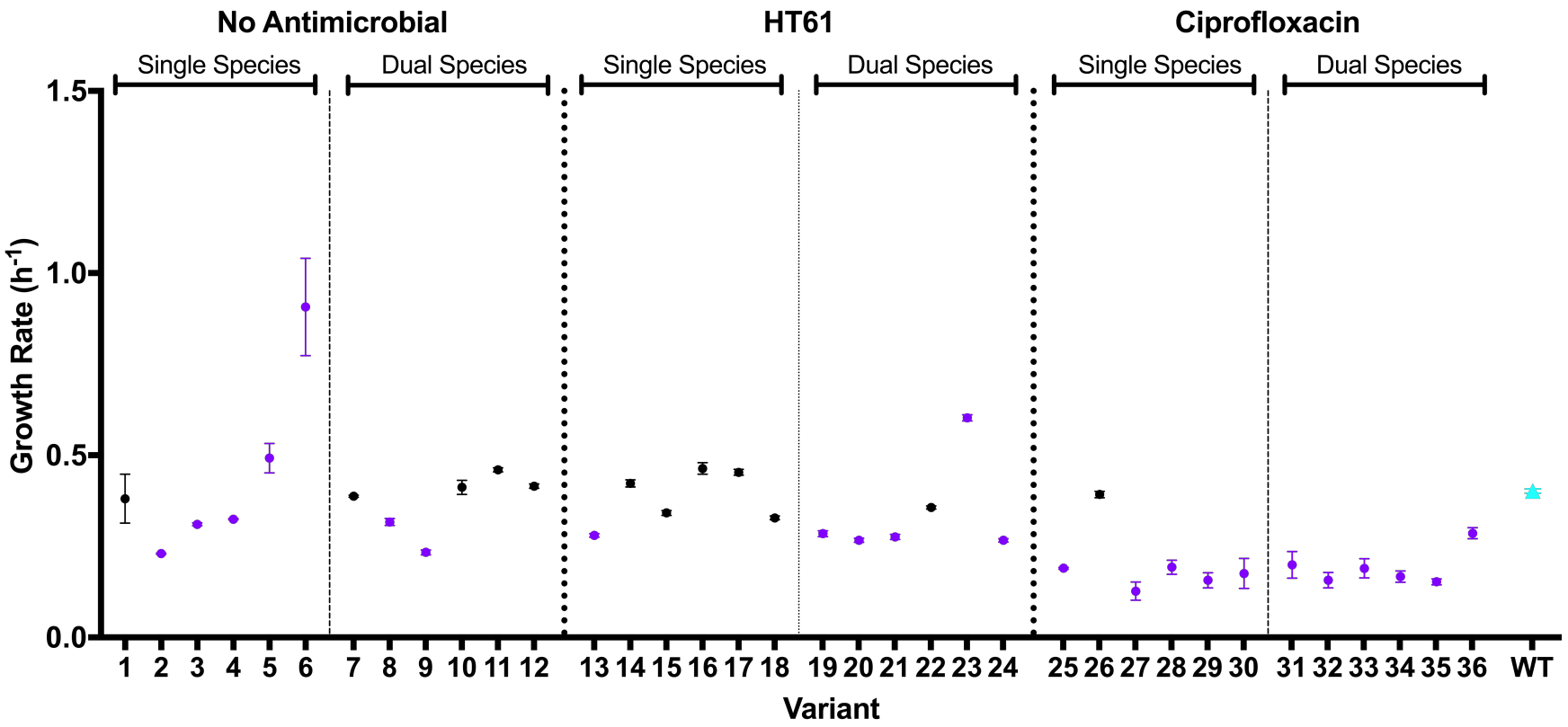

Figure 50: Exponential growth rates of biofilm derived variants of *P. aeruginosa*

Compared to the ancestral wild type (WT, light blue triangle to the right of the graph), 3 variants present with a statistically significant increase in growth rate and 21 variants with a statistically significant decrease in growth rate, according to Dunnet's post-hoc comparisons ($p < 0.05$). Variants with a statistically significant difference in growth rate are plotted with a purple point, those with a non-significant difference in growth rate are plotted with a black point. $3 \leq n \leq 9$. Wild type $n = 15$. Error bars represent standard error of the mean.

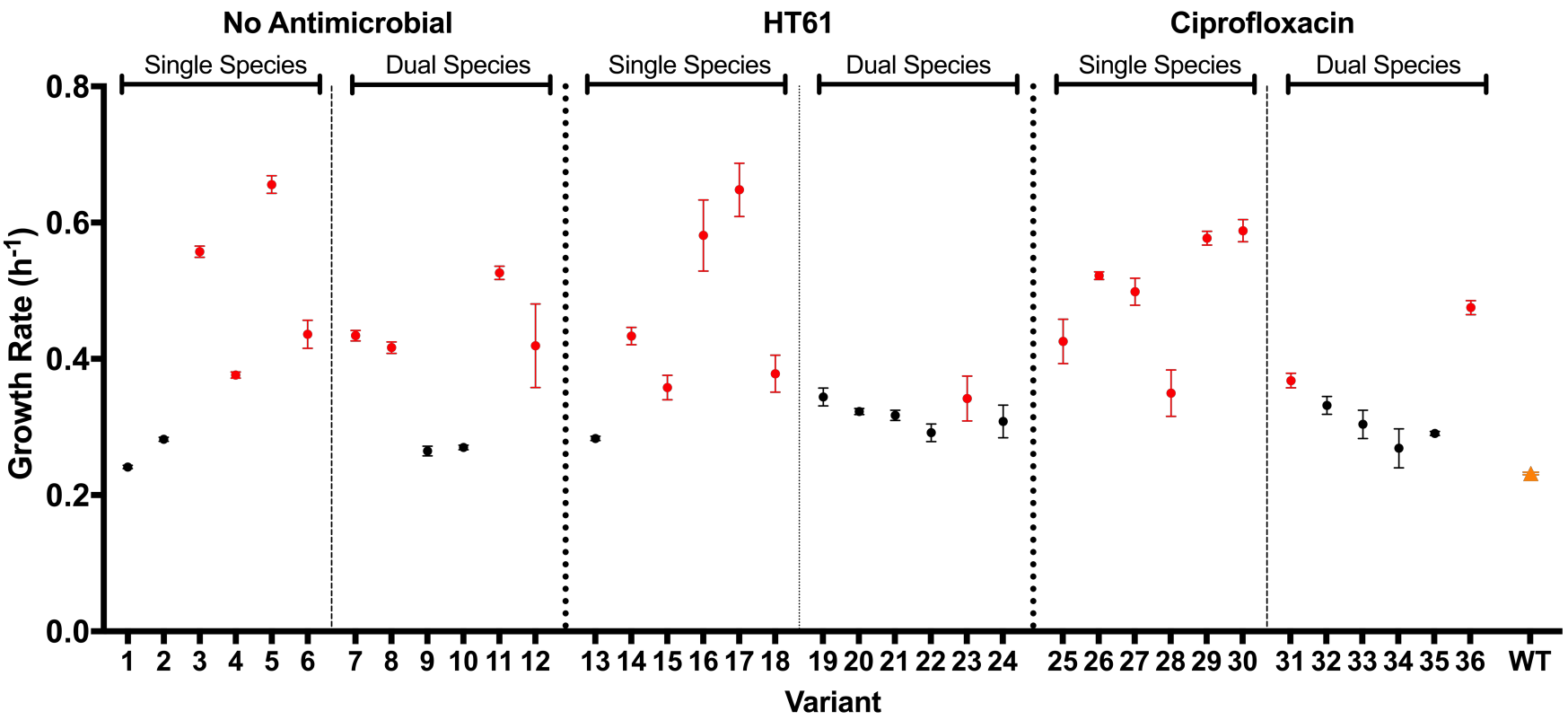

Figure 51: Exponential growth rates of biofilm derived variants of *S. aureus*

Compared to the ancestral wild type (WT, orange triangle to the right of the graph), 14 variants present with a statistically significant increase in growth rate, according to Dunnet's post-hoc comparisons ($p < 0.05$). Variants with a statistically significant difference in growth rate are plotted with a red point and those with a non-significant difference in growth rate are plotted with a black point. $3 \leq n \leq 9$. Wild type $n = 15$. Error bars represent standard error of the mean.

5.3.5 Biofilm Derived Variants are Genetically Distinct from The Ancestral Wild Type

5.3.5.1 Analysis of Variant Genome Assemblies

All 72 biofilm derived isolates (36 *P. aeruginosa* and 36 *S. aureus*), were subjected to whole genome sequencing in order to investigate whether biofilm co-culture altered the evolutionary dynamics of each species. In addition, the results were examined to identify any putative adaptive mechanisms to HT61 and ciprofloxacin.

Assembly and annotation details of the reference and variant genomes are fully listed in the appendices of this chapter. For both *P. aeruginosa* and *S. aureus*, the variant genomes were highly similar to the ancestral wild type suggesting the data was of good quality.

For *P. aeruginosa* variants, genomes assembled to an average of 106 contigs, with an average N50 (contig length at 50% of the assembly; half of the nucleotides are assembled in contigs greater than or equal to a length) of 135, 256 bp. Average assembly length was 6.7 Mb with 6160 CDS. Average coverage was equal to 99 x that of the annotated reference genome.

S. aureus variant assemblies were comprised of an average of 38 contigs, with an average N50 of 137, 364 bp. Average assembly length was 2.7 Mb and an average of 2542 CDS regions were identified. Average coverage compared to the ancestral wild type genome was approximately 126 x.

Assembly of PAV34 was not to the same quality of the other variants with a higher number of contigs, reduced N50 and a reduction in total genome size by approximately 1.2 Mb. Furthermore, programs utilised for subsequent analysis would routinely fail suggesting issues with the quality of the actual sequence data. Investigations into the raw sequence data supplied by MicrobesNG revealed that 29.59 % of the reads for PAV34 were unclassified and only 68.5 % were attributed to *Pseudomonadaceae.* For comparison, other samples contained approximately 0.1 to 2.5 % unclassified DNA, and at least 95 % classified as *Pseudomonadaceae*. This suggests high levels of contamination in the PAV34 reads and/or possible sequencing errors. For these reasons, it had to be excluded from all subsequent analyses.

Core and accessory genomes of both bacterial species were determined using ROARY. The core genome describes genes that are shared by 95 to 100% of isolates (Core = 99 to 100%, Soft core = 95 to 99%) while the accessory genome describes those genes that are shared by fewer isolates (although are still common, between each other)[321]. The core genome will typically incorporate essential genes and the accessory genome will often include features such as mobile elements and phage DNA. A summary table of the core genomes is shown in Table 18.

The core genome of both species is higher than typically identified in literature (*P. aeruginosa* core between 4455 and 5316 genes[330], and *S. aureus* of approximately 1485 genes[331]). However, these previous studies assess the genome between many different strains, whereas the calculations performed here only account for variation within a single strain (and a comparatively short time frame). As such, the number of core genes is naturally higher than if comparisons were made between different strains of each species.

Table 18: Pan genome analysis of *P. aeruginosa* and *S. aureus* calculated using ROARY

According to these data, the accessory genome, which incorporates mobile elements and phages, is considerably higher in *P. aeruginosa*, compared to *S. aureus*, comprising 3.62% and 1.25% respectively.

	Core Genome			Accessory Genome		
	Core Genes	Soft Core Genes	**Total Core**	Shell Genes	Cloud Genes	**Total Accessory**
P. aeruginosa	5740	339	**6079**	190	38	**228**
S. aureus	2516	10	**2526**	31	1	**32**

5.3.5.2 Whole Genome Sequence Analysis Identifies Genes That May Be Under Selection During Biofilm Growth

Following sequencing, variant genomes were analysed for SNPs and INDELs using the breseq software package[322,323]. Mutational profiles were evaluated to address three specific aims. First, to identify whether mutations could be attributed to the observed colony phenotypes, including growth rates, antimicrobial susceptibility and biofilm formation. Secondly, whether the spectrum of mutations could be differentiated between those colonies derived from single and dual species biofilms. Finally, whether mutations could be identified that provide insight into possible mechanisms of action/resistance of HT61.

Genomes of *P. aeruginosa* presented with an average of 48.2 mutations per genome, compared to the ancestral wild type. Comparatively, an average of 9.58 mutations were found per genome of the *S. aureus* biofilm derived colonies. No statistically significant variation in mutation frequency was observed between variants derived from single or dual species biofilms, or between groups treated with HT61, ciprofloxacin or without antimicrobial treatment for either species (*P. aeruginosa*: one-way ANOVA, $p = 0.7420$; *S. aureus*: one-way ANOVA, $p = 0.4976$).

The distribution of the types of mutations identified in biofilm derived variants of *P. aeruginosa* and *S. aureus* are graphically summarised in Figure 52, panels A and B, respectively. Across all 36 *P. aeruginosa* variants, an average of 41.1 mutations per isolate were classified as small insertions/deletions. Of the SNPs that were identified, intergenic SNPs were the most prevalent, with an average of 4.03 per isolate, followed by non-synonymous SNPs, which would result in a change in the amino acid sequence of associated proteins.

However, for *S. aureus*, over 50% of the total genomic mutations were large deletions greater than 10 bp. The remaining 50% of mutations consisted of small insertions/deletions (INDELs) and SNPs (non-synonymous, nonsense and intergenic).

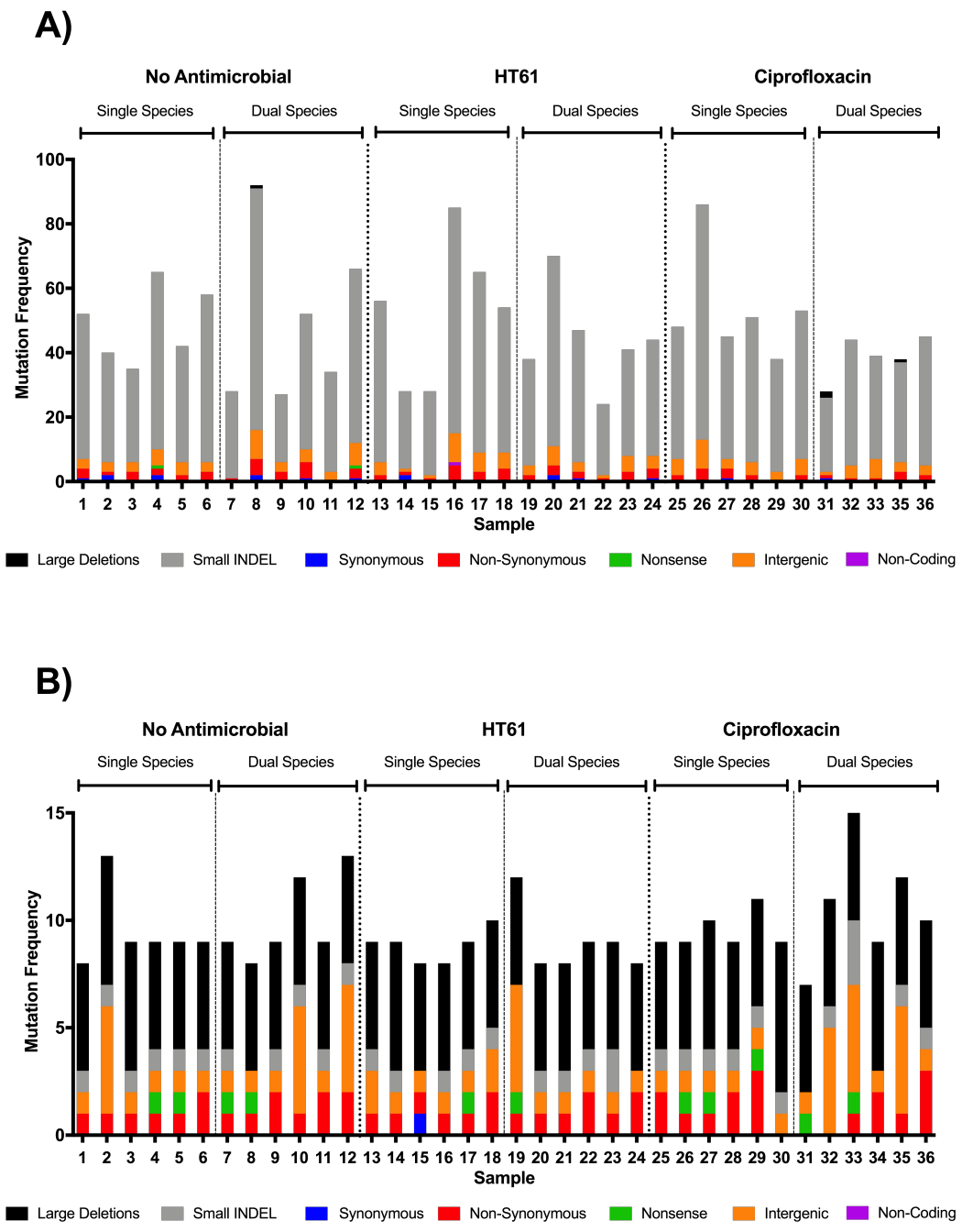

Figure 52: Distribution of mutation types identified in biofilm derived variants of *P. aeruginosa* (A) and *S. aureus* (B)

Large deletions represent those greater than 10 bp, small indels are insertions and deletions less than 10 bp. SNPs are categorised as synonymous if the codon output is unchanged, non-synonymous if codon output is altered to a different amino acid, nonsense if a stop codon is introduced prematurely, intergenic if occurring between two genes and non-coding if occurring in a region of a gene not implicated in coding e.g. regulatory sequences. Regions characterised using the breseq and gdtools software packages.

5.3.5.3 *P. aeruginosa* Genes Associated with Biofilm Formation, Virulence and Cell Division Are Under Selection During Biofilm Growth

Table 19 details genomic mutations identified in variants derived from non-antimicrobial treated biofilms and variants from at least one of the antimicrobial treated (HT61 or ciprofloxacin) populations. By considering the different biofilm populations together (single and dual species, with and without antimicrobial), it is possible to identify genes that may be under selection during biofilm growth in more general terms.

Annotated genes with known or predicted function that had mutated in non-antimicrobial, HT61 and ciprofloxacin treated populations included *ftsN* (19/35 variants, implicated in cell division), *comEC* (8/35, nuclease, important for DNA uptake and transformation[332]), *dipA* (12/35, putative ci-di-GMP phosphodiesterase associated with biofilm formation and virulence[333]), *trxB* (23/35, thioredoxin/peroxide reductase and stress[334]) , *maoC* (19/35, enoyl-coA hydratase[335]), *lipH* (10/35, lipase chaperone, important for the regulation of biofilm formation[336]) and *yhhY* (23/35, conserved acetyltransferase).

The mutations identified in *dipA* are notable as all identified SNPs were non-synonymous, with two in particular, isolated from PAV4 and PAV12, resulting in nonsense mutations and the premature introduction of a stop codon. These mutations, E238* and E636*, are located within the GAF domain and signal transducing/membrane spanning domains, implicating a loss of function. *dipA* knockout mutants exhibit markedly reduced biofilm dispersal, impaired swarming and improved biofilm attachment[333]. As such, it is possible that the mutations identified in the *P. aeruginosa* variants could contribute to the observed increased in biofilm formation described in Figure 48. This would only be one factor however, as mutations in *dipA* were not present in all biofilm derived variants.

Furthermore, there are a number of genes with unknown function that were mutated in all treatment groups such as various base insertions in PA3953 (24/35) and PA4697 (25/35) as well as a common non-synonymous SNP in PA4637 (GCT → GGT, A26G, in 22/35 variants).

Of the 165 mutations identified, 80 were classified as intergenic, located between both known and unknown genes. For example, common intergenic mutations included the insertions of an additional A, GCG and TC within the intergenic region between PA3835 and PA3836, identified in 35, 35 and 34 variants, respectively. The implications of these

intergenic mutations are currently unknown, but typically these regions of DNA include important modulatory sites such as promoter regions. A recent pre-print article has suggested that mutations in *P. aeruginosa* intergenic regions are important for altering protein expression and facilitating adaptation to a host environment[337].

There was no clear set of mutations to conclusively differentiate isolates of *P. aeruginosa* based on colony morphology or whether a colony was derived from a single or dual species biofilm (e.g. there were no common mutations present in all dual species derived variants). However, some mutations did appear to preferentially occur in variants from single or dual species biofilms.

For example, two separate non-synonymous mutations (L685Q and G55S) occurred in the gene *cheA3* in PAV2 and PAV6, each derived from separate single species biofilm populations. *cheA3* is a histidine kinase and is implicated in the negative regulation of chemotaxis and bacterial mobility, in particular, swarming and swimming motility[338,339]. Notably, the associated *cheB* gene was also found to be mutated but these mutations were not restricted to single or dual species biofilm derived isolates. While a 13 bp deletion was found in PAV6, a 16 bp duplication was identified in PAV14 and PAV20 (HT61 treated, single and dual species biofilm derived, respectively) and a non-synonymous SNP (A311V) was present in the gene of PAV11 (no antimicrobial, dual species).

Specific mutations associated with co-culture were also limited. PAV12, derived from a non-antimicrobial treated, dual species biofilm, contained a series of exclusive intergenic SNPs between *aguR* and *aguB,* which are components of the *aguBA* operon, associated with agmatine catabolism and associated polyamine metabolism[340]. PAV12 also harboured a non-synonymous mutation (R217C) in *nuoG*, a component of the electron transport chain and an aminoglycoside modifying enzyme that has been associated with resistance to aminoglycoside class antimicrobials[190,341].

A final mutation of mention was a non-synonymous SNP (Q157H) identified in *wspR* of PAV7, derived from a non-antimicrobial treated, dual species biofilm. *wspR* is a regulator of the Wsp signalling system which is associated with the generation of c-di-GMP and biofilm formation[52]. Recently, mutations in other members of the Wsp signalling system have been shown to exclusively occur in *P. aeruginosa* following planktonic co-evolution with *S. aureus* and not when cultured in isolation. *wsp* mutants exhibited reduced fitness

when in culture with *S. aureus* suggesting that adaptation in this gene is important for facilitating *P. aeruginosa* survival in planktonic co-culture[154]. As such, the mutation present in PAV7 may promote *P. aeruginosa* survival as well. Mutations in *wspR* in *P. aeruginosa* PAO1 have also been linked with the development of rugose colony variants[78]. However, this does not appear to apply to PAV7, which had a smaller, non-rugose colony morphology (Figure 42).

Table 19: SNPs and INDELs identified in common genes across *P. aeruginosa* PA21 variants derived from single and dual species biofilms, with or without antimicrobial supplementation

Dotted lines separate variants from the two separate biofilm populations, while thick, solid lines separate variants derived from single/dual species biofilms and antimicrobial treatment groups. Mutation column describes the base transition/transversion, insertion (signified by a +) or deletion (signified by a Δ). Effects of the mutation on specific codons are highlighted if known. Nonsense mutations are indicated by a *. Intergenic refers to a mutation occurring between two genes, described in the brackets, with the position relative to each gene indicated in the brackets that follow (+ or – indicate up or downstream of gene). Coding indicates the mutation has occurred in the coding region of a gene and the implicated nucleotides are specified in brackets. Green squares indicate the particular mutation was identified in the associated variant. DEL means the mutation was not found as the implicated genomic region was deleted. (1/3)

			No Antimicrobial												HT61												Ciprofloxacin											
			Single						Dual						Single						Dual						Single						Dual					
mutation	Effect	Gene	1			2			1			2			1			2			1			2			1			2			1			2		
			1	2	3	4	5	6	7	8	9	10	11	12	13	14	15	16	17	18	19	20	21	22	23	24	25	26	27	28	29	30	31	32	33	35	36
T→C	Y238C (TAC→TGC)	*pqsH*																																			
Δ1 bp	coding (290/1182 nt)	*atoB*																																			
+AC	intergenic (+41/-526)	*arfA →* / *→ mltB_3*																																			
+G	intergenic (+61/-506)																																				
G→A	intergenic (+63/-504)																																				
G→A	intergenic (+81/-486)																																				
+TGCCGC	intergenic (+95/-472)																																				
$(CCA)_{t2\rightarrow t1}$	coding (519-521/972 nt)	*czcD_2 →*																																			
47 bp→57 bp	coding (392-438/681 nt)	*ftsN_1 ←*																																			
+GCG	coding (435/681 nt)																																				
+G	coding (397/681 nt)																																				
+CT	coding (374/681 nt)																																				
A→G	A124A (GCT→GCC)																																				
A→G	L123L (TTG→CTG)																																				
+G	coding (357/681 nt)																																				
+GC	coding (343/681 nt)																																				
A→T	L685Q (CTG→CAG)	*cheA_3 ←*																																			
C→T	G55S (GGC→AGC)																																				
G→A	A311V (GCG→GTG)	*cheB_2 ←*																																			
Δ13 bp	coding (843-855/1008 nt)																																				
(CAATAATTCG CCACGC)$_{t1\rightarrow2}$	coding (776/1008 nt)																																				
C→T	G162D (GGT→GAT)																																				
+C	coding (1120/2220 nt)	*comEC ←*																																			
+C	coding (1036/2220 nt)																																				
A→G	Y893H (TAT→CAT)	*dipA*																																			
Δ1 bp	coding (2528/2700 nt)																																				
C→G	A843P (GCC→CCC)																																				
A→G	V839A (GTG→GCG)																																				
C→T	D825N (GAC→AAC)																																				
A→C	Y807D (TAC→GAC)																																				
C→A	G673V (GGC→GTC)																																				
C→A	E636* (GAG→TAG)																																				
C→G	A618P (GCC→CCC)																																				
Δ57 bp	coding (1776-1832/2700 nt)																																				
Δ1 bp	coding (1306/2700 nt)																																				
C→A	E238* (GAG→TAG)																																				
2 bp→CT	intergenic (-3/+414)	*gmr_1 ← / ← aceF*																																			
G→C	A142A (GCG→GCC)	*folP →*																																			
+A	intergenic (+127/-34)	*PA0387/hemN*																																			
+C	intergenic (+134/-27)																																				
+C	intergenic (+138/-23)																																				
+C	intergenic (+149/-12)																																				
G→A	S274F (TCC→TTC)	*flhA ←*																																			
Δ14 bp	coding (511-524/1137 nt)	*flhB_2 ←*																																			
C→T	R303C (CGC→TGC)	*trxB*																																			
+C	coding (914/1269 nt)																																				
+A	coding (931/1269 nt)																																				
+TC	coding (935/1269 nt)																																				
+G	coding (959/1269 nt)																																				
+T	coding (996/1269 nt)																																				
+TC	coding (1008/1269 nt)																																				
+C	coding (1020/1269 nt)																																				
C→T	R26C (CGC→TGC)	*wbpX*																																			
Δ11 bp	coding (665-675/1383 nt)																																				
Δ11 bp	coding (1201-1211/1383 nt)																																				
A→G	K13E (AAG→GAG)	*PA0141*																																			
C→A	V315V (GTG→GTT)	*urtC*																																			

Table 19 continued (2/3)

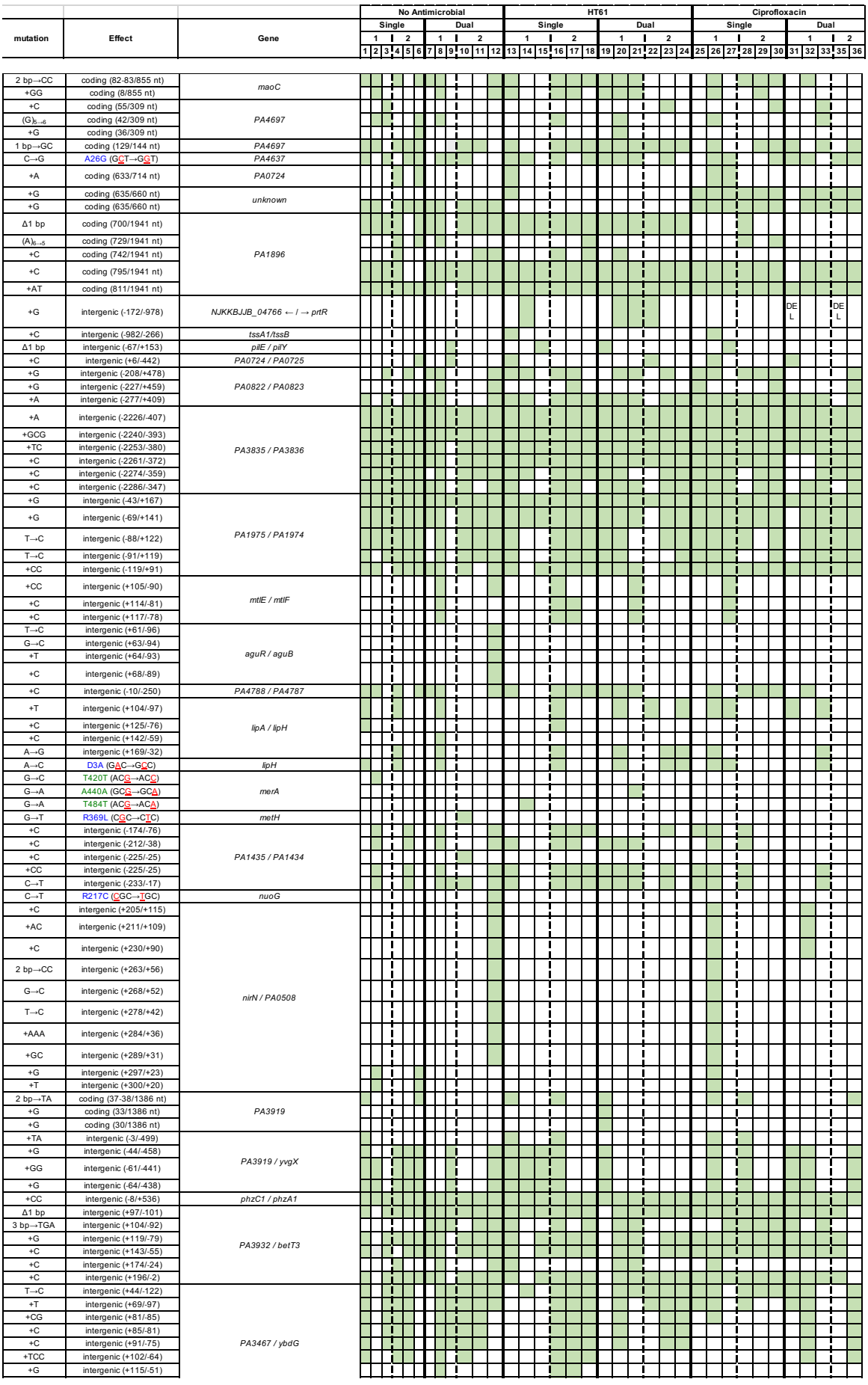

mutation	Effect	Gene	No Antimicrobial												HT61												Ciprofloxacin											
			Single						Dual						Single						Dual						Single						Dual					
			1			2			1			2			1			2			1			2			1			2			1			2		
			1	2	3	4	5	6	7	8	9	10	11	12	13	14	15	16	17	18	19	20	21	22	23	24	25	26	27	28	29	30	31	32	33	35	36
2 bp→CC	coding (82-83/855 nt)	*maoC*																																			
+GG	coding (8/855 nt)																																				
+C	coding (55/309 nt)	*PA4697*																																			
$(G)_{5\to6}$	coding (42/309 nt)																																				
+G	coding (36/309 nt)																																				
1 bp→GC	coding (129/144 nt)	*PA4697*																																			
C→G	A26G (GCT→GGT)	*PA4637*																																			
+A	coding (633/714 nt)	*PA0724*																																			
+G	coding (635/660 nt)	*unknown*																																			
+G	coding (635/660 nt)																																				
Δ1 bp	coding (700/1941 nt)	*PA1896*																																			
$(A)_{6\to5}$	coding (729/1941 nt)																																				
+C	coding (742/1941 nt)																																				
+C	coding (795/1941 nt)																																				
+AT	coding (811/1941 nt)																																				
+G	intergenic (-172/-978)	*NJKKBJJB_04766 ← / → prtR*																														DEL			DEL		
+C	intergenic (-982/-266)	*tssA1/tssB*																																			
Δ1 bp	intergenic (-67/+153)	*pilE / pilY*																																			
+C	intergenic (+6/-442)	*PA0724 / PA0725*																																			
+G	intergenic (-208/+478)	*PA0822 / PA0823*																																			
+G	intergenic (-227/+459)																																				
+A	intergenic (-277/+409)																																				
+A	intergenic (-2226/-407)	*PA3835 / PA3836*																																			
+GCG	intergenic (-2240/-393)																																				
+TC	intergenic (-2253/-380)																																				
+C	intergenic (-2261/-372)																																				
+C	intergenic (-2274/-359)																																				
+C	intergenic (-2286/-347)																																				
+G	intergenic (-43/+167)	*PA1975 / PA1974*																																			
+G	intergenic (-69/+141)																																				
T→C	intergenic (-88/+122)																																				
T→C	intergenic (-91/+119)																																				
+CC	intergenic (-119/+91)																																				
+CC	intergenic (+105/-90)	*mtlE / mtlF*																																			
+C	intergenic (+114/-81)																																				
+C	intergenic (+117/-78)																																				
T→C	intergenic (+61/-96)	*aguR / aguB*																																			
G→C	intergenic (+63/-94)																																				
+T	intergenic (+64/-93)																																				
+C	intergenic (+68/-89)																																				
+C	intergenic (-10/-250)	*PA4788 / PA4787*																																			
+T	intergenic (+104/-97)	*lipA / lipH*																																			
+C	intergenic (+125/-76)																																				
+C	intergenic (+142/-59)																																				
A→G	intergenic (+169/-32)																																				
A→C	D3A (GAC→GCC)	*lipH*																																			
G→C	T420T (ACG→ACC)	*merA*																																			
G→A	A440A (GCG→GCA)																																				
G→A	T484T (ACG→ACA)																																				
G→T	R369L (CGC→CTC)	*metH*																																			
+C	intergenic (-174/-76)	*PA1435 / PA1434*																																			
+C	intergenic (-212/-38)																																				
+C	intergenic (-225/-25)																																				
+CC	intergenic (-225/-25)																																				
C→T	intergenic (-233/-17)																																				
C→T	R217C (CGC→TGC)	*nuoG*																																			
+C	intergenic (+205/+115)	*nirN / PA0508*																																			
+AC	intergenic (+211/+109)																																				
+C	intergenic (+230/+90)																																				
2 bp→CC	intergenic (+263/+56)																																				
G→C	intergenic (+268/+52)																																				
T→C	intergenic (+278/+42)																																				
+AAA	intergenic (+284/+36)																																				
+GC	intergenic (+289/+31)																																				
+G	intergenic (+297/+23)																																				
+T	intergenic (+300/+20)																																				
2 bp→TA	coding (37-38/1386 nt)	*PA3919*																																			
+G	coding (33/1386 nt)																																				
+G	coding (30/1386 nt)																																				
+TA	intergenic (-3/-499)	*PA3919 / yvgX*																																			
+G	intergenic (-44/-458)																																				
+GG	intergenic (-61/-441)																																				
+G	intergenic (-64/-438)																																				
+CC	intergenic (-8/+536)	*phzC1 / phzA1*																																			
Δ1 bp	intergenic (+97/-101)	*PA3932 / betT3*																																			
3 bp→TGA	intergenic (+104/-92)																																				
+G	intergenic (+119/-79)																																				
+C	intergenic (+143/-55)																																				
+C	intergenic (+174/-24)																																				
+C	intergenic (+196/-2)																																				
T→C	intergenic (+44/-122)	*PA3467 / ybdG*																																			
+T	intergenic (+69/-97)																																				
+CG	intergenic (+81/-85)																																				
+C	intergenic (+85/-81)																																				
+C	intergenic (+91/-75)																																				
+TCC	intergenic (+102/-64)																																				
+G	intergenic (+115/-51)																																				

Table 19 continued (3/3)

mutation	Effect	Gene	No Antimicrobial												HT61												Ciprofloxacin											
			Single						Dual						Single						Dual						Single						Dual					
			1			2			1			2			1			2			1			2			1			2			1			2		
			1	2	3	4	5	6	7	8	9	10	11	12	13	14	15	16	17	18	19	20	21	22	23	24	25	26	27	28	29	30	31	32	33	35	36
$(G)_{9\rightarrow10}$	intergenic (-34/+51)	*PA1142 / PA1143*																																				
+G	intergenic (+31/+761)	*mk / cyaA*																																				
C→T	intergenic (+33/+759)																																					
+C	intergenic (+41/+751)																																					
+C	intergenic (+52/+740)																																					
+C	intergenic (+73/+719)																																					
C→A	Q157H (CAG→CAT)	*wspR*																																				
+G	intergenic (-26/+1)	*mviM / yggX*																																				
+A	coding (577/597 nt)	*yhhY*																																				
+T	coding (570/597 nt)																																					
1 bp→TT	coding (569/597 nt)																																					
+C	coding (537/597 nt)																																					
+CC	coding (531/597 nt)																																					
+A	coding (487/597 nt)																																					
+C	coding (560/1086 nt)	*PA3953*																																				
+T	coding (593/1086 nt)																																					
+C	coding (612/1086 nt)																																					
1 bp→GC	coding (642/1086 nt)																																					
Δ12 bp	coding (562-573/1035 nt)	*pilT*																																				

5.3.5.4 Antimicrobial Treatment Confers Specific Mutations in Virulence and Antimicrobial Resistance Genes in Biofilm Derived Isolates of *P. aeruginosa*

Table 20 describes mutations identified in *P. aeruginosa* variants that were exclusive to isolates derived from HT61 or ciprofloxacin treated biofilms and that were not present in variants isolated from the untreated biofilms. Consequently, these mutations could be directly associated with an evolutionary response to the antimicrobial and not biofilm growth in more general terms.

Regarding variants derived from biofilms treated with HT61, 6 exclusive mutations were identified. Of interest was a non-synonymous SNP (Q235L, found in PAV16 and PAV23) in *tpbB,* a regulator of ci-di-GMP and biofilm formation[342]. While this mutation could be linked to altered biofilm formation, it does not specifically infer a mechanism of action or resistance towards HT61. However, as HT61 has no demonstrated efficacy towards *P. aeruginosa* this was not unexpected.

In variants derived from ciprofloxacin treated biofilms, 12 exclusive mutations were identified. The genes encoding two glycosyltransferases, *wbpY* and *wbpZ*, required for the synthesis of cell surface antigens[343], were mutated in PAV27 and PAV29, respectively. Furthermore, two extremely large deletions of 41, 506 bp were identified in the dual species derived PAV31 and PAV35 variants. Despite the loss of 60 genes, (55 hypothetical), these variants were not phenotypically distinct from the other *P. aeruginosa* variants in terms of growth rates, biofilm formation or antimicrobial susceptibility (as per Table 16, Figure 48 and Figure 50).

Interestingly, an intergenic insertion of two cytosine residues between *phzC1* and *phzA1*, (components of the phenazine biosynthesis operon)[344], was present in all 23 variants, regardless of whether they were derived from HT61 or ciprofloxacin treated biofilms. This could imply a more general evolutionary response to antibiotic pressure and may be an important target for future treatment biofilm treatments.

While the mutation is not shared by any other variants, PAV26 harboured a 12 bp deletion within the coding region of *mexS. mexS* encodes a negative regulator of the mexT dependent MexEF-OprN multidrug efflux pump system[345]. Notably, numerous studies have shown that mutations within this gene can result in increased resistance to

fluoroquinolone antibiotics and is associated with genes that can alter biofilm formation[168,346]. Subsequently, the observed *mexS* deletion in PAV26 could explain why it was the least susceptible to ciprofloxacin treatment (MIC ≥ 1 μg ml^{-1}, Table 16) and also formed significantly more biofilm than the other *P. aeruginosa* variant colonies (see Figure 48).

Table 20: SNPs and INDELs exclusively identified in biofilm derived variants of *P. aeruginosa* PA21 following culture with HT61 or ciprofloxacin

Mutation column describes the base transition/transversion, insertion (signified by a +) or deletion (signified by a Δ). Effects of the mutation on specific codons are highlighted if known. Nonsense mutations are indicated by a *. Intergenic refers to a mutation occurring between two genes, described in the brackets, with the position relative to each gene indicated in the brackets that follow (+ or – indicate up or downstream of gene). Coding indicates the mutation has occurred in the coding region of a gene and the implicated nucleotides are specified in brackets. Green squares indicate the particular mutation was identified in the associated variant. DEL means the mutation was not found as the implicated genomic region was deleted.

			HT61												Ciprofloxacin											
			Single						Dual						Single						Dual					
			1			2			1			2			1			2			1			2		
Mutation	Effect	Gene	13	14	15	16	17	18	19	20	21	22	23	24	25	26	27	28	29	30	31	32	33	35	36	
A→G	noncoding (142/1531 nt)	*16S rRNA*																								
G→T	L7I (CTT→ATT)	*fliM*																								
G→A	G279G (GGC→GGT)	*PA1874*																								
+G	intergenic (-7/+82)	*PA5136 / yibQ*																								
+G	intergenic (-298/-87)	*hypothetical / PA1367*																								
A→G	N94N (AAT→AAC)	*PA1617*																								
+CC	intergenic (-8/+536)	*phzC1 / phzA1*																								
T→A	Q235L (CAG→CTG)	*tpbB (yfiN)*																								
A→T	E5V (GAA→GTA)	*PA3467*																								
G→A	R206Q (CGG→CAG)	*PA2212*																								
Δ41,506 bp	*60 genes; clpP_3, rusA, prtR_4, , spo0C, spxA + 55 hypothetical*																									
Δ14 bp	coding (523-536/1128 nt)	*wbpY*																								
Δ12 bp	coding (2963-2974/4200 nt)	*rpoC*																								
Δ14 bp	coding (720-733/915 nt)	*rmd →*																								
+GG	coding (726/1146 nt)	*WbpZ*																								
Δ143 bp	*PA3074 / PA3075*																									
C→T	V1175V (GTG→GTA)	*pchF*																								
C→T	intergenic (-195/-332)	*PA1972 / braZ*																								
Δ12 bp	coding (354-365/1020 nt)	*mexS*																								

5.3.5.5 Biofilm Derived Variants of *S. aureus* Harbour Mutated Genes Associated with Transcriptional Regulation and Stress Responses

Table 21 details genomic mutations identified in variants of *S. aureus* derived from non-antimicrobial treated biofilms and from at least one of the antimicrobial treated (HT61 or ciprofloxacin) populations. Compared to *P. aeruginosa,* the number of mutations identified, as well as the selection of genes is far more limited, encompassing 14 SNPs, 1 insertion and 3 deletions in 10 genetic targets, including intergenic regions.

Common to all 36 variants was an intergenic mutation between *osmC* and a hypothetical gene, suggesting parallel selection on this region. *osmC* is induced under osmotic stress and is important for the reduction of hydroperoxides[347], however the effect of this intergenic mutation is unknown. In addition, 24 variants harboured a non-synonymous SNP (G309D) in *whiA*. *whiA* encodes a transcription factor that has putative roles in cell division[348,349]. Therefore, positive selection for specific SNPs during biofilm growth may suggest an important function such as facilitating *S. aureus* survival. Curiously, this mutation is not present in any of the variants derived from biofilms treated with ciprofloxacin.

The gene *greA*, which encodes a transcription factor associated with the maintenance of transcriptional fidelity in *E. coli*[350] and may influence the expression of cell invasion virulence factors in *Francisella tularensis*[351], underwent numerous mutations in 10 of the *S. aureus* biofilm derived variants. These mutations appear to be linked to loss of function: the gene was either deleted fully (SAV2, SAV3 and SAV14), partially deleted (SAV30 – 84 bp deleted), or contained a nonsense SNP which would introduce a premature stop codon and lead to a truncated protein product (SAV4, SAV5, SAV7, SAV8, SAV26, SAV27, SAV30). Aside from SAV8, all of these mutations occurred in variants derived from single species biofilms.

Some gene mutations occurred in variants derived from single or dual species biofilms only, even though the genes in question are likely to interact. For example, non-synonymous SNPs were identified in genes associated with components of RNA polymerase[352], specifically *rpoA* (R289L) and *rpoD* (A138E and D277Y). However, *rpoA* was only mutated in variants derived from dual species biofilms (SAV11 and SAV24), while *rpoD* was only mutated in variants from single species biofilms (SAV6 and SAV28).

Mutations in either of these genes would likely affect transcriptional profiles of the implicated bacteria and it is possible that the differentiation between single and dual species derived mutation is necessary for the transcription of different sets of genes.

4 intergenic SNPs were identified between genes encoding hypothetical 23S and 16S ribosomal proteins. Curiously, these 4 SNPs occurred only as a complete set of 4 and, apart from identification in SAV2, occurred exclusively in variants derived from co-culture biofilms (SAV10, SAV12, SAV19, SAV32, SAV33 and SAV35). These could be important for modulating the translational output of the cell.

5.3.5.6 Treatment with HT61 or Ciprofloxacin Causes Mutations in Numerous Uncharacterised Proteins of *S. aureus*

Mutations exclusive to variants of *S. aureus* derived from biofilms treated with HT61 or ciprofloxacin (and not present in variants derived from untreated biofilms), are presented in Table 22.

Mutations exclusive to variants derived from HT61 treated biofilms included a single nucleotide deletion in *graS* (SAV16, SAV20, SAV21 and SAV23), two non-synonymous SNPs in *fmtC* (SAV17 and SAV18), a non-synonymous SNP in *walR* (SAV22), a nonsense mutation in a hypothetical gene (SAV19), a synonymous SNP in a second hypothetical gene (SAV15) and finally, an intergenic SNP between two hypothetical genes (SAV13 and SAV18). *graS* encodes a histidine kinase sensor that is important for bacterial survival to host antimicrobial peptides[353,354] while *fmtC* has been implicated in *S. aureus* resistance to β-lactam antimicrobials[355]. *walR* is part of the two-component *walRK* two component system and is linked to the modulation of peptidoglycan synthesis[356].

Variants derived from ciprofloxacin treated biofilms harboured a number of non-synonymous SNPs. However, these were largely in hypothetical genes so the precise impact of these mutations is difficult to discern or predict. Similar to those variants derived from HT61 treated biofilms was the identification of SNPs in *graS,* (SAV31 and SAV32, nonsense SNP), and *fmtC* (SAV30, insertion), suggesting that antimicrobial induced stress in general could be sufficient to select for mutations in these genes.

Table 21: SNPs and INDELs identified in common genes across *S. aureus* UAMS-1 variants derived from single and dual species biofilms, with or without antimicrobial supplementation

Dotted lines separate variants from the two separate biofilm populations, while thick, solid lines separate variants derived from single/dual species biofilms and antimicrobial treatment groups.

Mutation column describes the base transition/transversion, insertion (signified by a +) or deletion (signified by a Δ). Effects of the mutation on specific codons are highlighted if known. Nonsense mutations are indicated by a *. Intergenic refers to a mutation occurring between two genes, described in the brackets, with the position relative to each gene indicated in the brackets that follow (+ or – indicate up or downstream of gene). Coding indicates the mutation has occurred in the coding region of a gene and the implicated nucleotides are specified in brackets. Green squares indicate the particular mutation was identified in the associated variant. DEL means the mutation was not found as the implicated genomic region was deleted.

				No Antimicrobial												HT61												Ciprofloxacin											
				Single						Dual						Single						Dual						Single						Dual					
				1			2			1			2			1			2			1			2			1			2			1			2		
Type	mutation	Effect	Gene	1	2	3	4	5	6	7	8	9	10	11	12	13	14	15	16	17	18	19	20	21	22	23	24	25	26	27	28	29	30	31	32	33	34	35	36
SNP	T→C	intergenic (-174/+271)	*hypothetical 23S and 16S Ribosomal Proteins*																																				
SNP	G→A	intergenic (-199/+246)																																					
SNP	T→C	intergenic (-254/+191)																																					
SNP	C→T	intergenic (-257/+188)																																					
SNP	C→A	R289L (CGT→CTT)	*rpoA ←*																																				
SNP	C→T	R281C (CGT→TGT)	*walK →*																																				
INS	+31 bp	intergenic (+118/+49)	*hypothetical/GNAT AcetylTransferase*																																				
DEL	Δ9,307 bp	*11 genes;, udk, greA, accB_1, accC_1, lamB, mntH + 5 hypothetical*																																				
DEL	Δ3,670 bp	*greA, IIGICJAH_01684, AHS2, accB_1, accC_1*															DEL																						
SNP	T→A	Y7* (TAT→TAA)	*greA →*																																				
SNP	G→T	E20* (GAA→TAA)															DEL																						
SNP	G→T	E50* (GAG→TAG)			DEL	DEL											DEL																						
DEL	Δ84 bp	coding (150-233/477 nt)			DEL	DEL											DEL																						
SNP	C→A	S125* (TCA→TAA)			DEL	DEL											DEL																						
SNP	C→A	A138E (GCG→GAG)	*rpoD →*																																				
SNP	G→T	D277Y (GAC→TAC)																																					
SNP	C→T	intergenic (+234/-165)	*osmC → / → hypothetical*																																				
SNP	C→T	G309D (GGT→GAT)	*whiA ←*																																				

Table 22: SNPs and INDELs exclusively identified in biofilm derived variants of *S. aureus* UAMS-1 following culture with HT61 or ciprofloxacin

Dotted lines separate variants from the two separate biofilm populations, while thick, solid lines separate variants derived from single/dual species biofilms and antimicrobial treatment groups. Mutation column describes the base transition/transversion, insertion (signified by a +) or deletion (signified by a Δ). Effects of the mutation on specific codons are highlighted if known. Nonsense mutations are indicated by a *. Intergenic refers to a mutation occurring between two genes, described in the brackets, with the position relative to each gene indicated in the brackets that follow (+ or – indicate up or downstream of gene). Coding indicates the mutation has occurred in the coding region of a gene and the implicated nucleotides are specified in brackets. Green squares indicate the particular mutation was identified in the associated variant. DEL means the mutation was not found as the implicated genomic region was deleted.

				HT61												Ciprofloxacin											
Type	mutation	Effect	Gene	Single						Dual						Single						Dual					
				1			2			1			2			1			2			1			2		
				13	14	15	16	17	18	19	20	21	22	23	24	25	26	27	28	29	30	31	32	33	34	35	36
DEL	Δ14,734 bp	22 genes; eta_1, set14_1, groEL and 19 hypothetical																									
DEL	Δ3 bp	coding (1006-1008/1185 nt)	*hmrA* ←																								
SNP	G→T	A4E (GCG→GAG)	*hypothetical*																								
SNP	G→C	S321R (AGC→AGG)	*hypothetical*																								
INS	+31 bp	intergenic (+118/+49)	*hypothetical/hypothetical*																								
DEL	$(T)_{7\rightarrow6}$	coding (189/1041 nt)	*graS* →																								
SNP	C→T	Q256* (CAA→TAA)																									
DEL	Δ58 bp	intergenic (+193/-351)	*hypothetical/hypothetical*																								
SNP	G→T	E206* (GAA→TAA)	*hypothetical*																								
INS	$(AATGA)_{1\rightarrow2}$	coding (878/2937 nt)																									
SNP	C→T	P141L (CCG→CTG)	*hypothetical*																								
INS	+G	coding (865/1347 nt)	*hypothetical*																								
INS	+CC	coding (1523/2523 nt)	*fmtC* ←																								
SNP	A→C	V318G (GTG→GGG)																									
SNP	A→T	L176* (TTA→TAA)																									
SNP	A→T	F87I (TTT→ATT)	*hypothetical*																								
SNP	G→T	D16Y (GAT→TAT)	*walR* →																								
SNP	G→A	P228L (CCA→CTA)	*clpB* ←																								
SNP	C→A	G287V (GGT→GTT)	*rocD* ←																								
SNP	C→T	D904N (GAT→AAT)	*hypothetical*																								
SNP	C→A	Y16* (TAC→TAA)	*hypothetical*																								
SNP	A→G	F13F (TTT→TTC)	*hypothetical*																								
INS	C→A	intergenic (-26/-110)	*hypothetical/hypothetical*																								

5.4 Discussion

The aim of this chapter was to investigate how biofilm growth influenced phenotypic and genotypic characteristics of *P. aeruginosa* and *S. aureus* by analysing colonies derived from single and dual species biofilms. The primary hypothesis was that colonies derived from co-culture biofilms would be phenotypically and genotypically distinct from those derived from single species biofilms. Secondly, by incorporating antimicrobial treatment, the aim was to identify whether genes associated with adaptation, particularly to HT61, could be identified. The results described in this chapter do not fully satisfy either hypothesis, however they are discussed in length over the following sections.

5.4.1 Colony Origin or Phenotypic Characteristics could not be Determined Based on Colony Morphology

For each bacterial species, 36 colonies were isolated from a selection of bacterial populations, encompassing single and dual species biofilms, grown for 14 days with no antimicrobials or sub-inhibitory concentrations of HT61 or ciprofloxacin.

For *P. aeruginosa*, considerable variation in colony size and morphology was observed, with notably smaller colonies, as well as larger wrinkly colonies identified. However, variation between *S. aureus* colonies was more limited, with only slight discrepancies in size being observed and no difference in colony topography. In addition, the majority of variants from both species were able to form more biofilm than their respective ancestral wild type, which could be important for the establishment and maintenance of chronic infection. Measurement of variant growth rates showed that *P. aeruginosa* isolates were predominantly slower growing than the wild type ancestor and *S. aureus* variants were predominantly faster growing. However, no link could be made between colony morphology and phenotypic characteristics and no specific causal genomic mutations could be identified.

Variation in bacterial colony morphology is a well-known phenomenon and has been described extensively in both *P. aeruginosa* and *S. aureus* as well as numerous other bacterial species[8,83,84,86,357,358]. In certain instances, a change in colony morphology is associated with a specific phenotype. For example, rugose small colony variants of *P. aeruginosa* are more able to form biofilms and survive neutrophil attack than their wild type ancestors[78,79], while white variants of *S. aureus* present with a reduced ability to form biofilms[357].

Perhaps the most well researched colony variant of *P. aeruginosa* and *S. aureus* are small colony variants, which typically present with slower growth and increased capacity for biofilm formation[359]. Curiously, and despite a large body of evidence in the literature detailing how co-culture of *S. aureus* with *P. aeruginosa* facilitates the emergence of *S. aureus* SCVs[87,145,309], no small colonies of *S. aureus* were isolated from any biofilm population. This is despite the fact that SCVs and other colony variants of *S. aureus* have previously been isolated using both BPA and TSA plates[87,146,257]. SCVs of *S. aureus* are typically auxotrophic for hemin. Therefore, supplementation of media with hemin as per this chapter, may have complemented this phenotype so that the small colony phenotype was lost. Whether or not this is the case, it is clear that, similar to the findings of the previous chapter, that these types of variant will only emerge under very specific exogenous stressors.

5.4.2 Biofilm Derived Variants Present Altered Susceptibility to Antimicrobials, Even in the Absence of Antimicrobial Selection

The susceptibility of biofilm derived variants of *P. aeruginosa* and *S. aureus* was determined for both HT61 and ciprofloxacin. Additional whole genome sequencing was performed to identify potential evolutionary responses to antimicrobial pressure, and whether these responses differed in variants derived from single or dual species biofilms.

5.4.2.1 *S. aureus* Adaptation to HT61 May Involve Modulation of Cell Envelope

Intrinsic resistance to HT61 was maintained by all isolates of *P. aeruginosa*. This was not unexpected as HT61 has not demonstrated any inhibitory activity against *P. aeruginosa* in previous chapters or published studies[11]. Surprisingly, *S. aureus*, susceptibility to HT61 appeared to increase, with a revised MIC of 8 μg ml^{-1} for 6 isolates. This occurred in isolates from all biofilm populations, regardless of whether HT61 was supplemented, suggesting that the presence of HT61 was not exerting any selection for this phenotypic change. No resistance to HT61 was identified, corroborating previous studies[11].

In terms of possible routes of HT61 adaptation, limited information can be derived from the genomic data without further investigation. However, the impact of mutations only identified in HT61 treated variants can be hypothesised. For example, in *S. aureus,* one of the mutated genes, *fmtC*, has been linked to daptomycin resistance[360]. Point mutations in this gene leads to protein alterations and increased lysinylation of membrane phosphotidylglycerol, increasing the positive charge on the apical membrane surface,

causing daptomycin repulsion[360]. HT61 preferentially interacts with negatively charged membrane phospholipids[13] so mutations that increase the membrane charge could be linked to HT61 adaptation.

graS, was the only annotated gene mutated in both single and dual species derived variants of *S. aureus* following treatment with HT61. *graS* has been implicated in *S. aureus* resistance to cationic antimicrobial peptides via regulation of the *dltABCD* operon, which modulates the charge of the *Staphylococcal* cell envelope[353,354]. Furthermore, *walR* underwent a non-synonymous point mutation in one HT61 treated biofilm derived colony (SAV22). Mutations in the *walRK* two component system can perturb cell wall peptidoglycan maintenance and have previously been associated with resistance to vancomycin and daptomycin[211,361]. As *graS* and the *walRK* system are both associated with expression of cell wall associated proteins, (such as those implicated in the cell wall stress stimulon, shown to be induced following HT61 treatment in Chapter 2), mutations could be directly associated with HT61 adaptation.

As an aside, *walK* was only mutated in SAV9, which was derived from an untreated dual species biofilm, suggesting that there is also selective pressure on cell wall associated genes during co-culture, possibly as a result of *P. aeruginosa* mediated lysis[149].

As HT61 preferentially interacts with a negatively charged cell membrane[13], mutations in genes that interfere with envelope charge could result in altered HT61 efficacy. It is worth noting however, that this could culminate in both increased or decreased susceptibility depending on whether the charge is positive or negative.

5.4.2.2 Ciprofloxacin Resistance Can Spontaneously Emerge in the Absence of Antimicrobial Selection

A number of *S. aureus* and *P. aeruginosa* isolates were found to have decreased susceptibility to ciprofloxacin, implying the evolution of resistance mechanisms. As expected, the majority of less susceptible isolates were derived from biofilms treated with sub-inhibitory concentrations of ciprofloxacin. However, a number were derived from biofilms treated with HT61 or without antimicrobial supplementation, suggesting that short-term diversification within a biofilm was sufficient to generate *de novo* resistance to ciprofloxacin. There was no correlation with the emergence of resistance and whether a colony was derived from a single or dual species biofilm.

Of the *S. aureus* and *P. aeruginosa* colonies that exhibited resistance, all bar one, (PAV26), presented with an MIC two-fold higher than the respective ancestral wild types of each species. Genome sequencing of these isolates did not identify any shared mutations typically associated with ciprofloxacin resistance such as within *gyrA, gyrB, parC* or *parE*[362]. Furthermore, genome sequencing did not identify a shared genetic profile between resistant variants, although a number of non-synonymous mutations were identified in uncharacterised hypothetical proteins in both *P. aeruginosa* and *S. aureus* suggesting possibly novel routes of adaptation.

It is possible that the decreased susceptibility to ciprofloxacin is the result of several mutations, such as those in uncharacterised genes. These genes may either directly contribute to resistance or contribute via epistatic interactions with known resistance elements. Epistasis in the context of ciprofloxacin resistance has been examined in *E. coli* where certain mutations in *parC,* (which would not alter susceptibility in isolation), increase the MIC in a compounding rather than additive nature if they occur alongside mutations in *gyrA*[196,362].

5.4.3 Parallel Evolution Occurs Across Genes and Intergenic Regions in Single and Dual Species Biofilms of *P. aeruginosa* and *S. aureus*

The observation of differing colony morphologies alongside phenotypic changes implied that genotypic changes had occurred during biofilm growth. Whole genome sequencing was employed in an attempt to identify genomic signatures that could define isolates based on whether they were derived from single or dual species communities.

A large number of mutations were identified across biofilm derived isolates, including mutations in genes that are associated with biofilm formation and virulence such as *dipA* and *lipH* in *P. aeruginosa* and *greA* in *S. aureus.* Interestingly, in isolates of *P. aeruginosa*, a large proportion of mutations occurred in intergenic regions, with some such as between *PA3835* and *PA3836*, occurring in all 35 analysed isolates, suggesting high levels of parallelism. Intergenic mutations are not as well understood as intragenic mutations but by interfering with regulatory regions, they can modulate genes elsewhere in the genome[337,363]. For example, mutations in the *embC-embA* intergenic region of *M. tuberculosis* has been directly associated with increasing the binding affinity of the EmbR regulator, resulting in increased transcriptional activity of *embAB* by increasing the binding and resistance to ethambutol[363].

The identification of shared mutations or mutational targets across genomes from different populations implies parallel evolution, which suggests strong selective pressure on these regions[84,89]. As such, these areas could be important for biofilm growth and may be important targets for further research into the understandings of biofilm biology, or even potential targets for therapeutic intervention.

Unfortunately, no phenotype tested in this chapter (growth rate, antimicrobial susceptibility, ability to form biofilms, or colony morphology) could be universally ascribed to a specific genetic change without further investigation. For example, while mutations in *dipA* could explain an increase in biofilm formation for mutated variants of *P. aeruginosa*, this genotype does not explain increased biofilm formation in isolates harbouring a wild type *dipA* allele. PAV7 for example, contained no mutations in *dipA* but a non-synonymous SNP (Q157H) in *wspR,* a crucial component in the generation of c-di-GMP. If this amino acid change increases *wspR* activity, it could provide an alternative explanation for improved biofilm formation[364]. Generating knockout mutants of such genes and regions of interest on a case by case basis could assist in linking genotypes to phenotypes, especially if paired with expression level analysis using techniques such as qPCR or RNA-sequencing (RNA-seq).

5.4.4 Isolates from Single and Dual Species Biofilms Can Not Be Differentiated Based on Their Genomic Profiles

While numerous mutations were discovered, a clear genomic fingerprint was not identified to differentiate variants derived from single or dual species biofilms for either *S. aureus* or *P. aeruginosa*. A possible reason for this is that even though some genes were mutated in either single or dual species derived variants, the mutations were only present in a single colony or biofilm population. This reduces the statistical power and makes it difficult to draw substantial conclusions. Examples include non-synonymous SNPs in *flhA* and *wspR,* found in PAV1 and PAV7 only (single and dual species derived variants of *P. aeruginosa*), respectively. If these mutations were present in more colonies, across multiple biofilm populations, they could be designated as markers of single or dual species derived evolution with higher certainty.

Differing evolutionary trajectories have been described for *P. aeruginosa* and *S. aureus* following planktonic co-culture[154] as well as in cystic fibrosis isolates of *P. aeruginosa* sequenced over an extended time course[365,366]. These studies provide evidence that the growth environment can contribute in significant ways to community adaptation.

Surprisingly, this did not seem to be the case for the isolates sequenced in this chapter. There are several possible explanations for this.

Firstly, *P. aeruginosa* PA21 and *S. aureus* UAMS-1 are both clinical isolates: *P. aeruginosa* PA21 from the lung of a cystic fibrosis patient, *S. aureus* UAMS-1, from a chronic wound infection[215]. As such, the strains may experience a form of diminishing returns epistasis, where further genomic adaptation is limited as they have already undergone beneficial diversification and adaptation to a multispecies environment[101].

Secondly, certain mutations may not have fixed or were outcompeted within the biofilm populations. For a mutation to fix within a population, it must occur at a frequency that is high enough to overcome generalised genetic drift, which would otherwise cause extinction of that mutant lineage[367,368]. The required frequency is determined by the change in fitness conferred by the mutant genotype: a higher frequency is required for the fixation of mutations that confer lower fitness gains. If the change in fitness is not great enough/the critical frequency is not reached, the mutation will not fix[101]. Alternatively, if multiple beneficial mutant lineages are present, they can compete, with the lineage that confers the highest fitness prevailing in a process known as clonal interference[101,104]. The concepts of evolving lineage dynamics are elegantly illustrated in Figure 53 , taken from Cooper V. (2018). When this theory is applied to the results from this chapter, diversifying mutations may have occurred between single and dual species derived variants but they were either removed by genetic drift or outcompeted via clonal interference by more beneficial genotypes. Sampling at time points earlier than 14 days may have identified these mutations before they were swept to extinction. Alternatively, 14 days may have been too short of a timeframe for these differences to emerge, in which case, the experiment would need to be performed for a longer period of time.

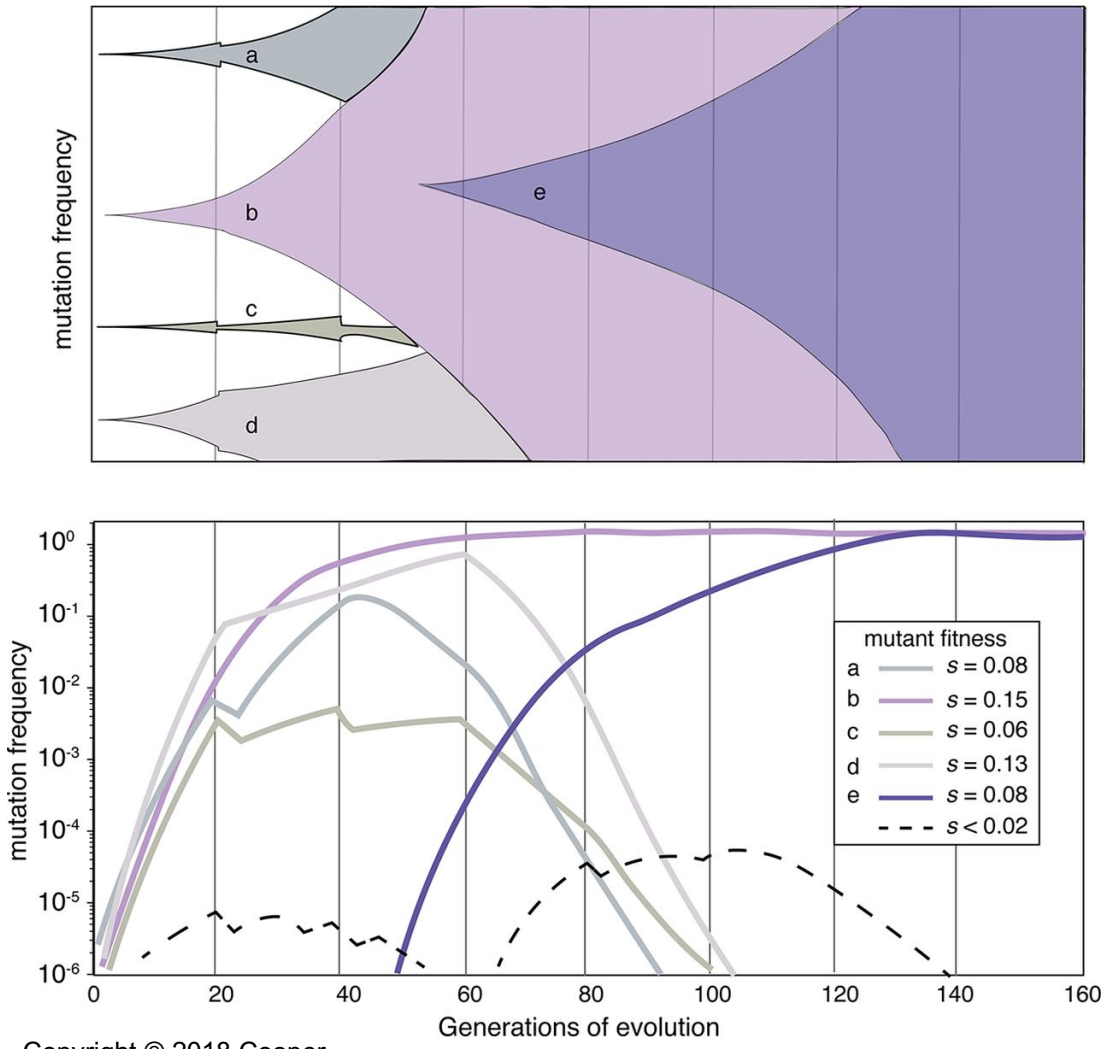

Figure 53: Representation of mutation frequency dynamics

Top figure shows how 4 mutant lineages adapt, with the most fit (b) eventually coming to fixation. A subsequent mutation creates a further lineage (e) that later comes to fixation.
Bottom figure shows fluctuations in mutant fitness, s, and how mutation frequency must rise by several orders of magnitude prior to detection and fixation. In this hypothetical experiment, a sample of a population is passaged multiple times: these transfer induced bottlenecks randomly alter the frequency of lineages. The dotted line highlights less frequent mutants that did not increase in frequency to a detectable level. In the context of the biofilm derived variants of *P. aeruginosa* and *S. aureus*, unique, low frequency mutations like this could have been outcompeted and subsequently not detected when harvested after 14 days.

5.4.5 Sequencing of Clonal Isolates Revealed No Difference in Mutation Rates Between Single and Dual Species Biofilms

By applying the Luria-Delbrück fluctuation test to co-culture biofilms, (Chapter 4), it was implied that *S. aureus* possessed a higher rate of mutation when in co-culture with *P. aeruginosa* compared to biofilm mono-culture. Higher rates of mutation have been linked to increased genomic diversity[369]. However, following sequencing, no difference in mutation frequency was observed between variants isolated from single or dual species biofilms, providing further evidence that the mutational dynamics within bacterial populations are perhaps more complicated than they first appear.

While unexpected, this discrepancy can be explained. Firstly, the culture conditions between biofilms used in the fluctuation tests and the flow cell biofilms were considerably different. The former were cultured at 37°C, 50 rpm for 24 hours in polystyrene 6 well plates, while the latter were cultured at room temperature with continuous flow for 14 days on glass. The large number of variables between the two culture conditions may mean the results are not immediately comparable. Furthermore, mutation rates can evolve over time. A 2018 study has shown that *E. coli* populations with very high mutation rates evolved lower mutation rates after 3000 generations[369]. Similar dynamics may have occurred for *S. aureus* during co-culture. For example, the mutation rate at 24 hours may have been elevated, but at an unknown point over the 14 day time course, it may have decreased (or increased in single species biofilm cultures), resulting in similar endpoint genetic profiles. Furthermore, while the rate of mutation may have increased, the increased potential for mutants will only be relevant if they fix within the population.

In addition, while the use of genome sequencing to measure mutation rates is theoretically the most accurate approach, if only clonal isolates are used, as per this chapter, only a small fraction of the population is measured. By comparison, the Luria-Delbrück fluctuation test accounts for the entire population, albeit at one genomic locus. This discrepancy may account for the observed differences. For an improved genomic comparison, a large number of whole biofilm populations would need to be sequenced and analysed.

The Luria-Delbrück fluctuation test employed in Chapter 4 specifically measured the rate of mutation of spontaneous rifampicin resistance, which is typically associated with mutations in *rpoB*[197]. Interestingly, no mutations in *rpoB* were identified in any of the sequenced isolates, which is unexpected, particularly if this gene can be relied on as a

marker for spontaneous mutation. Mutations in *rpoB* have previously been linked to decreased bacterial fitness in multiple studies[370–373], so if these mutant lineages occurred during earlier stages of biofilm growth, they may have been outcompeted following 14 days of culture.

5.4.6 Conclusions, Experimental Limitations and Future Work

The findings of this chapter demonstrate that extended single and dual species biofilm culture of *P. aeruginosa* and *S. aureus* can facilitate the emergence of phenotypic and genotypic variants. These variants can harbour characteristics that alter their virulence and propensity for chronic infection such as altered growth rates, ability to form biofilms and antimicrobial susceptibilities. Crucially, antimicrobial susceptibility can be affected in the absence of antimicrobial selection. Genomic analysis of these variants has identified regions of parallel evolution shared across single and dual species biofilms which could be important targets for future research into biofilm control. However, common phenotypic or genomic traits to distinguish isolates from single or dual species biofilms were not identified.

A major limitation of this chapter was the limited number of identical biofilm populations utilised. For each condition, only two biofilm populations were cultured. This was suitable for identifying general genomic mutations that occurred across all culture conditions (such as the intergenic SNP following *osmC* in all 36 isolates of *S. aureus)* but was not sufficient when looking within a single group, such as only dual species biofilms, without antimicrobial treatment. This limitation was particularly apparent if a mutation occurred at low frequency and/or was present in only one biological replicate, such as the mutation identified in *walK* of SAV9 and *walR* of SAV22. When considering rare mutations, this effect is compounded by the use of only 3 colonies per population because only a small subset of the population was sampled. Including more population replicates, as well as more colonies from each population, would address this concern.

The use of single colonies greatly limited the genotypes available for study and may have prevented the detection of rare alleles. In addition, the use of selective agar may have functioned as an additional selective bottleneck upon the biofilm population, reducing the diversity available for study. The use of selective agar may explain the limited phenotypic variation observed for *S. aureus*, although a study by Kipp *et al* showed that BPA should be suitable for the isolation of *S. aureus* small colony variants[374]. It is also possible that *S. aureus* variants were present following culture on BPA but reverted to a wild type

morphology following sub-culture on TSA plates. However, previous studies have shown that SCVs and other variants of *S. aureus* can grow successfully on TSA plates[87,146,257]. As such, if variants were plated onto the TSA, I would expect them to grow and maintain their phenotype.

Genotypic differences were also limited, with little difference in the evolutionary trajectories of variants derived from single and dual species biofilms. It is possible that the differential factor separating isolates evolved within a single or dual species biofilm is the abundance of genotypes rather than the distinct genomic differences. A population level analysis would provide a more accurate overview of these different allele frequencies, including rare genetic variants[89]. By incorporating additional sacrificial populations, thereby introducing a longitudinal element to the experiment, it would be possible to measure how allele abundance fluctuates over time.

There are two ways in which biofilm populations could be directly harvested and sequenced without the use of selective agar and these approaches, in theory, could be applied to biofilm co-culture. If the species were not separated prior to DNA extraction, the population could be sequenced and the reads filtered during post-processing[154]. However, regions of high similarity between species would be lost. The use of long read sequence technologies, such as Oxford Nanopore, or PacBio, could mitigate this as they would allow for improved resolution in repetitive and high similarity regions, as well as improved insight into structural arrangements of genes, aiding alignment to species specific reference genomes[375]. For example, consider three genes that are identical between two species, except for their arrangement within the chromosome. Long read sequencing could resolve the structural arrangement by sequencing all three genes in one read, which would, in this hypothetical example, allow for species separation without the use of selective agar.

Alternatively, bacterial species could be separated prior to DNA extraction, using techniques such as immunomagnetic separation. This technique uses species specific antibodies, which can be isolated from a mixed population with magnetic beads. This strategy has been successfully applied to the separation of *E. coli* from a dual species biofilm co-culture of *E. coli* and *Stenotrophomonas maltophila* for downstream microarray transcriptome analysis[376].

Limitations of sequencing aside, numerous genes were identified in variants of *P. aeruginosa* and *S. aureus* that could be important targets for biofilm control and

regulation of bacterial virulence, such as *dipA* in *P. aeruginosa* and *greA* in *S. aureus*. Furthermore, several hypothetical and intergenic regions were also frequently mutated compared to the ancestral wild type of either species. However, as these mutations were not exclusively associated with particular phenotypes, further investigation into the role of each gene would be required. The first stage would be to confirm mutations, either by targeted Sanger resequencing or by PCR, which could determine whether a gene product was truncated or extended due to deletions, nonsense mutations or insertions. Once a mutation was confirmed, the next stage would be to generate a knock out mutant to try and understand the role that the particular genomic region has on the bacterial cell. This could then be paired with additional phenotyping such as RNA-seq or quantitative proteomics to elucidate how the genomic region of interest altered the cell on a global level.

Another general issue with the work performed in this chapter focuses on the phenotyping experiments performed on the biofilm derived variants. Due to time limitations, growth rates and biofilm formation of the 72 variants were assessed using optical density and crystal violet-based assays, respectively. However, these measurements do not account for actual cell numbers. Both measurements could have been distorted by differing production of EPS rather than a change in actual cell numbers. Hence, incorporating CFU data into these assays would increase their accuracy. Furthermore, culturing and imaging biofilms formed by each variant over a time course using CLSM would provide further information into how the variants differ from the ancestral wild type. It would also have been desirable to perform more in-depth antimicrobial susceptibility testing, incorporating more antimicrobial classes such as aminoglycosides and β-lactams into the assays. Finally, if the variants could be tagged, for example with a constitutive GFP marker, the relative fitness of each variant compared to the ancestral wild type could be determined by culturing the two in competition and measuring the fluorescence profile of the culture.

A related phenotyping issue specifically refers to the calculation of the MIC for each variant. When performing MIC experiments, there is a known error of one two-fold dilution in either direction of the actual MIC; this error rate is even accounted for in clinical susceptibility testing[377,378]. As such, it is possible that there were no genomic determinants for altered antimicrobial susceptibility because the MIC had been calculated incorrectly and there were no associated mutations to find.

As of writing, this chapter describes the only dual species model of *P. aeruginosa* and *S. aureus* grown for 14 days in a flow cell, with the purpose of performing endpoint whole

genome sequencing of isolates. A flow model was chosen to ensure biofilms were granted a constant supply of nutrients and antimicrobials throughout the course of the experiment. However, this is not representative of a biofilm *in vivo,* not least because growth under flow is not common. Furthermore, issues regarding the use of artificial substrata, as well as only two bacterial species (discussed in Chapter 4), still apply.

The absence of mutations commonly associated with ciprofloxacin resistance suggests that the concentrations utilised in this chapter may have been outside the required selective concentration. In a clinical situation, the concentration of antimicrobials will typically surge at initial administration, before tapering off over time[376]. Consequently, an improvement to the experimental protocol that may grant a more realistic insight into the evolution of biofilms under antimicrobial pressure, would have been to treat biofilms with a clinically utilised concentration of antimicrobials periodically, rather than with a constant sub-inhibitory concentration.

In conclusion, this chapter has demonstrated that biofilm growth can facilitate the emergence of genotypic and phenotypic variants. I have discussed how a flow cell system can be used to culture both single and dual species biofilms of *P. aeruginosa* and *S. aureus* and also discussed the limitations associated with such an approach. Whole genome sequencing showed that parallel evolution can occur across various regions of the bacterial genome, encompassing metabolic, virulence and resistance determinants. However, when sampled after 14 days, no major genomic differences were identified between variants from single or dual species culture. Mutated genes of interest in *P. aeruginosa* included regulators of biofilm formation, such as *dipA* and *lipH,* regulators of stress responses such as *trxB,* as well as numerous uncharacterised and intergenic elements. For *S. aureus*, mutations in the transcription factors *whiA* and *greA* appeared common, which may lead to drastically altered expression profiles. Consistent sub-inhibitory treatment with HT61 caused adaptation in intergenic regions of the phenazine biosynthesis operon in *P. aeruginosa* and mutations in *graS* and *fmtC* in *S. aureus.* The latter two genes have previously been implicated in the modulation of the cell envelope. However, the precise implications of these mutations will require further investigation. Understanding the role of these genes and associated mutations could be important for the management of biofilm associated infections as well as the design of new antimicrobial compounds.

Chapter 6

Conclusions and Future Work

6 Conclusions and Future Work

6.1 Conclusions and Chapter Synthesis

Since the discovery and commercialisation of penicillin, antibiotic use and the prevalence of antibiotic resistance, has been increasing[15]. This has resulted in the emergence of resistant bacterial pathogens (so-called "super-bugs") which, thanks to a myriad of mechanisms, render current antimicrobial strategies ineffective. This ultimately leads to chronic, untreatable infections[14,20]. Contributing to disease chronicity are multicellular, sessile, bacterial communities, otherwise referred to as biofilms[6,7]. Biofilms exhibit numerous tolerance mechanisms which can facilitate bacterial survival against antimicrobial treatment, including but not limited to, the presence of slowly and non-dividing bacterial cells[6,7]. Biofilms also act as hubs of genetic diversity, harbouring multiple lineages and promoting the emergence of novel genotypes[8,9,82,84,89]. Furthermore, biofilms are typically comprised of more than one bacterial species. This can increase genetic diversity even further as well as alter resistance and virulence profiles[145,306].

When the aforementioned factors are considered, two points become clear. Firstly, there is a need for novel antimicrobial treatment strategies to effectively combat AMR bacteria. Secondly, there is a requirement to understand how biofilms, and associated interspecies interactions contribute to the emergence of novel genotypes, especially if those genotypes have the potential to spread AMR. By utilising the novel antimicrobial, HT61, both of these points have been investigated within this thesis. Using a combination of standard and newly adapted microbiological techniques as well as cutting edge proteomic and genomic methods, I have been able to provide clarity towards both the mechanism of action of HT61 and explore how biofilm growth and antimicrobial treatment affects the evolutionary trajectories of *P. aeruginosa* and *S. aureus*. The results from this thesis could inform the development of future antimicrobial compounds.

HT61 has previously shown to be effective against non-dividing bacterial cells[11,12], which can comprise a significant sub-population within biofilms contributing to tolerance[7]. With this in mind, Chapter 2 explored the effect of HT61 towards single species biofilms of numerous clinically relevant bacterial species. Against single species biofilms of *Staphylococcal spp.,* HT61 proved to be more effective than vancomycin although it was considerably less effective when used to treat Gram-negative species. High resolution SEM imaging of *S. aureus* and *P. aeruginosa* biofilms suggested a mechanism of action

focussed on the cell envelope, with apparent rupturing and blebbing in each species, respectively.

To investigate the mechanism of action of HT61 further, Chapter 3 described a label-free UPLC/MS_E proteomic strategy to study the cellular response of planktonic and biofilm cultures of *S. aureus* following treatment with sub-inhibitory and inhibitory concentrations of HT61. This work identified profound metabolic differences between early and late stationary phase planktonic growth, as well as biofilm cultures. Notably, biofilm growth was linked to increased arginine catabolism and activation of the ADI pathway and in late stationary phase planktonic cultures, proteins linked to cell wall biosynthesis were upregulated. Analysis of early stationary phase planktonic cultures (and to a lesser extent, biofilm cultures) revealed that HT61 treatment induced components of the cell wall stress stimulon and *dcw* cluster, while in late stationary phase planktonic cultures, autolytic enzymes were decreased in expression. Taken together, these findings suggest that HT61 exerts its killing effect by interfering with the integrity and maintenance of the bacterial cell wall, similar to other membrane active antibiotics, such as daptomycin[275]. The heightened efficacy towards late stationary phase cells is likely the result of dose-dependent kinetics mediated by increased accumulation of HT61 within the cell membrane, due to its increased negative charge[13]. Further work, such as TPP[277], would be required to understand the precise interactions that are occurring and whether HT61 directly interacts with cell wall components or whether the physical stress on the membrane and cell envelope is sufficient to induce cell lysis.

Following initial phenotypic studies of single species cultures, the natural progression was to assess the efficacy of HT61 against a more complex multispecies consortium to better represent the conditions of a clinical infection. Chapter 4 described the successful development of a dual species biofilm co-culture of *P. aeruginosa* and *S. aureus* that could be maintained over the course of 240 hours. Successful biofilm co-culture was influenced by both the choice of *P. aeruginosa* strain, as well as media composition, with the availability of iron (in the form of the exogenous hemin), proving to be particularly influential. As per previous studies, the antimicrobial susceptibility of the bacterial species within a dual species model was altered compared to single species culture[135,145,147,148]. HT61 was more effective at treating *S. aureus* within a biofilm co-culture, compared to a single species culture, with a 4-fold reduction in biofilm MBC. This could have been due to the comparatively lower cell density of *S. aureus* but could also be linked to slower *S. aureus* growth during co-culture with *P. aeruginosa*[145,146]. Furthermore, this chapter

describes the first application of the classic Luria-Delbrück fluctuation test to biofilm cultures, demonstrating that biofilm co-culture has the potential to greatly increase the bacterial mutation rate compared to planktonic cultures. This finding could have important implications for bacterial evolvability and the emergence of AMR.

The finding that mutation rates could be affected by biofilm co-culture informed the work of Chapter 5, which aimed to understand the differences in bacterial evolution between species grown within a single or dual species biofilm, both with and without antimicrobial pressure. Previous planktonic assays failed to obtain resistance to HT61[11] therefore if mutation rates were increased in biofilms, particularly for *S. aureus* during co-culture, it was hypothesised that biofilms could act as a catalyst to accelerate the emergence of HT61 resistance. Following 14 days of growth for both single and dual species biofilms of *P. aeruginosa* and *S. aureus,* a total of 72 colonies were isolated for phenotyping and whole genome sequencing. Alongside phenotypic changes many mutations were identified in isolates of both bacterial species, encompassing parallel SNPs and INDELs. However, analysis of mutation frequencies suggested no difference in mutation rates between isolates taken from single or dual species biofilms. Furthermore, it was not possible to distinguish whether an isolate was derived from a single or dual species biofilm based on an associated genotype. While these results were surprising, there are explanations. It is possible that the frequency of mutant lineages did increase in co-culture biofilms; however, by 14 days of culture they may have been outcompeted. Consequently, the frequency of mutations across all culture types may have "normalised" to only include those with the highest relative fitness. As discussed in Chapter 5, introducing a longitudinal element to the experiment may address this because less fit mutant genotypes would be analysed before they are outcompeted. Alternatively, the use of colony sequencing in this chapter, rather than population level sequencing may mean that genotypes were simply missed and not sequenced. This could explain both the lack of perceived differences in both mutation rates and genotypic signatures between isolates from single and dual species biofilms.

In terms of the genomic regions that were under selection, parallel evolution occurred across a number of regions within species. In both *P. aeruginosa* and *S. aureus,* a number of these mutations occurred in intergenic regions, which may suggest alterations in gene regulation opposed to alterations in a specific gene product[337,363]. These regions are typically ignored compared to mutations found in coding regions, however this work suggests selection within intergenic regions may be important in the context of biofilm evolution. As for understanding bacterial adaptation to HT61, genotypic evidence was

limited. However, several colonies of *S. aureus* derived from HT61 treated biofilms harboured mutations in genes associated with the regulation of cell wall biosynthesis (such as *graS* and *walR*) and membrane charge (*fmtC)*. These data complement the results of Chapter 2 suggesting both membrane and cell wall associated processes may be responsible for the action of HT61. The identification of genomic regions, including intergenic regions, which were under selection during biofilm growth may provide future targets for investigation that could be ultimately manipulated for the purposes of biofilm and infection control.

Over the entire course of this thesis, there has been no indication of resistance or adaptation to HT61. This could be because HT61 directly exerts its mechanism of action by binding to lipid components[13], which are less likely to undergo mutation. A published example is of the antimicrobial, teixobactin[5]. Teixobactin binds to highly conserved motifs of lipid II and lipid III, precursors of peptidoglycan and teichoic acid, respectively, leading to the inhibition of cell wall synthesis[5]. The authors suggest that targeting these motifs represents an "Achilles heel for antibiotic attack" and that resistance development is extremely unlikely[5]. It is possible that a similar mechanism is in place for HT61, making it essentially evolution-proof. However, resistance to other membrane active compounds such as daptomycin and colistin has occurred[162,360], which suggests it would be naïve to assume adaptation to HT61 cannot occur.

6.2 Future Work

Each chapter within this thesis has focussed on distinct bodies of work, albeit with an overarching narrative studying the effect of the novel antimicrobial HT61 within biofilm models. As such, in-depth critiques can be found within the Discussion sections of the respective results chapters. However, there are certain general limitations, both within chapters, and across the thesis as a whole which will be addressed here.

Even though HT61 was shown to be more effective at treating stationary phase planktonic cells, it is impossible to determine whether its effectiveness against biofilms, (particularly of *S. aureus* and *S. epidermidis*), is a result of this characteristic. In other words, it is difficult to discern whether HT61 is effectively killing the non-dividing biofilm sub-populations or simply functioning like a "typical" antimicrobial. Performing antimicrobial susceptibility testing on biofilms that are more mature (i.e. grown for longer than 72 hours), or have been nutrient limited by reducing the frequency of media exchanges, (thereby increasing the number of stationary phase cells), could help inform this.

It would also be interesting to investigate the effectiveness of HT61 against the archetypal non-growing persister cells, for *S. aureus* as well as other bacterial species. Isolation of persister cells can be performed by inducing activation of the SOS response using high concentrations of ciprofloxacin[379]. Firstly, planktonic cultures are grown to stationary phase prior to treatment with a high concentration of ciprofloxacin. The surviving cells comprise the persister population and can be subjected to further testing[379]. Certain membrane active antimicrobial peptides have recently been shown to be effective at the eradication of *P. aeruginosa* and *S. aureus* persister cells[380]. However, within the same study, daptomycin was shown to be ineffective at treating persister cells of *S. aureus*. This suggests that the ability for an antimicrobial to successfully treat persister cells is more nuanced and complex than simply determining whether or not it interacts with the cell membrane. The improved efficacy of HT61 against stationary phase cells is predicted to be a result of greater membrane accumulation due to an increase in anionic charge density within the cell membrane[13]. Persister cells are physically distinct from stationary phase cells[380] and it is likely that HT61 will prove ineffective unless the persister cell membrane content resembles that of stationary phase cultures. As such, analysis of the membrane composition of persister cells, along with biofilm populations could be useful in predicting the efficacy of membrane active antimicrobials such as HT61.

An interesting observation in both Chapters 2 and 3 was that biofilms of various species presented with a degree of biofilm tolerance to HT61. In Chapter 2, this was demonstrated by an increase in MBC for biofilm cultures of *S. epidermidis* and *A. baumannii*, while in Chapter 3, biofilms of *S. aureus* presented with a limited proteomic response following HT61 treatment compared to planktonic cultures. In biofilms of *S. epidermidis*, eDNA has been shown to sequester vancomycin imbuing tolerance[115]. A similar mechanism could function to impedes HT61 across the biofilm EPS. By fluorescently tagging HT61 it would be possible to track its movement throughout a biofilm and determine if it is accumulating within particular regions or is being sequestered by external factors such as DNA or even external lipid products, particularly if they are negatively charged.

While largely ineffective against the Gram-negative species tested, HT61 was shown to be effective against *A. baumannii* in certain instances. Planktonic susceptibility was similar to that of *S. aureus* UAMS-1 and while HT61 was less effective against stationary phase cultures, a biofilm MBC was obtained. As such, future investigations into the membrane composition of multiple Gram-negative species would be interesting to understand whether

differences in HT61 efficacy can be attributed to membrane structure in these species. For example, do cells of *A. baumannii* possess a membrane with a greater negative charge than *P. aeruginosa*, thereby explaining the improved efficacy of HT61? SEM of *P. aeruginosa* PAO1 biofilms treated with a high concentration of HT61 showed considerable membrane blebbing within the cells. This suggests a mechanism of action similar to that observed in *S. aureus*. As such, future work investigating the proteomic response of Gram-negative species to HT61 would also provide useful information, particularly if processes such as the cell wall stimulon are also implicated.

The second half of this thesis described the development of a dual species biofilm model of *P. aeruginosa* and *S. aureus* and attempted to investigate the impact of co-culture on bacterial evolution. Regarding the dual species model, future work should attempt to understand the factors that facilitate co-culture of these species. Whole genome comparisons of *P. aeruginosa* PAO1 and PA21 identified many genomic differences but due to time constraints, I was not able to investigate these differences further. By creating knockout mutants of particular genes, it may be possible to determine which factors are important for co-culture and biofilm colonisation. This could then inform the development of improved models, which utilise a greater number of bacterial species, or incorporation of *ex vivo* elements[312,314].

Application of the fluctuation test to the biofilm co-culture of *P. aeruginosa* and *S. aureus* suggested that the short-term mutation rate of *S. aureus* increases dramatically compared to rates calculated in single species biofilms. This is predicted to be a result of stress induced mutagenesis, possibly because *P. aeruginosa* is utilising *S. aureus* as a source of exogenous iron[149]. To investigate this, additional fluctuation tests could be performed with differing concentrations of exogenous iron (in the form of hemin, as well as other iron donors). If the mutation rate of *S. aureus* is higher in co-cultures with a lower concentration of exogenous iron, it could provide evidence that the increased mutation rate is associated with increased iron scavenging by *P. aeruginosa* (less iron results in more *P. aeruginosa* mediated *S. aureus* lysis, leading to higher *S. aureus* mutation rates). Linking this experiment to an expression-based study, such as RNA-seq or qPCR to determine changes in expression of *P. aeruginosa* genes encoding iron chelating/*S. aureus* suppression proteins such as *pqsA* and *pqsH,* would also be beneficial[307]. Alternatively, the mutation rate of *S. aureus* could be measured during growth in the presence of *P. aeruginosa* exoproducts to identify whether the secreted products in isolation are able to increase *S. aureus* mutation rates.

A related experiment would be to investigate how the mutation rates of each species evolved over time. If the mutation rate of *S. aureus* varied during the course of biofilm co-culture with *P. aeruginosa*, this could explain why mutation frequency was identical in isolates derived from single and dual species biofilm populations.

As for Chapter 5, which assessed the evolution of *P. aeruginosa* and *S. aureus* following biofilm culture, there are several major limitations that would need to be addressed in future investigations. The most obvious improvement would be to sequence more biofilm derived colonies. A total of 240 colonies were actually isolated (120 of each species) but due to financial constraints, only a limited selection (36 of each species) could be sequenced. By analysing the remaining colonies, it could be possible to identify missed genomic markers, such as genotypic signatures between single and dual species biofilm derived isolates. However, if this work was to be repeated, a greater emphasis should also be placed on using more replicate populations as well. Increasing replicates in this manner makes the identification of parallel evolution and areas under strong selection far easier because the populations, by definition, are isolated. As such, if a genotype occurs across multiple populations it is easier to be certain that it is true example of parallel evolution.

A secondary aim of Chapter 5 was to investigate whether resistance to HT61 could be obtained. Unfortunately, and similar to previous planktonic studies[11], this was not possible. In previous publications, selection for resistance was attempted using a multiple passage experiment, maintaining the concentration of HT61 at a value half the MIC[11]. Within this thesis, the concentration of HT61 was maintained at a quarter of the calculated MIC. In both instances, this may not have exerted sufficient selective pressure. A simple modification in future investigations would be to perform a passage experiment with a steadily increasing concentration of HT61, thereby facilitating the evolution of resistance in a stepwise manner[193,381].

A notable facet that was not explored in this thesis was the impact of bacterial communication and HGT on evolution. If this work was to be expanded, the impact of QS molecules on evolution could be determined by experimentally evolving single species communities in the presence of the exogenous secretions of another species. Rates of plasmid exchange could be measured in both single and dual species biofilms to identify whether community structure influences the dissemination of plasmid-borne traits, such as AMR mechanisms.

6.3 Concluding Statement

This project aimed to characterise the effect of the novel antimicrobial HT61 on clinically relevant bacterial biofilms in order to understand its mechanism of action. By combining numerous scientific methodologies, it has been shown that HT61 appears to influence components of the cell wall stimulon in *S. aureus*, leading to membrane permeabilisation. A reproducible dual species biofilm model of *P. aeruginosa* and *S. aureus,* which is more clinically relevant than single species biofilm cultures, was developed and HT61 was shown to retain its efficacy towards *S. aureus*. Investigations into bacterial evolvability during co-culture suggested that mutation rates are increased during biofilm growth, which could preclude the rapid evolution of AMR mechanisms. Whole genome sequencing of biofilm derived isolates of *P. aeruginosa* and *S. aureus* highlighted numerous regions that were under selection that could be targets for therapeutic intervention. While resistance to HT61 was not obtained, mutations in genes associated with maintenance of the cell envelope were linked to its use.

While there are limitations to the work, this thesis has emphasised the importance of research into multi-species biofilm communities and presented important preliminary findings regarding the efficacy of HT61. By combining both phenotypic and genotypic datasets, the findings of this thesis could be used to inform the development of future biofilm focused antimicrobials by providing insight into bacterial evolution alongside bacterial pathways and processes that can be exploited. Understanding mechanisms of antimicrobial action alongside evolution within biofilms will prove critical in developing new compounds to tackle chronic infection and limit the emergence of AMR.

Chapter 7

Appendices

7 Appendices

7.1 Chapter 2

7.1.1 Effect of HT61 on Early Biofilm Development

Below are the analysed data for the planktonic data sets taken at each time point. They detail the effect of HT61 on the surrounding planktonic suspension.

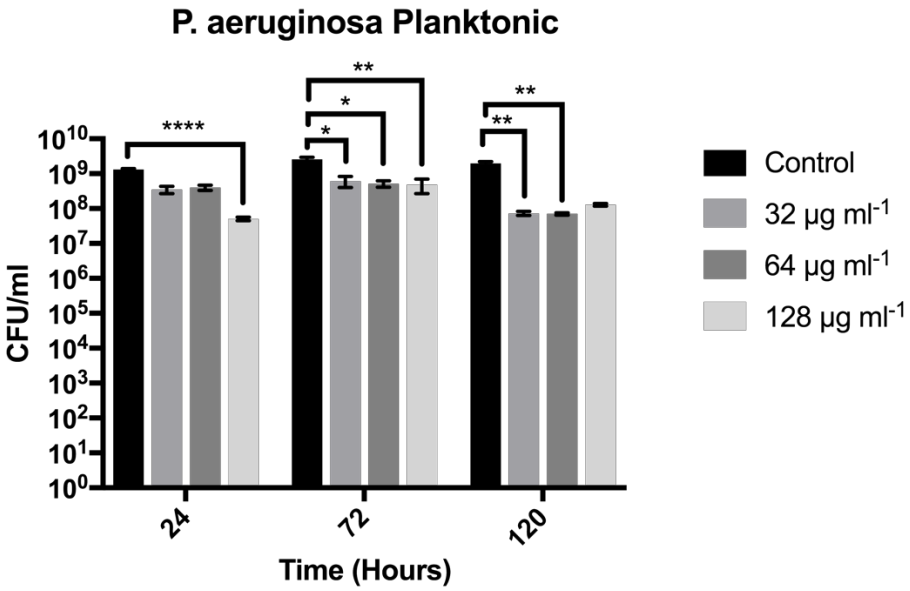

Figure S 1: Effect of HT61 on the planktonic suspension during early biofilm development of *P. aeruginosa* PAO1. Error bars represent standard error of the mean (n=6 from 3 experimental repeats). Statistical significance calculated using Kruskal-Wallis test, with Dunn's multiple comparison within each time point. Kruskal Wallis *p* values determining variation in medians within each time point: 24 hours p = 0.0002, 72 hours p = 0.0047, 120 hours p = 0.0004. Asterisks state significance values following post-hoc Dunn's multiple comparison. *: $p < 0.05$, **: $p < 0.01$, ****: $p < 0.0001$.

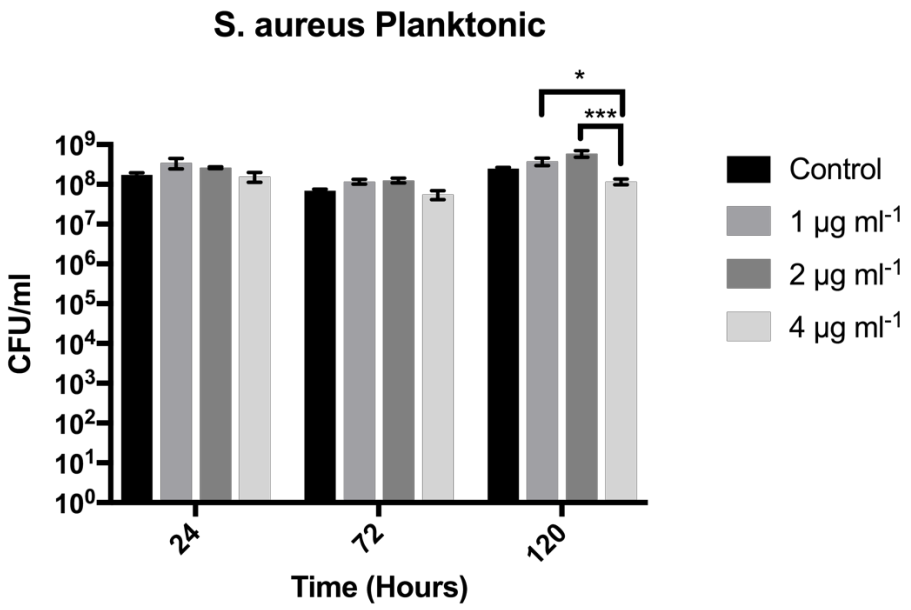

Figure S 2: Effect of HT61 on the planktonic suspension during early biofilm development of *S. aureus* UAMS-1. Error bars represent standard error of the mean (n=6 from 3 experimental repeats). Statistical significance calculated using Kruskal-Wallis test, with Dunn's multiple comparison within each time point. Kruskal Wallis p values determining variation in medians within each time point: 24 hours $p = 0.1262$, 72 hours $p = 0.0154$, 120 hours $p = 0.0007$. Asterisks state significance values following post-hoc Dunn's multiple comparison. *: $p < 0.05$, ***: $p < 0.001$.

7.2 Chapter 3

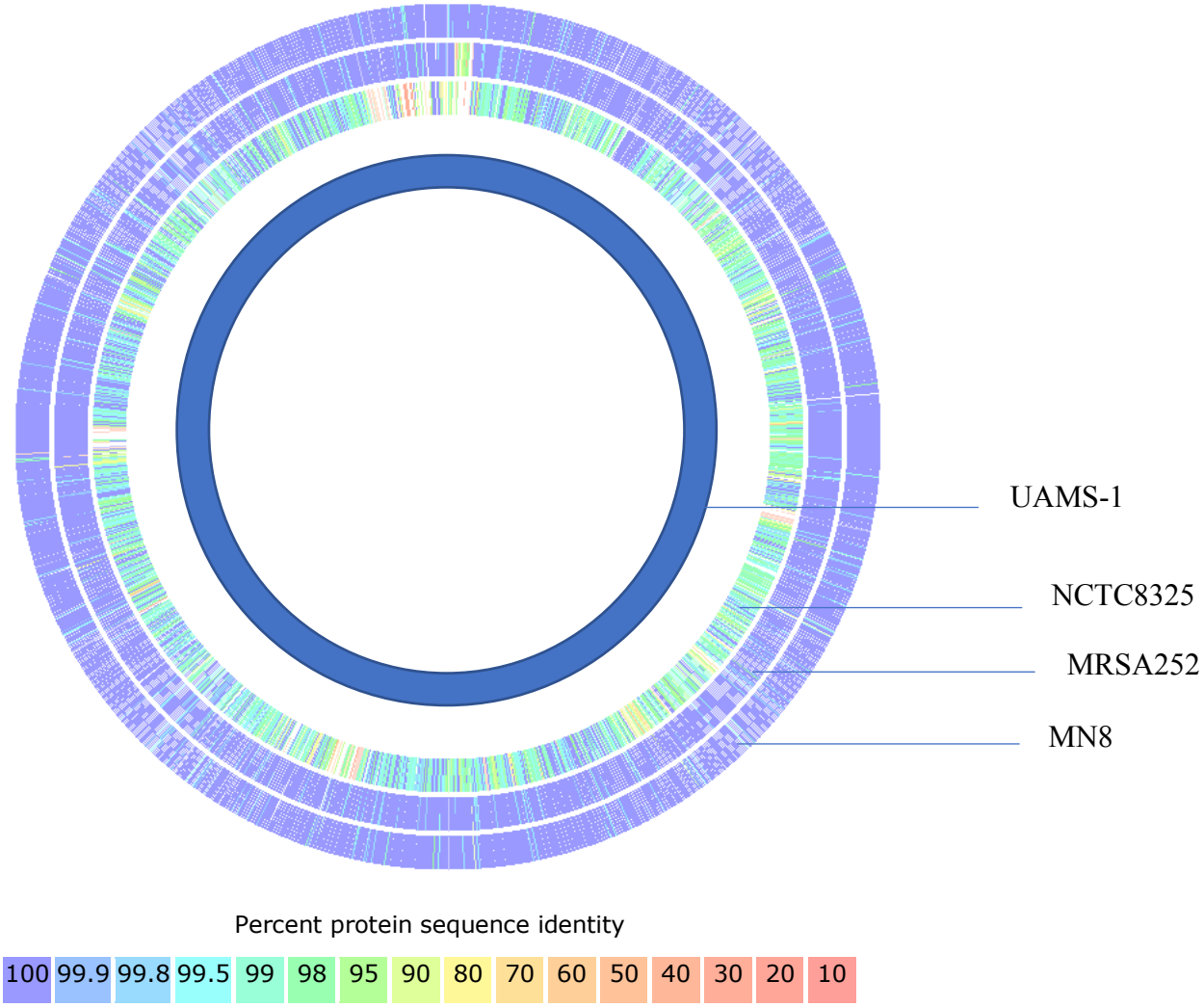

Figure S 3: Genome comparison utilised to choose reference proteome. *S. aureus* MN8 had the highest similarity.

7.3 Chapter 4

7.3.1 Kruskall Wallis with Dunn's Multiple Comparison Results

Strain CFU Comparison – Single Species Biofilms, Different Hemin Concentrations				
Bacterial Species	**Time Point**	**Media Composition**	**Adjusted *p* Value (Holm-Sidak Correction)**	**Summar**
***P. aeruginosa* PAO1 vs *P. aeruginosa* PA21**	**24 hr**	No Hemin	**1.34×10^{-6}**	****
		2 μM Hemin	**4.09×10^{-8}**	****
		20 μM Hemin	**1.21×10^{-6}**	****
		100 μM Hemin	**1.41×10^{-11}**	****
	72 hr	No Hemin	0.1121	NS
		2 μM Hemin	**0.0218**	*
		20 μM Hemin	0.9835	NS
		100 μM Hemin	0.9165	NS
	168 hr	No Hemin	0.2266	NS
		2 μM Hemin	0.7075	NS
		20 μM Hemin	0.8090	NS
		100 μM Hemin	**0.0005**	****
	240 hr	No Hemin	0.1865	NS
		2 μM Hemin	0.7075	NS
		20 μM Hemin	0.2628	NS
		100 μM Hemin	0.5159	NS
***S. aureus* UAMS-1 vs *S. aureus* LAC**	**24 hr**	No Hemin	0.4222	NS
		2 μM Hemin	0.2932	NS
		20 μM Hemin	0.3429	NS
		100 μM Hemin	0.1423	NS
	72 hr	No Hemin	0.5993	NS
		2 μM Hemin	0.0906	NS
		20 μM Hemin	0.3429	NS
		100 μM Hemin	0.8657	NS
	168 hr	No Hemin	**0.0006**	****
		2 μM Hemin	**0.0203**	*
		20 μM Hemin	**0.0022**	**
		100 μM Hemin	**0.0066**	**
	240 hr	No Hemin	**3.8×10^{-9}**	****
		2 μM Hemin	**1.20×10^{-9}**	****
		20 μM Hemin	**2.6×10^{-6}**	****
		100 μM Hemin	**2.5×10^{-6}**	****

P. aeruginosa PA21 and *S. aureus* UAMS-1 Biofilm Co-Culture				
Bacterial Species	**Time Point**	**Media Comparison**	**Adjusted *p* Value**	**Summary**
P. aeruginosa PA21	**24 hr**	No Hemin vs 2 uM	> 0.9999	NS
		No Hemin vs 20 μM	> 0.9999	NS
		No Hemin vs 100 μM	> 0.9999	NS
		2 μM vs 20 μM	0.1106	NS
		2 μM vs 100 μM	0.8310	NS
		20 μM vs 100 μM	> 0.9999	NS
	72 hr	No Hemin vs 2 uM	0.0003	***
		No Hemin vs 20 μM	0.0615	NS
		No Hemin vs 100 μM	0.0001	***
		2 μM vs 20 μM	0.8701	NS
		2 μM vs 100 μM	> 0.9999	NS
		20 μM vs 100 μM	0.4937	NS
	168 hr	No Hemin vs 2 uM	> 0.9999	NS
		No Hemin vs 20 μM	> 0.9999	NS
		No Hemin vs 100 μM	> 0.9999	NS
		2 μM vs 20 μM	> 0.9999	NS
		2 μM vs 100 μM	> 0.9999	NS
		20 μM vs 100 μM	0.8337	NS
	240 hr	No Hemin vs 2 uM	> 0.9999	NS
		No Hemin vs 20 μM	0.0541	NS
		No Hemin vs 100 μM	0.1780	NS
		2 μM vs 20 μM	0.2350	NS
		2 μM vs 100 μM	0.6246	NS
		20 μM vs 100 μM	> 0.9999	NS
S. aureus UAMS1	**24 hr**	No Hemin vs 2 uM	> 0.9999	NS
		No Hemin vs 20 μM	0.0095	**
		No Hemin vs 100 μM	0.8184	NS
		2 μM vs 20 μM	0.0124	*
		2 μM vs 100 μM	0.7016	NS
		20 μM vs 100 μM	< 0.0001	****
	72 hr	No Hemin vs 2 uM	> 0.9999	NS
		No Hemin vs 20 μM	0.0013	**
		No Hemin vs 100 μM	0.1092	NS
		2 μM vs 20 μM	0.0092	**
		2 μM vs 100 μM	0.3985	NS
		20 μM vs 100 μM	> 0.9999	NS
	168 hr	No Hemin vs 2 uM	> 0.9999	NS
		No Hemin vs 20 μM	0.0009	***
		No Hemin vs 100 μM	0.0218	*
		2 μM vs 20 μM	< 0.0001	****
		2 μM vs 100 μM	0.0031	**
		20 μM vs 100 μM	> 0.9999	NS
	240 hr	No Hemin vs 2 uM	> 0.9999	NS
		No Hemin vs 20 μM	< 0.0001	***
		No Hemin vs 100 μM	0.0297	*

P. aeruginosa PA21 and *S. aureus* AH1279 Biofilm Co-Culture				
Bacterial Species	**Time Point**	**Media Comparison**	**Adjusted *p* Value**	**Summary**
P. aeruginosa PA21	**24 hr**	No Hemin vs 2 uM	0.0272	*
		No Hemin vs 20 μM	> 0.9999	NS
		No Hemin vs 100 μM	0.4465	NS
		2 μM vs 20 μM	0.0411	*
		2 μM vs 100 μM	> 0.9999	NS
		20 μM vs 100 μM	0.5944	NS
	72 hr	No Hemin vs 2 uM	0.2156	NS
		No Hemin vs 20 μM	> 0.9999	NS
		No Hemin vs 100 μM	0.0165	*
		2 μM vs 20 μM	0.1366	NS
		2 μM vs 100 μM	< 0.0001	****
		20 μM vs 100 μM	0.0292	*
	168 hr	No Hemin vs 2 uM	0.3779	NS
		No Hemin vs 20 μM	0.8357	NS
		No Hemin vs 100 μM	0.6704	NS
		2 μM vs 20 μM	> 0.9999	NS
		2 μM vs 100 μM	> 0.9999	NS
		20 μM vs 100 μM	> 0.9999	NS
	240 hr	No Hemin vs 2 uM	> 0.9999	NS
		No Hemin vs 20 μM	> 0.9999	NS
		No Hemin vs 100 μM	0.1899	NS
		2 μM vs 20 μM	> 0.9999	NS
		2 μM vs 100 μM	0.0040	**
		20 μM vs 100 μM	0.1060	NS
S. aureus LAC	**24 hr**	No Hemin vs 2 uM	> 0.9999	NS
		No Hemin vs 20 μM	0.7185	NS
		No Hemin vs 100 μM	0.0003	***
		2 μM vs 20 μM	> 0.9999	NS
		2 μM vs 100 μM	0.0018	**
		20 μM vs 100 μM	0.0753	NS
	72 hr	No Hemin vs 2 uM	> 0.9999	NS
		No Hemin vs 20 μM	0.0041	**
		No Hemin vs 100 μM	0.0007	***
		2 μM vs 20 μM	0.0038	**
		2 μM vs 100 μM	0.0007	***
		20 μM vs 100 μM	> 0.9999	NS
	168 hr	No Hemin vs 2 uM	> 0.9999	NS
		No Hemin vs 20 μM	< 0.0001	****
		No Hemin vs 100 μM	0.0157	*
		2 μM vs 20 μM	0.0001	***
		2 μM vs 100 μM	0.0910	NS
		20 μM vs 100 μM	0.4190	NS
	240 hr	No Hemin vs 2 uM	> 0.9999	NS
		No Hemin vs 20 μM	0.0033	**
		No Hemin vs 100 μM	0.0013	**

P. aeruginosa PAO1 and *S. aureus* UAMS-1 Biofilm Co-Culture				
Bacterial Species	**Time Point**	**Media Comparison**	**Adjusted *p* Value**	**Summary**
P. aeruginosa PAO1	**24 hr**	No Hemin vs 2 uM	> 0.9999	NS
		No Hemin vs 20 μM	> 0.9999	NS
		No Hemin vs 100 μM	0.0527	NS
		2 μM vs 20 μM	> 0.9999	NS
		2 μM vs 100 μM	0.0067	**
		20 μM vs 100 μM	0.3001	NS
	72 hr	No Hemin vs 2 uM	0.4489	NS
		No Hemin vs 20 μM	0.2110	NS
		No Hemin vs 100 μM	> 0.9999	NS
		2 μM vs 20 μM	> 0.9999	NS
		2 μM vs 100 μM	0.0598	NS
		20 μM vs 100 μM	0.022	*
	168 hr	No Hemin vs 2 uM	> 0.9999	NS
		No Hemin vs 20 μM	0.0602	NS
		No Hemin vs 100 μM	0.1230	NS
		2 μM vs 20 μM	0.0025	**
		2 μM vs 100 μM	0.0065	**
		20 μM vs 100 μM	> 0.9999	NS
	240 hr	No Hemin vs 2 uM	> 0.9999	NS
		No Hemin vs 20 μM	0.0145	*
		No Hemin vs 100 μM	0.0318	*
		2 μM vs 20 μM	0.2428	NS
		2 μM vs 100 μM	0.4287	NS
		20 μM vs 100 μM	> 0.9999	NS
S. aureus UAMS1	**24 hr**	No Hemin vs 2 uM	0.0167	*
		No Hemin vs 20 μM	> 0.9999	NS
		No Hemin vs 100 μM	0.0139	*
		2 μM vs 20 μM	0.0095	**
		2 μM vs 100 μM	> 0.9999	NS
		20 μM vs 100 μM	0.0078	**
	72 hr	No Hemin vs 2 uM	0.0829	NS
		No Hemin vs 20 μM	0.2651	NS
		No Hemin vs 100 μM	0.0006	***
		2 μM vs 20 μM	> 0.9999	NS
		2 μM vs 100 μM	0.9201	NS
		20 μM vs 100 μM	0.3627	NS
	168 hr	No Hemin vs 2 uM	All values zero	
		No Hemin vs 20 μM	All values zero	
		No Hemin vs 100 μM	All values zero	
		2 μM vs 20 μM	All values zero	
		2 μM vs 100 μM	All values zero	
		20 μM vs 100 μM	All values zero	
	240 hr	No Hemin vs 2 uM	All values zero	
		No Hemin vs 20 μM	All values zero	
		No Hemin vs 100 μM	All values zero	

P. aeruginosa PAO1 and *S. aureus* AH1279 Biofilm Co-Culture				
Bacterial Species	**Time Point**	**Media Comparison**	**Adjusted *p* Value**	**Summary**
P. aeruginosa PAO1	**24 hr**	No Hemin vs 2 uM	> 0.9999	NS
		No Hemin vs 20 μM	> 0.9999	NS
		No Hemin vs 100 μM	0.1301	NS
		2 μM vs 20 μM	> 0.9999	NS
		2 μM vs 100 μM	0.2560	NS
		20 μM vs 100 μM	**0.0404**	*
	72 hr	No Hemin vs 2 uM	> 0.9999	NS
		No Hemin vs 20 μM	> 0.9999	NS
		No Hemin vs 100 μM	**0.0177**	*
		2 μM vs 20 μM	> 0.9999	NS
		2 μM vs 100 μM	**0.0071**	**
		20 μM vs 100 μM	**0.0001**	***
	168 hr	**No Hemin vs 2 uM**	**0.0340**	*
		No Hemin vs 20 μM	> 0.9999	NS
		No Hemin vs 100 μM	**0.0043**	**
		2 μM vs 20 μM	**0.0329**	*
		2 μM vs 100 μM	> 0.9999	NS
		20 μM vs 100 μM	**0.0041**	**
	240 hr	No Hemin vs 2 uM	> 0.9999	NS
		No Hemin vs 20 μM	> 0.9999	NS
		No Hemin vs 100 μM	0.2316	NS
		2 μM vs 20 μM	> 0.9999	NS
		2 μM vs 100 μM	0.4543	NS
		20 μM vs 100 μM	0.4543	NS
S. aureus LAC	**24 hr**	No Hemin vs 2 uM	> 0.9999	NS
		No Hemin vs 20 μM	**0.0042**	**
		No Hemin vs 100 μM	0.3132	NS
		2 μM vs 20 μM	**0.0052**	**
		2 μM vs 100 μM	0.3563	NS
		20 μM vs 100 μM	0.8863	NS
	72 hr	No Hemin vs 2 uM	0.7089	NS
		No Hemin vs 20 μM	**0.0015**	**
		No Hemin vs 100 μM	**0.0241**	*
		2 μM vs 20 μM	0.2169	NS
		2 μM vs 100 μM	> 0.9999	NS
		20 μM vs 100 μM	> 0.9999	NS
	168 hr	No Hemin vs 2 uM	All values zero	
		No Hemin vs 20 μM	All values zero	
		No Hemin vs 100 μM	All values zero	
		2 μM vs 20 μM	All values zero	
		2 μM vs 100 μM	All values zero	
		20 μM vs 100 μM	All values zero	
	240 hr	No Hemin vs 2 uM	All values zero	
		No Hemin vs 20 μM	All values zero	
		No Hemin vs 100 μM	All values zero	

7.3.2 Genes Not Identified in *P. aeruginosa* PA21

Gene	Length	Gene id	function
2472	91	fig|6666666.315499.peg.2472	10.1 kDa protein (ORF 90)
4029	165	fig|6666666.315499.peg.4029	Acyl-CoA dehydrogenase; probable dibenzothiophene desulfurization enzyme
2003	83	fig|6666666.315499.peg.2003	coat protein B of bacteriophage Pf1)
2466	83	fig|6666666.315499.peg.2466	coat protein B of bacteriophage Pf1)
1344	622	fig|6666666.315499.peg.1344	FIG00450309: hypothetical protein
504	57	fig|6666666.315499.peg.504	FIG00953081: hypothetical protein
4030	116	fig|6666666.315499.peg.4030	FIG00954095: hypothetical protein
1336	121	fig|6666666.315499.peg.1336	FIG00955484: hypothetical protein
123	142	fig|6666666.315499.peg.123	FIG00956262: hypothetical protein
661	487	fig|6666666.315499.peg.661	FIG00957630: hypothetical protein
1477	52	fig|6666666.315499.peg.1477	FIG00957790: hypothetical protein
3085	238	fig|6666666.315499.peg.3085	FIG00957922: hypothetical protein
4031	85	fig|6666666.315499.peg.4031	FIG00958178: hypothetical protein
508	90	fig|6666666.315499.peg.508	FIG00958543: hypothetical protein
814	470	fig|6666666.315499.peg.814	FIG00960399: hypothetical protein
815	223	fig|6666666.315499.peg.815	FIG00960864: hypothetical protein
3957	385	fig|6666666.315499.peg.3957	FIG00964184: hypothetical protein
2008	71	fig|6666666.315499.peg.2008	FIG00965801: hypothetical protein
4039	364	fig|6666666.315499.peg.4039	FIG00966085: hypothetical protein
4042	351	fig|6666666.315499.peg.4042	FIG00966085: hypothetical protein
1901	271	fig|6666666.315499.peg.1901	Hnh endonuclease
5639	318	fig|6666666.315499.peg.5639	HrgA protein
232	202	fig|6666666.315499.peg.232	hypothetical protein
464	139	fig|6666666.315499.peg.464	hypothetical protein
465	243	fig|6666666.315499.peg.465	hypothetical protein
466	340	fig|6666666.315499.peg.466	hypothetical protein
467	216	fig|6666666.315499.peg.467	hypothetical protein
545	45	fig|6666666.315499.peg.545	hypothetical protein
662	269	fig|6666666.315499.peg.662	hypothetical protein
1343	234	fig|6666666.315499.peg.1343	hypothetical protein
1345	251	fig|6666666.315499.peg.1345	hypothetical protein
1739	73	fig|6666666.315499.peg.1739	hypothetical protein
1740	208	fig|6666666.315499.peg.1740	hypothetical protein
1999	34	fig|6666666.315499.peg.1999	hypothetical protein
2010	442	fig|6666666.315499.peg.2010	hypothetical protein
2462	34	fig|6666666.315499.peg.2462	hypothetical protein

2470	115	fig|6666666.315499.peg.2470	hypothetical protein
2471	97	fig|6666666.315499.peg.2471	hypothetical protein
3441	45	fig|6666666.315499.peg.3441	hypothetical protein
3969	42	fig|6666666.315499.peg.3969	hypothetical protein
4038	47	fig|6666666.315499.peg.4038	hypothetical protein
4862	345	fig|6666666.315499.peg.4862	hypothetical protein
5370	411	fig|6666666.315499.peg.5370	hypothetical protein
5560	439	fig|6666666.315499.peg.5560	hypothetical protein
5633	106	fig|6666666.315499.peg.5633	hypothetical protein
5638	202	fig|6666666.315499.peg.5638	hypothetical protein
5640	75	fig|6666666.315499.peg.5640	hypothetical protein
4243	210	fig|6666666.315499.peg.4243	Inner membrane protein
1346	475	fig|6666666.315499.peg.1346	ISPsy6, transposase
505	295	fig|6666666.315499.peg.505	Manganese catalase (EC 1.11.1.6)
370	339	fig|6666666.315499.peg.370	Mobile element protein
468	402	fig|6666666.315499.peg.468	Mobile element protein
2600	339	fig|6666666.315499.peg.2600	Mobile element protein
3838	339	fig|6666666.315499.peg.3838	Mobile element protein
4354	339	fig|6666666.315499.peg.4354	Mobile element protein
4917	339	fig|6666666.315499.peg.4917	Mobile element protein
5678	339	fig|6666666.315499.peg.5678	Mobile element protein
5205	412	fig|6666666.315499.peg.5205	O-antigen flippase Wzx
5204	439	fig|6666666.315499.peg.5204	Oligosaccharide repeat unit polymerase Wzy
2007	97	fig|6666666.315499.peg.2007	Phage protein
762	143	fig|6666666.315499.peg.762	possible DNA helicase
1628	221	fig|6666666.315499.peg.1628	Predicted sugar nucleotidyltransferases
2002	359	fig|6666666.315499.peg.2002	Probable coat protein A precursor
2465	358	fig|6666666.315499.peg.2465	Probable coat protein A precursor
4863	1100	fig|6666666.315499.peg.4863	probable phospholipase
506	170	fig|6666666.315499.peg.506	Protein YciE
4040	112	fig|6666666.315499.peg.4040	Putative dUTPase
4481	361	fig|6666666.315499.peg.4481	putative integrase protein
5207	377	fig|6666666.315499.peg.5207	putitive LPS biosynthesis protein
2011	284	fig|6666666.315499.peg.2011	Retron-type RNA-directed DNA polymerase (EC 2.7.7.49)
1630	254	fig|6666666.315499.peg.1630	SAM-dependent methyltransferases
765	489	fig|6666666.315499.peg.765	Superfamily I DNA and RNA helicase
1342	712	fig|6666666.315499.peg.1342	Superfamily I DNA and RNA helicases
124	276	fig|6666666.315499.peg.124	Trans-aconitate 2-methyltransferase (EC 2.1.1.144)

5635	458	fig|6666666.315499.peg.5635	Type I restriction-modification system, specificity subunit S (EC 3.1.21.3)
4480	128	fig|6666666.315499.peg.4480	Type II secretory pathway, component ExeA (predicted ATPase)
5200	317	fig|6666666.315499.peg.5200	UDP-2-acetamido-2-deoxy-D-glucuronic acid dehydrogenase (NAD+ cofactor)

7.3.3 Genes Only Identified in *P. aeruginosa* PA21

Gene	Length	Gene id	function
4617	158	fig|6666666.315743.peg.4617	2-C-methyl-D-erythritol 2,4-cyclodiphosphate synthase (EC 4.6.1.12)
3650	758	fig|6666666.315743.peg.3650	5-methylcytosine-specific restriction enzyme McrB related protein
2641	205	fig|6666666.315743.peg.2641	Acetyltransferase (isoleucine patch superfamily)
2636	75	fig|6666666.315743.peg.2636	Acyl carrier protein
792	401	fig|6666666.315743.peg.792	acyltransferase 3
2377	325	fig|6666666.315743.peg.2377	alternative bacteriophage tail fiber C-terminus
2913	352	fig|6666666.315743.peg.2913	aminoglycoside phosphotransferase
1039	586	fig|6666666.315743.peg.1039	Arsenical pump-driving ATPase (EC 3.6.3.16)
1034	354	fig|6666666.315743.peg.1034	Arsenical-resistance protein ACR3
2947	83	fig|6666666.315743.peg.2947	Asl7591 protein
1025	571	fig|6666666.315743.peg.1025	ATP-dependent DNA helicase UvrD/PcrA
1026	619	fig|6666666.315743.peg.1026	ATP-dependent endonuclease family protein
3408	875	fig|6666666.315743.peg.3408	ATPase involved in DNA repair
2990	248	fig|6666666.315743.peg.2990	Bacteriophage protein gp37
3633	562	fig|6666666.315743.peg.3633	Bipolar DNA helicase HerA
5451	601	fig|6666666.315743.peg.5451	Bipolar DNA helicase HerA
3474	378	fig|6666666.315743.peg.3474	Butyryl-CoA dehydrogenase (EC 1.3.8.1)
3412	127	fig|6666666.315743.peg.3412	Candidate type III effector Hop protein
4085	372	fig|6666666.315743.peg.4085	Capsular polysaccharide synthesis enzyme Cap5F
3482	350	fig|6666666.315743.peg.3482	Chalcone synthase (EC 2.3.1.74)
2771	307	fig|6666666.315743.peg.2771	Chromate resistance protein ChrB
3360	292	fig|6666666.315743.peg.3360	Chromosome partitioning ATPase in PFGI-1-like cluster, ParA-like
3369	212	fig|6666666.315743.peg.3369	Cobalt-zinc-cadmium resistance protein CzcD
2156	401	fig|6666666.315743.peg.2156	COG0582: Integrase
4661	553	fig|6666666.315743.peg.4661	COG1156: Archaeal/vacuolar-type H+-ATPase subunit B
2162	182	fig|6666666.315743.peg.2162	COG1896: Predicted hydrolases of HD superfamily
3430	106	fig|6666666.315743.peg.3430	COGs COG2002
3640	305	fig|6666666.315743.peg.3640	COGs COG2378
2940	333	fig|6666666.315743.peg.2940	Cointegrate resolution protein T
3642	575	fig|6666666.315743.peg.3642	conserved hypothetical protein
2959	281	fig|6666666.315743.peg.2959	Cytochrome c family protein
4704	254	fig|6666666.315743.peg.4704	Cytosine methylase, phage-associated

1558	93	fig|6666666.315743.peg.1558	Death on curing protein, Doc toxin
4503	265	fig|6666666.315743.peg.4503	DNA adenine methyltransferase, phage-associated
2177	913	fig|6666666.315743.peg.2177	DNA primase (bacterial type)
2346	280	fig|6666666.315743.peg.2346	DNA replication protein DnaC
2160	591	fig|6666666.315743.peg.2160	DNA-cytosine methyltransferase (EC 2.1.1.37)
4467	389	fig|6666666.315743.peg.4467	Eha
2187	333	fig|6666666.315743.peg.2187	elements of external origin; phage-related functions and prophages
2799	198	fig|6666666.315743.peg.2799	EXTRACYTOPLASMIC FUNCTION ALTERNATIVE SIGMA FACTOR
2804	214	fig|6666666.315743.peg.2804	EXTRACYTOPLASMIC FUNCTION ALTERNATIVE SIGMA FACTOR
5142	260	fig|6666666.315743.peg.5142	FIG000557: hypothetical protein co-occurring with RecR
3373	71	fig|6666666.315743.peg.3373	FIG00464742: hypothetical protein
3363	187	fig|6666666.315743.peg.3363	FIG004780: hypothetical protein in PFGI-1-like cluster
2305	394	fig|6666666.315743.peg.2305	FIG005429: hypothetical protein
2755	668	fig|6666666.315743.peg.2755	FIG006126: DNA helicase, restriction/modification system component YeeB
3425	466	fig|6666666.315743.peg.3425	FIG00715740: hypothetical protein
2304	1102	fig|6666666.315743.peg.2304	FIG007317: Chromosome segregation protein SMC-like
5452	424	fig|6666666.315743.peg.5452	FIG00806694: hypothetical protein
3641	1611	fig|6666666.315743.peg.3641	FIG00808534: hypothetical protein
3376	246	fig|6666666.315743.peg.3376	FIG00902157: hypothetical protein
2362	108	fig|6666666.315743.peg.2362	FIG00953426: hypothetical protein
4666	828	fig|6666666.315743.peg.4666	FIG00954405: hypothetical protein
3395	107	fig|6666666.315743.peg.3395	FIG00954465: hypothetical protein
3405	183	fig|6666666.315743.peg.3405	FIG00954712: hypothetical protein
2355	110	fig|6666666.315743.peg.2355	FIG00954937: hypothetical protein
4813	93	fig|6666666.315743.peg.4813	FIG00955190: hypothetical protein
2929	296	fig|6666666.315743.peg.2929	FIG00955335: hypothetical protein
2795	137	fig|6666666.315743.peg.2795	FIG00955907: hypothetical protein
2998	121	fig|6666666.315743.peg.2998	FIG00956135: hypothetical protein
4664	566	fig|6666666.315743.peg.4664	FIG00956273: hypothetical protein
4657	94	fig|6666666.315743.peg.4657	FIG00956286: hypothetical protein
3424	316	fig|6666666.315743.peg.3424	FIG00956406: hypothetical protein
2349	95	fig|6666666.315743.peg.2349	FIG00956875: hypothetical protein
3396	102	fig|6666666.315743.peg.3396	FIG00957490: hypothetical protein
3426	120	fig|6666666.315743.peg.3426	FIG00958347: hypothetical protein
2963	53	fig|6666666.315743.peg.2963	FIG00958355: hypothetical protein
3475	546	fig|6666666.315743.peg.3475	FIG00958574: hypothetical protein
2642	383	fig|6666666.315743.peg.2642	FIG00959623: hypothetical protein
4700	101	fig|6666666.315743.peg.4700	FIG00959863: hypothetical protein

4014	261	fig|6666666.315743.peg.4014	FIG00959928: hypothetical protein
4672	106	fig|6666666.315743.peg.4672	FIG00960527: hypothetical protein
2938	160	fig|6666666.315743.peg.2938	FIG00960741: hypothetical protein
2361	68	fig|6666666.315743.peg.2361	FIG00961661: hypothetical protein
2320	510	fig|6666666.315743.peg.2320	FIG00962130: hypothetical protein
2157	216	fig|6666666.315743.peg.2157	FIG00962931: hypothetical protein
2158	243	fig|6666666.315743.peg.2158	FIG00962931: hypothetical protein
2330	221	fig|6666666.315743.peg.2330	FIG00962931: hypothetical protein
4464	227	fig|6666666.315743.peg.4464	FIG00962931: hypothetical protein
4707	501	fig|6666666.315743.peg.4707	FIG00962931: hypothetical protein
4702	179	fig|6666666.315743.peg.4702	FIG00963381: hypothetical protein
4662	135	fig|6666666.315743.peg.4662	FIG00963969: hypothetical protein
2344	77	fig|6666666.315743.peg.2344	FIG00964051: hypothetical protein
4669	65	fig|6666666.315743.peg.4669	FIG00964642: hypothetical protein
4698	83	fig|6666666.315743.peg.4698	FIG00964821: hypothetical protein
3646	317	fig|6666666.315743.peg.3646	FIG00965493: hypothetical protein
4658	187	fig|6666666.315743.peg.4658	FIG00965686: hypothetical protein
2316	343	fig|6666666.315743.peg.2316	FIG00965705: hypothetical protein
2796	80	fig|6666666.315743.peg.2796	FIG00967047: hypothetical protein
3636	1429	fig|6666666.315743.peg.3636	FIG00967058: hypothetical protein
4660	196	fig|6666666.315743.peg.4660	FIG00967075: hypothetical protein
4705	83	fig|6666666.315743.peg.4705	FIG00967252: hypothetical protein
3428	126	fig|6666666.315743.peg.3428	FIG00976384: hypothetical protein
3414	120	fig|6666666.315743.peg.3414	FIG01210404: hypothetical protein
3423	149	fig|6666666.315743.peg.3423	FIG01211007: hypothetical protein
3374	131	fig|6666666.315743.peg.3374	FIG01211190: hypothetical protein
3375	229	fig|6666666.315743.peg.3375	FIG01219358: hypothetical protein
3478	450	fig|6666666.315743.peg.3478	FIG022199: FAD-binding protein
3481	505	fig|6666666.315743.peg.3481	FIG022199: FAD-binding protein
3394	370	fig|6666666.315743.peg.3394	FIG023873: Plasmid related protein
3393	217	fig|6666666.315743.peg.3393	FIG026997: Hypothetical protein
3389	230	fig|6666666.315743.peg.3389	FIG034376: Hypothetical protein
3361	90	fig|6666666.315743.peg.3361	FIG034647: hypothetical protein in PFGI-1-like cluster
5450	394	fig|6666666.315743.peg.5450	FIG036446: hypothetical protein
3390	114	fig|6666666.315743.peg.3390	FIG036757: Plasmid-related protein
2303	250	fig|6666666.315743.peg.2303	FIG039767: hypothetical protein
3392	87	fig|6666666.315743.peg.3392	FIG041301: Hypothetical protein
3358	249	fig|6666666.315743.peg.3358	FIG041388: hypothetical protein in PFGI-1-like cluster

2756	927	fig|6666666.315743.peg.2756	FIG045374: Type II restriction enzyme, methylase subunit YeeA
3391	136	fig|6666666.315743.peg.3391	FIG046709: Hypothetical protein
3386	255	fig|6666666.315743.peg.3386	FIG049434: Periplasmic protein TonB, links inner and outer membranes
3387	302	fig|6666666.315743.peg.3387	FIG049434: Periplasmic protein TonB, links inner and outer membranes
2974	355	fig|6666666.315743.peg.2974	FIG074102: hypothetical protein
3379	63	fig|6666666.315743.peg.3379	FIG076210: Hypothetical protein
3385	87	fig|6666666.315743.peg.3385	FIG076210: Hypothetical protein
3378	275	fig|6666666.315743.peg.3378	FIG076676: Hypothetical protein
3365	264	fig|6666666.315743.peg.3365	FIG141694: hypothetical protein in PFGI-1-like cluster
734	390	fig|6666666.315743.peg.734	FIG141751: hypothetical protein in PFGI-1-like cluster
3364	413	fig|6666666.315743.peg.3364	FIG141751: hypothetical protein in PFGI-1-like cluster
2302	451	fig|6666666.315743.peg.2302	FIG149030: hypothetical protein
2921	320	fig|6666666.315743.peg.2921	Flavohemoprotein (Hemoglobin-like protein) (Flavohemoglobin) (Nitric oxide dioxygenase) (EC 1.14.12.17)
2759	467	fig|6666666.315743.peg.2759	FOG: GGDEF domain
2359	215	fig|6666666.315743.peg.2359	Gene Transfer Agent prohead protease
2807	252	fig|6666666.315743.peg.2807	Glutamate synthase [NADPH] large chain (EC 1.4.1.13)
2953	264	fig|6666666.315743.peg.2953	Glutamate synthase [NADPH] large chain (EC 1.4.1.13)
2788	385	fig|6666666.315743.peg.2788	Glutathione S-transferase
1048	320	fig|6666666.315743.peg.1048	Glutathione synthase/Ribosomal protein S6 modification enzyme (glutaminyl transferase)
2966	421	fig|6666666.315743.peg.2966	Heavy metal RND efflux outer membrane protein, CzcC family
2317	289	fig|6666666.315743.peg.2317	Histidinol-phosphatase (EC 3.1.3.15)
3442	203	fig|6666666.315743.peg.3442	Histone acetyltransferase HPA2 and related acetyltransferases
4685	116	fig|6666666.315743.peg.4685	Holliday junction resolvase / Crossover junction endodeoxyribonuclease rusA (EC 3.1.22.-)
2988	470	fig|6666666.315743.peg.2988	Homospermidine synthase (EC 2.5.1.44)
1028	254	fig|6666666.315743.peg.1028	HTH-type transcriptional activator RhaS
3448	272	fig|6666666.315743.peg.3448	Hydrogen peroxide-inducible genes activator
3410	225	fig|6666666.315743.peg.3410	hypothetical gene
673	44	fig|6666666.315743.peg.673	hypothetical protein
677	314	fig|6666666.315743.peg.677	hypothetical protein
679	38	fig|6666666.315743.peg.679	hypothetical protein
730	249	fig|6666666.315743.peg.730	hypothetical protein
755	316	fig|6666666.315743.peg.755	hypothetical protein
757	477	fig|6666666.315743.peg.757	hypothetical protein
759	323	fig|6666666.315743.peg.759	hypothetical protein
760	245	fig|6666666.315743.peg.760	hypothetical protein

1021	699	fig|6666666.315743.peg.1021	hypothetical protein
1024	46	fig|6666666.315743.peg.1024	hypothetical protein
1029	146	fig|6666666.315743.peg.1029	hypothetical protein
1038	266	fig|6666666.315743.peg.1038	hypothetical protein
1044	45	fig|6666666.315743.peg.1044	hypothetical protein
1045	215	fig|6666666.315743.peg.1045	hypothetical protein
1046	52	fig|6666666.315743.peg.1046	hypothetical protein
1047	221	fig|6666666.315743.peg.1047	hypothetical protein
1049	112	fig|6666666.315743.peg.1049	hypothetical protein
1053	134	fig|6666666.315743.peg.1053	hypothetical protein
1055	64	fig|6666666.315743.peg.1055	hypothetical protein
1056	86	fig|6666666.315743.peg.1056	hypothetical protein
1057	74	fig|6666666.315743.peg.1057	hypothetical protein
1527	45	fig|6666666.315743.peg.1527	hypothetical protein
1676	232	fig|6666666.315743.peg.1676	hypothetical protein
2142	546	fig|6666666.315743.peg.2142	hypothetical protein
2148	73	fig|6666666.315743.peg.2148	hypothetical protein
2152	37	fig|6666666.315743.peg.2152	hypothetical protein
2163	245	fig|6666666.315743.peg.2163	hypothetical protein
2166	79	fig|6666666.315743.peg.2166	hypothetical protein
2167	123	fig|6666666.315743.peg.2167	hypothetical protein
2168	95	fig|6666666.315743.peg.2168	hypothetical protein
2170	103	fig|6666666.315743.peg.2170	hypothetical protein
2171	70	fig|6666666.315743.peg.2171	hypothetical protein
2173	77	fig|6666666.315743.peg.2173	hypothetical protein
2174	74	fig|6666666.315743.peg.2174	hypothetical protein
2175	68	fig|6666666.315743.peg.2175	hypothetical protein
2176	167	fig|6666666.315743.peg.2176	hypothetical protein
2180	246	fig|6666666.315743.peg.2180	hypothetical protein
2183	75	fig|6666666.315743.peg.2183	hypothetical protein
2186	212	fig|6666666.315743.peg.2186	hypothetical protein
2188	94	fig|6666666.315743.peg.2188	hypothetical protein
2189	146	fig|6666666.315743.peg.2189	hypothetical protein
2190	68	fig|6666666.315743.peg.2190	hypothetical protein
2191	251	fig|6666666.315743.peg.2191	hypothetical protein
2195	336	fig|6666666.315743.peg.2195	hypothetical protein
2196	287	fig|6666666.315743.peg.2196	hypothetical protein
2197	587	fig|6666666.315743.peg.2197	hypothetical protein

2198	79	fig|6666666.315743.peg.2198	hypothetical protein
2203	116	fig|6666666.315743.peg.2203	hypothetical protein
2306	784	fig|6666666.315743.peg.2306	hypothetical protein
2307	1025	fig|6666666.315743.peg.2307	hypothetical protein
2308	347	fig|6666666.315743.peg.2308	hypothetical protein
2309	210	fig|6666666.315743.peg.2309	hypothetical protein
2310	270	fig|6666666.315743.peg.2310	hypothetical protein
2311	48	fig|6666666.315743.peg.2311	hypothetical protein
2312	33	fig|6666666.315743.peg.2312	hypothetical protein
2313	257	fig|6666666.315743.peg.2313	hypothetical protein
2314	220	fig|6666666.315743.peg.2314	hypothetical protein
2315	60	fig|6666666.315743.peg.2315	hypothetical protein
2318	375	fig|6666666.315743.peg.2318	hypothetical protein
2319	232	fig|6666666.315743.peg.2319	hypothetical protein
2324	182	fig|6666666.315743.peg.2324	hypothetical protein
2326	110	fig|6666666.315743.peg.2326	hypothetical protein
2334	85	fig|6666666.315743.peg.2334	hypothetical protein
2335	78	fig|6666666.315743.peg.2335	hypothetical protein
2338	104	fig|6666666.315743.peg.2338	hypothetical protein
2339	96	fig|6666666.315743.peg.2339	hypothetical protein
2340	103	fig|6666666.315743.peg.2340	hypothetical protein
2341	93	fig|6666666.315743.peg.2341	hypothetical protein
2342	78	fig|6666666.315743.peg.2342	hypothetical protein
2351	74	fig|6666666.315743.peg.2351	hypothetical protein
2352	105	fig|6666666.315743.peg.2352	hypothetical protein
2354	66	fig|6666666.315743.peg.2354	hypothetical protein
2363	109	fig|6666666.315743.peg.2363	hypothetical protein
2364	65	fig|6666666.315743.peg.2364	hypothetical protein
2366	129	fig|6666666.315743.peg.2366	hypothetical protein
2367	169	fig|6666666.315743.peg.2367	hypothetical protein
2368	115	fig|6666666.315743.peg.2368	hypothetical protein
2369	76	fig|6666666.315743.peg.2369	hypothetical protein
2376	222	fig|6666666.315743.peg.2376	hypothetical protein
2378	214	fig|6666666.315743.peg.2378	hypothetical protein
2751	551	fig|6666666.315743.peg.2751	hypothetical protein
2753	32	fig|6666666.315743.peg.2753	hypothetical protein
2760	88	fig|6666666.315743.peg.2760	hypothetical protein
2761	212	fig|6666666.315743.peg.2761	hypothetical protein

2763	217	fig|6666666.315743.peg.2763	hypothetical protein
2764	78	fig|6666666.315743.peg.2764	hypothetical protein
2774	45	fig|6666666.315743.peg.2774	hypothetical protein
2775	234	fig|6666666.315743.peg.2775	hypothetical protein
2783	100	fig|6666666.315743.peg.2783	hypothetical protein
2789	71	fig|6666666.315743.peg.2789	hypothetical protein
2798	36	fig|6666666.315743.peg.2798	hypothetical protein
2813	40	fig|6666666.315743.peg.2813	hypothetical protein
2860	60	fig|6666666.315743.peg.2860	hypothetical protein
2920	51	fig|6666666.315743.peg.2920	hypothetical protein
2931	221	fig|6666666.315743.peg.2931	hypothetical protein
2939	215	fig|6666666.315743.peg.2939	hypothetical protein
2944	120	fig|6666666.315743.peg.2944	hypothetical protein
2949	576	fig|6666666.315743.peg.2949	hypothetical protein
2950	400	fig|6666666.315743.peg.2950	hypothetical protein
2952	105	fig|6666666.315743.peg.2952	hypothetical protein
2955	87	fig|6666666.315743.peg.2955	hypothetical protein
2969	121	fig|6666666.315743.peg.2969	hypothetical protein
2971	163	fig|6666666.315743.peg.2971	hypothetical protein
2972	244	fig|6666666.315743.peg.2972	hypothetical protein
2981	88	fig|6666666.315743.peg.2981	hypothetical protein
2987	243	fig|6666666.315743.peg.2987	hypothetical protein
2989	439	fig|6666666.315743.peg.2989	hypothetical protein
2992	74	fig|6666666.315743.peg.2992	hypothetical protein
3229	111	fig|6666666.315743.peg.3229	hypothetical protein
3357	167	fig|6666666.315743.peg.3357	hypothetical protein
3377	93	fig|6666666.315743.peg.3377	hypothetical protein
3398	260	fig|6666666.315743.peg.3398	hypothetical protein
3409	351	fig|6666666.315743.peg.3409	hypothetical protein
3413	78	fig|6666666.315743.peg.3413	hypothetical protein
3415	137	fig|6666666.315743.peg.3415	hypothetical protein
3417	306	fig|6666666.315743.peg.3417	hypothetical protein
3429	153	fig|6666666.315743.peg.3429	hypothetical protein
3449	40	fig|6666666.315743.peg.3449	hypothetical protein
3479	89	fig|6666666.315743.peg.3479	hypothetical protein
3620	436	fig|6666666.315743.peg.3620	hypothetical protein
3627	41	fig|6666666.315743.peg.3627	hypothetical protein
3629	46	fig|6666666.315743.peg.3629	hypothetical protein

3634	381	fig|6666666.315743.peg.3634	hypothetical protein
3635	259	fig|6666666.315743.peg.3635	hypothetical protein
3637	441	fig|6666666.315743.peg.3637	hypothetical protein
3643	116	fig|6666666.315743.peg.3643	hypothetical protein
3648	60	fig|6666666.315743.peg.3648	hypothetical protein
3649	526	fig|6666666.315743.peg.3649	hypothetical protein
3798	43	fig|6666666.315743.peg.3798	hypothetical protein
4000	36	fig|6666666.315743.peg.4000	hypothetical protein
4084	57	fig|6666666.315743.peg.4084	hypothetical protein
4087	435	fig|6666666.315743.peg.4087	hypothetical protein
4089	363	fig|6666666.315743.peg.4089	hypothetical protein
4304	78	fig|6666666.315743.peg.4304	hypothetical protein
4456	183	fig|6666666.315743.peg.4456	hypothetical protein
4460	230	fig|6666666.315743.peg.4460	hypothetical protein
4461	208	fig|6666666.315743.peg.4461	hypothetical protein
4469	325	fig|6666666.315743.peg.4469	hypothetical protein
4471	87	fig|6666666.315743.peg.4471	hypothetical protein
4476	53	fig|6666666.315743.peg.4476	hypothetical protein
4479	107	fig|6666666.315743.peg.4479	hypothetical protein
4480	101	fig|6666666.315743.peg.4480	hypothetical protein
4491	68	fig|6666666.315743.peg.4491	hypothetical protein
4668	251	fig|6666666.315743.peg.4668	hypothetical protein
4678	248	fig|6666666.315743.peg.4678	hypothetical protein
4679	66	fig|6666666.315743.peg.4679	hypothetical protein
4680	80	fig|6666666.315743.peg.4680	hypothetical protein
4683	125	fig|6666666.315743.peg.4683	hypothetical protein
4684	100	fig|6666666.315743.peg.4684	hypothetical protein
4687	69	fig|6666666.315743.peg.4687	hypothetical protein
4688	266	fig|6666666.315743.peg.4688	hypothetical protein
4689	100	fig|6666666.315743.peg.4689	hypothetical protein
4692	69	fig|6666666.315743.peg.4692	hypothetical protein
4693	69	fig|6666666.315743.peg.4693	hypothetical protein
4694	63	fig|6666666.315743.peg.4694	hypothetical protein
4695	50	fig|6666666.315743.peg.4695	hypothetical protein
4699	105	fig|6666666.315743.peg.4699	hypothetical protein
4701	126	fig|6666666.315743.peg.4701	hypothetical protein
4706	70	fig|6666666.315743.peg.4706	hypothetical protein
4708	80	fig|6666666.315743.peg.4708	hypothetical protein

4709	215	fig|6666666.315743.peg.4709	hypothetical protein
4710	121	fig|6666666.315743.peg.4710	hypothetical protein
4711	65	fig|6666666.315743.peg.4711	hypothetical protein
4786	41	fig|6666666.315743.peg.4786	hypothetical protein
5339	60	fig|6666666.315743.peg.5339	hypothetical protein
5834	81	fig|6666666.315743.peg.5834	hypothetical protein
5882	327	fig|6666666.315743.peg.5882	hypothetical protein
5883	398	fig|6666666.315743.peg.5883	hypothetical protein
5903	51	fig|6666666.315743.peg.5903	hypothetical protein
6085	81	fig|6666666.315743.peg.6085	hypothetical protein
6090	283	fig|6666666.315743.peg.6090	hypothetical protein
2777	374	fig|6666666.315743.peg.2777	Inner membrane protein
2785	183	fig|6666666.315743.peg.2785	Inner membrane protein forms channel for type IV secretion of T-DNA complex (VirB10)
2808	155	fig|6666666.315743.peg.2808	INTEGRAL MEMBRANE PROTEIN (Rhomboid family)
726	400	fig|6666666.315743.peg.726	Integrase
733	288	fig|6666666.315743.peg.733	Integrase
2161	262	fig|6666666.315743.peg.2161	Integrase
2973	400	fig|6666666.315743.peg.2973	Integrase
3454	648	fig|6666666.315743.peg.3454	Integrase
3630	371	fig|6666666.315743.peg.3630	Integrase
3366	176	fig|6666666.315743.peg.3366	Integrase regulator R
2782	263	fig|6666666.315743.peg.2782	Isochorismatase (EC 3.3.2.1)
3443	136	fig|6666666.315743.peg.3443	Isopropylmalate/homocitrate/citramalate synthases
6086	746	fig|6666666.315743.peg.6086	lipase family protein
6088	36	fig|6666666.315743.peg.6088	lipase family protein
6087	264	fig|6666666.315743.peg.6087	lipoprotein
6089	264	fig|6666666.315743.peg.6089	lipoprotein
4478	208	fig|6666666.315743.peg.4478	Lipoprotein, phage-associated
3452	272	fig|6666666.315743.peg.3452	LysR family transcriptional regulator YbhD
4090	411	fig|6666666.315743.peg.4090	Membrane protein involved in the export of O-antigen and teichoic acid
2986	302	fig|6666666.315743.peg.2986	membrane protein, putative
3381	117	fig|6666666.315743.peg.3381	Mercuric transport protein, MerT
3402	217	fig|6666666.315743.peg.3402	Methyl-accepting chemotaxis protein
2201	268	fig|6666666.315743.peg.2201	Methyl-directed repair DNA adenine methylase (EC 2.1.1.72)
2978	117	fig|6666666.315743.peg.2978	Mlr6156 protein
3437	445	fig|6666666.315743.peg.3437	Mlr6914 protein
1050	105	fig|6666666.315743.peg.1050	Mobile element protein

2786	989	fig|6666666.315743.peg.2786	Mobile element protein
2790	113	fig|6666666.315743.peg.2790	Mobile element protein
2791	419	fig|6666666.315743.peg.2791	Mobile element protein
2793	263	fig|6666666.315743.peg.2793	Mobile element protein
2794	719	fig|6666666.315743.peg.2794	Mobile element protein
2970	290	fig|6666666.315743.peg.2970	Mobile element protein
2985	1005	fig|6666666.315743.peg.2985	Mobile element protein
2993	103	fig|6666666.315743.peg.2993	Mobile element protein
3384	214	fig|6666666.315743.peg.3384	Mobile element protein
3446	424	fig|6666666.315743.peg.3446	Mobile element protein
3447	343	fig|6666666.315743.peg.3447	Mobile element protein
3618	99	fig|6666666.315743.peg.3618	Mobile element protein
4486	370	fig|6666666.315743.peg.4486	Mu-like prophage FluMu I protein
4483	525	fig|6666666.315743.peg.4483	Mu-like prophage FluMu protein gp29
2957	104	fig|6666666.315743.peg.2957	Multicopper oxidase
3644	323	fig|6666666.315743.peg.3644	Mycobacteriophage Barnyard protein gp56
3639	708	fig|6666666.315743.peg.3639	N-6 DNA methylase
2778	98	fig|6666666.315743.peg.2778	NreA-like protein
2976	86	fig|6666666.315743.peg.2976	NreA-like protein
4665	174	fig|6666666.315743.peg.4665	PE-PGRS virulence associated protein
3382	96	fig|6666666.315743.peg.3382	Periplasmic mercury(+2) binding protein
1030	411	fig|6666666.315743.peg.1030	Permease of the major facilitator superfamily
4484	413	fig|6666666.315743.peg.4484	Phage (Mu-like) virion morphogenesis protein
2343	257	fig|6666666.315743.peg.2343	Phage DNA binding protein Roi
2297	108	fig|6666666.315743.peg.2297	Phage DNA-binding protein
3621	95	fig|6666666.315743.peg.3621	Phage DNA-binding protein
4498	273	fig|6666666.315743.peg.4498	Phage FAD/FMN-containing dehydrogenase
4682	111	fig|6666666.315743.peg.4682	phage holin, lambda family
2765	207	fig|6666666.315743.peg.2765	Phage integrase family protein
2348	426	fig|6666666.315743.peg.2348	phage integrase, putative
3631	486	fig|6666666.315743.peg.3631	phage integrase, putative
2360	405	fig|6666666.315743.peg.2360	Phage major capsid protein
4488	299	fig|6666666.315743.peg.4488	Phage major capsid protein
2358	406	fig|6666666.315743.peg.2358	Phage portal protein
4674	549	fig|6666666.315743.peg.4674	Phage portal protein
2184	489	fig|6666666.315743.peg.2184	Phage portal protein, lambda family
92	147	fig|6666666.315743.peg.92	Phage protein
2144	225	fig|6666666.315743.peg.2144	Phage protein

2159	144	fig|6666666.315743.peg.2159	Phage protein
2164	270	fig|6666666.315743.peg.2164	Phage protein
2192	1091	fig|6666666.315743.peg.2192	Phage protein
2193	137	fig|6666666.315743.peg.2193	Phage protein
2202	89	fig|6666666.315743.peg.2202	Phage protein
2327	240	fig|6666666.315743.peg.2327	Phage protein
2328	64	fig|6666666.315743.peg.2328	Phage protein
2329	39	fig|6666666.315743.peg.2329	Phage protein
2331	112	fig|6666666.315743.peg.2331	Phage protein
2336	71	fig|6666666.315743.peg.2336	Phage protein
2350	186	fig|6666666.315743.peg.2350	Phage protein
3628	111	fig|6666666.315743.peg.3628	Phage protein
4457	189	fig|6666666.315743.peg.4457	Phage protein
4458	156	fig|6666666.315743.peg.4458	Phage protein
4459	64	fig|6666666.315743.peg.4459	Phage protein
4462	67	fig|6666666.315743.peg.4462	Phage protein
4463	178	fig|6666666.315743.peg.4463	Phage protein
4465	95	fig|6666666.315743.peg.4465	Phage protein
4466	114	fig|6666666.315743.peg.4466	Phage protein
4472	163	fig|6666666.315743.peg.4472	Phage protein
4473	77	fig|6666666.315743.peg.4473	Phage protein
4474	168	fig|6666666.315743.peg.4474	Phage protein
4475	99	fig|6666666.315743.peg.4475	Phage protein
4487	135	fig|6666666.315743.peg.4487	Phage protein
4489	172	fig|6666666.315743.peg.4489	Phage protein
4490	151	fig|6666666.315743.peg.4490	Phage protein
4492	247	fig|6666666.315743.peg.4492	Phage protein
4493	161	fig|6666666.315743.peg.4493	Phage protein
4495	319	fig|6666666.315743.peg.4495	Phage protein
4496	308	fig|6666666.315743.peg.4496	Phage protein
4497	569	fig|6666666.315743.peg.4497	Phage protein
4499	77	fig|6666666.315743.peg.4499	Phage protein
4500	737	fig|6666666.315743.peg.4500	Phage protein
4501	383	fig|6666666.315743.peg.4501	Phage protein
4654	91	fig|6666666.315743.peg.4654	Phage protein
4659	64	fig|6666666.315743.peg.4659	Phage protein
4670	157	fig|6666666.315743.peg.4670	Phage protein
4671	110	fig|6666666.315743.peg.4671	Phage protein

4675	72	fig|6666666.315743.peg.4675	Phage protein
4691	85	fig|6666666.315743.peg.4691	Phage protein
2365	191	fig|6666666.315743.peg.2365	Phage protein, HK97, gp10
4686	124	fig|6666666.315743.peg.4686	phage recombination protein
2172	229	fig|6666666.315743.peg.2172	Phage repressor
728	714	fig|6666666.315743.peg.728	Phage T7 exclusion protein
4663	137	fig|6666666.315743.peg.4663	Phage tail fibers
4494	1196	fig|6666666.315743.peg.4494	Phage tail length tape-measure protein
2182	672	fig|6666666.315743.peg.2182	Phage terminase, large subunit
2357	560	fig|6666666.315743.peg.2357	Phage terminase, large subunit
4482	558	fig|6666666.315743.peg.4482	Phage terminase, large subunit
4676	660	fig|6666666.315743.peg.4676	Phage terminase, large subunit
2356	164	fig|6666666.315743.peg.2356	Phage terminase, small subunit
4481	183	fig|6666666.315743.peg.4481	Phage terminase, small subunit
4468	595	fig|6666666.315743.peg.4468	Phage transposase
3622	109	fig|6666666.315743.peg.3622	Phage-related protein
4703	206	fig|6666666.315743.peg.4703	Phage-related protein
1843	462	fig|6666666.315743.peg.1843	Pilin glycosylation enzyme
3401	154	fig|6666666.315743.peg.3401	PilL protein
3416	230	fig|6666666.315743.peg.3416	Possible exported protein
1032	172	fig|6666666.315743.peg.1032	Predicted protein-tyrosine phosphatase
4696	289	fig|6666666.315743.peg.4696	Predicted transcriptional regulators
1559	93	fig|6666666.315743.peg.1559	Prevent host death protein, Phd antitoxin
2345	345	fig|6666666.315743.peg.2345	Primosomal protein I
2149	238	fig|6666666.315743.peg.2149	Probable coat protein A precursor
3403	242	fig|6666666.315743.peg.3403	probable exported protein STY4558
2983	93	fig|6666666.315743.peg.2983	probable lipoprotein
2185	391	fig|6666666.315743.peg.2185	Prophage Clp protease-like protein
3645	334	fig|6666666.315743.peg.3645	Protein gp47, recombination-related [Bacteriophage A118]
2936	289	fig|6666666.315743.peg.2936	Protein involved in biosynthesis of mitomycin antibiotics/polyketide fumonisin
3388	276	fig|6666666.315743.peg.3388	protein of unknown function DUF932
3362	560	fig|6666666.315743.peg.3362	Protein with ParB-like nuclease domain in PFGI-1-like cluster
2780	226	fig|6666666.315743.peg.2780	putative (L31491) ORF2; putative [Plasmid pTOM9]
2980	211	fig|6666666.315743.peg.2980	putative (L31491) ORF2; putative [Plasmid pTOM9]
2914	119	fig|6666666.315743.peg.2914	Putative acyl-CoA dehydrogenase
4455	123	fig|6666666.315743.peg.4455	putative bacteriophage transcriptional regulator
2181	197	fig|6666666.315743.peg.2181	Putative bacteriophage-related protein
2169	190	fig|6666666.315743.peg.2169	putative deoxynucleotide monophosphate kinase

3418	477	fig|6666666.315743.peg.3418	putative exported protein
2752	766	fig|6666666.315743.peg.2752	putative integrase
3419	147	fig|6666666.315743.peg.3419	putative lipoprotein
2705	260	fig|6666666.315743.peg.2705	putative membrane protein
3407	250	fig|6666666.315743.peg.3407	putative membrane protein
3427	506	fig|6666666.315743.peg.3427	putative membrane protein
2779	246	fig|6666666.315743.peg.2779	putative ORF1 [Plasmid pTOM9]
2979	246	fig|6666666.315743.peg.2979	putative ORF1 [Plasmid pTOM9]
2333	279	fig|6666666.315743.peg.2333	putative serine protease
2801	91	fig|6666666.315743.peg.2801	Putative signal peptide protein
2805	91	fig|6666666.315743.peg.2805	Putative signal peptide protein
2750	416	fig|6666666.315743.peg.2750	putative site specific recombinase
2194	1184	fig|6666666.315743.peg.2194	PUTATIVE TRANSMEMBRANE PROTEIN
2325	398	fig|6666666.315743.peg.2325	putative transposase
3431	615	fig|6666666.315743.peg.3431	Pyruvate/2-oxoglutarate dehydrogenase complex, dihydrolipoamide acyltransferase (E2) component, and related enzymes
2758	196	fig|6666666.315743.peg.2758	Response regulator
3638	507	fig|6666666.315743.peg.3638	restriction modification system DNA specificity domain
2773	108	fig|6666666.315743.peg.2773	Rhodanese-like protein ChrE
3984	71	fig|6666666.315743.peg.3984	Ribosome modulation factor
2800	194	fig|6666666.315743.peg.2800	RNA polymerase sigma-70 factor, ECF subfamily
140	54	fig|6666666.315743.peg.140	Shufflon-specific DNA recombinase
3367	147	fig|6666666.315743.peg.3367	Single-stranded DNA-binding protein in PFGI-1-like cluster
1052	265	fig|6666666.315743.peg.1052	SIR2 family protein
1023	453	fig|6666666.315743.peg.1023	Site-specific recombinase, phage integrase family
4712	368	fig|6666666.315743.peg.4712	site-specific recombinase, phage integrase family
1022	655	fig|6666666.315743.peg.1022	Site-specific recombinase, phage integrase family domain protein
3404	197	fig|6666666.315743.peg.3404	Soluble lytic murein transglycosylase and related regulatory proteins (some contain LysM/invasin domains)
1027	272	fig|6666666.315743.peg.1027	Sterol desaturase
4677	182	fig|6666666.315743.peg.4677	Terminase small subunit
1040	455	fig|6666666.315743.peg.1040	Thioredoxin reductase (EC 1.8.1.9)
2941	331	fig|6666666.315743.peg.2941	Tn4652, cointegrate resolution protein S
2991	324	fig|6666666.315743.peg.2991	Tn4652, cointegrate resolution protein S
2816	560	fig|6666666.315743.peg.2816	TniA putative transposase
2817	303	fig|6666666.315743.peg.2817	TniB NTP-binding protein
1054	95	fig|6666666.315743.peg.1054	transcriptional regulator
3359	71	fig|6666666.315743.peg.3359	Transcriptional regulator in PFGI-1-like cluster

4470	105	fig|6666666.315743.peg.4470	Transcriptional regulator, IclR family
4697	129	fig|6666666.315743.peg.4697	Transcriptional regulator, LuxR family
2982	315	fig|6666666.315743.peg.2982	Transcriptional regulator, LysR family
3444	302	fig|6666666.315743.peg.3444	Transcriptional regulator, LysR family
2928	194	fig|6666666.315743.peg.2928	Transcriptional regulator, TetR family
2757	74	fig|6666666.315743.peg.2757	Transcriptional regulator, XRE family
2762	385	fig|6666666.315743.peg.2762	Transcriptional regulator, XRE family
2165	116	fig|6666666.315743.peg.2165	Translation elongation factors (GTPases)
2996	360	fig|6666666.315743.peg.2996	Tricarboxylate transport membrane protein TctA
2937	400	fig|6666666.315743.peg.2937	Trx
731	376	fig|6666666.315743.peg.731	Type I restriction-modification system, specificity subunit S (EC 3.1.21.3)
1842	155	fig|6666666.315743.peg.1842	Type IV pilin PilA
2984	124	fig|6666666.315743.peg.2984	Type IV secretion system protein VirD4
3420	961	fig|6666666.315743.peg.3420	Type IV secretory pathway, VirB4 components
3406	729	fig|6666666.315743.peg.3406	Type IV secretory pathway, VirD4 components
3411	301	fig|6666666.315743.peg.3411	unnamed protein product
4485	192	fig|6666666.315743.peg.4485	virion morphogenesis protein
2754	397	fig|6666666.315743.peg.2754	YeeC-like protein

7.4 Chapter 5

7.4.1 Crystal Violet Statistics

7.4.1.1 *P. aeruginosa*

ANOVA summary	
F	48.04
P value	<0.0001
P value summary	****
Significant diff. among means (P < 0.05)?	Yes
R square	0.9034

Dunnett's multiple comparisons test	Mean Diff.	95.00% CI of diff.	Significant?	Summary	Adjusted P Value
WT vs. 1	-0.941	-1.471 to -0.4107	Yes	****	<0.0001
WT vs. 2	-1.458	-1.988 to -0.9273	Yes	****	<0.0001
WT vs. 3	-0.9265	-1.457 to -0.3962	Yes	****	<0.0001
WT vs. 4	-1.017	-1.547 to -0.4867	Yes	****	<0.0001
WT vs. 5	-1.111	-1.641 to -0.5807	Yes	****	<0.0001
WT vs. 6	-1.849	-2.38 to -1.319	Yes	****	<0.0001
WT vs. 7	-1.091	-1.621 to -0.5607	Yes	****	<0.0001
WT vs. 8	-1.17	-1.701 to -0.6402	Yes	****	<0.0001
WT vs. 9	-0.936	-1.466 to -0.4057	Yes	****	<0.0001
WT vs. 10	-0.7293	-1.26 to -0.199	Yes	**	0.0010
WT vs. 11	-1.413	-1.943 to -0.8827	Yes	****	<0.0001
WT vs. 12	-0.7697	-1.3 to -0.2393	Yes	***	0.0004
WT vs. 13	-0.3873	-0.9177 to 0.143	No	ns	0.3391
WT vs. 14	-0.7855	-1.316 to -0.2552	Yes	***	0.0003
WT vs. 15	-0.9942	-1.525 to -0.4638	Yes	****	<0.0001
WT vs. 16	-0.5225	-1.053 to 0.007847	No	ns	0.0567
WT vs. 17	-0.6905	-1.221 to -0.1602	Yes	**	0.0024
WT vs. 18	-0.8303	-1.361 to -0.3	Yes	****	<0.0001
WT vs. 19	-0.547	-1.077 to -0.01665	Yes	*	0.0381
WT vs. 20	-0.615	-1.145 to -0.08465	Yes	*	0.0113
WT vs. 21	-0.1523	-0.6827 to 0.378	No	ns	0.9986
WT vs. 22	-0.9213	-1.452 to -0.391	Yes	****	<0.0001
WT vs. 23	-0.6685	-1.199 to -0.1382	Yes	**	0.0039
WT vs. 24	-0.3912	-0.9215 to 0.1392	No	ns	0.3257
WT vs. 25	-1.568	-2.099 to -1.038	Yes	****	<0.0001
WT vs. 26	-5.444	-5.975 to -4.914	Yes	****	<0.0001
WT vs. 27	-1.197	-1.727 to -0.6665	Yes	****	<0.0001
WT vs. 28	-1.246	-1.776 to -0.7157	Yes	****	<0.0001
WT vs. 29	-1.602	-2.133 to -1.072	Yes	****	<0.0001
WT vs. 30	-1.255	-1.785 to -0.7243	Yes	****	<0.0001
WT vs. 31	-0.9973	-1.528 to -0.467	Yes	****	<0.0001
WT vs. 32	-1.235	-1.766 to -0.7048	Yes	****	<0.0001
WT vs. 33	-1.467	-1.998 to -0.9372	Yes	****	<0.0001
WT vs. 34	-0.7808	-1.311 to -0.2505	Yes	***	0.0003
WT vs. 35	-1.439	-1.97 to -0.9088	Yes	****	<0.0001
WT vs. 36	-1.093	-1.623 to -0.5625	Yes	****	<0.0001

7.4.1.2 *S. aureus*

ANOVA summary	
F	104
P value	<0.0001
P value summary	****
Significant diff. among means (P < 0.05)?	Yes
R square	0.9529

Dunnett's multiple comparisons test	Mean Diff.	95.00% CI of diff.	Significant?	Summary	Adjusted P Value
WT vs. 1	-0.4277	-1.165 to 0.3095	No	ns	0.6865
WT vs. 2	-1.318	-2.055 to -0.5805	Yes	****	<0.0001
WT vs. 3	-1.143	-1.88 to -0.4055	Yes	***	0.0001
WT vs. 4	-2.134	-2.871 to -1.397	Yes	****	<0.0001
WT vs. 5	-0.9693	-1.706 to -0.2322	Yes	**	0.0021
WT vs. 6	-0.7443	-1.481 to -0.007178	Yes	*	0.0460
WT vs. 7	-1.376	-2.113 to -0.6388	Yes	****	<0.0001
WT vs. 8	-2.711	-3.448 to -1.974	Yes	****	<0.0001
WT vs. 9	-1.863	-2.6 to -1.126	Yes	****	<0.0001
WT vs. 10	-1.323	-2.06 to -0.5857	Yes	****	<0.0001
WT vs. 11	-0.5493	-1.286 to 0.1878	No	ns	0.3116
WT vs. 12	-0.9512	-1.688 to -0.214	Yes	**	0.0028
WT vs. 13	-1.016	-1.753 to -0.2783	Yes	**	0.0010
WT vs. 14	-4.018	-4.755 to -3.281	Yes	****	<0.0001
WT vs. 15	-2.889	-3.626 to -2.152	Yes	****	<0.0001
WT vs. 16	-4.599	-5.336 to -3.862	Yes	****	<0.0001
WT vs. 17	-3.571	-4.308 to -2.834	Yes	****	<0.0001
WT vs. 18	-0.2427	-0.9798 to 0.4945	No	ns	0.9983
WT vs. 19	-3.821	-4.558 to -3.084	Yes	****	<0.0001
WT vs. 20	-4.844	-5.581 to -4.107	Yes	****	<0.0001
WT vs. 21	-0.7587	-1.496 to -0.02151	Yes	*	0.0388
WT vs. 22	-0.6093	-1.346 to 0.1278	No	ns	0.1873
WT vs. 23	-0.6027	-1.34 to 0.1345	No	ns	0.1990
WT vs. 24	-1.486	-2.223 to -0.7488	Yes	****	<0.0001
WT vs. 25	-1.128	-1.865 to -0.3905	Yes	***	0.0002
WT vs. 26	-4.143	-4.88 to -3.406	Yes	****	<0.0001
WT vs. 27	-4.281	-5.018 to -3.544	Yes	****	<0.0001
WT vs. 28	-1.52	-2.257 to -0.7828	Yes	****	<0.0001
WT vs. 29	-5.318	-6.055 to -4.581	Yes	****	<0.0001
WT vs. 30	-0.2785	-1.016 to 0.4587	No	ns	0.9855
WT vs. 31	-0.1427	-0.8798 to 0.5945	No	ns	0.9992
WT vs. 32	-6.011	-6.748 to -5.274	Yes	****	<0.0001
WT vs. 33	-0.211	-0.9482 to 0.5262	No	ns	0.9986
WT vs. 34	-0.09183	-0.829 to 0.6453	No	ns	0.9995
WT vs. 35	-0.2518	-0.989 to 0.4853	No	ns	0.9933
WT vs. 36	-0.1993	-0.9365 to 0.5378	No	ns	0.9987

7.4.2 Growth Kinetics of Biofilm Derived Variants

A) PAV1 - PAV12

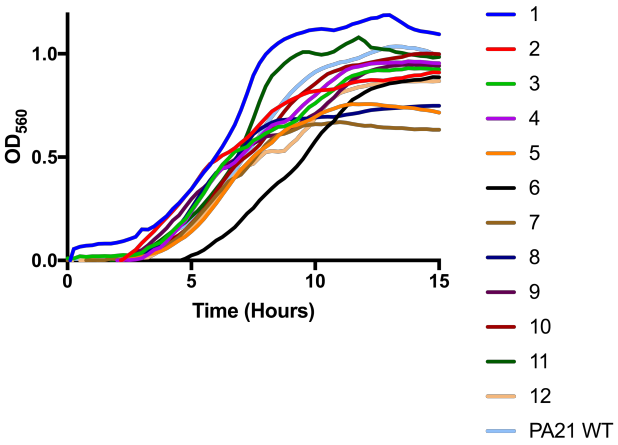

B) PAV13 - PAV24

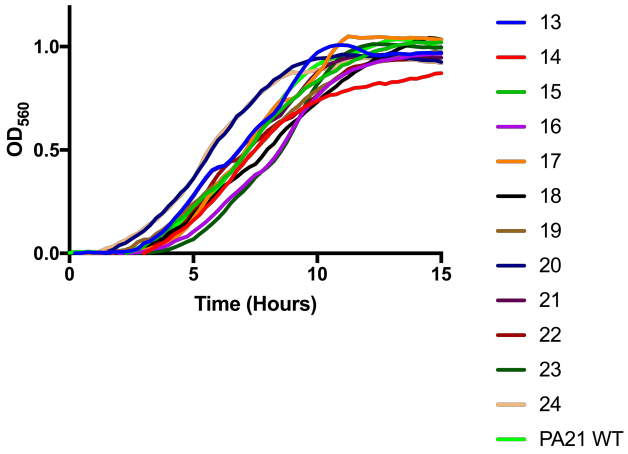

C) PAV25 - PAV36

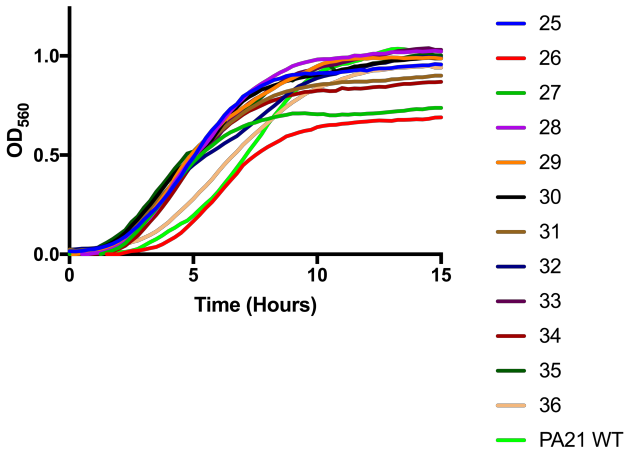

A) SAV1 - SAV12

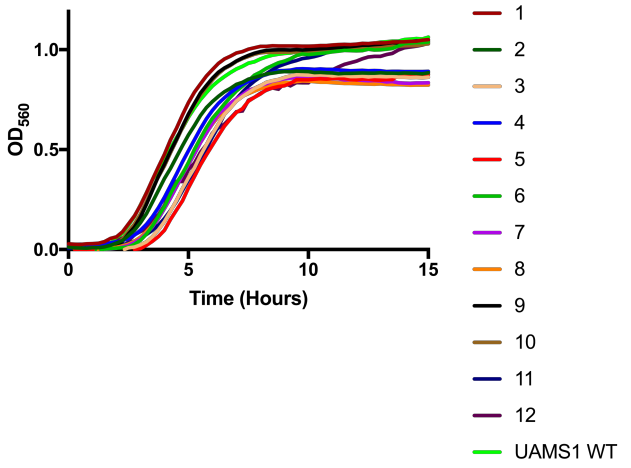

B) SAV13 - SAV24

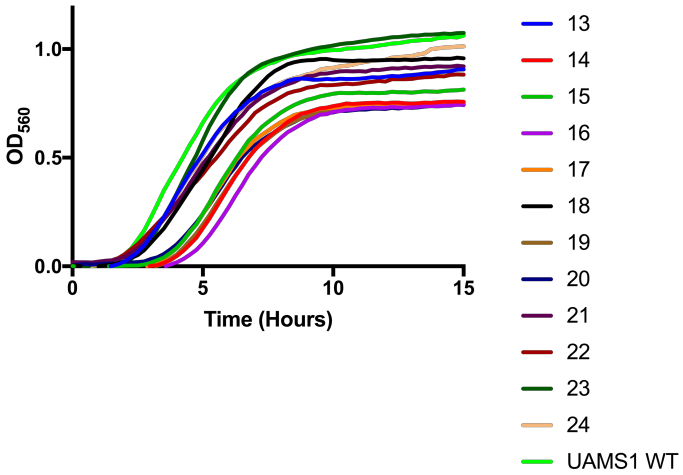

C) SAV25 - SAV36

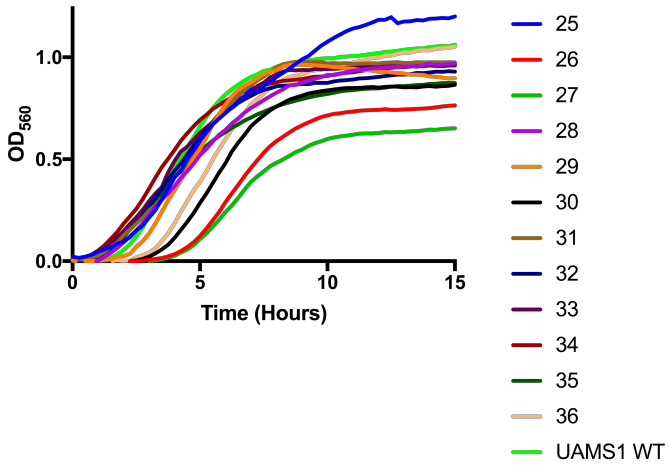

7.4.3 Statistical Comparisons of Rates

7.4.3.1 *P. aeruginosa*

ANOVA summary	
F	34.99
P value	<0.0001
P value summary	****
Significant diff. among means (P < 0.05)?	Yes
R square	0.8961

Dunnett's multiple comparisons test	Mean Diff.	95.00% CI of diff.	Significant?	Summary
WT vs. 1	0.02117	-0.07618 to 0.1185	No	ns
WT vs. 2	0.1721	0.07479 to 0.2695	Yes	****
WT vs. 3	0.09148	0.01741 to 0.1655	Yes	**
WT vs. 4	0.07739	0.00332 to 0.1515	Yes	*
WT vs. 5	-0.09002	-0.1545 to -0.02555	Yes	***
WT vs. 6	-0.5052	-0.6026 to -0.4079	Yes	****
WT vs. 7	0.01436	-0.0597 to 0.08843	No	ns
WT vs. 8	0.0851	0.02064 to 0.1496	Yes	**
WT vs. 9	0.1685	0.07118 to 0.2659	Yes	****
WT vs. 10	-0.009986	-0.07445 to 0.05448	No	ns
WT vs. 11	-0.05802	-0.125 to 0.008978	No	ns
WT vs. 12	-0.01335	-0.08742 to 0.06072	No	ns
WT vs. 13	0.1219	0.05489 to 0.1889	Yes	****
WT vs. 14	-0.02084	-0.1182 to 0.07651	No	ns
WT vs. 15	0.06042	-0.03692 to 0.1578	No	ns
WT vs. 16	-0.06185	-0.1263 to 0.002618	No	ns
WT vs. 17	-0.05133	-0.1254 to 0.02274	No	ns
WT vs. 18	0.07386	-0.02349 to 0.1712	No	ns
WT vs. 19	0.1171	0.01974 to 0.2144	Yes	**
WT vs. 20	0.1354	0.03801 to 0.2327	Yes	***
WT vs. 21	0.1262	0.05605 to 0.1963	Yes	****
WT vs. 22	0.04552	-0.02855 to 0.1196	No	ns
WT vs. 23	-0.2004	-0.2745 to -0.1264	Yes	****
WT vs. 24	0.1355	0.03813 to 0.2328	Yes	***
WT vs. 25	0.2123	0.1149 to 0.3096	Yes	****
WT vs. 26	0.009545	-0.0878 to 0.1069	No	ns
WT vs. 27	0.275	0.1777 to 0.3724	Yes	****
WT vs. 28	0.2092	0.1118 to 0.3065	Yes	****
WT vs. 29	0.245	0.1476 to 0.3423	Yes	****
WT vs. 30	0.2264	0.1291 to 0.3238	Yes	****
WT vs. 31	0.2025	0.1052 to 0.2999	Yes	****
WT vs. 32	0.2447	0.1474 to 0.342	Yes	****
WT vs. 33	0.2125	0.1151 to 0.3098	Yes	****
WT vs. 34	0.2349	0.1375 to 0.3322	Yes	****
WT vs. 35	0.2493	0.152 to 0.3467	Yes	****
WT vs. 36	0.1161	0.0188 to 0.2135	Yes	**

7.4.3.2 *S. aureus*

ANOVA summary	
F	19.68
P value	<0.0001
P value summary	****
Significant diff. among means (P < 0.05)?	Yes
R square	0.834

Dunnett's multiple comparisons test	Mean Diff.	95.00% CI of diff.	Significant?	Summary	Adjusted P Value
WT vs. 1	-0.009519	-0.09789 to 0.07885	No	ns	0.9996
WT vs. 2	-0.05015	-0.1302 to 0.02994	No	ns	0.5669
WT vs. 3	-0.3254	-0.4138 to -0.2371	Yes	****	<0.0001
WT vs. 4	-0.1445	-0.2329 to -0.05611	Yes	****	<0.0001
WT vs. 5	-0.424	-0.5124 to -0.3356	Yes	****	<0.0001
WT vs. 6	-0.2043	-0.2927 to -0.116	Yes	****	<0.0001
WT vs. 7	-0.2023	-0.2907 to -0.1139	Yes	****	<0.0001
WT vs. 8	-0.1847	-0.2731 to -0.09635	Yes	****	<0.0001
WT vs. 9	-0.03305	-0.1214 to 0.05532	No	ns	0.9857
WT vs. 10	-0.03828	-0.1266 to 0.05009	No	ns	0.9596
WT vs. 11	-0.2946	-0.383 to -0.2062	Yes	****	<0.0001
WT vs. 12	-0.1874	-0.2646 to -0.1103	Yes	****	<0.0001
WT vs. 13	-0.05142	-0.1671 to 0.06428	No	ns	0.9478
WT vs. 14	-0.2016	-0.3173 to -0.08586	Yes	****	<0.0001
WT vs. 15	-0.1261	-0.2418 to -0.01042	Yes	*	0.0225
WT vs. 16	-0.3493	-0.465 to -0.2336	Yes	****	<0.0001
WT vs. 17	-0.4163	-0.532 to -0.3006	Yes	****	<0.0001
WT vs. 18	-0.1465	-0.2622 to -0.03077	Yes	**	0.0038
WT vs. 19	-0.1123	-0.228 to 0.003442	No	ns	0.0641
WT vs. 20	-0.09096	-0.2067 to 0.02474	No	ns	0.2415
WT vs. 21	-0.08529	-0.201 to 0.03042	No	ns	0.3238
WT vs. 22	-0.05981	-0.1755 to 0.05589	No	ns	0.8299
WT vs. 23	-0.11	-0.1984 to -0.02165	Yes	**	0.0048
WT vs. 24	-0.07626	-0.1534 to 0.0008751	No	ns	0.0550
WT vs. 25	-0.1939	-0.274 to -0.1139	Yes	****	<0.0001
WT vs. 26	-0.2905	-0.4062 to -0.1748	Yes	****	<0.0001
WT vs. 27	-0.2667	-0.3824 to -0.151	Yes	****	<0.0001
WT vs. 28	-0.1179	-0.2336 to -0.002232	Yes	*	0.0424
WT vs. 29	-0.3454	-0.4611 to -0.2296	Yes	****	<0.0001
WT vs. 30	-0.3564	-0.4721 to -0.2407	Yes	****	<0.0001
WT vs. 31	-0.1364	-0.2521 to -0.02065	Yes	**	0.0095
WT vs. 32	-0.09993	-0.2156 to 0.01577	No	ns	0.1441
WT vs. 33	-0.07208	-0.1878 to 0.04362	No	ns	0.5747
WT vs. 34	-0.03689	-0.1526 to 0.07881	No	ns	0.9984
WT vs. 35	-0.05875	-0.1745 to 0.05696	No	ns	0.8488
WT vs. 36	-0.2435	-0.3592 to -0.1278	Yes	****	<0.0001

7.4.4 Assembly Metrics

Table S 1 Assembly and Annotation Statistics for *P. aeruginosa* PA21 and the associated biofilm derived variants. All genomes were assembled de novo with Unicycler. Reference genomes were assembled with a combination of Illumina short read and Oxford Nanopore long read data, with the maximum coverage equal to the sum of the two datasets. Coverage was calculated by aligning raw sequence reads to the reference genome with bwa mem, and subsequent calculation with samtools. Assembly and annotation information calculated by PROKKA and QUAST. Contigs refers to those greater than or equal to 500 bp.

Species	Isolate	Contigs	N50	Coverage Depth (x)	Bases (Mb)	CDS	tRNA
P. aeruginosa	**Reference**	**3**	**2 692 404**	**110**	**6.78**	**6206**	**74**
	1	104	123 466	113.6	6.73	6187	68
	2	110	133 947	102	6.71	6152	68
	3	117	121 825	59.9	6.75	6204	68
	4	100	136 708	61.8	6.72	6179	67
	5	95	136 708	86.7	6.72	6248	68
	6	96	136 142	130.3	6.75	6090	68
	7	107	123 426	68.7	6.74	6210	67
	8	85	233 983	295.4	6.76	6228	68
	9	146	912 18	31.2	6.62	6059	66
	10	105	126 469	73.1	6.75	6214	68
	11	105	135 637	71.0	6.76	6223	68
	12	91	168 097	98.3	6.76	6228	68
	13	103	136 708	173.0	6.74	6208	68
	14	113	123 466	51.1	6.71	6172	67
	15	118	119 829	43.6	6.66	6109	66
	16	89	168 097	180.0	6.76	6223	68
	17	88	185 716	133.4	6.76	6228	68
	18	96	140 570	118.8	6.76	6221	68
	19	102	124 688	86.8	6.76	6218	67
	20	90	142 487	173.7	6.76	6229	68
	21	99	135 596	126.2	6.76	6217	68
	22	131	119 641	42.8	6.72	6181	67
	23	100	136 699	69.6	6.71	6155	67
	24	105	123 466	102.8	6.66	6129	68
	25	97	168 097	93.6	6.75	6214	68
	26	114	135 507	110.5	6.75	6216	68
	27	103	136 028	94.9	6.75	6216	68
	28	107	123 466	73.9	6.75	6218	68

	29	102	126 489	95.5	6.75	6215	68
	30	99	133 947	137.1	6.75	6219	68
	31	116	123 463	57.2	6.70	6150	67
	32	104	158 694	61.8	6.72	6175	68
	33	101	124 661	100.6	6.76	6222	68
	34	156	64 644	76.3	5.55	5048	71
	35	107	126 189	75.2	6.71	6163	68
	36	106	123 463	101.4	6.75	6217	68

Table S 2: Assembly and Annotation Statistics for S.aureus UAMS-1 and the associated biofilm derived variants. All genomes were assembled de novo with Unicycler. Reference genomes were assembled with a combination of Illumina short read and Oxford Nanopore long read data, with the maximum coverage the sum of the two datasets. Coverage was calculated by aligning raw sequence reads to the reference genome with bwa mem, and subsequent calculation with samtools. Assembly and annotation information calculated by PROKKA and QUAST.

Species	Isolate	Contigs	N50	Coverage Depth (x)	Bases (Mb)	CDS	tRNA
S. aureus	**Reference**	**8**	**1 405 315**	**177**	**2.79**	**2570**	**60**
	1	37	142 178	141.5	2.74	2545	57
	2	40	124 398	213.4	2.74	2539	57
	3	39	138 508	136.4	2.73	2538	57
	4	39	142 178	69.9	2.74	2543	57
	5	41	120 069	53.2	2.73	2542	57
	6	37	142 178	103.1	2.74	2544	57
	7	37	142 178	117.7	2.74	2545	57
	8	39	142 178	138.2	2.74	2543	57
	9	37	142 178	283.6	2.74	2544	57
	10	37	142 178	167.1	2.74	2544	57
	11	37	142 178	181.2	2.74	2545	57
	12	37	142 178	89.7	2.74	2544	57
	13	38	124 398	252.2	2.74	2545	57
	14	43	124 398	36.1	2.72	2527	57
	15	37	142 178	81.5	2.74	2545	57
	16	38	124 398	61.8	2.74	2545	57
	17	38	124 398	208.6	2.74	2545	57
	18	37	142 178	148.6	2.74	2543	57
	19	37	142 178	91.3	2.74	2545	57
	20	37	142 178	71.8	2.74	2545	57
	21	37	142 178	88.2	2.74	2545	57

	22	37	142 178	161.4	2.74	2544	57
	23	37	124 398	106.2	2.74	2544	57
	24	38	124 398	70.5	2.74	2543	57
	25	40	124 398	142.5	2.74	2545	57
	26	39	142 178	206.5	2.74	2543	57
	27	39	150 122	171.1	2.72	2521	57
	28	40	120 996	48.1	2.74	2542	57
	29	37	142 178	207.5	2.74	2544	57
	30	39	150 122	69.4	2.72	2523	57
	31	37	142 178	79.6	2.74	2545	57
	32	37	142 178	87.3	2.74	2543	57
	33	37	142 179	169.6	2.74	2545	57
	34	37	142 178	101.2	2.74	2544	57
	35	37	142 178	114.4	2.74	2545	57
	36	37	142 178	88.3	2.74	2545	57

Chapter 8

References

8 References

1. Bosch, F. & Rosich, L. The contributions of Paul Ehrlich to pharmacology: A tribute on the occasion of the centenary of his Nobel prize. *Pharmacology* **82,** 171–179 (2008).
2. Houbraken, J., Frisvad, J. C. & Samson', R. A. Fleming's penicillin producing strain is not *Penicillium chrysogenum* but *P. rubens*. *IMA Fungus* **2,** 87–95 (2011).
3. Aminov, R. I. A brief history of the antibiotic era: lessons learned and challenges for the future. *Front. Microbiol.* **1,** 134 (2010).
4. Coates, A. R., Halls, G. & Hu, Y. Novel classes of antibiotics or more of the same? *Br. J. Pharmacol.* **163,** 184–194 (2011).
5. Ling, L. L. *et al.* A new antibiotic kills pathogens without detectable resistance. *Nature* **517,** 455–459 (2015).
6. Flemming, H.-C. *et al.* Biofilms: an emergent form of bacterial life. *Nat. Rev. Microbiol.* **14,** 563–575 (2016).
7. Hall, C. W. & Mah, T.-F. Molecular mechanisms of biofilm-based antibiotic resistance and tolerance in pathogenic bacteria. *FEMS Microbiol. Rev.* **41,** 276–301 (2017).
8. Boles, B. R., Thoendel, M. & Singh, P. K. Self-generated diversity produces 'insurance effects' in biofilm communities. *Proc. Natl. Acad. Sci.* **101,** 16630–16635 (2004).
9. Boles, B. R. & Singh, P. K. Endogenous oxidative stress produces diversity and adaptability in biofilm communities. *Proc. Natl. Acad. Sci.* **105,** 12503–12508 (2008).
10. Koo, H., Allan, R. N., Howlin, R. P., Stoodley, P. & Hall-Stoodley, L. Targeting microbial biofilms: current and prospective therapeutic strategies. *Nat. Rev. Microbiol.* **15,** 740 (2017).
11. Hu, Y., Shamaei-Tousi, A., Liu, Y. & Coates, A. A new approach for the discovery of antibiotics by targeting non-multiplying bacteria: A novel topical antibiotic for Staphylococcal infections. *PLoS One* **5,** e11818 (2010).
12. Hu, Y. & Coates, A. R. M. Enhancement by novel anti-methicillin-resistant *Staphylococcus aureus* compound HT61 of the activity of neomycin, gentamicin, mupirocin and chlorhexidine: *in vitro* and *in vivo* studies. *J. Antimicrob. Chemother.* **68,** 374–384 (2013).
13. Hubbard, A. T. M. *et al.* Mechanism of action of a membrane-active quinoline-based antimicrobial on natural and model bacterial membranes. *Biochemistry* **56,**

1163–1174 (2017).

14. Boucher, H. W. *et al.* Bad bugs, no drugs: no ESKAPE! An update from the Infectious diseases society of America. *Clin. Infect. Dis.* **48,** 1–12 (2009).
15. Tacconelli, E. *et al.* Discovery, research, and development of new antibiotics: the WHO priority list of antibiotic-resistant bacteria and tuberculosis. *Lancet. Infect. Dis.* **0,** (2017).
16. Popescu, A. & Doyle, R. J. The Gram stain after more than a century. *Biotech. Histochem.* **71,** 145–51 (1996).
17. Silhavy, T. J., Kahne, D. & Walker, S. The bacterial cell envelope. *Cold Spring Harb. Perspect. Biol.* **2,** a000414 (2010).
18. Brown, L., Wolf, J. M., Prados-Rosales, R. & Casadevall, A. Through the wall: extracellular vesicles in Gram-positive bacteria, mycobacteria and fungi. *Nat. Rev. Microbiol.* **13,** 620–630 (2015).
19. John, U. V. & Carvalho, J. *Enterococcus*: review of its physiology, pathogenesis, diseases and the challenges it poses for clinical microbiology. *Front. Biol. (Beijing).* **6,** 357–366 (2011).
20. Pendleton, J. N., Gorman, S. P. & Gilmore, B. F. Clinical relevance of the ESKAPE pathogens. *Expert Rev. Anti. Infect. Ther.* **11,** 297–308 (2013).
21. Foster, T. J. The *Staphylococcus aureus* 'superbug'. *J. Clin. Invest.* **114,** 1693–1696 (2004).
22. Deurenberg, R. H. & Stobberingh, E. E. The evolution of *Staphylococcus aureus*. *Infect. Genet. Evol.* **8,** 747–763 (2008).
23. Boswihi, S. S. & Udo, E. E. Methicillin-resistant *Staphylococcus aureus*: An update on the epidemiology, treatment options and infection control. *Curr. Med. Res. Pract.* **8,** 18–24 (2018).
24. Chang, S. *et al.* Infection with vancomycin-resistant *Staphylococcus aureus* containing the *vanA* resistance gene. *N. Engl. J. Med.* **348,** 1342–1347 (2003).
25. Podschun, R. & Ullmann, U. *Klebsiella spp.* as nosocomial pathogens: epidemiology , taxonomy, typing methods and pathogenicity factors. *Clin. Microbiol. Rev.* **11,** 589–603 (1998).
26. Friedman, N. D., Carmeli, Y., Walton, A. L. & Schwaber, M. J. Carbapenem-Resistant Enterobacteriaceae: a strategic roadmap for infection control. *Infect. Control Hosp. Epidemiol.* **38,** 580–594 (2017).
27. Yong, D. *et al.* Characterization of a new metallo-β-lactamase gene, *bla* NDM-1, and a novel erythromycin esterase gene carried on a unique genetic structure in *Klebsiella pneumoniae* sequence type 14 from India. *Antimicrob. Agents*

Chemother. **53,** 5046–5054 (2009).

28. Harding, C. M., Hennon, S. W. & Feldman, M. F. Uncovering the mechanisms of *Acinetobacter baumannii* virulence. *Nat. Rev. Microbiol.* **16,** 91–102 (2017).
29. Giammanco, A., Calà, C., Fasciana, T. & Dowzicky, M. J. Global assessment of the activity of tigecycline against multidrug-resistant Gram-negative pathogens between 2004 and 2014 as part of the tigecycline evaluation and surveillance trial. *mSphere* **2,** (2017).
30. Cisneros, J. M. *et al.* Bacteremia due to *Acinetobacter baumannii*: epidemiology, clinical findings, and prognostic features. *Clin. Infect. Dis.* **22,** 1026–1032 (1996).
31. Scott, P. *et al.* An outbreak of multidrug-resistant *Acinetobacter baumannii*-calcoaceticus complex infection in the US military health care system associated with military operations in Iraq. *Clin. Infect. Dis.* **44,** 1577–1584 (2007).
32. Gellatly, S. L. & Hancock, R. E. W. *Pseudomonas aeruginosa*: new insights into pathogenesis and host defenses. *Pathog. Dis.* **67,** 159–173 (2013).
33. Moradali, M. F., Ghods, S. & Rehm, B. H. A. *Pseudomonas aeruginosa* lifestyle: a paradigm for adaptation, survival, and persistence. *Front. Cell. Infect. Microbiol.* **7,** 39 (2017).
34. Davin-Regli, A. & Pagès, J.-M. *Enterobacter aerogenes* and *Enterobacter cloacae*; versatile bacterial pathogens confronting antibiotic treatment. *Front. Microbiol.* **6,** 392 (2015).
35. Szabó, D. *et al.* SHV-type extended-spectrum beta-lactamase production is associated with reduced cefepime susceptibility in *Enterobacter cloacae*. *J. Clin. Microbiol.* **43,** 5058–5064 (2005).
36. Majewski, P. *et al.* Emergence of OXA-48 carbapenemase-producing *Enterobacter cloacae* ST89 infection in Poland. *Int. J. Infect. Dis.* **25,** 107–109 (2014).
37. Hubaux, N., Wells, G. & Morgenroth, E. Impact of coexistence of flocs and biofilm on performance of combined nitritation-anammox granular sludge reactors. *Water Res.* **68,** 127–139 (2015).
38. Hobley, L., Harkins, C., Macphee, C. E. & Stanley-Wall, N. R. Giving structure to the biofilm matrix: an overview of individual strategies and emerging common themes. *FEMS Microbiol. Rev.* **015,** 649–669 (2015).
39. National Institutes of Health. NIH Public Announcements PA-03-047. (2002).
40. Valenza, G. *et al.* Prevalence and antimicrobial susceptibility of microorganisms isolated from sputa of patients with cystic fibrosis. *J. Cyst. Fibros.* **7,** 123–127 (2008).
41. Dobretsov, S., Abed, R. M. M. & Teplitski, M. Mini-review: inhibition of

biofouling by marine microorganisms. *Biofouling* **29,** 423–441 (2013).

42. Srey, S., Kabir, I. & Jessore, J. Biofilm formation in food industries : a food safety concern . Food Control. *Food Control* **31,** 572–581 (2013).
43. Bleich, R., Watrous, J. D., Dorrestein, P. C., Bowers, A. A. & Shank, E. A. Thiopeptide antibiotics stimulate biofilm formation in *Bacillus subtilis*. *Proc. Natl. Acad. Sci.* **112,** 3086–3091 (2015).
44. Hoffman, L., D'Argenio, D. & MacCoss, M. Aminoglycoside antibiotics induce bacterial biofilm formation. *Nature* **436,** 1171–1175 (2005).
45. Rutherford, S. T. & Bassler, B. L. Bacterial quorum sensing: its role in virulence and possibilities for its control. *Cold Spring Harb. Perspect. Med.* **2,** (2012).
46. Verbeke, F. *et al.* Peptides as quorum sensing molecules: measurement techniques and obtained levels *in vitro* and *in vivo*. *Front. Neurosci.* **11,** 183 (2017).
47. Pereira, C. S., Thompson, J. A. & Xavier, K. B. AI-2-mediated signalling in bacteria. *FEMS Microbiol. Rev.* **37,** 156–181 (2013).
48. Lee, J. *et al.* A cell-cell communication signal integrates quorum sensing and stress response. *Nat. Chem. Biol.* **9,** 339–343 (2013).
49. Lee, J. & Zhang, L. The hierarchy quorum sensing network in *Pseudomonas aeruginosa. Protein Cell* **6,** 26–41 (2015).
50. Le, K. Y. & Otto, M. Quorum-sensing regulation in staphylococci-an overview. *Front. Microbiol.* **6,** 1174 (2015).
51. Mund, A., Diggle, S. P. & Harrison, F. The fitness of *Pseudomonas aeruginosa* quorum sensing signal cheats is influenced by the diffusivity of the environment. *MBio* **8,** (2017).
52. Valentini, M. & Filloux, A. Biofilms and cyclic di-GMP (c-di-GMP) signaling: lessons from *Pseudomonas aeruginosa* and other bacteria. *J. Biol. Chem.* **291,** 12547–55 (2016).
53. Liu, C. *et al.* Insights into biofilm dispersal regulation from the crystal structure of the PAS-GGDEF-EAL region of RbdA from *Pseudomonas aeruginosa*. *J. Bacteriol.* **200,** e00515-17 (2017).
54. McDougald, D., Rice, S. A., Barraud, N., Steinberg, P. D. & Kjelleberg, S. Should we stay or should we go: mechanisms and ecological consequences for biofilm dispersal. *Nat. Rev. Microbiol.* **10,** 39–50 (2011).
55. Corrigan, R. M., Abbott, J. C., Burhenne, H., Kaever, V. & Gründling, A. C-di-amp is a new second messenger in *Staphylococcus aureus* with a role in controlling cell size and envelope stress. *PLoS Pathog.* **7,** (2011).
56. Oppenheimer-Shaanan, Y., Wexselblatt, E., Katzhendler, J., Yavin, E. & Ben-

Yehuda, S. c-di-AMP reports DNA integrity during sporulation in *Bacillus subtilis*. *EMBO Rep.* **12,** 594–601 (2011).

57. Woodward, J. J., Iavarone, A. T. & Portnoy, D. A. c-di-AMP secreted by intracellular *Listeria monocytogenes* activates a host Type I interferon response. *Science (80-.).* **328,** 1703–1705 (2010).
58. Fahmi, T., Port, G. C. & Cho, K. H. c-di-AMP: an essential molecule in the signaling pathways that regulate the viability and virulence of Gram-positive bacteria. *Genes (Basel).* **8,** (2017).
59. Hermansson, M. The DLVO theory in microbial adhesion. *Colloids Surfaces B Biointerfaces* **14,** 105–119 (1999).
60. Bayoudh, S., Othmane, A., Mora, L. & Ben Ouada, H. Assessing bacterial adhesion using DLVO and XDLVO theories and the jet impingement technique. *Colloids Surfaces B Biointerfaces* **73,** 1–9 (2009).
61. Ramsey, M. M. & Whiteley, M. *Pseudomonas aeruginosa* attachment and biofilm development in dynamic environments. *Mol. Microbiol.* **53,** 1075–1087 (2004).
62. Secor, P. R. *et al.* Filamentous bacteriophage promote biofilm assembly and function. *Cell Host Microbe* **18,** 549–559 (2015).
63. Boles, B. R. & Horswill, A. R. Agr-mediated dispersal of *Staphylococcus aureus* biofilms. *PLoS Pathog.* **4,** e1000052 (2008).
64. Davies, D. G. *et al.* The involvement of cell-to-cell signals in the development of a bacterial biofilm. *Science* **280,** 295–8 (1998).
65. Haagensen, J. A. J. *et al.* Differentiation and distribution of colistin- and sodium dodecyl sulfate-tolerant cells in *Pseudomonas aeruginosa* biofilms. *J. Bacteriol.* **189,** 28–37 (2007).
66. Moscoso, M., García, E. & López, R. Pneumococcal biofilms. *Int. Microbiol.* **12,** 77–85 (2009).
67. Kaplan, J. B. Biofilm Dispersal: Mechanisms, Clinical Implications, and Potential Therapeutic Uses. *J. Dent. Res.* **89,** 205–218 (2010).
68. Purevdorj-Gage, B., Costerton, W. J. & Stoodley, P. Phenotypic differentiation and seeding dispersal in non-mucoid and mucoid *Pseudomonas aeruginosa* biofilms. *Microbiology* **151,** 1569–1576 (2005).
69. Barraud, N. *et al.* Involvement of nitric oxide in biofilm dispersal of *Pseudomonas aeruginosa*. *J. Bacteriol.* **188,** 7344–7353 (2006).
70. Webb, J. S. *et al.* Cell death in *Pseudomonas aeruginosa* biofilm development. *J. Bacteriol.* **185,** 4585–92 (2003).
71. Kolodkin-Gal, I. *et al.* D-amino acids trigger biofilm disassembly. *Science (80-.).*

328, 627–629 (2010).

72. Stewart, P. S. & Franklin, M. J. Physiological heterogeneity in biofilms. *Nat. Rev. Microbiol.* **6,** 199–210 (2008).
73. Rani, S. A. *et al.* Spatial patterns of DNA replication, protein synthesis, and oxygen concentration within bacterial biofilms reveal diverse physiological states. *J. Bacteriol.* **189,** 4223–4233 (2007).
74. Vroom, J. M. *et al.* Depth penetration and detection of pH gradients in biofilms by two-photon excitation microscopy. *Appl. Environ. Microbiol.* **65,** 3502–11 (1999).
75. Okabe, S., Itoh, T., Satoh, H. & Watanabe, Y. Analyses of spatial distributions of sulfate-reducing bacteria and their activity in aerobic wastewater biofilms. *Appl. Environ. Microbiol.* **65,** 5107–16 (1999).
76. Williamson, K. S. *et al.* Heterogeneity in *Pseudomonas aeruginosa* biofilms includes expression of ribosome hibernation factors in the antibiotic-tolerant subpopulation and hypoxia-induced stress response in the metabolically active population. *J. Bacteriol.* **194,** 2062–2073 (2012).
77. Proctor, R. A. *et al.* Small colony variants: a pathogenic form of bacteria that facilitates persistent and recurrent infections. *Nat. Rev. Microbiol.* **4,** 295–305 (2006).
78. Starkey, M. *et al. Pseudomonas aeruginosa* rugose small-colony variants have adaptations that likely promote persistence in the cystic fibrosis lung. *J. Bacteriol.* **191,** 3492–503 (2009).
79. Pestrak, M. J. *et al. Pseudomonas aeruginosa* rugose small-colony variants evade host clearance, are hyper-inflammatory, and persist in multiple host environments. *PLOS Pathog.* **14,** e1006842 (2018).
80. Singh, R., Ray, P., Das, A. & Sharma, M. Role of persisters and small-colony variants in antibiotic resistance of planktonic and biofilm-associated *Staphylococcus aureus*: an *in vitro* study. *J. Med. Microbiol.* **58,** 1067–1073 (2009).
81. Brandis, G., Cao, S., Huseby, D. L. & Hughes, D. Having your cake and eating it - *Staphylococcus aureus* small colony variants can evolve faster growth rate without losing their antibiotic resistance. *Microb. cell (Graz, Austria)* **4,** 275–277 (2017).
82. Cooper, V. S., Staples, R. K., Traverse, C. C. & Ellis, C. N. Parallel evolution of small colony variants in *Burkholderia cenocepacia* biofilms. *Genomics* **104,** 447–452 (2014).
83. Tashiro, Y., Eida, H., Ishii, S., Futamata, H. & Okabe, S. Generation of small colony variants in biofilms by *Escherichia coli* harboring a conjugative F plasmid. *Microbes Environ.* **32,** 40–46 (2017).

84. Churton, N. W. V *et al.* Parallel evolution in *Streptococcus pneumoniae* biofilms. *Genome Biol. Evol.* **8,** 1316–1326 (2016).
85. Allegrucci, M. & Sauer, K. Characterization of colony morphology variants isolated from *Streptococcus pneumoniae* biofilms. *J. Bacteriol.* **189,** 2030–2038 (2007).
86. Allegrucci, M. & Sauer, K. Formation of *Streptococcus pneumoniae* non-phase-variable colony variants is due to increased mutation frequency present under biofilm growth conditions. *J. Bacteriol.* **190,** 6330–6339 (2008).
87. Biswas, L., Biswas, R., Schlag, M., Bertram, R. & Götz, F. Small-colony variant selection as a survival strategy for *Staphylococcus aureus* in the presence of *Pseudomonas aeruginosa*. *Appl. Environ. Microbiol.* **75,** 6910–2 (2009).
88. Huse, H. K. *et al.* Parallel evolution in *Pseudomonas aeruginosa* over 39,000 generations *in vivo*. *MBio* **1,** e00199-10 (2010).
89. McElroy, K. E. *et al.* Strain-specific parallel evolution drives short-term diversification during *Pseudomonas aeruginosa* biofilm formation. *Proc. Natl. Acad. Sci.* **111,** E1419–E1427 (2014).
90. Sommer, L. M. *et al.* Bacterial evolution in PCD and CF patients follows the same mutational steps. *Sci. Rep.* **6,** 28732 (2016).
91. Driffield, K., Miller, K., Bostock, J. M., O'neill, A. J. & Chopra, I. Increased mutability of *Pseudomonas aeruginosa* in biofilms. *J. Antimicrob. Chemother.* **61,** 1053–1056 (2008).
92. Ryder, V. J., Chopra, I. & O'Neill, A. J. Increased mutability of *Staphylococci* in biofilms as a consequence of oxidative stress. *PLoS One* **7,** e47695 (2012).
93. Conibear, T. C. R., Collins, S. L. & Webb, J. S. Role of mutation in *Pseudomonas aeruginosa* biofilm development. *PLoS One* **4,** e6289 (2009).
94. Savage, V. J., Chopra, I. & O'Neill, A. J. *Staphylococcus aureus* biofilms promote horizontal transfer of antibiotic resistance. *Antimicrob. Agents Chemother.* **57,** 1968–1970 (2013).
95. Li, Y. H., Lau, P. C., Lee, J. H., Ellen, R. P. & Cvitkovitch, D. G. Natural genetic transformation of *Streptococcus mutans* growing in biofilms. *J. Bacteriol.* **183,** 897–908 (2001).
96. Stalder, T. & Top, E. Plasmid transfer in biofilms: a perspective on limitations and opportunities. *npj Biofilms Microbiomes* **2,** 16022 (2016).
97. Christensen, B. B., Sternberg, C. & Molin, S. Bacterial plasmid conjugation on semi-solid surfaces monitored with the green fluorescent protein (GFP) from *Aequorea victoria* as a marker. *Gene* **173,** 59–65 (1996).
98. Millan, A. S. *et al.* Positive selection and compensatory adaptation interact to

stabilize non-transmissible plasmids. *Nat. Commun.* **5,** 5208 (2014).

99. Fox, R. E., Zhong, X., Krone, S. M. & Top, E. M. Spatial structure and nutrients promote invasion of IncP-1 plasmids in bacterial populations. *ISME J.* **2,** 1024–1039 (2008).
100. Banas, J. A. *et al.* Evidence that accumulation of mutants in a biofilm reflects natural selection rather than stress-induced adaptive mutation. *Appl. Environ. Microbiol.* **73,** 357–361 (2007).
101. Cooper, V. S. Experimental evolution as a high-throughput screen for genetic adaptations. *mSphere* **3,** e00121-18 (2018).
102. Steenackers, H. P., Parijs, I., Foster, K. R. & Vanderleyden, J. Experimental evolution in biofilm populations. *FEMS Microbiol. Rev.* **40,** 373–397 (2016).
103. Klausen, M., Aaes-Jørgensen, A., Molin, S. & Tolker-Nielsen, T. Involvement of bacterial migration in the development of complex multicellular structures in *Pseudomonas aeruginosa* biofilms. *Mol. Microbiol.* **50,** 61–68 (2003).
104. Traverse, C. C., Mayo-Smith, L. M., Poltak, S. R. & Cooper, V. S. Tangled bank of experimentally evolved *Burkholderia* biofilms reflects selection during chronic infections. *Proc. Natl. Acad. Sci. U. S. A.* **110,** E250-9 (2013).
105. Rakoff-Nahoum, S., Foster, K. R. & Comstock, L. E. The evolution of cooperation within the gut microbiota. *Nature* **533,** 255–9 (2016).
106. Brauner, A., Fridman, O., Gefen, O. & Balaban, N. Q. Distinguishing between resistance, tolerance and persistence to antibiotic treatment. *Nat. Rev. Microbiol.* **14,** 320–330 (2016).
107. Brooun, A., Liu, S. & Lewis, K. A dose-response study of antibiotic resistance in *Pseudomonas aeruginosa* biofilms. *Antimicrob. Agents Chemother.* **44,** 640–646 (2000).
108. Stewart, P. S. Antimicrobial tolerance in biofilms. *Microb. Biofilms, 2nd Ed.* **3,** 269–285 (2015).
109. Thien-fah, C. M. & Toole, G. A. O. Mechanisms of biofilm resistance to antimicrobial agents. *Trends Microbiol.* **9,** 34–39 (2001).
110. Singh, R., Sahore, S., Kaur, P., Rani, A. & Ray, P. Penetration barrier contributes to bacterial biofilm-associated resistance against only select antibiotics, and exhibits genus-, strain- and antibiotic-specific differences. *Pathog. Dis.* **74,** (2016).
111. Stewart, P. S. Diffusion in biofilms. *J. Bacteriol.* **185,** 1485–1491 (2003).
112. Anderl, J. N., Franklin, M. J. & Stewart, P. S. Role of antibiotic penetration limitation in *Klebsiella pneumoniae* biofilm resistance to ampicillin and ciprofloxacin. *Antimicrob. Agents Chemother.* **44,** 1818–1824 (2000).

113. Nichols, W. W., Dorrington, S. M., Slack, M. P. E. & Walmsley, H. L. Inhibition of tobramycin diffusion by binding to alginate. *Antimicrob. Agents Chemother.* **32,** 518–523 (1988).
114. Billings, N. *et al.* The extracellular matrix component Psl provides fast-acting antibiotic defense in *Pseudomonas aeruginosa* biofilms. *PLoS Pathog.* **9,** e1003526 (2013).
115. Doroshenko, N. *et al.* Extracellular DNA impedes the transport of vancomycin in Staphylococcus epidermidis biofilms preexposed to subinhibitory concentrations of vancomycin. *Antimicrob. Agents Chemother.* **58,** 7273–7282 (2014).
116. Borriello, G. *et al.* Oxygen limitation contributes to antibiotic tolerance of *Pseudomonas aeruginosa* in biofilms. *Antimicrob. Agents Chemother.* **48,** 2659–2664 (2004).
117. Eng, R. H. K., Padberg, F. T., Smith, S. M., Tan, E. N. & Cherubin, C. E. Bactericidal effects of antibiotics. *Antimicrob. Agents Chemother.* **35,** 1824–1828 (1991).
118. Pamp, S. J., Gjermansen, M., Johansen, H. K. & Tolker-Nielsen, T. Tolerance to the antimicrobial peptide colistin in *Pseudomonas aeruginosa* biofilms is linked to metabolically active cells, and depends on the *pmr* and *mexAB-oprM* genes. *Mol. Microbiol.* **68,** 223–240 (2008).
119. Thomas, J. *et al.* The affect of pH and bacterial phenotypic state on antibiotic efficacy. *Int. Wound J.* **9,** 428–435 (2012).
120. Wilton, M., Charron-Mazenod, L., Moore, R. & Lewenza, S. Extracellular DNA acidifies biofilms and induces aminoglycoside resistance in *Pseudomonas aeruginosa*. *Antimicrob. Agents Chemother.* **60,** 544–553 (2016).
121. Lewis, K. Persister Cells. *Annu. Rev. Microbiol.* **64,** 357–372 (2010).
122. Li, Y. & Zhang, Y. PhoU is a persistence switch involved in persister formation and tolerance to multiple antibiotics and stresses in *Escherichia coli*. *Antimicrob. Agents Chemother.* **51,** 2092–2099 (2007).
123. Carvalho, G., Balestrino, D., Forestier, C. & Mathias, J.-D. How do environment-dependent switching rates between susceptible and persister cells affect the dynamics of biofilms faced with antibiotics? *npj Biofilms Microbiomes* **4,** 6 (2018).
124. Fasani, R. A. & Savageau, M. A. Molecular mechanisms of multiple toxin-antitoxin systems are coordinated to govern the persister phenotype. *Proc. Natl. Acad. Sci.* **110,** E2528–E2537 (2013).
125. Nguyen, D. *et al.* Active Starvation Responses Mediate Antibiotic Tolerance in Biofilms and Nutrient-Limited Bacteria. *Science (80-.).* **334,** 982–986 (2011).

126. Conlon, B. P. *et al.* Persister formation in *Staphylococcus aureus* is associated with ATP depletion. *Nat. Microbiol.* **1,** 16051 (2016).
127. Stewart, P. S. *et al.* Contribution of stress responses to antibiotic tolerance in *Pseudomonas aeruginosa* biofilms. *Antimicrob. Agents Chemother.* **59,** 3838–3847 (2015).
128. Mah, T. *et al.* A genetic basis for *Pseudomonas aeruginosa* biofilm antibiotic resistance. *Nature* **426,** 306–10 (2003).
129. Baugh, S., Phillips, C. R., Ekanayaka, A. S., Piddock, L. J. V & Webber, M. A. Inhibition of multidrug efflux as a strategy to prevent biofilm formation. *J. Antimicrob. Chemother.* **69,** 673–681 (2014).
130. Bjarnsholt, T. *et al. Pseudomonas aeruginosa* tolerance to tobramycin, hydrogen peroxide and polymorphonuclear leukocytes is quorum-sensing dependent. *Microbiology* **151,** 373–383 (2005).
131. Que, Y. A. *et al.* A quorum sensing small volatile molecule promotes antibiotic tolerance in bacteria. *PLoS One* **8,** e80140 (2013).
132. Larsen, T. & Fiehn, N.-E. Dental biofilm infections - an update. *APMIS* **125,** 376–384 (2017).
133. Baldan, R. *et al.* Adaptation of *Pseudomonas aeruginosa* in cystic fibrosis airways influences virulence of *Staphylococcus aureus in vitro* and murine models of co-Infection. *PLoS One* **9,** e89614 (2014).
134. Dunne, E. M. *et al.* Carriage of *Streptococcus pneumoniae, Haemophilus influenzae, Moraxella catarrhalis*, and *Staphylococcus aureus* in Indonesian children: a cross-sectional study. *PLoS One* **13,** e0195098 (2018).
135. Burmølle, M., Ren, D., Bjarnsholt, T. & Sørensen, S. J. Interactions in multispecies biofilms: do they actually matter? *Trends Microbiol.* **22,** 84–91 (2014).
136. Hotterbeekx, A., Kumar-Singh, S., Goossens, H. & Malhotra-Kumar, S. *In vivo* and *in vitro* interactions between *Pseudomonas aeruginosa* and *Staphylococcus spp*. *Front. Cell. Infect. Microbiol.* **7,** 106 (2017).
137. Cox, M. J. *et al.* Airway Microbiota and Pathogen Abundance in Age-Stratified Cystic Fibrosis Patients. *PLoS One* **5,** e11044 (2010).
138. Fazli, M. *et al.* Nonrandom distribution of *Pseudomonas aeruginosa* and *Staphylococcus aureus* in chronic wounds. *J. Clin. Microbiol.* **47,** 4084–9 (2009).
139. Sagel, S. D. *et al.* Impact of *Pseudomonas* and *Staphylococcus* infection on inflammation and clinical status in young children with cystic fibrosis. *J. Pediatr.* **154,** 183–188.e3 (2009).
140. Seth, A. K. *et al.* Comparative analysis of single-species and polybacterial wound

biofilms using a quantitative, *in vivo*, rabbit ear model. *PLoS One* **7,** e42897 (2012).

141. Pastar, I. *et al.* Interactions of methicillin resistant *Staphylococcus aureus* USA300 and *Pseudomonas aeruginosa* in polymicrobial wound infection. *PLoS One* **8,** e56846 (2013).
142. Seth, A. K. *et al.* Quantitative comparison and analysis of species-specific wound biofilm virulence using an *in vivo*, rabbit-ear model. *J. Am. Coll. Surg.* **215,** 388–399 (2012).
143. Cigana, C. *et al. Staphylococcus aureus* impacts *Pseudomonas aeruginosa* chronic respiratory disease in murine models. *J. Infect. Dis.* **217,** 933–942 (2018).
144. Ahlgren, H. G. *et al.* Clinical outcomes associated with *Staphylococcus aureus* and *Pseudomonas aeruginosa* airway infections in adult cystic fibrosis patients. *BMC Pulm. Med.* **15,** 67 (2015).
145. Orazi, G. & O'Toole, G. A. *Pseudomonas aeruginosa* alters *Staphylococcus aureus* sensitivity to vancomycin in a biofilm model of cystic fibrosis infection. *MBio* **8,** e00873-17 (2017).
146. Filkins, L. M. *et al.* Coculture of *Staphylococcus aureus* with *Pseudomonas aeruginosa* drives *S. aureus* towards fermentative metabolism and reduced viability in a cystic fibrosis model. *J. Bacteriol.* **197,** 2252–2264 (2015).
147. Radlinski, L. *et al. Pseudomonas aeruginosa* exoproducts determine antibiotic efficacy against *Staphylococcus aureus*. *PLOS Biol.* **15,** e2003981 (2017).
148. Beaudoin, T. *et al. Staphylococcus aureus* interaction with *Pseudomonas aeruginosa* biofilm enhances tobramycin resistance. *npj Biofilms Microbiomes* **3,** 25 (2017).
149. Mashburn, L. M., Jett, A. M., Akins, D. R. & Whiteley, M. *Staphylococcus aureus* serves as an iron source for *Pseudomonas aeruginosa* during in vivo coculture. *J. Bacteriol.* **187,** 554–566 (2005).
150. Limoli, D. H. *et al. Pseudomonas aeruginosa* alginate overproduction promotes coexistence with *Staphylococcus aureus* in a model of cystic fibrosis respiratory infection. *MBio* **8,** e00186-17 (2017).
151. DeLeon, S. *et al.* Synergistic interactions of *Pseudomonas aeruginosa* and *Staphylococcus aureus* in an *in vitro* wound model. *Infect. Immun.* **82,** 4718–4728 (2014).
152. Banin, E., Vasil, M. L. & Greenberg, E. P. Iron and *Pseudomonas aeruginosa* biofilm formation. *Proc. Natl. Acad. Sci. U. S. A.* **102,** 11076–81 (2005).
153. Hunter, R. C. *et al.* Ferrous Iron Is a Significant Component of Bioavailable Iron in Cystic Fibrosis Airways. *MBio* **4,** e00557-13-e00557-13 (2013).

154. Tognon, M. *et al.* Co-evolution with *Staphylococcus aureus* leads to lipopolysaccharide alterations in *Pseudomonas aeruginosa*. *ISME J.* **11,** 2233–2243 (2017).
155. Davies, J. & Davies, D. Origins and evolution of antibiotic resistance. *Microbiol. Mol. Biol. Rev.* **74,** 417–433 (2010).
156. D'Costa, V. M. *et al.* Antibiotic resistance is ancient. *Nature* **477,** 457–461 (2011).
157. Nyquist, A.-C. Antibiotic prescribing for children with colds, upper respiratory tract infections, and bronchitis. *Jama* **279,** 875 (1998).
158. Chastre, J. *et al.* Comparison of 8 vs 15 days of antibiotic therapy for ventilator-associated pneumonia in adults. *Jama* **290,** 2588 (2003).
159. Acar, J., Casewell, M., Freeman, J., Friis, C. & Goossens, H. Avoparcin and virginiamycin as animal growth promoters: A plea for science in decision-making. *Clin. Microbiol. Infect.* **6,** 477–482 (2000).
160. Coque, T. M., Tomayko, J. F., Ricke, S. C., Okhyusen, P. C. & Murray, B. E. Vancomycin-resistant enterococci from nosocomial, community, and animal sources in the United States. *Antimicrob. Agents Chemother.* **40,** 2605–2609 (1996).
161. Aarestrup, F. M. *et al.* Effect of abolishment of the use of antimicrobial agents for growth promotion on occurrence of antimicrobial resistance in fecal enterococci from food animals in Denmark. *Antimicrob. Agents Chemother.* **45,** 2054–2059 (2001).
162. Liu, Y. Y. *et al.* Emergence of plasmid-mediated colistin resistance mechanism MCR-1 in animals and human beings in China: a microbiological and molecular biological study. *Lancet Infect. Dis.* **16,** 161–168 (2016).
163. Lindberg, R. H. *et al.* Environmental risk assessment of antibiotics in the Swedish environment with emphasis on sewage treatment plants. *Water Res.* **41,** 613–619 (2007).
164. Graham, D. W. *et al.* Antibiotic resistance gene abundances associated with waste discharges to the Almendares river near Havana, Cuba. *Environ. Sci. Technol.* **45,** 418–424 (2011).
165. Kumar, A. & Schweizer, H. P. Bacterial resistance to antibiotics: active efflux and reduced uptake. *Adv. Drug Deliv. Rev.* **57,** 1486–1513 (2005).
166. Piddock, L. J. V. Multidrug-resistance efflux pumps — not just for resistance. *Nat. Rev. Microbiol.* **4,** 629–636 (2006).
167. Costa, S. S. Multidrug Efflux Pumps in *Staphylococcus aureus*: an Update. *Open Microbiol. J.* **7,** 59–71 (2013).
168. Morita, Y., Tomida, J. & Kawamura, Y. Efflux-mediated fluoroquinolone resistance

in the multidrug-resistant *Pseudomonas aeruginosa* clinical isolate PA7: identification of a novel MexS variant involved in upregulation of the *mexEF-oprN* multidrug efflux operon. *Front. Microbiol.* **6,** 8 (2015).

169. Wright, G. D. & D., W. Bacterial resistance to antibiotics: enzymatic degradation and modification. *Adv. Drug Deliv. Rev.* **57,** 1451–70 (2005).
170. Tomasz, A. The mechanism of the irreversible antimicrobial effects of penicillins: how the beta-lactam antibiotics kill and lyse bacteria. *Annu. Rev. Microbiol.* **33,** 113–137 (1979).
171. Palzkill, T. Metallo-beta-lactamase structure and function. *Ann. N. Y. Acad. Sci.* **1277,** 91–104 (2013).
172. Magnet, S., Smith, T. A., Zheng, R., Nordmann, P. & Blanchard, J. S. Aminoglycoside resistance resulting from tight drug binding to an altered aminoglycoside acetyltransferase. *Antimicrob. Agents Chemother.* **47,** 1577–1583 (2003).
173. Noguchi, N., Tamura, Y., Katayama, J. & Narui, K. Expression of the *mphB* gene for macrolide 2'-phosphotransferase II from *Escherichia coli* in *Staphylococcus aureus*. *FEMS Microbiol. Lett.* **159,** 337–342 (1998).
174. Jiang, Y. *et al.* Complete nucleotide sequence of *Klebsiella pneumoniae* multidrug resistance plasmid pKP048, carrying *blaKPC-2, blaDHA-1, qnrB4,* and *armA*. *Antimicrob. Agents Chemother.* **54,** 3967–3969 (2010).
175. Nakamura, A. *et al.* Detection and characterization of a macrolide 2'-phosphotransferase from a *Pseudomonas aeruginosa* clinical isolate. *Antimicrob. Agents Chemother.* **44,** 3241–3242 (2000).
176. Cao, M., Bernat, B. A., Wang, Z., Armstrong, R. N. & Helmann, J. D. FosB, a cysteine-dependent fosfomycin resistance protein under the control of sigmaW, an extracytoplasmic-function sigma factor in *Bacillus subtilis*. *J. Bacteriol.* **183,** 2380–2383 (2001).
177. Lambert, P. A. Bacterial resistance to antibiotics: modified target sites. *Adv. Drug Deliv. Rev.* **57,** 1471–1485 (2005).
178. Kosowska, K., Jacobs, M. R., Bajaksouzian, S., Koeth, L. & Appelbaum, P. C. Alterations of penicillin-binding proteins 1A, 2X, and 2B in *Streptococcus pneumoniae* isolates for which amoxicillin MICs are higher than penicillin MICs. *Antimicrob. Agents Chemother.* **48,** 4020–4022 (2004).
179. Hanssen, A. M., Kjeldsen, G. & Ericson Sollid, J. U. Local variants of Staphylococcal Cassette Chromosome *mec* in sporadic methicillin-resistant *Staphylococcus aureus* and methicillin-resistant coagulase-negative Staphylococci:

evidence of horizontal gene transfer? *Antimicrob. Agents Chemother.* **48,** 285–296 (2004).

180. Whiley, D. M., Limnios, E. A., Ray, S., Sloots, T. P. & Tapsall, J. W. Diversity of *penA* alterations and subtypes in *Neisseria gonorrhoeae* strains from Sydney, Australia, that are less susceptible to ceftriaxone. *Antimicrob. Agents Chemother.* **51,** 3111–3116 (2007).
181. Vashist, J., Tiwari, V., Das, R., Kapil, A. & Rajeswari, M. R. Analysis of penicillin-binding proteins (PBPs) in carbapenem resistant *Acinetobacter baumannii*. *Indian J. Med. Res.* **133,** 332–338 (2011).
182. Bellido, F., Veuthey, C., Blaser, J., Banernfeind, A. & Pechére, J. C. Novel resistance to imipenem associated with an altered PBP-4 in a *Pseudomonas aeruginosa* clinical isolate. *J. Antimicrob. Chemother.* **25,** 57–68 (1990).
183. Rice, L. B. *et al.* Impact of specific PBP5 mutations on expression of β-lactam resistance in *Enterococcus faecium*. *Antimicrob. Agents Chemother.* **48,** 3028–3032 (2004).
184. Fuda, C., Suvorov, M., Vakulenko, S. B. & Mobashery, S. The basis for resistance to beta-lactam antibiotics by penicillin-binding protein 2a of methicillin-resistant *Staphylococcus aureus*. *J. Biol. Chem.* **279,** 40802–40806 (2004).
185. Cui, L. *et al.* Cell wall thickening is a common feature of vancomycin resistance in *Staphylococcus aureus*. *J. Clin. Microbiol.* **41,** 5–14 (2003).
186. Alekshun, M. N. & Levy, S. B. Molecular mechanisms of antibacterial multidrug resistance. *Cell* **128,** 1037–1050 (2007).
187. Bonomo, R. A. & Szabo, D. Mechanisms of Multidrug Resistance in *Acinetobacter* Species and *Pseudomonas aeruginosa*. *Clin. Infect. Dis.* **43,** S49–S56 (2006).
188. Andersson, D. I. & Hughes, D. Microbiological effects of sublethal levels of antibiotics. *Nat. Rev. Microbiol.* **12,** 465–478 (2014).
189. Gullberg, E. *et al.* Selection of resistant bacteria at very low antibiotic concentrations. *PLoS Pathog.* **7,** e1002158 (2011).
190. Wistrand-Yuen, E. *et al.* Evolution of high-level resistance during low-level antibiotic exposure. *Nat. Commun.* (2017). doi:10.1038/s41467-018-04059-1
191. Melnyk, A. H., Wong, A. & Kassen, R. The fitness costs of antibiotic resistance mutations. *Evol. Appl.* **8,** 273–283 (2015).
192. San Millan, A. Evolution of plasmid-mediated antibiotic resistance in the clinical context. *Trends Microbiol.* **0,** (2018).
193. Baym, M. *et al.* Spatiotemporal microbial evolution on antibiotic landscapes. *Science (80-.).* **353,** 1147–1151 (2016).

194. Conley, Z. C., Bodine, T. J., Chou, A. & Zechiedrich, L. Wicked: The untold story of ciprofloxacin. *PLOS Pathog.* **14,** e1006805 (2018).
195. Hawkey, P. M. Mechanisms of quinolone action and microbial response. *J. Antimicrob. Chemother.* **51,** 29–35 (2003).
196. Huseby, D. L. *et al.* Mutation supply and relative fitness shape the genotypes of ciprofloxacin-resistant *Escherichia coli. Mol. Biol. Evol.* **34,** 1029–1039 (2017).
197. Taniguchi, H. *et al.* Rifampicin resistance and mutation of the *rpoB* gene in *Mycobacterium tuberculosis. FEMS Microbiol. Lett.* **144,** 103–8 (1996).
198. Hakenbeck, R. *et al.* Acquisition of five high-Mr penicillin-binding protein variants during transfer of high-level beta-lactam resistance from *Streptococcus mitis* to *Streptococcus pneumoniae. J. Bacteriol.* **180,** 1831–40 (1998).
199. Colavecchio, A., Cadieux, B., Lo, A. & Goodridge, L. D. Bacteriophages contribute to the spread of antibiotic resistance genes among foodborne pathogens of the Enterobacteriaceae family - a review. *Front. Microbiol.* **8,** 1108 (2017).
200. Aranda, J. *et al.* Identification of a DNA-Damage-Inducible regulon in *Acinetobacter baumannii*. *J. Bacteriol.* **195,** 5577–5582 (2013).
201. Beaber, J. W., Hochhut, B. & Waldor, M. K. SOS response promotes horizontal dissemination of antibiotic resistance genes. *Nature* **427,** 72–74 (2004).
202. Torres-Barceló, C., Kojadinovic, M., Moxon, R. & MacLean, R. C. The SOS response increases bacterial fitness, but not evolvability, under a sublethal dose of antibiotic. *Proc. R. Soc. B Biol. Sci.* **282,** 20150885 (2015).
203. Gutierrez, A. *et al.* β-lactam antibiotics promote bacterial mutagenesis via an RpoS-mediated reduction in replication fidelity. *Nat. Commun.* **4,** 1610 (2013).
204. Boutte, C. C. & Crosson, S. Bacterial lifestyle shapes the regulation of stringent response activation. *Trends Microbiol.* **21,** 174–180 (2013).
205. Aedo, S. & Tomasz, A. Role of the stringent stress response in the antibiotic resistance phenotype of methicillin-resistant *Staphylococcus aureus*. *Antimicrob. Agents Chemother.* **60,** 2311–2317 (2016).
206. Kim, C. *et al.* The mechanism of heterogeneous beta-lactam resistance in MRSA: key role of the stringent stress response. *PLoS One* **8,** e82814 (2013).
207. Levin-Reisman, I. *et al.* Antibiotic tolerance facilitates the evolution of resistance. *Science* **355,** 826–830 (2017).
208. Boudjemaa, R. *et al.* New insight into daptomycin bioavailability and localization in *Staphylococcus aureus* biofilms by dynamic fluorescence imaging. *Antimicrob. Agents Chemother.* **60,** 4983–4990 (2016).
209. Frost, I. *et al.* Cooperation, competition and antibiotic resistance in bacterial

colonies. *ISME J.* 1 (2018). doi:10.1038/s41396-018-0090-4

210. Koch, G. *et al.* Evolution of resistance to a last-resort antibiotic in *Staphylococcus aureus* via bacterial competition. *Cell* **158,** 1060–1071 (2014).
211. Li, S. *et al.* Fitness cost of daptomycin-resistant *Staphylococcus aureus* obtained from *in vitro* daptomycin selection pressure. *Front. Microbiol.* **8,** 2199 (2017).
212. Reffuveille, F., De La Fuente-Nũnez, C., Mansour, S. & Hancock, R. E. W. A broad-spectrum antibiofilm peptide enhances antibiotic action against bacterial biofilms. *Antimicrob. Agents Chemother.* **58,** 5363–5371 (2014).
213. Howlin, R. P. *et al.* Low-dose nitric oxide as targeted anti-biofilm adjunctive therapy to treat chronic *Pseudomonas aeruginosa* infection in cystic fibrosis. *Mol. Ther.* **25,** 2104–2116 (2017).
214. Oosterhof, J. J. H. *et al.* The influence of antimicrobial peptides and mucolytics on the integrity of biofilms consisting of bacteria and yeasts as affecting voice prosthetic air flow resistances. *Biofouling* **19,** 347–353 (2003).
215. Gillaspy, A. F. *et al.* Role of the accessory gene regulator (agr) in pathogenesis of staphylococcal osteomyelitis. *Infect. Immun.* **63,** 3373–80 (1995).
216. Odds, F. C. Synergy, antagonism, and what the chequerboard puts between them. *J. Antimicrob. Chemother.* **52,** (2003).
217. Ceri, H. *et al.* The Calgary Biofilm Device : new technology for rapid determination of antibiotic susceptibilities of bacterial biofilms. *J. Clin. Microbiol.* **37,** 1771 (1999).
218. Heydorn, A. *et al.* Quantication of biofilm structures by the novel computer program. *Image Process.* **146,** 2395–2407 (2000).
219. Allan, R. N. *et al.* Pronounced metabolic changes in adaptation to biofilm growth by *Streptococcus pneumoniae*. *PLoS One* **9,** e107015 (2014).
220. Miller, S. I. Antibiotic resistance and regulation of the Gram-negative bacterial outer membrane barrier by host innate immune molecules. *MBio* **7,** e01541-16 (2016).
221. Ramón-García, S. *et al.* Synergistic drug combinations for tuberculosis therapy identified by a novel high-throughput screen. *Antimicrob. Agents Chemother.* **55,** 3861–3869 (2011).
222. Worthington, R. J. & Melander, C. Combination approaches to combat multidrug-resistant bacteria. *Trends Biotechnol.* **31,** 177–184 (2013).
223. Soren, O. *et al.* Antimicrobial peptide novicidin synergizes with rifampin, ceftriaxone, and ceftazidime against antibiotic-resistant Enterobacteriaceae in vitro. *Antimicrob. Agents Chemother.* **59,** 6233–6240 (2015).
224. Gifford, D. R. *et al.* Identifying and exploiting genes that potentiate the evolution of

antibiotic resistance. *Nat. Ecol. Evol.* (2018). doi:10.1038/s41559-018-0547-x

225. Thirumurugan, G., Seshagiri Rao, J. V. L. N. & Dhanaraju, M. D. Elucidating pharmacodynamic interaction of silver nanoparticle - topical deliverable antibiotics. *Sci. Rep.* **6,** 29982 (2016).
226. Ichimiya, T. *et al.* The influence of azithromycin on the biofilm formation of *Pseudomonas aeruginosa in vitro. Chemotherapy* **42,** 186–91 (1996).
227. Wagner, T., Soong, G., Sokol, S., Saiman, L. & Prince, A. Effects of azithromycin on clinical isolates of *Pseudomonas aeruginosa* from cystic fibrosis patients. *Chest* **128,** 912–919 (2005).
228. Kulp, A. & Kuehn, M. J. Biological functions and biogenesis of secreted bacterial outer membrane vesicles. *Annu. Rev. Microbiol.* **64,** 163–84 (2010).
229. Alves, C. S. *et al. Escherichia coli* cell surface perturbation and disruption induced by antimicrobial peptides BP100 and PepR. *J. Biol. Chem.* **285,** 27536–44 (2010).
230. Werneburg, M. *et al.* Inhibition of lipopolysaccharide transport to the outer membrane in *Pseudomonas aeruginosa* by peptidomimetic antibiotics. *ChemBioChem* **13,** 1767–1775 (2012).
231. Kamata, H. *et al.* Impact of chronic *Pseudomonas aeruginosa* infection on health-related quality of life in *Mycobacterium avium* complex lung disease. *BMC Pulm. Med.* **17,** 198 (2017).
232. Smith, I. *Mycobacterium tuberculosis* pathogenesis and molecular determinants of virulence. *Clin. Microbiol. Rev.* **16,** 463–96 (2003).
233. Abouelhassan, Y. *et al.* Discovery of quinoline small molecules with potent dispersal activity against methicillin-resistant *Staphylococcus aureus* and *Staphylococcus epidermidis* biofilms using a scaffold hopping strategy. *Bioorganic Med. Chem. Lett.* **24,** 5076–5080 (2014).
234. LaMontagne, M. P., Markovac, A. & Khan, M. S. Antimalarials. 13. 5-Alkoxy Analogues of 4-Methylprimaquine. *J. Med. Chem.* **25,** 964–968 (1982).
235. Berry, H., Coquelin, J. P., Gordon, A. & Seymour, D. Antrafenine, naproxen and placebo in osteoarthritis: a comparative study. *Rheumatology* **22,** 89–94 (1983).
236. Ahmed, N. *et al.* Bioorganic & medicinal chemistry synthesis and anti-HIV activity of alkylated quinoline 2,4-diols. *Bioorg. Med. Chem.* **18,** 2872–2879 (2010).
237. Pérez-Llarena, F. J. & Bou, G. Proteomics as a tool for studying bacterial virulence and antimicrobial resistance. *Front. Microbiol.* **7,** 410 (2016).
238. Savaryn, J. P., Toby, T. K. & Kelleher, N. L. A researcher's guide to mass spectrometry-based proteomics. *Proteomics* **16,** 2435–43 (2016).
239. Wiese, S., Reidegeld, K. A., Meyer, H. E. & Warscheid, B. Protein labeling by

iTRAQ: a new tool for quantitative mass spectrometry in proteome research. *Proteomics* **7,** 340–350 (2007).

240. Thai, V. C., Lim, T. K., Le, K. P. U., Lin, Q. & Nguyen, T. T. H. iTRAQ-based proteome analysis of fluoroquinolone-resistant *Staphylococcus aureus*. *J. Glob. Antimicrob. Resist.* **8,** 82–89 (2017).
241. Allan, R. N. *et al.* Low concentrations of nitric oxide modulate *Streptococcus pneumoniae* biofilm metabolism and antibiotic tolerance. *Antimicrob. Agents Chemother.* (2016). doi:10.1128/AAC.02432-15
242. Liu, X., Hu, Y., Pai, P.-J., Chen, D. & Lam, H. Label-free quantitative proteomics analysis of antibiotic response in *Staphylococcus aureus* to oxacillin. *J. Proteome Res.* **13,** 1223–1233 (2014).
243. Wick, R. R., Judd, L. M., Gorrie, C. L. & Holt, K. E. Unicycler: resolving bacterial genome assemblies from short and long sequencing reads. *PLOS Comput. Biol.* **13,** e1005595 (2017).
244. Seemann, T. Prokka: rapid prokaryotic genome annotation. *Bioinformatics* **30,** 2068–2069 (2014).
245. Overbeek, R. *et al.* The SEED and the Rapid Annotation of microbial genomes using Subsystems Technology (RAST). *Nucleic Acids Res.* **42,** D206-14 (2014).
246. Aziz, R. K. *et al.* The RAST Server: Rapid Annotations using Subsystems Technology. *BMC Genomics* **9,** 75 (2008).
247. Brettin, T. *et al.* RASTtk: A modular and extensible implementation of the RAST algorithm for building custom annotation pipelines and annotating batches of genomes. *Sci. Rep.* **5,** 8365 (2015).
248. Søe, N. H. *et al.* A novel knee prosthesis model of implant-related osteomyelitis in rats. *Acta Orthop.* **84,** 92–7 (2013).
249. Mi, H. *et al.* PANTHER version 11: expanded annotation data from Gene Ontology and Reactome pathways, and data analysis tool enhancements. *Nucleic Acids Res.* **45,** D183–D189 (2017).
250. Szklarczyk, D. *et al.* The STRING database in 2017: quality-controlled protein–protein association networks, made broadly accessible. *Nucleic Acids Res.* **45,** D362–D368 (2017).
251. Imber, M. *et al.* The aldehyde dehydrogenase AldA contributes to the hypochlorite defense and is redox-controlled by protein S-bacillithiolation in *Staphylococcus aureus*. *Redox Biol.* **15,** 557–568 (2018).
252. Bertin, Y. *et al.* The gluconeogenesis pathway is involved in maintenance of enterohaemorrhagic *Escherichia coli* O157:H7 in bovine intestinal content. *PLoS*

One **9,** e98367 (2014).

253. Maghnouj, A., de Sousa Cabral, T. F., Stalon, V. & Vander Wauven, C. The *arcABDC* gene cluster, encoding the arginine deiminase pathway of *Bacillus licheniformis*, and its activation by the arginine repressor ArgR. *J. Bacteriol.* **180,** 6468–75 (1998).
254. Somerville, G. A. & Proctor, R. A. At the crossroads of bacterial metabolism and virulence factor synthesis in Staphylococci. *Microbiol. Mol. Biol. Rev.* **73,** 233–48 (2009).
255. Barreteau, H. *et al.* Cytoplasmic steps of peptidoglycan biosynthesis. *FEMS Microbiol. Rev.* **32,** 168–207 (2008).
256. Choby, J. E. & Skaar, E. P. Heme synthesis and acquisition in bacterial pathogens. *J. Mol. Biol.* **428,** 3408–28 (2016).
257. Lobo, S. A. L. *et al. Staphylococcus aureus* haem biosynthesis: characterisation of the enzymes involved in final steps of the pathway. *Mol. Microbiol.* **97,** 472–487 (2015).
258. Halsey, C. R. *et al.* Amino acid catabolism in *Staphylococcus aureus* and the function of carbon catabolite repression. *MBio* **8,** e01434-16 (2017).
259. Poulsen, C., Panjikar, S., Holton, S. J., Wilmanns, M. & Song, Y.-H. WXG100 Protein Superfamily Consists of Three Subfamilies and Exhibits an α-Helical C-Terminal Conserved Residue Pattern. *PLoS One* **9,** e89313 (2014).
260. Tamames, J., González-Moreno, M., Mingorance, J., Valencia, A. & Vicente, M. Bringing gene order into bacterial shape. *Trends Genet.* **17,** 124–126 (2001).
261. Pucci, M. J., Thanassi, J. A., Discotto, L. F., Kessler, R. E. & Dougherty, T. J. Identification and characterization of cell wall-cell division gene clusters in pathogenic Gram-positive cocci. *Journal of bacteriology* **179,** (1997).
262. Anton, B. P. *et al.* Functional characterization of the YmcB and YqeV tRNA methylthiotransferases of *Bacillus subtilis. Nucleic Acids Res.* **38,** 6195–205 (2010).
263. Weiss, A. *et al.* The ω subunit governs RNA polymerase stability and transcriptional specificity in *Staphylococcus aureus*. *J. Bacteriol.* **199,** (2017).
264. Lindgren, J. K. *et al.* Arginine deiminase in *Staphylococcus epidermidis* functions to augment biofilm maturation through pH homeostasis. *J. Bacteriol.* **196,** 2277–89 (2014).
265. Brown, S., Santa Maria, J. P., Walker, S. & Walker, S. Wall teichoic acids of Gram-positive bacteria. *Annu. Rev. Microbiol.* **67,** 313–36 (2013).
266. Somerville, G. A. *et al. Staphylococcus aureus* aconitase inactivation unexpectedly inhibits post-exponential-phase growth and enhances stationary-phase survival.

Infect. Immun. **70,** 6373–82 (2002).

267. Gaupp, R., Schlag, S., Liebeke, M., Lalk, M. & Götz, F. Advantage of upregulation of succinate dehydrogenase in *Staphylococcus aureus* biofilms. *J. Bacteriol.* **192,** 2385–94 (2010).
268. Resch, A. *et al.* Comparative proteome analysis of *Staphylococcus aureus* biofilm and planktonic cells and correlation with transcriptome profiling. *Proteomics* **6,** 1867–1877 (2006).
269. Resch, A., Rosenstein, R., Nerz, C. & Götz, F. Differential gene expression profiling of *Staphylococcus aureus* cultivated under biofilm and planktonic conditions. *Appl. Environ. Microbiol.* **71,** 2663–76 (2005).
270. Mengin-Lecreulx, D. & van Heijenoort, J. Effect of growth conditions on peptidoglycan content and cytoplasmic steps of its biosynthesis in *Escherichia coli. J. Bacteriol.* **163,** 208–12 (1985).
271. Sieradzki, K. & Tomasz, A. Alterations of cell wall structure and metabolism accompany reduced susceptibility to vancomycin in an isogenic series of clinical isolates of *Staphylococcus aureus*. *J. Bacteriol.* **185,** 7103–10 (2003).
272. Borisova, M. *et al.* Peptidoglycan recycling in Gram-positive bacteria is crucial for survival in stationary phase. *MBio* **7,** e00923-16 (2016).
273. Utaida, S. *et al.* Genome-wide transcriptional profiling of the response of *Staphylococcus aureus* to cell-wall-active antibiotics reveals a cell-wall-stress stimulon. *Microbiology* **149,** 2719–2732 (2003).
274. Straus, S. K. & Hancock, R. E. W. Mode of action of the new antibiotic for Gram-positive pathogens daptomycin: comparison with cationic antimicrobial peptides and lipopeptides. *Biochim. Biophys. Acta - Biomembr.* **1758,** 1215–1223 (2006).
275. Muthaiyan, A., Silverman, J. A., Jayaswal, R. K. & Wilkinson, B. J. Transcriptional profiling reveals that daptomycin induces the *Staphylococcus aureus* cell wall stress stimulon and genes responsive to membrane depolarization. *Antimicrob. Agents Chemother.* **52,** 980–90 (2008).
276. Dawe, H. *et al.* D-methionine interferes with non-typeable *Haemophilus influenzae* peptidoglycan synthesis during growth and biofilm formation. *Microbiology* **163,** 1093–1104 (2017).
277. Mateus, A., Määttä, T. A. & Savitski, M. M. Thermal proteome profiling: unbiased assessment of protein state through heat-induced stability changes. *Proteome Sci.* **15,** 13 (2016).
278. Lin, Y., Lin, H., Liu, Z., Wang, K. & Yan, Y. Improvement of a sample preparation method assisted by sodium deoxycholate for mass-spectrometry-based shotgun

membrane proteomics†. *J. Sep. Sci.* **37,** 3321–3329 (2014).

279. Serra, R. *et al.* Chronic wound infections: the role of *Pseudomonas aeruginosa* and *Staphylococcus aureus*. *Expert Rev. Anti. Infect. Ther.* **13,** 605–613 (2015).
280. Rosche, W. A. & Foster, P. L. Determining mutation rates in bacterial populations. *Methods* **20,** 4–17 (2000).
281. Foster, P. L. Methods for determining spontaneous mutation rates. *Methods Enzymol.* **409,** 195–213 (2006).
282. Luria, S. E. & Delbrück, M. Mutations of bacteria from virus sensitivity to virus resistance. *Genetics* **28,** 491–511 (1943).
283. Hall, B. M., Ma, C. X., Liang, P. & Singh, K. K. Fluctuation analysis calculator: A web tool for the determination of mutation rate using Luria-Delbück fluctuation analysis. *Bioinformatics* **25,** 1564–1565 (2009).
284. Zheng, Q. Methods for comparing mutation rates using fluctuation assay data. *Mutat. Res. - Fundam. Mol. Mech. Mutagen.* **777,** 20–22 (2015).
285. Lauderdale, K. J., Malone, C. L., Boles, B. R., Morcuende, J. & Horswill, A. R. Biofilm dispersal of community-associated methicillin-resistant *Staphylococcus aureus* on orthopedic implant material. *J. Orthop. Res.* **28,** 55–61 (2010).
286. Duignan, C. M. Influence of low-dose nitric oxide on mono- and mixed-species biofilms formed by bacteria isolated from cystic fibrosis patients. (University of Southampton, 2017).
287. Wick, R. R., Judd, L. M., Gorrie, C. L. & Holt, K. E. Completing bacterial genome assemblies with multiplex MinION sequencing. doi:10.1099/mgen.0.000132
288. Zhou, Y., Liang, Y., Lynch, K. H., Dennis, J. J. & Wishart, D. S. PHAST: a fast phage search tool. *Nucleic Acids Res.* **39,** W347–W352 (2011).
289. Arndt, D. *et al.* PHASTER: a better, faster version of the PHAST phage search tool. *Nucleic Acids Res.* **44,** W16–W21 (2016).
290. MacGregor-Fors, I. & Payton, M. E. Contrasting diversity values: statistical inferences based on overlapping confidence intervals. *PLoS One* **8,** e56794 (2013).
291. Zheng, Q. New algorithms for Luria-Delbrück fluctuation analysis. *Math. Biosci.* **196,** 198–214 (2005).
292. Tyrrell, J. & Callaghan, M. Iron acquisition in the cystic fibrosis lung and potential for novel therapeutic strategies. *Microbiology* **162,** 191–205 (2016).
293. Lansky, I. B. *et al.* The cytoplasmic heme-binding protein (PhuS) from the heme uptake system of *Pseudomonas aeruginosa* is an intracellular heme-trafficking protein to the delta-regioselective heme oxygenase. *J. Biol. Chem.* **281,** 13652–62 (2006).

294. MacLean, R. C. & San Millan, A. Microbial evolution: towards resolving the plasmid paradox. *Curr. Biol.* **25,** R764–R767 (2015).
295. Kaplan, J. B. Antibiotic-induced biofilm formation. *Int. J. Artif. Organs* **34,** 737–51 (2011).
296. McCarthy, R. R. *et al.* Cyclic-di-GMP regulates lipopolysaccharide modification and contributes to *Pseudomonas aeruginosa* immune evasion. *Nat. Microbiol.* **2,** 17027 (2017).
297. Whittaker, J. W. Non-heme manganese catalase--the 'other' catalase. *Arch. Biochem. Biophys.* **525,** 111–20 (2012).
298. Liu, M., Zhang, Y., Inouye, M. & Woychik, N. A. Bacterial addiction module toxin Doc inhibits translation elongation through its association with the 30S ribosomal subunit. *Proc. Natl. Acad. Sci. U. S. A.* **105,** 5885–90 (2008).
299. Noinaj, N., Guillier, M., Barnard, T. J. & Buchanan, S. K. TonB-dependent transporters: regulation, structure, and function. *Annu. Rev. Microbiol.* **64,** 43–60 (2010).
300. Bonamore, A. & Boffi, A. Flavohemoglobin: Structure and reactivity. *IUBMB Life* **60,** 19–28 (2007).
301. Niemann, V. *et al.* The NreA protein functions as a nitrate receptor in the Staphylococcal nitrate regulation system. *J. Mol. Biol.* **426,** 1539–1553 (2014).
302. Gordon, J. E. *et al.* Use of chimeric type IV secretion systems to define contributions of outer membrane subassemblies for contact-dependent translocation. *Mol. Microbiol.* **105,** 273–293 (2017).
303. James, C. E. *et al.* Lytic activity by temperate phages of *Pseudomonas aeruginosa* in long-term cystic fibrosis chronic lung infections. *ISME J.* **9,** 1391–1398 (2015).
304. Sharples, G. J., Bolt, E. L. & Lloyd, R. G. RusA proteins from the extreme thermophile *Aquifex aeolicus* and lactococcal phage r1t resolve Holliday junctions. *Mol. Microbiol.* **44,** 549–559 (2002).
305. Palmer, K. L., Mashburn, L. M., Singh, P. K. & Whiteley, M. Cystic fibrosis sputum supports growth and cues key aspects of *Pseudomonas aeruginosa* physiology. *J. Bacteriol.* **187,** 5267–77 (2005).
306. Miller, C. L. *et al.* Global transcriptome responses including small RNAs during mixed-species interactions with methicillin-resistant *Staphylococcus aureus* and *Pseudomonas aeruginosa*. *Microbiologyopen* **6,** 1–22 (2017).
307. Nguyen, A. T. & Oglesby-Sherrouse, A. G. Spoils of war: iron at the crux of clinical and ecological fitness of *Pseudomonas aeruginosa*. *BioMetals* **28,** 433–443 (2015).
308. Nguyen, A. T., Jones, J. W., Ruge, M. A., Kane, M. A. & Oglesby-Sherrouse, A. G.

Iron depletion enhances production of antimicrobials by *Pseudomonas aeruginosa*. *J. Bacteriol.* **197,** 2265–2275 (2015).

309. Hoffman, L. R. *et al.* Selection for *Staphylococcus aureus* small-colony variants due to growth in the presence of *Pseudomonas aeruginosa*. *Proc. Natl. Acad. Sci. U. S. A.* **103,** 19890–5 (2006).
310. Krašovec, R. *et al.* Spontaneous mutation rate is a plastic trait associated with population density across domains of life. *PLOS Biol.* **15,** e2002731 (2017).
311. Lebeaux, D., Chauhan, A., Rendueles, O. & Beloin, C. From *in vitro* to *in vivo* models of bacterial biofilm-related infections. *Pathog. (Basel, Switzerland)* **2,** 288–356 (2013).
312. Walker, W. T. *et al.* Primary ciliary dyskinesia ciliated airway cells show increased susceptibility to *Haemophilus influenzae* biofilm formation. *Eur. Respir. J.* **50,** 1700612 (2017).
313. Harrison, F. & Diggle, S. P. An *ex vivo* lung model to study bronchioles infected with *Pseudomonas aeruginosa* biofilms. *Microbiology* **162,** 1755–1760 (2016).
314. Harrison, F., Muruli, A., Higgins, S. & Diggle, S. P. Development of an *ex vivo* porcine lung model for studying growth, virulence, and signaling of *Pseudomonas aeruginosa*. **82,** (2014).
315. Alves, P. M. *et al.* Interaction between *Staphylococcus aureus* and *Pseudomonas aeruginosa* is beneficial for colonisation and pathogenicity in a mixed biofilm. *Pathog. Dis.* **76,** (2018).
316. Huse, H. K. *et al.* Parallel evolution in *Pseudomonas aeruginosa* over 39,000 generations *in vivo*. *MBio* **1,** e00199-10 (2010).
317. Li, H. Aligning sequence reads, clone sequences and assembly contigs with BWA-MEM. (2013).
318. Li, H. *et al.* The Sequence Alignment/Map format and SAMtools. *Bioinformatics* **25,** 2078–2079 (2009).
319. Li, H. A statistical framework for SNP calling, mutation discovery, association mapping and population genetical parameter estimation from sequencing data. *Bioinformatics* **27,** 2987–2993 (2011).
320. Gurevich, A., Saveliev, V., Vyahhi, N. & Tesler, G. QUAST: quality assessment tool for genome assemblies. *Bioinformatics* **29,** 1072–1075 (2013).
321. Page, A. J. *et al.* Roary: rapid large-scale prokaryote pan genome analysis. *Bioinformatics* **31,** 3691–3 (2015).
322. Deatherage, D. E. & Barrick, J. E. Identification of mutations in laboratory-evolved microbes from next-generation sequencing data using breseq. *Methods Mol. Biol.*

1151, 165–88 (2014).

323. Barrick, J. E. *et al.* Identifying structural variation in haploid microbial genomes from short-read resequencing data using breseq. *BMC Genomics* **15,** 1039 (2014).
324. Thorvaldsdottir, H., Robinson, J. T. & Mesirov, J. P. Integrative Genomics Viewer (IGV): high-performance genomics data visualization and exploration. *Brief. Bioinform.* **14,** 178–192 (2013).
325. Robinson, J. T. *et al.* Integrative genomics viewer. *Nat. Biotechnol.* **29,** 24–26 (2011).
326. Johnson, M. *et al.* NCBI BLAST: a better web interface. *Nucleic Acids Res.* **36,** W5–W9 (2008).
327. Boratyn, G. M. *et al.* BLAST: a more efficient report with usability improvements. *Nucleic Acids Res.* **41,** W29–W33 (2013).
328. Altschul, S. F., Gish, W., Miller, W., Myers, E. W. & Lipman, D. J. Basic local alignment search tool. *J. Mol. Biol.* **215,** 403–410 (1990).
329. Winsor, G. L. *et al.* Enhanced annotations and features for comparing thousands of *Pseudomonas* genomes in the Pseudomonas genome database. *Nucleic Acids Res.* **44,** D646–D653 (2016).
330. Valot, B. *et al.* What it takes to be a *Pseudomonas aeruginosa*? The core genome of the opportunistic pathogen updated. *PLoS One* **10,** e0126468 (2015).
331. Snipen, L., Almøy, T. & Ussery, D. W. Microbial comparative pan-genomics using binomial mixture models. *BMC Genomics* **10,** 385 (2009).
332. Baker, J. A., Simkovic, F., Taylor, H. M. C. & Rigden, D. J. Potential DNA binding and nuclease functions of ComEC domains characterized *in silico*. *Proteins* **84,** 1431–42 (2016).
333. Roy, A. B., Petrova, O. E. & Sauer, K. The phosphodiesterase DipA (PA5017) is essential for *Pseudomonas aeruginosa* biofilm dispersion. *J. Bacteriol.* **194,** 2904–15 (2012).
334. Somprasong, N. *et al. Pseudomonas aeruginosa* thiol peroxidase protects against hydrogen peroxide toxicity and displays atypical patterns of gene regulation. *J. Bacteriol.* **194,** 3904–12 (2012).
335. Park, S. J. & Lee, S. Y. Identification and characterization of a new enoyl coenzyme A hydratase involved in biosynthesis of medium-chain-length polyhydroxyalkanoates in recombinant *Escherichia coli. J. Bacteriol.* **185,** 5391–7 (2003).
336. Rosenau, F. *et al.* Lipase LipC affects motility, biofilm formation and rhamnolipid production in *Pseudomonas aeruginosa*. *FEMS Microbiol. Lett.* **309,** no-no (2010).

337. Khademi, H. & Jelsbak, L. Host adaptation mediated by intergenic evolution in a bacterial pathogen. *bioRxiv* 236000 (2017). doi:10.1101/236000
338. Li, X. *et al.* The 3.2 Å resolution structure of a receptor: CheA:CheW signaling complex defines overlapping binding sites and key residue interactions within bacterial chemosensory arrays. *Biochemistry* **52,** 3852–3865 (2013).
339. Fedi, S. *et al.* The role of *cheA* genes in swarming and swimming motility of *Pseudomonas pseudoalcaligenes* KF707. *Microbes Environ.* **31,** 169–72 (2016).
340. Chou, H. T., Kwon, D.-H., Hegazy, M. & Lu, C.-D. Transcriptome analysis of agmatine and putrescine catabolism in *Pseudomonas aeruginosa* PAO1. *J. Bacteriol.* **190,** 1966–75 (2008).
341. Poonsuk, K. & Chuanchuen, R. Contribution of the MexXY multidrug efflux pump and other chromosomal mechanisms on aminoglycoside resistance in *Pseudomonas aeruginosa* isolates from canine and feline infections. *J. Vet. Med. Sci.* **74,** 1575–82 (2012).
342. Ueda, A. & Wood, T. K. Tyrosine phosphatase TpbA of *Pseudomonas aeruginosa* controls extracellular DNA via cyclic diguanylic acid concentrations. *Environ. Microbiol.* **2,** 449–55 (2010).
343. Wang, S. *et al.* Biosynthesis of the common polysaccharide antigen of *Pseudomonas aeruginosa* PAO1: characterization and role of GDP-d-rhamnose:GlcNAc/GalNAc-diphosphate-lipid α1,3-d-rhamnosyltransferase WbpZ. *J. Bacteriol.* **197,** 2012–2019 (2015).
344. Nowroozi, J., Akhavan Sepahi, A. & Rashnonejad, A. Pyocyanine biosynthetic genes in clinical and environmental isolates of *Pseudomonas aeruginosa* and detection of pyocyanine's antimicrobial effects with or without colloidal silver nanoparticles. *Cell J.* **14,** 7–18 (2012).
345. Hilliam, Y. *et al. Pseudomonas aeruginosa* adaptation and diversification in the non-cystic fibrosis bronchiectasis lung. *Eur Respir J* **49,** (2017).
346. Llanes, C. *et al.* Role of the MexEF-OprN efflux system in low-level resistance of *Pseudomonas aeruginosa* to ciprofloxacin. *Antimicrob. Agents Chemother.* **55,** 5676–84 (2011).
347. Saikolappan, S., Das, K. & Dhandayuthapani, S. Inactivation of the organic hydroperoxide stress resistance regulator OhrR enhances resistance to oxidative stress and isoniazid in *Mycobacterium smegmatis. J. Bacteriol.* **197,** 51–62 (2015).
348. Surdova, K. *et al.* The conserved DNA-binding protein WhiA is involved in cell division in *Bacillus subtilis. J. Bacteriol.* **195,** 5450–60 (2013).
349. Bush, M. J., Bibb, M. J., Chandra, G., Findlay, K. C. & Buttner, M. J. Genes

required for aerial growth, cell division, and chromosome segregation are targets of WhiA before sporulation in *Streptomyces venezuelae. MBio* **4,** e00684-13 (2013).

350. Traverse, C. C. & Ochman, H. A Genome-Wide Assay Specifies Only GreA as a Transcription Fidelity Factor in *Escherichia coli. G3 (Bethesda).* g3.200209.2018 (2018). doi:10.1534/g3.118.200209
351. Cui, G., Wang, J., Qi, X. & Su, J. Transcription elongation factor GreA plays a key role in cellular invasion and virulence of *Francisella tularensis* subsp. novicida. *Sci. Rep.* **8,** 6895 (2018).
352. Lee, J. & Borukhov, S. Bacterial RNA polymerase-DNA interaction—the driving force of gene expression and the target for drug action. *Front. Mol. Biosci.* **3,** 73 (2016).
353. Cheung, A. L. *et al.* Site-specific mutation of the sensor kinase GraS in *Staphylococcus aureus* alters the adaptive response to distinct cationic antimicrobial peptides. *Infect. Immun.* **82,** 5336–5345 (2014).
354. Chaili, S. *et al.* The GraS sensor in *Staphylococcus aureus* mediates resistance to host defense peptides differing in mechanisms of action. *Infect. Immun.* **84,** 459–466 (2016).
355. Komatsuzawa, H. *et al.* Cloning and sequencing of the gene, *fmtC* , which affects oxacillin resistance in methicillin-resistant *Staphylococcus aureus*. *FEMS Microbiol. Lett.* **203,** 49–54 (2001).
356. Dubrac, S., Bisicchia, P., Devine, K. M. & Msadek, T. A matter of life and death: cell wall homeostasis and the WalKR (YycGF) essential signal transduction pathway. *Mol. Microbiol.* **70,** 1307–1322 (2008).
357. Savage, V. J., Chopra, I. & O'Neill, A. J. Population diversification in *Staphylococcus aureus* biofilms may promote dissemination and persistence. *PLoS One* **8,** e62513 (2013).
358. Conlon, K. M., Humphreys, H. & O'Gara, J. P. Inactivations of *rsbU* and *sarA* by IS256 represent novel mechanisms of biofilm phenotypic variation in Staphylococcus epidermidis. *J. Bacteriol.* **186,** 6208–6219 (2004).
359. Johns, B. E., Purdy, K. J., Tucker, N. P. & Maddocks, S. E. Phenotypic and genotypic characteristics of small colony variants and their role in chronic infection. *Microbiol. insights* **8,** 15–23 (2015).
360. Peleg, A. Y. *et al.* Whole genome characterization of the mechanisms of daptomycin resistance in clinical and laboratory derived isolates of *Staphylococcus aureus. PLoS One* **7,** e28316 (2012).
361. Cameron, D. R., Jiang, J.-H., Kostoulias, X., Foxwell, D. J. & Peleg, A. Y.

Vancomycin susceptibility in methicillin-resistant *Staphylococcus aureus* is mediated by YycHI activation of the WalRK essential two-component regulatory system. *Sci. Rep.* **6,** 30823 (2016).

362. Hughes, D. & Andersson, D. I. Environmental and genetic modulation of the phenotypic expression of antibiotic resistance. *FEMS Microbiol. Rev.* **41,** 374–391 (2017).
363. Cui, Z. *et al.* Mutations in the *embC-embA* intergenic region contribute to *Mycobacterium tuberculosis* resistance to ethambutol. *Antimicrob. Agents Chemother.* **58,** 6837–43 (2014).
364. Hickman, J. W., Tifrea, D. F. & Harwood, C. S. A chemosensory system that regulates biofilm formation through modulation of cyclic diguanylate levels. *Proc. Natl. Acad. Sci. U. S. A.* **102,** 14422–7 (2005).
365. Sherrard, L. J. *et al.* Within-host whole genome analysis of an antibiotic resistant *Pseudomonas aeruginosa* strain sub-type in cystic fibrosis. *PLoS One* **12,** e0172179 (2017).
366. Frydenlund Michelsen, C. *et al.* Evolution of metabolic divergence in *Pseudomonas aeruginosa* during long-term infection facilitates a proto-cooperative interspecies interaction. *ISME J.* **10,** 1323–36 (2016).
367. Levy, S. F. *et al.* Quantitative evolutionary dynamics using high-resolution lineage tracking. *Nature* **519,** 181–186 (2015).
368. Desai, M. M. & Fisher, D. S. Beneficial mutation selection balance and the effect of linkage on positive selection. *Genetics* **176,** 1759–98 (2007).
369. Sprouffske, K., Aguilar-Rodríguez, J., Sniegowski, P. & Wagner, A. High mutation rates limit evolutionary adaptation in *Escherichia coli. PLoS Genet.* **14,** e1007324 (2018).
370. Gifford, D. R., Moss, E. & MacLean, R. C. Environmental variation alters the fitness effects of rifampicin resistance mutations in *Pseudomonas aeruginosa*. *Evolution (N. Y).* **70,** 725–730 (2016).
371. Wi, Y. M. *et al.* Rifampicin resistance in *Staphylococcus epidermidis*: molecular characterisation and fitness cost of *rpoB* mutations. *Int. J. Antimicrob. Agents* **51,** 670–677 (2018).
372. Wichelhaus, T. A. *et al.* Biological cost of rifampin resistance from the perspective of *Staphylococcus aureus. Antimicrob. Agents Chemother.* **46,** 3381–5 (2002).
373. Hall, A. R., Iles, J. C. & MacLean, R. C. The fitness cost of rifampicin resistance in *Pseudomonas aeruginosa* depends on demand for RNA polymerase. *Genetics* **187,** 817–822 (2011).

374. Kipp, F. *et al.* Evaluation of two chromogenic agar media for recovery and identification of *Staphylococcus aureus* small-colony variants. *J. Clin. Microbiol.* **43,** 1956–9 (2005).
375. Leggett, R. M. & Clark, M. D. A world of opportunities with nanopore sequencing. *J. Exp. Bot.* **68,** 5419–5429 (2017).
376. Dai, D., Holder, D., Raskin, L. & Xi, C. Separation of the bacterial species, *Escherichia coli*, from mixed-species microbial communities for transcriptome analysis. *BMC Microbiol.* **11,** 59 (2011).
377. Brennan-Krohn, T., Smith, K. P. & Kirby, J. E. The poisoned well: enhancing the predictive value of antimicrobial susceptibility testing in the era of multidrug resistance. *J. Clin. Microbiol.* **55,** 2304–2308 (2017).
378. Jorgensen, J. H., Ferraro, M. J., Jorgensen, J. H. & Ferraro, M. J. Antimicrobial susceptibility testing: a review of general principles and contemporary practices. *Clin. Infect. Dis.* **49,** 1749–1755 (2009).
379. Mina, E. G. & Marques, C. N. H. Interaction of *Staphylococcus aureus* persister cells with the host when in a persister state and following awakening. *Sci. Rep.* **6,** 31342 (2016).
380. Cho, J., Carr, A. N., Whitworth, L., Johnson, B. & Wilson, K. S. MazEF toxin-antitoxin proteins alter *Escherichia coli* cell morphology and infrastructure during persister formation and regrowth. *Microbiology* **163,** 308–321 (2017).
381. Bell, G. & MacLean, C. The search for ‘evolution-proof’ antibiotics. *Trends Microbiol.* (2017). doi:10.1016/J.TIM.2017.11.005